

**STUDY OF THE MIXING BEHAVIOR OF SOME
COMPOUND FORMING BINARY LIQUID ALLOYS
(Bi-Pb, Cu-In etc)**



**A THESIS SUBMITTED TO THE
CENTRAL DEPARTMENT OF PHYSICS
INSTITUTE OF SCIENCE AND TECHNOLOGY
TRIBHUVAN UNIVERSITY
NEPAL**

**FOR THE AWARD OF
DOCTOR OF PHILOSOPHY
IN PHYSICS**

By
INDRA BAHADUR BHANDARI

OCTOBER 2023

**STUDY OF THE MIXING BEHAVIOR OF SOME
COMPOUND FORMING BINARY LIQUID ALLOYS
(Bi-Pb, Cu-In etc)**



**A THESIS SUBMITTED TO THE
CENTRAL DEPARTMENT OF PHYSICS
INSTITUTE OF SCIENCE AND TECHNOLOGY
TRIBHUVAN UNIVERSITY
NEPAL**

**FOR THE AWARD OF
DOCTOR OF PHILOSOPHY
IN PHYSICS**

By
INDRA BAHADUR BHANDARI

OCTOBER 2023



TRIBHUVAN UNIVERSITY
Institute of Science and Technology
DEAN'S OFFICE

Kirtipur, Kathmandu, Nepal

Reference No.:

EXTERNAL EXAMINERS

The Title of Ph.D. Thesis: " Study of the Mixing Behavior of Some Compound Forming Binary Liquid Alloys (Bi-Pb, Cu-In etc) "

Name of Candidate: Indra Bahadur Bhandari

External Examiners:

- (1) Dr. Krishna Raj Adhikari
Institute of Engineering
Pashchimanchal Campus
Tribhuvan University,
Pokhara, NEPAL
- (2) Prof. Dr. Jagdhar Mandal
T.M. Bhagalpur University
INDIA
- (3) Dr. Rudra Aryal
Franklin Pierce University
Rindge NH, USA

October 11, 2023

(Dr. Surendra Kumar Gautam)
Asst. Dean

DECLARATION

This thesis entitled “**STUDY OF THE MIXING BEHAVIOR OF SOME COMPOUND FORMING BINARY LIQUID ALLOYS (Bi-Pb, Cu-In etc)**” which is being submitted to the Central Department of Physics, Institute of Science and Technology (IoST), Tribhuvan University, Nepal for the award of the degree of Doctor of Philosophy (Ph.D.); is a research work carried out by me under the supervision of Prof. Dr. Ishwar Koirala, of Central Department of Physics, Tribhuvan University, Kirtipur, Kathmandu, Nepal.

This research is original and has not been submitted earlier in part or full in this or any other form to any university or institute, here or elsewhere, for the award of any degree.



Indra Bahadur Bhandari

RECOMMENDATION

This is to recommend that **Mr. Indra Bahadur Bhandari** has carried out research entitled “**STUDY OF THE MIXING BEHAVIOR OF SOME COMPOUND FORMING BINARY LIQUID ALLOYS (Bi-Pb, Cu-In etc)**” for the award of Doctor of Philosophy (Ph.D.) in **Physics** under my supervision. To my knowledge, this work has not been submitted for any other degree.

He has fulfilled all the requirements laid down by the Institute of Science and Technology (IoST), Tribhuvan University, Kirtipur for the submission of the thesis for the award of Ph.D. degree.



.....
Dr. Ishwar Koirala

Supervisor

(Professor)

Central Department of Physics,

Tribhuvan University,

Kirtipur, Kathmandu, Nepal

APRIL 20, 2023



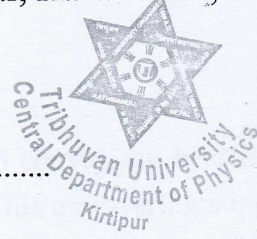
TRIBHUVAN UNIVERSITY

CENTRAL DEPARTMENT OF PHYSICS

Kirtipur, Kathmandu, Nepal

☎ 4331054

www.tucdp.edu.np



Ref. No.: (F.No) CDP

Date:

LETTER OF APPROVAL

Date: 20/04/2023

On the recommendation of **Prof. Dr. Ishwar Koirala**, this Ph.D. thesis submitted by **Mr. Indra Bahadur Bhandari**, entitled “**STUDY OF THE MIXING BEHAVIOR OF SOME COMPOUND FORMING BINARY LIQUID ALLOYS (Bi-Pb, Cu-In etc)**” is forwarded by Central Department Research Committee (CDRC) to the Dean, Institute of Science and Technology (IoST), Tribhuvan University.

OP Niraula

Dr. Om Prakash Niraula
(Professor)

Head,

Central Department of Physics,

Tribhuvan University,

Kirtipur, Kathmandu, Nepal

ACKNOWLEDGMENTS

First and foremost, I would like to convey my heartfelt thanks to Prof. Dr. Ishwar Koirala, my Ph. D. supervisor, for his unwavering support, patience, encouragements, excitement, and depth knowledge. His advice was invaluable during the research and writing of this thesis. Working and studying under his instruction was a wonderful honor and privilege.

Besides my supervisor, I would like to express my sincere thanks to Prof. Dr. Om Prakash Niraula, Head of Central Department of Physics, Tribhuvan University, Kirtipur, Kathmandu, Nepal. I would also like to thank Prof. Dr. Devendra Adhikari for his valuable guidance throughout my academic years. He provided the guidance that I needed to choose the right direction and also successfully publish my research works. I would like to thank the rest of central department research committee members: Prof. Dr. Raju Khanal, Prof. Dr. Narayan Prasad Adhikari, and Dr. Bal Ram Ghimire, for their encouragements, insightful comments and suggestions. During the second semester of this Ph. D. study, Prof. Dr. Narayan Prasad Adhikari introduced us to advanced research methodologies and computational physics. I am equally thankful to Prof. Dr. Binil Aryal, Dean of Institute of Science and Technology (IoST), Tribhuvan University, Kirtipur, Kathmandu, Nepal for sharing his knowledge about “error analysis” and “journal ranking” in my second semester. Furthermore, I am grateful to all of the Department’s recognized instructors and staffs who directly or indirectly assisted and supported me when I began my research career at the Department.

I’d like to thank my batch mates Mr. Basudev Ghimire, Mr. Daya Nidhi Chhatkuli, Mr. Dinesh Kumar Chaudhary, Mr. Jiwan Regmi, Mr. Prakash Man Shrestha, Mr. Raj Kumar Rai, Mr. Ram Babu Roy, Mr. Ramesh Kumar Gohivar, Dr. Suresh Basnet, Mr. Tarun Chaudhary, Mr. Upendra , and Mrs. Usha Joshi for their moral support and suggestions.

I would like to extend my special gratitude to Dr. Basu Dev Oli, West Virginia University, USA, and Dr. Uttar Pudasaini, The College of William and Mary, USA for their generous cooperation in supplying literature review materials. I am thankful to my student Er. Dipendra Marasaini, for giving me with python expertise. I want to express my gratitude to my beloved brother Mr. Sudeep Gaire for always being there for me, both physically and mentally. My friends Er. Bal Krishna Neupane, Mr. Deepak Dhakal, Dr. Hari Krishna Neupane, Mr. Jagadish Gyawali, Dr. Jeevan Kafle, Mr. Kishor Dhungana, Mr. Narayan Panthi, Mr. Prem Prasad Poudel, and Mr. Youb Raj Gaire deserve special

gratitude for their encouragements and valuable suggestions. I am thankful to Mr. Shyam Shrestha for providing stationery goods.

I am extremely grateful to my father, Mr. Gopal Singh Bhandari, and mother, Late Mrs. Kalasa Devi Bhandari, for their love, prayers, care, and sacrifices in educating and preparing me for my future. My wife, Mrs. Kopila Khatri, deserve special thanks for her love, understanding, prayers, and unwavering support to accomplish this research project. My son, Mr. Eelesh Bhandari, and my daughter, Ms. Eenaya Bhandari, whose adorable smiles and giggles made me feel at ease even when I had to work hard for a long time. I also like to thank my sister-in-law, Mrs. Amita Khatri, and niece, Ms. Manisha Dhama, for their help and prayers.

Mr. Arun Kumar Bhandari, Chief Executive Director, Everest Engineering College, who is not only my elder brother but also a guardian for me, deserves special recognition for his love, care, support, and keen interest in seeing this dissertation through to completion.

Finally, I would like to express my gratitude to Everest Engineering College (EEC), Sanepa, Lalitpur, Nepal, for funding my research project and the Institute of Engineering, Purwanchal Campus, Dharan, Nepal, for giving paid vacation throughout my Ph. D. study.

Indra Bahadur Bhandari
April 2023

ABSTRACT

Alloys are produced by combining two or more metals, and they often develop from their liquid states. Only a small number of metals are used in their pure form; the majority of applications use alloys instead because they have distinctive qualities above and beyond those of the component metals. In the study of liquid science, it is essential to comprehend the properties of liquid alloys because most solid alloys are produced by cooling them from the corresponding liquid states. Liquid alloys are regarded as disordered materials because they lack long-range atomic or magnetic organization. Because disordered materials show a wide range of atomic configurations, this topic is of significant interest to both theoretical and experimental researchers. They have long sought to comprehend the anomalies in the mixing properties of liquid alloys in order to fully comprehend alloying behavior. Theoretical methods can reduce the amount of time and effort necessary and are quite useful in forecasting the mixing properties. So, we have created focused on a theoretical model to study how alloys behave when they are molten. Commonly, the effectiveness of binary alloy is assessed based on observed thermo-physical characteristics that depart from the ideal mixing state. Departures from ideality manifest as asymmetries in thermodynamic and structural characteristics away from equiatomic composition and are typically attributed to one or more of the following: the size effect, different electronegativity, interactions between solute and solvent atoms, complex formation, or a combination of these factors. The binary liquid alloys can be divided into two categories symmetric and asymmetric, based on the symmetry of the curves reflecting the thermodynamic and microscopic functions.

Numerous theoretical approaches have been devised and implemented to examine the thermodynamic and structural properties of binary systems. The Complex Formation Model (CFM) is founded on a fundamental theoretical model. This model makes it possible to express the energetics of a system in terms of the interaction parameters that reproduce the system's thermodynamic properties, as well as the ordering and phase separation processes that are observed in liquid binary alloys. The CFM makes the assumption that, if compounds are formed in the solid state at one or more stoichiometric compositions, then it follows that they are very likely to exist in the liquid state at those same compositions. The alloying behavior of binary solutions can be investigated by making the assumption that complexes are present near to melting points. The molten alloy is considered to be composed of a ternary mixture of A and B atoms, as well as a number of chemical complexes A_pB_q in chemical equilibrium with one another. In this case, p and q are both pairs of small integers that stand for stoichiometric indices of the

complex.

In the present work, we have examined and explained the mixing behavior of two liquid binary alloys based on Bi, such as Bi-Mg at 975 K and Bi-Pb at 700 K, as well as two In-based alloys, such as Cu-In at 1073 K and In-Pb at 673 K, using the CFM framework. For the aforementioned liquid alloys at a given temperature, the thermodynamic properties, such as free energy of mixing (G_M), enthalpy of mixing (H_M), and entropy of mixing (S_M), structural properties, such as concentration fluctuation in long wave length limit ($S_{cc}(0)$) and chemical short range order parameter (α_1), and transport property, such as ratio of diffusion coefficients (D_M/D_{id}), have been examined. We have calculated the interaction energy parameters (Ψ_{ij} , $i, j = 1, 2, 3$, $i \neq j$), the energy of complex formation (χ), and the number of complexes (n_3) for this purpose. These parameters are used to compute the free energy of mixing (G_M/RT) for each system. Enthalpy of mixing (H_M/RT) and entropy of mixing (S_M/R) have been calculated using these parameters and their temperature coefficients ($\partial\Psi_{ij}/\partial T$ and $\partial\chi/\partial T$). Comparing the thermodynamic characteristics of the selected systems, it can be seen that they are in very well agreement with the experimental data reported in the literature. The Bi-Mg system is the most interactive, followed by the Cu-In and Bi-Pb systems, according to a comparison of structural properties ($S_{cc}(0)$ and α_1), the ratio of diffusion coefficients (D_M/D_{id}), using the same interaction parameters, and thermodynamic properties. The analysis of these mixing characteristics in the In-Pb liquid alloy, however, shows that segregation does occur in this alloy.

We have also used the Budai-Benko-Kaptay (BBK) model to study the viscosity (η) of the selected liquid alloys. For the liquid alloys of Bi-Pb and In-Pb, symmetric viscosity isotherms have been reported; however, Bi-Mg and Cu-In exhibit asymmetry. Within the framework of the updated Butler model, the surface properties of the aforementioned binary alloys, such as surface concentration (c_i^s) and surface tension (σ), have been investigated. Theoretical analyses show that the component in binary liquid alloys whose surface concentration values are higher than the corresponding ideal values segregates across the surface.

It is found that the interaction parameters depend on temperature rather than concentration. To optimize the values of interaction parameters at high temperatures, temperature coefficients and their values at a certain temperature are used. The mixing characteristics of Bi-Pb liquid alloys at 900 K, 1100 K, 1300 K, and 1500 K have been investigated using these optimized values of interaction parameters. The compound-forming propensity of binary liquid systems diminishes with increase in temperature, according to the high temperature investigation of Bi-Pb liquid alloy. The properties of binary liquid alloys at the needed temperature can be carried using this expanded CFM, which is expected to be highly helpful in future work.

केही मिश्रण बनाउने binary तरल मिश्रहरू (Bi-Pb, Cu-In आदि) को मिसिने व्यवहारको अध्ययन

शोधसार

मिश्र दुई वा दुई भन्दा वढी धातुहरू संयोजन गरेर उत्पादन गरिन्छ र तिनीहरू प्राय तरल अवस्थाबाट बनाइन्छ । केवल थोरै संख्यामा शुद्ध धातुहरू प्रयोग गरिन्छ, धेरै जसो applications मा मिश्रहरू प्रयोग हुन्छन किनकि तिनीहरूसंग शुद्ध धातुहरूको भन्दा विशिष्ट गुणहरू हुन्छन् । तरल विज्ञानको अध्ययनमा तरल मिश्रका गुणहरू बुझ्नु आवश्यक छ किनकि धेरै ठोस मिश्रहरू सम्बन्धित तरल मिश्रहरूबाट चिसो गरेर उत्पादन गरिन्छ । तरल मिश्रलाई अव्यवस्थित पदार्थको रूपमा लिइन्छ किनकि यिनीहरूमा लामो दुरीको आणविक वा चुम्बकीय संगठनको अभाव छ । यिनीहरूमा धेरै किसिमको आणविक संरचना हुन्छ त्यसैले यो विषय सैद्धान्तिक तथा प्रयोगात्मक अनुसन्धान कर्ताहरूको लागि महत्वपूर्ण चासोको विषय छ। अनुसन्धानकर्ताहरूले लामो समयदेखि तरल मिश्रको मिसिने गुणहरूमा हुने anomalies हरु बुझ्न खोजेका छन् ताकि मिश्रको गुणहरूलाई पूर्ण रूपमा बुझ्न सकियोस । सैद्धान्तिक विधिहरूबाट थोरै समय र प्रयासमा मिश्रको गुणहरू अनुसन्धान गर्नमा उपयोगी हुने भएकोले हामीले सैद्धान्तिक विधिबाट अध्ययन गरेका छौ । Binary मिश्रको गुणहरू र प्रभावकारिता अध्ययन गर्न thermophysical विशेषताहरूको आधारमा मूल्यांकन गरिन्छ जुन ideal मिश्रबाट फरक पर्ने गुणहरूको आधारमा हुन्छ र यी फरक पर्ने गुणहरूको कारणमा निम्न मध्ये एक वा बढीलाई श्रेय दिइन्छ आकार प्रभाव, electronegativity को फरक, घोलक र घुलित बिचको अन्तरक्रिया, complex बन्ने स्थिति वा यी कारकहरूको संयुक्त अन्तरक्रिया । Thermodynamic र microscopic गुणहरूको रेखाचित्रको आधारमा binary तरल मिश्रलाई symmetric र asymmetric वर्गमा विभाजन गर्न सकिन्छ । Binary मिश्रहरूको thermodynamic र संरचनात्मक गुणहरूको अध्ययन गर्न धेरै सैद्धान्तिक विधिहरू बनाइएको र कार्यान्वयन गरिएको छ । जसमध्ये complex formation model (CFM) एक आधारभुत सैद्धान्तिक विधिको रूपमा स्थापित छ । यो model बाट thermodynamic प्रयोगात्मक data हरु प्रयोग गरी interaction parameter हरु पत्ता लगाइन्छ र मिश्र बन्ने वा नबन्ने कुराको निश्चित गर्न सकिन्छ । CFM को अनुसार यदि यौगिक हरु एक वा वढी stoichiometric concentration मा ठोस पदार्थको रूपमा बन्न सक्छ भने त्यही concentration मा तरल अवस्थामा पनि बन्न सक्छ । binary मिश्रहरूको अध्ययन तिनीहरूको पग्लिने तापक्रममा गरिएको छ । CFM ले तरल मिश्रलाई A तत्व, B तत्व र A_pB_q पदार्थको ternary मिश्रको रूपमा मानेको छ जहाँ तिनीहरू एक आपसमा रासायनिक सन्तुलनमा हुन्छन । यहाँ p र q दुवै साना पूर्णांकहरू हुन जुनले stoichiometric सूचकांक जनाउँछन।

यो अध्यायमा CFM प्रयोग गरी Bismuth मा आधारित दुईवटा Bi-Mg र Bi-Pb तरल binary मिश्रको अध्ययन 975 K र 700 K मा गरेका छौं । साथै दुईवटा Indium मा आधारित Cu-In र In-Pb मिश्रहरूको अध्ययन 1073 K र 675 K मा गरेका छौं । यस उद्देश्यको लागि, हामीले interaction energy parameters (Ψ_{ij} , $i, j=1, 2, 3, i \neq j$), formation energy of complex (χ) र complex number (n_3) निर्धारण गरेका छौं। यी parameter हरु प्रयोग गरी माथि उल्लेखित प्रत्येक मिश्र हरुको free energy of mixing (G_M/RT) निकालिएको छ। यी प्यारामिटरहरू सँगै तिनीहरूका temperature coefficients ($\partial\Psi_{ij}/\partial T$ र $\partial\chi/\partial T$) प्रयोग गरी मिश्रणको enthalpy of mixing (H_M/RT) र entropy of mixing (S_M/R) को अध्ययन गरिएको छ। CFM प्रयोग गरी हामीले गरेको अध्ययन पूर्व प्रकाशित प्रयोगात्मक अनुसन्धानसँग मेल खाएको छ । संरचनात्मक गुणहरू जस्तै concentration fluctuation at long wave length limit ($S_{cc}(0)$) chemical short order parameter (α_1) transport properties जस्तै diffusion coefficient (D_M/D_{id}) हरुको अध्ययन उहाँ interaction parameter हरुको प्रयोग गरी गरिएको छ । हाम्रो अध्ययन अनुसार Bi-Mg मिश्र सबैभन्दा interactive हो र त्यसपछिको interactive मा Cu-In र Bi-Pb क्रमशः पर्दछन । यसै अध्ययनले In-Pb को मिश्र चाहिँ नबन्ने देखाउँदछ । चुनिएका मिश्रहरूको viscosity को अध्ययन Budai-Benko-Kaptay (BBK) विधिबाट अध्ययन गरिएको छ । Bi-Pb र In-Pb को लागि viscosity को graph symmetric पाइयो भने Cu-In र Bi-Mg को चाहिँ asymmetric पाइयो । Surface concentration र surface tension को अध्ययन George-Kaptay ले परिमार्जन गरेको Butler model बाट गरिएको छ । यो अध्ययनको अनुसार जुन तत्वको surface concentration सम्बन्धित bulk concentration भन्दा बढी हुन्छ त्यो तत्व मिश्रको सतहमा segregate हुन्छ । Interaction parameter हरु concentration मा निर्भर हुँदैनन्तर तापक्रममा चाँहि हुन्छन । हामीले CFM लाई विस्तार गरी Bi-Pb मिश्रको लागी interaction parameter हरुको मान उच्च तापक्रमहरू जस्तै 900 K, 1100 K, 1300 K र 1500 K को लागी पत्ता लगायो र Bi-Pb मिश्रको गुणहरू यी तापक्रमहरूमा अध्ययन गर्यो । यो अध्ययन अनुसार तापक्रम बढाउँदा binary मिश्रहरू बन्ने प्रवृत्ति घट्दै जाने देखिन्छ । विस्तारित CFM प्रयोग गरी आवश्यक तापक्रममा गर्न सकिने यो अध्ययन भविष्यको कामका लागि अत्याधिक सहयोगी हुने विश्वास गरिन्छ ।

LIST OF ACRONYMS AND ABBREVIATIONS

BBK	:Budai-Benko-Kaptay Model
CFM	:Complex Formation Model
FVM	:Free Volume Model
LCG	:Local Composition Guggenheim's Equation
LSG	:Local Surface Guggenheim's Equation
QCA	:Quasi Chemical Approximation
QLT	:Quasi Lattice Theory
RASM	:Regular Associated Solution Model
RKPM	:Redlich-Kister Polynomial Method
RST	:Regular Solution Theory
SAM	:Self Association Model
SRO	:Short Range Order
SSM	:Simple Statistical Model

LIST OF SYMBOLS

a_i	:Activity of i^{th} Component
a_i^b	:Activity of Component i in the Bulk Phase
a_i^s	:Activity of component i in the surface phase
A, B	:Components of a binary liquid alloy
$A - B$:Type of binary liquid alloy
$A_p B_q$:Type of complex
c	:Bulk concentration of the component A in the alloy
c_i^s	:Surface concentration of i^{th} component in the alloy
C_p^{XS}	:Excess heat capacity
d_i	:Diameter of the space that an atom occupies in meter
D_M/D_{id}	:Ratio of mutual to intrinsic diffusion coefficient
E_i	:Activation energy of viscous flow for pure liquid i in J/mol
G	:Total Gibbs free energy before mixing
G'	:Free energy of mixing of the ternary mixture of A , B , and $A_p B_q$
$G_i^{(0)}$:Chemical potential per atom of species i in its unmixed form
G_M	:Free energy of mixing
G_M^{ideal}	:Ideal value of G_M
G_M^{XS}	:Excess Gibb's free energy of mixing
$G_i^{XS,b}$:Partial excess free energy of the components in bulk
$G_i^{XS,s}$:Partial excess free energy of the components in the surface
H_M	:Enthalpy of mixing
\vec{k}_1	:Initial wave vector
\vec{k}_2	:Final wave vector
k_B	:Boltzmann constant
n_1	:Number of A components
n_2	:Number of B components
n_3	:Number of $A_p B_q$ complexes
n_{AA}	:Number of $A - A$ interactions
n_{BB}	:Number of $B - B$ interactions
n_{AB}	:Number of $A - B$ interactions
N_{AV}	:Avogadro number
p, q	:Stoichiometry indices of complex
R	:Molar gas constant
$\vec{R}_j(t)$:Position operator of the atom j at time t

$S_{cc}(0)$:Concentration fluctuation in long wavelength limit
$S_{cc}(\vec{q})$:Concentration-concentration structure factor
$S_{Nc}(\vec{q})$:Number-concentration structure factor
$S_{NN}(\vec{q})$:Number-number structure factor
$S_{cc}^{(ideal)}(0)$:Ideal value of $S_{cc}(0)$
S_i	:Monolayer surface area of component i ($i = A$ or B)
S_M	:Entropy of mixing
S^{XS}	:Excess entropy of mixing
T	:Working temperature
$T_{m,i}$:Melting point of pure liquid metal i in Kelvin
u	:Coordination fraction
V_i	:Molar volume of liquid metal i at its melting point in m^3/mol
$W_j(q)$:Pseudo-potential matrix element of the ion j in the alloy
Y^∞	:Infinite dilute activity coefficients
z	:Coordination number
α_1	:Chemical short range order parameter
χ	:Formation energy of the complex
$\partial\chi/\partial T, \partial\Psi_{ij}/\partial T$:Temperature coefficients of χ and Ψ_{ij} respectively
δ	:Dilation factor
$\Delta_c U_i$:Cohesion energy of the liquid metal
Δz_i	:Number of broken bonds that occur during viscous flow
η	:Viscosity of binary liquid alloy
γ_i	:Activity coefficient of i^{th} component
Γ_{AB}	:Nearest neighbor correlation parameter
$\Gamma(\vec{k}, \omega)$:Function which determines the scattering of an electron from the initial wave vector state \vec{k}_1 to the final wave-vector state \vec{k}_2 in the alloy
Ψ_{ij} ($i, j = 1,2,3, i \neq j$)	:Interaction energy parameters
σ	:Surface tension of binary liquid alloy
σ_A	:Surface tension of pure component A
σ_B	:Surface tension of pure component B
Υ_i^b	:Activity coefficient of component i in the bulk phases
Υ_i^s	:Activity coefficient of component i in the surface phases

LIST OF TABLES

	Page No.
Table 1: Stoichiometric indices and interaction parameters.	70
Table 2: Temperature coefficient values for the interaction parameter	72
Table 3: Input activity data for the calculation of experimental $S_{cc}(0)$ (Hultgren et al., 1973)	76
Table 4: Input parameters for calculation of viscosity (Brandes & Brook, 2013).	79
Table 5: Excess bulk free energies of the components of the alloys in corresponding alloys (Hultgren et al., 1973)	81
Table 6: Input parameters for calculation of surface tension (Brandes & Brook, 2013).	81
Table 7: Interaction energy parameters at higher temperatures.	85

LIST OF FIGURES

	Page No.
Figure 1: Schematic diagram of substitutional and interstitial alloys (Dossett & Boyer, 2006).	4
Figure 2: Free energy of mixing ($G_M(RT)^{-1}$) versus concentration of Pb (C_{Pb}) for Pb-Sb liquid alloy at 905 K (Bhandari, Panthi, & Koirala, 2021b).	5
Figure 3: Free energy of mixing ($G_M(RT)^{-1}$) versus concentration of Bi (C_{Bi}) for Bi-Mg liquid alloy at 975 K (Bhandari, Koirala, & Adhikari, 2021).	6
Figure 4: Illustration of (a) demixing and (b) mixing tendency in binary liquid alloys (Polak & Rubinovich, 2000).	7
Figure 5: Schematic diagram demonstrating industrial applications of the alloys.	10
Figure 6: Concentration fluctuations ($S_{cc}(0)$) for Na-Cs system (Y. Tanaka et al., 1983; Bhatia & March, 1975b; Ichikawa et al., 1974; R. N. Singh & Bhatia, 1984; Neale & Cusack, 1982; Huijben et al., 1979).	23
Figure 7: Different behaviors exhibited by $S_{cc}(0)$ (Ivanov & Berezutski, 1996; I. Koirala et al., 2014b; Novakovic et al., 2006; Adhikari, Singh, et al., 2010; Novakovic et al., 2002).	27
Figure 8: The phase diagram and the composition dependence of $S_{cc}(0)$ at 1054 K in the system Ba-Mg (Ramachandrarao et al., 1984).	28
Figure 9: Free energy of mixing ($G_M(RT)^{-1}$) versus bulk concentration for (a) Bi-Mg, (b) Bi-Pb, (c) Cu-In, and (d) In-Pb alloys at 975 K, 700 K, 1073 K and 673 K respectively.	71
Figure 10: Heat of mixing ($H_M(RT)^{-1}$) versus bulk concentration for a) Bi-Mg, b) Bi-Pb, c) Cu-In and d) In-Pb alloys at 975 K, 700 K, 1073 K and 673 K respectively.	73
Figure 11: Entropy of mixing ($S_M R^{-1}$) versus bulk concentration for a) Bi-Mg, b) Bi-Pb, c) Cu-In and d) In-Pb alloys at 975 K, 700 K, 1073 K and 673 K respectively.	74

Figure 12: Concentration fluctuation at long wavelength limit $S_{cc}(0)$ versus bulk concentration for a) Bi-Mg, b) Bi-Pb, c) Cu-In and d) In-Pb alloys at 975 K, 700 K, 1073 K and 673 K respectively.	75
Figure 13: Chemical short range order (α_1) versus bulk concentration for a) Bi-Mg, b) Bi-Pb, c) Cu-In and d) In-Pb alloys at 975 K, 700 K, 1073 K and 673 K, respectively.	77
Figure 14: Ratio of mutual and intrinsic diffusion coefficients ($D_M D_{id}^{-1}$) versus bulk concentration for a) Bi-Mg, b) Bi-Pb, c) Cu-In and d) In-Pb alloys at 975 K, 700 K, 1073 K and 673 K respectively.	78
Figure 15: Viscosity (η) versus bulk concentration for a) Bi-Mg, b) Bi-Pb, c) Cu-In and d) In-Pb alloys at 975 K, 700 K, 1073 K and 673 K respectively.	80
Figure 16: a) c_{Bi}^s versus c_{Bi} in Bi-Mg liquid alloy at 975 K. b) c_{Bi}^s versus c_{Bi} in Bi-Pb liquid alloy at 700 K. c) c_{Cu}^s versus c_{Cu} in Cu-In liquid alloy at 1073 K. d) c_{In}^s versus c_{In} in In-Pb liquid alloy at 673 K.	83
Figure 17: Surface tension (σ) versus bulk concentration for a) Bi-Mg, b) Bi-Pb, c) Cu-In and d) In-Pb alloys at 975K, 700K, 1073K and 673K respectively.	84
Figure 18: Compositional dependence of free energy of mixing ($G_M(RT)^{-1}$) in liquid Bi-Pb alloy at different temperatures.	85
Figure 19: Compositional dependence of $S_{cc}(0)$ in liquid Bi-Pb alloy at different temperatures.	86
Figure 20: Compositional dependence of SRO parameter (α_1) in liquid Bi-Pb alloy at different temperatures.	86
Figure 21: Compositional dependence of ratio of mutual and intrinsic diffusion coefficients (D_M/D_{id}) versus concentration of Bismuth (c_{Bi}) in the liquid Bi-Pb alloy at different temperatures.	87
Figure 22: Compositional dependence of viscosity (η) of liquid Bi-Pb alloy at different temperatures.	87
Figure 23: Compositional dependence of surface concentration of Bismuth (c_{Bi}^s) versus concentration of Bismuth (c_{Bi}) in the liquid Bi-Pb alloy at different temperatures.	88
Figure 24: Compositional dependence of surface tension (σ) of liquid Bi-Pb alloy at different temperatures.	88

TABLE OF CONTENTS

	Page No.
Declaration	i
Recommendation	ii
Letter of Approval	iii
Acknowledgements	iv
Abstract	vi
List of Abbreviations	x
List of Symbols	xi
List of Tables	xiii
List of Figures	xiv
CHAPTER 1	1
1. INTRODUCTION	1
1.1 Background of Alloys	1
1.2 General Methods of Preparation of Alloys	2
1.3 Classifications of Alloys	4
1.3.1 Substitution and interstitial alloys	4
1.3.2 Symmetric and asymmetric alloys	4
1.4 Mixing Behavior of Binary Liquid Alloys	6
1.5 Significance of Research Work	6
1.6 Motivation	9
1.7 Objectives	12
1.8 Outline of Thesis	12
CHAPTER 2	14

2. LITERATURE REVIEW	14
2.1 Background of Structure Factors	14
2.2 Review and Technical Description of $S_{cc}(0)$	16
2.3 Literature Methods	17
2.3.1 Complex formation model (CFM)	17
2.3.2 Quasi chemical approximation (QCA)	19
2.3.3 Quasi lattice theory (QLT)	24
2.3.4 Regular associated solution model (RASM)	25
2.3.5 Simple statistical model (SSM)	29
2.3.6 Self-association model (SAM)	30
2.3.7 Redlich-Kister polynomial method (RKPM)	35
 CHAPTER 3	 37
3. MATERIALS AND METHODOLOGY	37
3.1 Thermodynamic Properties	38
3.2 Structural Properties	48
3.3 Transport Properties	59
3.4 Surface Properties	64
 CHAPTER 4	 69
4. RESULTS AND DISCUSSION	69
4.1 Thermodynamic Properties	69
4.2 Structural Properties	74
4.3 Transport Properties	77
4.4 Surface Properties	80
4.5 Temperature Dependent Behavior of Binary Liquid Alloys	84
 CHAPTER 5	 89
5. CONCLUSION AND RECOMMENDATIONS	89
5.1 Conclusion	89
5.2 Recommendations for Future Work	93
 CHAPTER 6	 95
6. SUMMARY	95
6.1 Summary	95
 REFERENCES	 98

APPENDIX

CHAPTER 1

INTRODUCTION

1.1 Background of Alloys

In general, a single crystal of highly pure metal is soft and flexible. Because this may not be desired, most metals are utilized in the form of alloys. The word “alloy” comes from the Latin word “alligare”, which means “to bond to” (Matson & Orbaek, 2013). Combining a metal with other metals, nonmetals, or metalloids results in an alloy. Alloys are employed because they have unique characteristics that make them more appealing than pure metals. Some alloys, for example, have high strength, while others have low melting temperatures, are particularly corrosion resistant, or have favorable magnetic, thermal, or electrical properties (Callister & Rethwisch, 2018). Copper and zinc are used to make brass. Steel is a nonmetal alloy made up of iron and carbon. Steel is alloyed with other metals to create alloy steels; stainless steel, for example, is chromium-nickel steel. Ferrosilicon is an iron and silicon alloy. Amalgams are mercury-containing alloys (Smith, 1970). Only a few metals are utilized in their pure form; copper is used in electrical applications as pure metal, while it is used in construction applications as an alloy (Wright, 2011). A pure metal has a high electrical conductivity, whereas an alloy is typically harder and has a lesser conductivity. Chemically, pure metals are reactive. Pure metals corrode as a result of moisture and gasses in the atmosphere. Metals in alloy form, on the other hand, are more corrosion resistant. They improve the durability and usability of metals. They get a lot of tensile strength. The qualities of alloy mixtures are difficult to anticipate based on knowledge of the individual metals (Bauccio et al., 1993; Mills, 1922). Copper and nickel, for example, both have strong electrical conductivity, but they combine to make alloys with extremely low conductivity, making them useful as electrical resistance lines (Davis et al., 2001). Corrosion resistance, oxidation resistance at raised temperatures, abrasion or wear resistance, good bearing qualities, creep strength at elevated temperatures, and impact toughness are some of the other attributes that alloys can acquire to a far greater degree than pure metal (Habashi, 2008).

1.2 General Methods of Preparation of Alloys

Alloys are formed by melting the primary metal in liquid form and dissolving it in an exact proportion with another metal or metals. After that, the mixture is allowed to cool and harden. There are numerous metal alloys and their use in our daily lives. When metals are alloyed with different elements, their qualities such as corrosion resistance, conductivity, modulus of elasticity, ductility, and hardness can be improved (Dossett & Boyer, 2006). Alloys are prepared in one of following four ways (Angelo & Subramanian, 2008; Habashi, 2008):

- 1) Melting and combining the components. This is the most used method. Except for a few metals, such as iron and lead, all metals are miscible in their molten condition.
- 2) Combining and crushing the ingredients in powder form.
- 3) Electrolysis of a solution containing the components' salts.
- 4) Simultaneous reduction of component metal oxides.

When molten alloys harden, they may remain soluble in one another or may separate mechanically into intimate combinations of the pure constituent metals. Typically, partial solubility exists in the solid state, and the structure is composed of a mixture of saturated solid solutions. As a result, the behavior of metals during the alloying process is classified as follows:

Completely soluble:

After the components are melted, they form a homogeneous mixture that remains homogeneous when the alloy solidifies. The two metals combine to form a substance known as a "solid solution" or "mixed crystals" (Dossett & Boyer, 2006). The following classifications are possible:

- 1) **Solid-solution substitution:** This is the case, for example, with copper and nickel. By combining nickel and copper, new qualities are created that neither copper nor nickel alone possesses. Nickel atoms are incorporated into the crystal structure of copper. The grains of the alloy appear to be identical to those of copper. Gold and silver, silver and platinum, nickel and chromium, cobalt and chromium, and lead and antimony are further examples.
- 2) **Solid-solution addition:** This is the case, for example, with certain alloys containing boron or carbon. Due to their short atomic radius, boron and carbon can enter the metal's crystal structure in interstitial places (Dossett & Boyer, 2006).

Partially soluble:

This is the scenario when the components melt as a homogeneous mixture but solidify as two or more distinct types of grains. These are solid solutions of the two metals in varying amounts. For example, lead and tin, as well as some types of brass, a copper-zinc alloy, have this structure (Habashi, 2008).

Insoluble:

This is the circumstance where the components melt together but separate during solidification due to their insoluble nature; examples include cadmium and bismuth, as well as gold and lead. Under specific conditions, a eutectic combination with a melting point lower than both metals is formed, and when solidified, the eutectic alloy consists of an intimate mixture of fine crystals of almost pure metals (Polak & Rubinovich, 2000).

Inter-metallic compounds:

In this situation, the metals combine to generate a compound that has a different crystal and grain structure than either of the pure metals. When equal parts of calcium and magnesium are melted together and allowed to cool slowly, the crystals that initially precipitate from the liquid have the composition Ca_3Mg_4 . Numerous similar compounds are known, including MgZn_2 , CuZn , CuBe , AgCd , AuZn , LiHg_3 , and Cu_5Sn , among others (Friauf, 1927; Westbrook, 1977). While inter-metallic compounds are often hard and brittle, their presence in trace levels in an alloy is advantageous. The toughness of solid solutions is combined with the hardness of inter-metallic compounds in these alloys (Nakamura, 1995; Westbrook, 1996). The alloy is not always formed of a single phase; in most situations, it contains many phases. For instance, in an aluminum-copper alloy, a trace of copper forms a solid solution with the aluminum, while the remainder of the copper mixes with the aluminum to produce an inter-metallic compound made of two aluminum atoms and one copper atom. Thus, the aluminum-copper alloy is composed of three constituents: a significant amount of aluminum, a trace amount of copper in solid solution, and minute particles of the inter-metallic compound (Westbrook, 1977). Additionally, novel procedures for producing additional types of alloys are created, including electron-beam refining, solidification, single crystal super-alloys, and metallic glass (Habashi, 2008).

1.3 Classifications of Alloys

1.3.1 Substitution and interstitial alloys

There are three major kinds of alloys based on how the alloying element is incorporated into the metal. These are referred to as substitution alloys, interstitial alloys, and interstitial and substitutional alloys as shown in Figure 1. In substitution alloys, the parent metal's atoms are literally replaced with atoms of a similar size from another material. Brass is an example of a copper-zinc replacement alloy. In interstitial alloys, the atoms of the injected metal are arranged in the interstitial location of the original metal's crystal lattice. Interstitial and substitutional processes coexist in certain alloys (Dossett & Boyer, 2006).

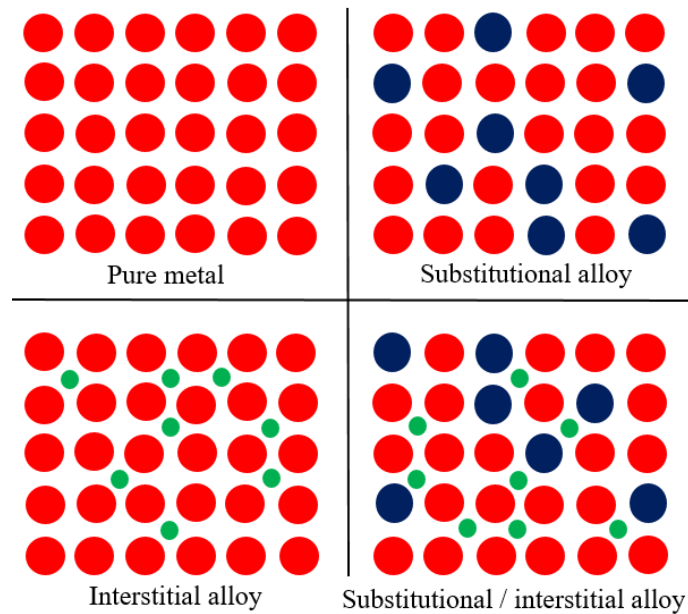


Figure 1: Schematic diagram of substitutional and interstitial alloys (Dossett & Boyer, 2006).

1.3.2 Symmetric and asymmetric alloys

The divergence of alloy properties from the ideal mixing condition is explained in terms of the energy interaction of the alloy's constituent species. As a result of the preceding, the fundamental parameter for selecting a thermodynamic alloy is the degree to which the thermodynamic characteristics of liquid alloys vary from the ideal values (Adhikari, 2018). An alloy can be classified as a compound forming liquid alloy (hetero-coordinated) or a segregating (homo-coordinated) system based on its divergence from ideal thermodynamic parameters. Departures from ideality are visible as asymmetries in thermodynamic properties away from equiatomic composition and are typically attributed to one of the following factors: size effect, differences in electronegativity,

interactions between solute and solvent atoms, or a combination of these factors (Novakovic et al., 2011; Adhikari, 2011; I. Koirala et al., 2014b). The industrial applications of liquid alloys could also provide a strong basis for further research. In terms of the symmetry of the curves representing thermodynamic functions G_M , H_M , S_M , and so on, the binary liquid alloys can be divided into two groups: symmetric and asymmetric. This class includes binary liquid alloys such as K-Na, Fe-V, Fe-Ti, Al-Ga, Al-Ge, Si-Ti, Al-Mn, In-Pb, In-Sn and so on (Akinlade & Boyo, 2004; Rafique & Kumar, 2007; Novakovic et al., 2008; Anusionwu, Adebayo, & Madu, 2009; Awe et al., 2011; Adhikari et al., 2012b; I. Koirala et al., 2013; R. P. Koirala, Kumar, et al., 2014; Gohivar, Yadav, et al., 2020). Figure 2 depicts the compositional dependency of free energy of mixing in liquid Pb-Sb alloys at 905 K, which represent symmetric binary liquid alloys. The experimental data are taken from literature (Hultgren et al., 1973). Whereas in the later class of alloys, the thermodynamic functions are not symmetric at equiatomic composition, hence their extremum values are found at different stoichiometric compositions. Binary liquid alloys such as Cd-Na, Pb-Te, Bi-Mg, Cu-Mg, Cd-Hg, Cu-Sn, Al-Sn etc are classified as asymmetric (Akasofu et al., 2020; Shrestha, Singh, Jha, Singh, & Adhikari, 2017; Adhikari, Singh, et al., 2010; Bhandari, Koirala, & Adhikari, 2021; Godbole et al., 2004; I. Koirala et al., 2015; Panthi et al., 2021). Figure 3 depicts the compositional dependence of the Gibbs free energy of mixing of Bi-Mg liquid alloy at 975 K, which represents the asymmetric class of alloy.

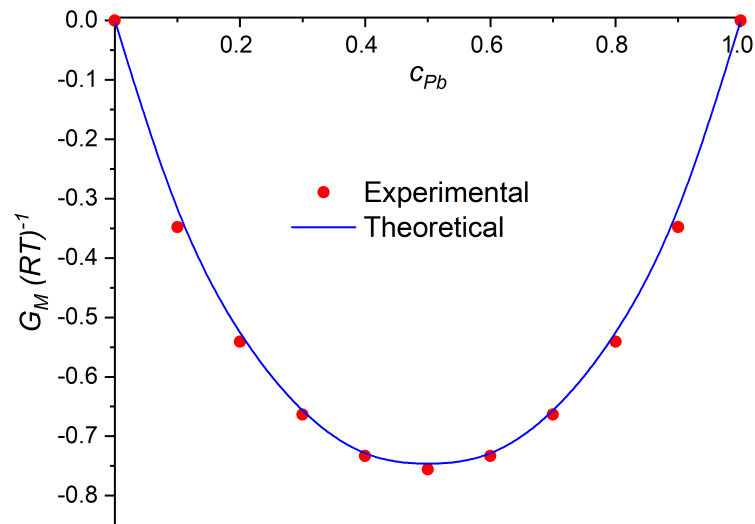


Figure 2: Free energy of mixing ($G_M(RT)^{-1}$) versus concentration of Pb (C_{Pb}) for Pb-Sb liquid alloy at 905 K (Bhandari, Panthi, & Koirala, 2021b).

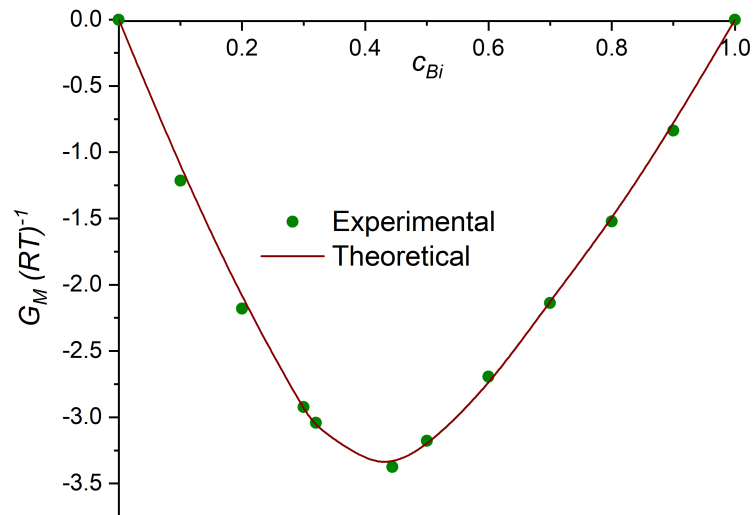


Figure 3: Free energy of mixing ($G_M(RT)^{-1}$) versus concentration of Bi (C_{Bi}) for Bi-Mg liquid alloy at 975 K (Bhandari, Koirala, & Adhikari, 2021).

1.4 Mixing Behavior of Binary Liquid Alloys

The mixing behavior of two metals that combine to produce binary alloys is a result of the interaction of energetic and structural reorganization of the constituent atoms. When A and B atoms are mixed, they can either prefer to remain self-coordinated, forming A-A or B-B pairs, or they can develop a strong interaction between dissimilar atoms, forming hetero-coordinated A-B pairings. All liquid binary alloys can be classified into two broad categories based on their deviations from the additive rule of mixing (Raoult's law): segregating (positive deviation) and ordering or short-range ordered (negative deviation) alloys (B. P. Singh et al., 2014; Bhatia & Hargrove, 1974; Novakovic et al., 2008; R. N. Singh & Sommer, 1997; R. N. Singh, 1987; Adhikari et al., 2012a; Bhatia & Singh, 1984). However, some liquid alloys do not fall neatly into either of the preceding two categories. For example, the excess Gibbs energy associated with mixing G_M^{XS} for Ag-Ge and Cd-Na is negative in some compositions but positive in others (R. N. Singh & Sommer, 1997). Additionally, in liquid alloys such as Au-Bi, Bi-Cd, and Bi-Sb, the enthalpy of mixing (H_M) is a positive value, whereas G_M^{XS} is a negative value. Bi-Pb possesses positive H_M and G_M^{XS} values in the solid phase, but negative values in the liquid phase. Additionally, some systems, such as Au-Ni and Cr-Mo, exhibit immiscibility in the solid phase that is not readily apparent in the liquid phase (R. N. Singh & Sommer, 1997).

1.5 Significance of Research Work

To build new alloys and improve existing ones, it is necessary to have a detailed understanding of the thermodynamic variables of the constituent systems. To completely

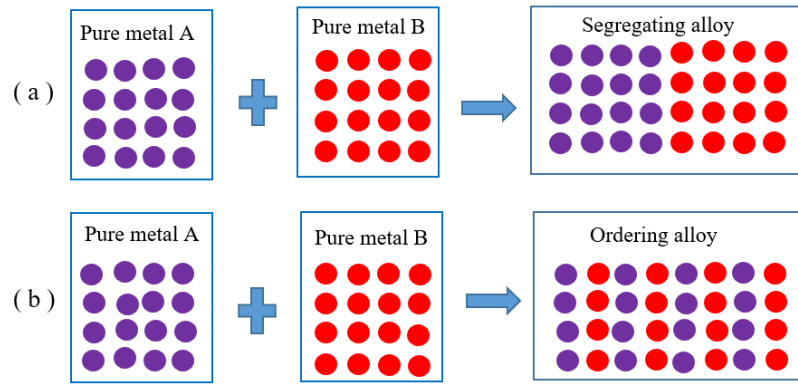


Figure 4: Illustration of (a) demixing and (b) mixing tendency in binary liquid alloys (Polak & Rubinovich, 2000).

grasp the observed behaviors, it may be necessary to have a thorough theoretical understanding of the structural readjustment and energy preferences of atoms in binary liquid metallic systems, in addition to an understanding of the empirical metallurgical structures (Anusionwu, 2003; R. N. Singh & Sommer, 1992a; Ogundeji et al., 2021; Awe et al., 2011). These advancements have been made possible by integrating a number of easy theoretical tools or models for explaining deviations and anomalies in terms of hetero- or self-coordination species that can exist in liquid. Understanding the properties of liquid alloys is critical in the study of liquid science, as the majority of solid alloys are created through cooling from their respective liquid states. Though our everyday experience attests to the division of matter into three distinct classical phases: solid, liquid, and gas. Solids are hard and produce clear Bragg reflections when investigated by diffraction. Diffraction tests have demonstrated that liquids in general, and metallic liquids in particular, exhibit some form of short-range order (SRO), indicating the absence of long-range order among the atoms or molecules (R. N. Singh, 1987; Bhatia & Singh, 1982a; Müller, 2003; Sommer, 1990). To model the thermodynamic, structural, and surface properties of liquid binary alloys and liquid metals, it is necessary to know their structures and the relevant forces that quantify inter-atomic interactions. This is why many physicists, chemists, and metallurgists have been studying the mixing behavior of two elemental metals producing a binary alloy (Akinlade et al., 1998; Kaban et al., 2003; Adhikari, 2011; Arzpeyma et al., 2013; I. Koirala, 2018; Ogundeji et al., 2021; Bhandari, Panthi, Gaire, & Koirala, 2021). Numerous theoretical approaches have been developed and applied to the study of binary systems thermodynamic and structural features. Several of these models include the complex formation model (Bhatia & Hargrove, 1974; A. K. Mishra et al., 1994; Akinlade & Boyo, 2004; Prasad et al., 2007; Novakovic et al., 2012, 2016; Bhandari, Panthi, & Koirala, 2021a), the electron theory (Ashcroft & Stroud, 1978), and the ab-initio methods (Jank & Hafner, 1988; Kresse & Hafner, 1993), which involve the computation of thermodynamic quantities using the pseudo-potential

formalism. The first is based on a basic theoretical model that enables the energetic of a system to be expressed in terms of the interaction parameters that reproduce its thermodynamic properties, as well as the ordering and phase separation processes observed in liquid binary alloys. Additionally, thermophysical features such as surface tension (Butler, 1932; Mekler & Kaptay, 2008; Kaptay, 2019), viscosity (Ganesan et al., 1987; Kaptay, 2005b; Budai et al., 2005, 2007; R. N. Singh & Sommer, 2012), and chemical diffusion (R. N. Singh & Sommer, 1997, 1998) can be defined. The purpose of this work is to investigate the complex formation propensity and mixing behavior of two binary liquid alloys based on Bi (Bi-Mg and Bi-Pb) and two binary liquid alloys based on In (Cu-In and In-Pb) using theoretical models. The liquid alloys examined have been discovered to have a wide variety of applications in a variety of fields. Lead alloys such as Bi-Pb and In-Pb are primarily used in lead-acid ammunition batteries, cable sheathing, sheet, pipe, and solder construction, bearings, gaskets, special castings, anodes, fusible alloys, shielding, and weights. Due to lead alloys' corrosion resistance, their applications are also linked to the production of a protective corrosion coating (Ilinčev, 2002). Despite their numerous beneficial applications, lead and its compounds are compounded poisons and should be handled with caution. These compounds should not be included in diets or other consumables (Fratesi et al., 1984). In-Pb alloys are often recommended as alternative solders for soldering gold since they do not easily leach or dissolve the metal. Additionally, due to their low melting points, In-Pb alloys are employed as contact alloys for metal-glass or metal-ceramic contacts (Minic et al., 2001; Deloffre et al., 2004; Yu et al., 2006). Because elemental Pb and In are difficult to volatilize, data collected at elevated temperatures are sufficiently realistic, making it beneficial to research the characteristics of In-Pb melts. Lead-bismuth alloys are advantageous due to their corrosion resistance and wear resistance (Barbin et al., 2013). Lead-bismuth alloys are being investigated as a possible heat transfer medium for nuclear power plants (Klement Jr, 1963; Kurata et al., 2002). The Bi-Mg system is intriguing theoretically because it forms the stable inter-metallic complex Bi_2Mg_3 (Bhatia & Hargrove, 1974). Bi_2Mg_3 in liquid form is a well-known example of a liquid semiconductor with a conductivity of $45 \text{ ohm}^{-1}\text{cm}^{-1}$. Binary Bi-Mg systems are also fascinating for high temperature magnesium alloys. Magnesium alloys have generated considerable interest in the automotive and aerospace industries recently due to their low density in comparison to aluminum and steel alloys. Sn, Si, Sb, and Bi are being evaluated as alloying elements for the development of novel magnesium alloys for use in high-temperature applications (Jung et al., 2007; Paliwal & Jung, 2009). Additionally, the Bi - Mg alloys may be used as phase change materials for thermal energy storage (Chunju et al., 2012; Fang et al., 2016). Cu-In are potential candidates for Pb-free solders in electronic packaging, which are gaining traction in the industry in response to the growing demand for environmental protection (Liu et al., 2002). The primary

objective of this work was to synthesize experimental and theoretical data in order to establish a reasonable understanding between experimental results and theoretical approaches via a theoretical determination of a few binary liquid alloys' thermodynamic, structural, and transport properties. One objective was to deduce the role of enthalpic as well as entropic effects on mixing, which is presented within the context of the complex formation model. The two effects compete for control of the system's degree of segregation/ordering. This has been investigated further in light of what is known about surface and transport properties. R. N. Singh & Sommer (1992b) notified that the inter-atomic pair potentials found in first principle theory have a clear relationship with the order energy found as a free parameter in the complex formation model. These models are then extended to predict the properties indicated previously at elevated temperatures

1.6 Motivation

Alloys have an unlimited number of uses in a variety of fields, including medical, military, commercial, industrial, residential, manufacturing, and scientific research. Figure 5 demonstrates some of the industrial applications of alloys. The various categories of liquid alloys are categorized according to their intended use. Bearing alloys are utilized for metals that come into contact with another surface when compressed (Clarke & Sarkar, 1979; Kostrivas & Lippold, 1999; Marrocco et al., 2006; Equey et al., 2011). Certain alloys are resistant to corrosion due to their noble metal composition (Porter, 1994; Ghali, 2010; Akimoto et al., 2018). The precious-metal alloys are one of these (Baran & Woodland, 1981; Givan, 2014). Other alloys are resistant to corrosion due to the formation of a protective oxide film on the metal surface (Shih et al., 2000; Ruzankina & Vasiliev, 2016). Dental alloys based on silver amalgam are composed primarily of silver and contain trace amounts of tin, copper, and zinc for hardening purposes. Dental alloys based on gold are favored over pure gold due to gold's greater softness (Knosp et al., 2003; Von Fraunhofer, 2013). Die-Casting alloys have low enough melting points that they may be injected under pressure into steel dies in their liquid state (Wang et al., 1995). These castings are employed in the manufacture of vehicle components as well as office and domestic equipment with relatively complex shapes (Vinarcik, 2002). Fusible alloys are a class of alloys with melting temperatures lower than that of tin (232°C). The majority of these materials are mixtures of metals with low melting points, including tin, bismuth, and lead. Fusible alloys are used as solder, in safety sprinklers that automatically spray out water when the alloy melts due to the heat of a fire, and in fuses that interrupt an electrical circuit when the current exceeds a certain threshold (Schwartz, 2002, 2014). In power plants, jet engines, and gas turbines, high-temperature or refractory alloys with high strengths at elevated temperatures are required. Furthermore, these alloys are resistant to oxidation caused by fuel-air combinations and steam

(R. Tanaka, 2000; Muktinutalapati, 2011).



Figure 5: Schematic diagram demonstrating industrial applications of the alloys.

Both nickel-base and cobalt-base alloys, collectively referred to as super alloys, are capable of performing useful activities at temperatures from 800 to 1100°C (Reed, 2008). Metals are joined together through the application of joining alloys during welding, brazing, or soldering. The brazing and soldering alloys are chosen to give a filler metal with a melting point significantly lower than the joined parts (Campbell, 2011). Light-metal alloys have become of great importance in the construction of transportation equipment and as a result of their employment, the total weight of transportation equipment has been reduced significantly. Aircraft building is one of the most common uses for light metal alloys. The majority of light alloys are made up of aluminum and magnesium, which have densities of 2.7 and 1.75 g/cm³, respectively (Polmear, 2005; Monteiro, 2014). Low-expansion alloys, such as Invar (64% Fe, 36% Ni), maintain their dimensions over the ambient temperature range (Shiga, 1996). They are particularly well-suited for use in watches and other temperature-sensitive electronics (Harner, 1994). Magnetic alloys are utilized in transformer and motor magnetic cores and must be easily magnetized and demagnetized. Silicon-ferrite is a material that is frequently utilized in alternating current applications. Permalloy (a nickel-iron alloy) and several similar cobalt-base alloys have extremely high permeability's at low field strengths and are consequently

employed in the communications industry. Cobalt and rare-earth metal alloys are used to make hard magnets (Strnat & Strnat, 1991; Hasegawa, 2001; Shokrollahi & Janghorban, 2007; Shokrollahi, 2009). Metallic glasses and meta-stable crystalline alloys may be the world's strongest, toughest, most corrosion-resistant, most easily magnetizable materials. The atomic size ratio of an alloy, its crystallization temperature and melting point, and the enthalpy of formation of compounds all affect its capacity to produce a metallic glass (Egami & Waseda, 1984; Suryanarayana & Inoue, 2017). Sterling silver is the most common precious metal alloy, comprising 92.5 percent silver and the remaining copper. Copper strengthens and hardens the alloy, making it superior than pure silver (Praiphruk et al., 2013; Ortiz-Corona & Rodriguez-Gomez, 2019). Yellow gold is an alloy of Au, Ag, and Cu with a ratio of roughly 2:1:1. White gold is an alloy containing between ten and eighteen karats of gold with the remainder of nickel, silver, or zinc (Rapson, 1990; Cretu & Van Der Lingen, 1999). Internal prostheses, i.e., surgical implants such as artificial hips and knees, are made of prosthetic alloys. The most often used prosthetic alloys are corrosion-resistant high-strength ferrous, cobalt-based, or titanium-based alloys (Semlitsch & Willert, 1980; Jovanović et al., 2007). When heated or cooled, shape-memory alloys retain their shape. This thermoelastic feature is due to the fact that when they are cooled or heated, they undergo a reversible change in crystal structure that does not involve diffusion. They are suitable for thermostats as well as couplings on hydraulic lines and electrical circuits (Van Humbeeck, 1999, 2001). At low temperatures, superconducting alloys exhibit no resistance to the flow of electric current. This feature enables advancements in technology, such as the development of powerful magnetic fields (Yao & Ma, 2021). Thermocouple alloys are extremely useful for temperature measurements ranging from 20° C to several hundreds (Pollock, 2018). Certain alloys with a wide range of applications are categorized according to their metal constituents. Aluminum, bismuth, indium, copper, zinc, tin, nickel, magnesium, titanium, chromium, silver, gold and so on alloys are employed in a wide variety of vital applications (Habashi, 2008).

Many researchers have concentrated their efforts on understanding the properties of binary liquid alloys. Some of the early initiatives were experimental in nature (Kleppa & Thalmayer, 1959; Alcock et al., 1969; Brillo et al., 2006; Arzpeyma et al., 2013; Kobatake et al., 2015), while others were more theoretical in nature (Faber & Ziman, 1965; Bhatia & Hargrove, 1974; Prasad & Jha, 2005; Awe et al., 2011; B. P. Singh et al., 2014; Shrestha, Singh, Jha, Singh, & Adhikari, 2017; Gohivar, Yadav, Koirala, & Adhikari, 2021a). Recent advancements in the use of liquid alloys and their composites in a wide range of high-temperature applications necessitate a better understanding of the thermodynamic and dynamical properties of liquid alloys to aid in the development of new alloys and the improvement of existing ones (Müller, 2003; Novakovic & Tanaka,

2006; Awe et al., 2011; R. P. Koirala, Kumar, et al., 2014). As a result, theoretical study on several binary liquid alloys at fixed and higher temperatures is currently lacking, which would provide data on thermophysical properties that may be utilized to investigate further prospects of binary liquid alloy.

1.7 Objectives

The general objective of this work is to:

study of the mixing behavior of some binary liquid alloys (Bi-Pb, Cu-In etc.)

The specific objectives of the proposed work are:

- 1) to study the thermodynamic behavior of liquid alloys (Free energy, enthalpy and entropy of mixing).
- 2) to study the structural dependence of binary liquid alloys (concentration fluctuation in long wavelength limit and chemical short range order parameter).
- 3) to study the transport properties of liquid alloys (diffusion coefficient and viscosity).
- 4) to study the surface properties of liquid alloys (surface concentration and surface tension).

1.8 Outline of Thesis

Using the complex formation model, the thermodynamic properties, including free energy of mixing (G_M), enthalpy of formation (H_M), and entropy of mixing (S_M) of Bi-Mg, Bi-Pb, In-Pb, and Cu-In binary liquid alloys have been investigated. The extended CFM is employed to examine structural features such as concentration fluctuation in long wavelength limit ($S_{cc}(0)$) and chemical short range order parameter (α_1). The model is extended to investigate the diffusion coefficient of the previously mentioned binary liquid alloys. Transport properties such as viscosity have been studied within the framework of the Budai-Benko-Kaptay (BBK) model. By using improved Butler's equation, surface properties such as surface concentration and surface tension have been investigated. The models are further expanded in order to investigate the aforementioned features of Bi-Pb liquid alloys at elevated temperatures. The study of thermo-physical properties of binary liquid alloys at different temperatures remains an active area of research in the field of material science, as it has a rising number of applications in numerous disciplines of science and industry. This study investigates the various thermophysical properties of binary liquid alloys and the degree of ordering or segregation in the chosen binary systems. In addition, a comparison is made between the theoretical results and

the available experimental results, and it is determined that the results are qualitatively in agreement.

This thesis work is organized as follows:

Chapter-1: Introduction, the chapter discusses the introduction to alloys, background of alloys, general methods of alloy preparation, types of alloys, introduction to the presented research work, and the motivation for the work.

Chapter-2: Literature review, in this part, the literature review of study of binary liquid alloys with numerous models have been presented.

Chapter-3: Material and methods, here the chapter provides the insight of fundamental concept of complex formation model, BBK model and Buttlar equation. The extension of complex formation to analyse chemical short range order parameter and diffusion coefficient has also been presented.

Chapter-4: Results and discussion, this section discusses the obtained results and their interpretations.

Chapter-5: Conclusion and recommendation, conclusions of the study and recommendations for the future work have been presented.

Chapter-6: Finally, the work is summarized.

CHAPTER 2

LITERATURE REVIEW

2.1 Background of Structure Factors

The structured characteristics of the electrical resistivity of binary alloys were examined by introducing three new structure factors: $S_{NN}(\vec{k})$, $S_{cc}(\vec{k})$ and $S_{Nc}(\vec{k})$. For liquid alloys, the approximation is precise, while for solids it is simply approximate. These structure factors were derived from the Fourier Transform of the local ion concentration and number density. In the weak scattering approximation, the function, $\Gamma(\vec{k}, \omega)$ describing the scattering of an electron from the initial wave vector state (\vec{k}_1) to the final wave vector state (\vec{k}_2) in the alloy is given by (Bhatia & Thornton, 1970).

$$\Gamma(\vec{k}, \omega) = 1/(2\pi N) \int e^{(-i\omega t)} dt \langle A^*(\vec{k}, 0) A(\vec{k}, t) \rangle \quad (2.1)$$

where N represents the total number of atoms present in the crystal and $\Gamma(\vec{k}, \omega)$ is related to the alloy's resistivity in the same way as it is in the case of pure metal (Bhatia & Gupta, 1969). Here $\hbar\omega = E_{\vec{k}_1} - E_{\vec{k}_2}$ and $\vec{k} = \vec{k}_1 - \vec{k}_2$. The function $A(\vec{k}, t)$ is defined as

$$A(\vec{k}, t) = \sum_j W_j(k) e^{(i\vec{k} \cdot \vec{R}_j(t))}. \quad (2.2)$$

Here $\vec{R}_j(t)$ is the position operator of the atom j at time t , and $A^*(\vec{k}, 0)$ is the complex conjugate of the operator ($A(\vec{k}, 0)$). The pseudo-potential matrix element ($W_j(k)$) of the ion j in the alloy is given by

$$W_j(k) = \int e^{i\vec{k} \cdot (\vec{r} - \vec{R}_j)} V_j(\vec{r} - \vec{R}_j) d^3r \quad (2.3)$$

where the term $(V_j(\vec{r} - \vec{R}_j))$ is the effective potential due to the j^{th} ion centered at (\vec{R}_j) . Equation 2.1 is simplified as (Bhatia & Thornton, 1970):

$$\Gamma(\vec{k}, \omega) = (\overline{W})^2 S_{\text{NN}}(\vec{k}, \omega) + (W_1 - W_2)^2 S_{\text{cc}}(\vec{k}, \omega) + 2\overline{W}(W_1 - W_2) S_{\text{Nc}}(\vec{k}, \omega) \quad (2.4)$$

where $W_1 = W_1(k)$, $W_2 = W_2(k)$, and $\overline{W} = cW_1 + (1 - c)W_2$.

Here, the structure factors $S_{\text{NN}}(\vec{k})$, $S_{\text{cc}}(\vec{k})$ and $S_{\text{Nc}}(\vec{k})$ are functions of their respective dynamic structure factors $S_{\text{NN}}(\vec{k}, \omega)$, $S_{\text{cc}}(\vec{k}, \omega)$, $S_{\text{Nc}}(\vec{k}, \omega)$, ω and $1/T$.

$$S_{\text{NN}}(\vec{k}) = \int \left[\frac{\beta\omega}{(\exp(\beta\omega) - 1)} \right] S_{\text{NN}}(\vec{k}, \omega) d\omega$$

here, $\beta = \hbar/k_B T$. After some simplification the expressions for structure factors are obtained as,

$$S_{\text{NN}}(\vec{k}) = N^{-1} \langle N^*(k) N(k) \rangle,$$

$$S_{\text{cc}}(\vec{k}) = N \langle c^*(k) c(k) \rangle \text{ and}$$

$$S_{\text{Nc}}(\vec{k}) = Re \langle N^*(k) c(\vec{k}) \rangle$$

Here $N(\vec{k})$ and $c(\vec{k})$ (number and concentration factors) refer to the same time and hence need not be considered as quantum operators. The asterisk denotes the complex conjugate in this case. All structure factors in liquid alloys are solely determined by the magnitude k of \vec{k} only. It is also noted that the substantial temperature dependence of an alloy's resistivity at its critical point is due to the temperature dependence of concentration fluctuations. For liquid alloys and some above the Debye temperature, these structure factors have the property that at the long wave length limit ($k \rightarrow 0$), $S_{\text{cc}}(k)$ represents the mean square fluctuation in concentration (Bhatia & Thornton, 1970).

$$S_{\text{cc}}(\vec{k}) = S_{\text{cc}}(0) = N \langle (\Delta c)^2 \rangle \quad (2.5)$$

Similarly, it was demonstrated at the long wavelength limit $k \rightarrow 0$ that (Bhatia & Thornton, 1970),

$$S_{\text{NN}}(\vec{k}) = S_{\text{NN}}(0) = \langle (\Delta N)^2 \rangle / N \quad (2.6)$$

$$S_{\text{Nc}}(\vec{k}) = S_{\text{Nc}}(0) = \langle \Delta N \Delta c \rangle \quad (2.7)$$

Here, $\langle (\Delta c)^2 \rangle$ represents the mean square fluctuation in concentration, $\langle (\Delta N)^2 \rangle$ rep-

resents the mean square fluctuation in number, and $\langle \Delta N \Delta c \rangle$ represents the correlation between the two fluctuations, Δc and ΔN . The mean square fluctuations in concentration, $\langle (\Delta c)^2 \rangle$ is defined as (Ramachandrarao et al., 1984),

$$\Delta c = \frac{c_2 \Delta N_1 - c_1 \Delta N_2}{N_{AV}} \quad (2.8)$$

where N_{AV} is the Avogadro's number, ΔN_1 and ΔN_2 correspondingly represent the fluctuation in the particle density of species 1 and 2. Further research was done on the structure factors at zero wave number and how they can be changed into thermodynamic variables (Bhatia & Hargrove, 1974). Bhatia & Thornton (1971) extended the idea of structural factor in the long wave length limit of solid alloy by taking the complete complement of stress and strain variables into consideration. Bhatia & March (1972) extended the conformal solution theory to determine the liquidus curve of the binary Na-K system with respect to the potassium atomic percentage. The formation of a complex has been confirmed with the aid of a computed phase diagram.

2.2 Review and Technical Description of $S_{cc}(\mathbf{0})$

If V_1 and V_2 are the partial molar volumes per atom of two different species, then the dilation factor is defined as

$$\delta = \frac{V_1 - V_2}{c_1 V_1 + c_2 V_2} \quad (2.9)$$

Regular solution is one in which (δ) is small ($\delta \ll 1$). For such solution with no super lattice where the difference in partial volumes of components is very small, complex formation model (CFM) or regular solution theory (RST) can be applied. When partial molar volumes V_1 and V_2 differ significantly, the Flory formula is a more accurate approximation (Bhatia & Hargrove, 1974). For this kind of solution without a super lattice

$$S_{cc}(\mathbf{0}) = \frac{c_1 c_2}{1 - 2c_1 c_2 \Psi_{12}/RT} \quad (2.10)$$

For an ideal solution $\Psi_{12} = 0$. This is the random solution, which means that the resistivity due to alloying is proportional to $c(1-c)$ and temperature independent. Hence, the long wave length limit of the partial structure factor contains direct information on the ideality and non-ideality of the mixture. It is conceivable, in principle, to collect information about the structural changes that take place as a result of alloy formation because there is a direct correlation between the atomic structure of liquid alloys and their thermodynamic properties (Bhatia et al., 1973). When a single complex is formed, the idea of $S_{cc}(\mathbf{0})$ is also used to study the thermodynamics of eutectic type liquidus curve

in a compound forming binary system (Bhatia et al., 1974; Bhatia & March, 1975a). Predel (1976) created a model that successfully describes the deviation from regular behavior of various alloy systems such as Cd-Hg, Cd-Na, and Mg-Ca. Using argon, sodium, potassium, and copper as reference liquids, Johnson et al. (1975) investigated the dependence of concentration fluctuation on wave number. On the basis of complex formation, structure factors for binary systems are obtained and used to the Li-Pb system (Bhatia & Ratti, 1975). For metal salt solutions such as Na-NaCl at 1173 K and K-KBr at 1033 K, the partial structure factor was studied as a function of concentration for small q values (Durham & Greenwood, 1976).

The above mentioned type works for a variety of binary systems have been designed and expanded to investigate their additional potential (Ratti & Bhatia, 1975; March et al., 1976; Bhatia & Ratti, 1977; Ratti & Bhatia, 1977; Swamy et al., 1977; Bhatia & March, 1978; Ratti & Bhatia, 1978; Bhatia et al., 1980; Bhatia & Singh, 1980; Alonso & March, 1982). The binary liquid alloys in different prospect have been studied by numerous researcher (Bhatia & March, 1979; Tamaki et al., 1982; Laty et al., 1978; Lee & Aaronson, 1980; Alonso & Gallego, 1985).

2.3 Literature Methods

2.3.1 Complex formation model (CFM)

Bhatia & Hargrove (1974) developed the complex formation model on the basis of conformal solution theory of Guggenheim (Guggenheim, 1952). The expressions for free energy, enthalpy, entropy, activity and concentration fluctuation in long wave length limit are presented. The model is successfully applied to Bi-Mg, Tl-Te, Cu-Sn and Ag-Al liquid alloys. The model is applied in many way by numerous researchers. In Li-Pb and Na-Pb liquid alloys, the electrical resistivity and entropy exhibit anomalous behavior as a function of concentration. This anomalous behavior is explained by the complex formation hypothesis (A. K. Mishra et al., 1990). The hetero coordination in Mg-Sn was observed by R. N. Singh, Jha, & Pandey (1993) and that in K-Te by Akinlade (1994). The mixing behavior was observed in Hg-Na and Hg-K (A. K. Mishra et al., 1994), Hg-In (Attri et al., 1995), K-Bi (Akinlade, 1996) Hg-In (Attri et al., 1996) , Al-Mg (Prasad et al., 1996), Thermodynamic and structural property of Al-Fe (Akinlade et al., 2000), Mg-Zn (N. Jha et al., 2001), Li-Pb (Rukhaiyar et al., 2001), In -Cu (Akinlade & Singh, 2002), Ca-Mg (P. P. Mishra et al., 2002), Te-Ga and Te-Tl (Awe et al., 2003), Fe-V and Fe-Ti (Akinlade & Boyo, 2004), Cu-Mg (Godbole et al., 2004), Na-Cs (Boyo, 2005), Cd-Na (I. S. Jha & Singh, 2005). Salmon (1992) studied the 2:1 binary system's structure using the Bhatia-Thornton formalism (Bhatia & Thornton, 1970), which was represented as MX_2 ($MgCl_2$, $CaCl_2$, $SrCl_2$, $BaCl_2$, $NiCl_2$, $NiBr_2$, NiI_2 , $ZnCl_2$, $GeSe_2$),

where M is an electropositive chemical species, and X is an electronegative one.

On the basis of the CFM and the pseudo-potential technique, the alloying behavior of a Cu-Mg alloy close to the melting point was explored. The former has been used to calculate the microscopic functions, thermodynamic, surface, partial and total structure factors. The latter was utilized to calculate the local screened factor required for calculating the alloy's electrical resistivity. The outcomes are in a fair degree of agreement with the experiment (Kumar et al., 2005). The development of the chemical complex CaMg_2 served as the foundation for the investigation of the Ca-Mg alloy. On this basis, the partial and total structure factors $S_{ij}(k)$ and $S(k)$ have been calculated and analyzed. Additionally, the local screening factor and, subsequently, the electrical resistivity of the alloy have been calculated using the Shaw model of pseudo potential. In the context of the complex formation model, a number of thermodynamical properties, including the heat of formation, entropy of mixing, concentration fluctuation at long wavelength limit $S_{cc}(0)$, and chemical short range order parameter (SRO), have also been investigated (Kumar et al., 2006). It was found that in the case of the liquid alloy Al-Mg, various factors such size difference and electronegativity difference are too small to justify the asymmetric behavior. The reported asymmetry indicates that in the liquid alloy, Al_3Mg_2 complexes occur. This suggests that, in any complexes stoichiometric composition lying at the certain composition other than equiatomic composition creates asymmetry around stoichiometric composition (A. K. Mishra & Milanarun, 2006). The CFM is also applied to Au-In (Novakovic et al., 2006), Al-Co and Co-Ni (Novakovic & Tanaka, 2006), Cd-Na (A. K. Mishra, 2007), Cu-Sn (Prasad et al., 2007), Cd-Zn (Rafique & Kumar, 2007), Cu-In (Oduote, 2008), Bi-In (Novakovic et al., 2009), Na-Cd (Chatterjee et al., 2011), Sb-Sn, (Novakovic et al., 2011), Al- Ti (Novakovic et al., 2012), Hg-Pb and Hg-In (Sharma et al., 2013) liquid alloys.

Infinite dilute activity coefficients (Y^∞) of binary liquids have been calculated using a new approach. The method mainly involves utilizing a complex formation model to calculate Y^∞ 's using experimental thermodynamic integral free energy of mixing data. Twenty-two binary alloys were chosen, and the computed activities for each were compared to the experimental activities that were available. In most of the chosen alloys, it was found that the findings of the suggested technique exhibited higher agreement with experimental activity data. As a result, the method is recommended as an alternative and more trustworthy method of determining Y^∞ 's of binary liquid alloys (Awe & Oshakuade, 2016). The CFM is further applied to explore the mixing behavior in Co-Si (Novakovic et al., 2016), Bi-Sb, Bi-Sn and Sb-Sn (Adedipe et al., 2019), Ga-Zn (Bhandari et al., 2019), Bi-Pb and In-Pb (Bhandari, Panthi, Koirala, & Adhikari, 2021) binary systems.

From Guggenheim's quasi lattice model and Wilson's local composition conception, Vera et al. (1977) constructed a novel formula for the excess Gibbs energy of liquid

mixture. The new equations are known as the local surface Guggenheim's (LSG) equation and the local composition Guggenheim's equation (LCG). The new equations only need two adjustable parameters for each binary, and there are no higher order parameters needed for the equations to be extended to multi-component systems. Ab initio method was used by R. N. Singh (1981) to determine the free energy of mixing and the heat of mixing for a liquid alloy of NaK, KRb, and NaCs. The hard-sphere reference system and pseudo potential theory were utilized for this study. It was noticed that during alloying, the diameter of heavier elements decreases while the diameter of lighter elements increases. It was also noted that the structural component of energy contributes significantly to the free energy. Alonso & March (1982) used semi empirical theory to develop a concentration dependent interchange energy $\Psi(c)$, which is a modification of the concentration-independent interchange energy employed in conformal theory of liquid solution. The concentration fluctuation in liquid Na-K alloy is then studied using $\Psi(c)$. The model is also used to investigate the concentration dependence of heat of formation in alkali metal liquid alloys such as Na-Cs, Na-Rb, Na-K, K-Cs, K-Rb, and Rb-Cs (Gallego et al., 1983). A statistical model that permits the configurational entropy of compound producing binary liquid alloys was established by Bergman and colleagues (Bergman et al., 1982). The researchers compared the entropies that were calculated based on ideal mixing with those that were calculated using the Flory model. The model is applied to Tl-Te and Cu-Si alloys by making the assumption that the regular associated solution is composed of A and B atoms along with their respective chemical associates, $A_p B_q$. The thermodynamic data of liquid Hg-Na alloys were analyzed by Tamaki et al. (1982) in terms of the concept of compound formation. In addition, the magnetic susceptibility and resistivity of the same system were measured at 373 K.

2.3.2 Quasi chemical approximation (QCA)

To understand short range order (SRO) in a number of regular alloys, Bhatia & Singh (1982a) modified the conformal solution model and hence the complex formation model to the quasi-chemical approximation (QCA). To deal with SRO in alloys, they set up the grand partition function. In a weak interaction approximation, Bhatia & Singh (1982b) made the quasi-chemical approximation even easier to understand and used it to describe Ag-Al alloy. Though conformal solution model (Longuet-Higgins, 1951) and consequently complex formation model (Bhatia & Hargrove, 1974) have successfully inferred $S_{cc}(0)$ using interchange energy, they did not provide any information about SRO because the models neglects the extent of local ordering. Knowledge of $S_{cc}(0)$ as well as the local ordering measured in terms of the Cowley-Warren short range order parameter for the nearest neighbor shell can give insight on the phenomenon of easy glass formation in numerous binary molten alloys (R. N. Singh, 1987).

For use in molten alloys belonging to the weakly interacting compound family, such as Ag-Al, Ca-Mg, Cu-Sn, Mg-Zn, etc., Bhatia & Singh (1984) further simplified the QCA. In the event that no complexes are formed, the complex formation model, and hence the quasi-chemical approximation, will be reduced to the conformational solution expression. The formula for chemical short range order parameter (α_1) in the quasi-chemical approximation may only be utilized for qualitative information at temperatures below and close to the critical temperature. The quasi-chemical approximation is known to perform poorly at $T \leq T_c$, even for alloys with long range order. However, can be utilized more confidently for temperatures higher than T_c . The value of the short-range order parameter in the compound forming system is determined by 1) A-B contacts that are in the mixture outside the complex and 2) A-B contacts that lie within the complex itself. It is also crucial to understand that coordination number (z), which is typically between 6 and 12 ($z = 6, 8$ and 12 for sc, bcc, and fcc), should not greatly influence $S_{cc}(0)$, but its inclusion is significant for SRO study. Within quasi lattice theory (QLT), one can easily obtain the two approximations: the conformational solution and Flory's, which were used in Bhatia and Hargrove's work (Bhatia & Hargrove, 1974) by setting $z = 2$ and $z = \infty$. The free energy expression in a quasi-lattice model is:

$$G_m = RT \left[n_1 \ln \frac{n_1}{N} + n_2 \ln \frac{n_2}{N} + n_3 \ln \left(\frac{(p+q)n_3}{N} \right) - \frac{1}{2} z q_3 n_3 \ln \frac{p+q}{q_3} - \frac{1}{2} z \mathbb{N} \ln \frac{\mathbb{N}}{N} \right] + \frac{1}{\mathbb{N}} \sum_{i < j} \sum n_i n_j \Psi_{ij} \quad (2.11)$$

where $n = n_1 + n_2 + q_3 n_3$ and q_3 can be stated as follows for an open chained structure of the complex:

$$q_3 = (p+q) - 2 \frac{(p+q-1)}{z} \quad (2.12)$$

and

$$\mathbb{N} = N - \xi n_3, \quad \xi = p+q - q_3 = \frac{2(p+q-1)}{z}$$

Setting $z = 2$, equation 2.12, results $q_3 = 1$ and $\mathbb{N} = n_1 + n_2 + n_3 = n$. When these values are substituted for equation 2.11, once we get,

$$G_M = RT \sum_{i=1}^3 n_i \ln \left(\frac{n_i}{n} \right) + \sum_{i < j} \sum \left(\frac{n_i n_j}{n} \right) \Psi_{ij} \quad (2.13)$$

This is the conformational solution formula for the ternary mixture's free energy of mixing.

For $z \rightarrow \infty$, the equations 2.11 and 2.12 permit us to write

$$G_M = RT \left[n_1 \ln \frac{n_1}{N} + n_2 \ln \frac{n_2}{N} + n_3 \ln \left(\frac{(p+q)n_3}{N} \right) \right] + \sum_{i < j} \sum \left(\frac{n_i n_j}{n} \right) \Psi_{ij} \quad (2.14)$$

This equation is commonly referred to as Flory's formula for free energy. The quasi chemical technique was modified by Pelton & Blander (1986) to account for the concentration dependence of numerous binary slag systems, such as CaO-SiO₂, FeO-SiO₂ and CaO-FeO. The calculations were expanded to include a ternary SiO₂ – CaO – FeO slag system. R. N. Singh et al. (1987) used quasi chemical theory to investigate the activity, heat of mixing, concentration fluctuation in the long wave length limit $S_{cc}(0)$, and chemical short range order parameter in Li-Mg alloys. As a result of considering the exchange energy as a function of temperature, numerous thermodynamic quantities are determined at high temperatures. The model is applied to investigate the energetic of mixing in Mg-Sn and Cu-Sn (Prasad et al., 1995), As-Zn and As-Cd (Akinlade, 1998), Zn -Au (Anusionwu, 2000), Cu-Zr and Cu-Si (Anusionwu & Adebayo, 2001) and weak association in Li-Mg alloy (Anusionwu, 2002). QCA has been used to confirm the possible compounds present in the liquid Cu-Hf alloys at 1650 and 1873 K. It was found that CuHf₂ is a more stable molecule at higher temperatures, despite the fact that its existence appears to be more prevalent at lower concentrations of Hf (Anusionwu et al., 2003). The structural, surface, and thermodynamic properties of Ge-Ga and Ge-Sb liquid alloys were investigated and the QCA is extended to study the surface $S_{cc}(0)$ as well (Anusionwu, 2004). The approximation is also used to observe the alloying behavior in Cd-Mg, and Cd-Ga (A. K. Mishra & Milanarun, 2005), Ag-Cu (Novakovic, Ricci, et al., 2005), Au-Sn (Novakovic, Ricci, et al., 2005), Ga-Sn and Ga-Zn (Ga-X) (Novakovic & Zivkovic, 2005), Sb-Sn and In-Sn (Anusionwu, 2006) liquid alloys. All thermodynamic and phase diagram data for the Mg-Si and Mg-Sn binary systems, as well as the Mg-Sn-Si ternary system, were analyzed critically. To produce a single set of model parameters for the Gibbs's energies of the liquid as functions of composition and temperature, all reliable data were simultaneously optimized. To describe the strong ordering in Mg-Si and Mg-Sn liquids, the liquid phase was studied using the modified Quasi chemical model (Jung et al., 2007). The Al-Ce, Al-Y, Al-Se, and Mg-Sc system were subjected to rigorous critical analysis and optimization. For the liquid phase, which displays a high level of short-range ordering, the modified quasi-chemical model is applied. All of the accessible and credible experimental data, including phase diagrams, enthalpies of mixing in liquid alloys, and heats of intermetallic phase formation, are accurately reproduced within the experimental error limitations (Kang et al., 2008). The mixing behavior of an In-Sn liquid alloy was investigated using the quasi-chemical approximation and the complex formation model, with the compound assumed to be energetically favorable. At equi-atomic composition, the thermodynamic functions of

mixing exhibit symmetry, whereas the microscopic functions and diffusivities exhibit asymmetrical behavior (Novakovic et al., 2008). The applications of QCA were made on Ga-Sn, Ga-Mg and Al-Ga (Awe et al., 2008), Al-Ga and Al-Ge (Anusionwu, Adebayo, & Madu, 2009), Cu-B (Passerone et al., 2009), Si-Ti (Awe et al., 2011), Al-Cr and Cr-Ni (Novakovic et al., 2011), Na-K (Adhikari et al., 2012b), Ge-Si (Amore et al., 2014), Fe-Cr (Novakovic & Brillo, 2014) and Al-X (Al-Sn, Al-Ge, Al-Cu) (Oduote, 2014) liquid systems to observe their mixing behavior. At 673 K, the Gibbs free energy, enthalpy, entropy, and activity as well as the concentration fluctuation in the long wave length limit and chemical short range order parameter of the Tl-Na alloy have been studied. The viscosities of the alloy determined using the BBK model, Singh and Sommer's formulation, and the Kaptay equation were compared. The results of the surface tension calculation show that the results from the layered structure approach and the compound formation model are reasonably in agreement in the Tl-rich side of the composition and are in good agreement in the Na-rich side, whereas those obtained from the Butler equation show a noticeable deviation in the intermediate compositions. The Tl-Na melt has been observed to have hetero-coordination in the complete range of concentrations and has been found to be a significantly interacting system by negative divergence from the Raultian behavior (I. S. Jha et al., 2016). The approximation is further continued to employee in Ag-Ge (Delsante et al., 2019), Au-X (X = Cu, Zn, Pb, Ni, Sn, Al) (Oduote & Popoola, 2019) and Bi-Sn (Giuranno & Novakovic, 2020) binary systems to explore their thermophysical characteristics.

The time of flight (ToF) spectrometer was used to conduct the neutron scattering experiment (Soltwisch et al., 1983). The authors reported quasi-elastic neutron scattering data that yield experimental knowledge regarding the microscopic dynamics of concentration fluctuation. A different method for determining concentration dependent interaction energy $W(c)$ is also described. In accordance with the conformal solution model, for $q = 0$ we have,

$$S_{cc}(0) = \frac{S_{cc}^{(ideal)}(0)}{1 + 2W(c) S_{cc}^{(ideal)}(0)/K_B T} \quad (2.15)$$

where $W(c)$ is proportional to enthalpy of mixing H_M

$$W(c) = \frac{H_M}{N c_A c_B}$$

Excess thermodynamic fluctuations, structure factors, and concentration fluctuations in Na-Rb, Na-Cs, K-Rb, and Rb-Cs liquid alkali alloys were examined in the framework of Vander Waals theory, where a liquid alloy was treated as a mixture of hard spheres immersed in a homogeneous background potential (Y. Tanaka et al., 1983).

The conformal solution theory was widely applicable to the mixtures in which the difference in volume between the species was not significant. However, for systems such as Na-Cs and Na-Rb in which the volume ratio is large (≈ 3), Bhatia & March (1975b) offered an alternate method and successfully explained the size effects in a Na-Cs liquid alloy by considering only one interaction energy parameter. In 1984, R. N. Singh & Bhatia (1984) introduced the temperature-dependent interaction energy (W) and investigated the entropy and free energy of mixing of Na-Cs liquid alloy. The size impact in the Na-Cs system was resolved by inserting a temperature-dependent interaction energy term. The dependence of $S_{cc}(0)$ on temperature is also studied. The size effect in the Na-Cs liquid alloy in terms of $S_{cc}(0)$ had been explained through various approaches as demonstrate in figure 6. The open circles are theoretical at $T = 384$ K (Y. Tanaka et al., 1983), the full circles are for theoretical at $T = 383$ K (Bhatia & March, 1975b), the stars are experimental at $T = 383$ K (Ichikawa et al., 1974), solid curves are theoretical with $T = 383$ K (R. N. Singh & Bhatia, 1984), the broken curves are experimental at 473 K (Neale & Cusack, 1982) and the plus signs are from neutron diffraction experiment at 373 K. (Huijben et al., 1979).

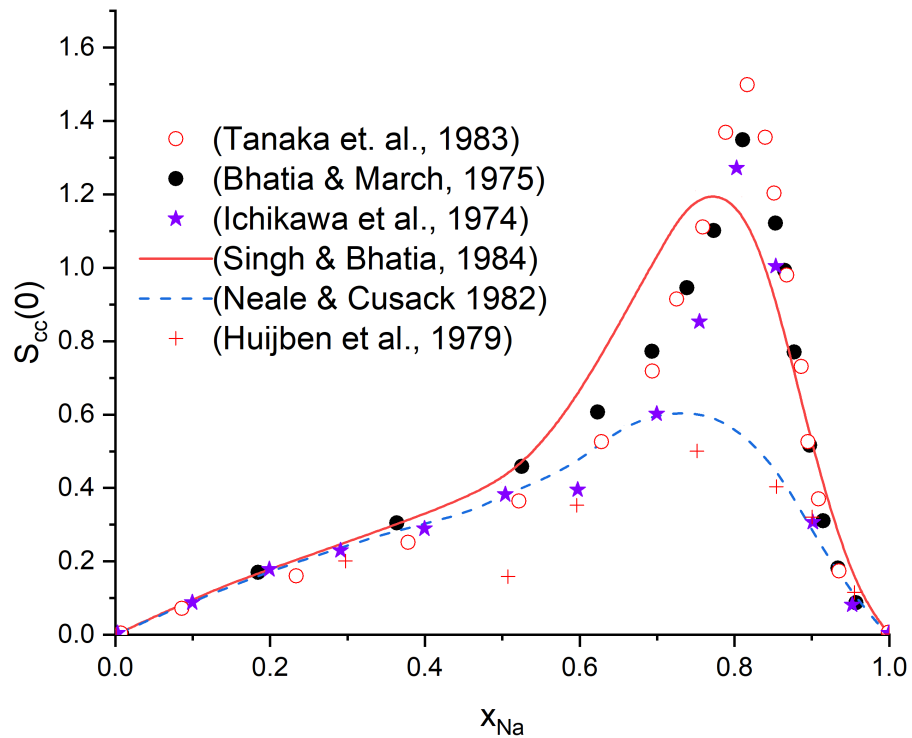


Figure 6: Concentration fluctuations ($S_{cc}(0)$) for Na-Cs system (Y. Tanaka et al., 1983; Bhatia & March, 1975b; Ichikawa et al., 1974; R. N. Singh & Bhatia, 1984; Neale & Cusack, 1982; Huijben et al., 1979).

2.3.3 Quasi lattice theory (QLT)

Bhatia & Singh (1984) demonstrated that the thermodynamic properties of compound forming $A - B$ alloys are able to be explained by using a quasi-lattice picture. In this picture, the alloy is viewed as a pseudo ternary mixture of A atoms, B atoms, and A_pB_q complexes, all of which are in equilibrium with one another. It is assumed that all atoms occupy lattice positions. Each location has z closest neighbors. If the size difference between two types of atoms A and B is less than fifty percent, each atom can be considered a monomer. The large majority of compound-forming alloys come under this category. The complex A_pB_q is therefore $(p + q)$ -mer or occupies a $(p + q)$ lattice site. This approach gives a formulation for the short range order parameter for nearest neighbors, unlike the Bhatia-Hargrove approach. If the total number of lattice sites be N , then it is equal to the total number of atoms present in the alloy, $N = n_1 + n_2 + (p + q) n_3$. In conclusion, it is assumed that the interaction between the atoms is of a short range, and this interaction is represented by the energies of the nearest bond or the contact. To explain the alloying behavior of liquid Au-Zn alloys, the QLT has been used. The hetero coordination in the Au-Zn melt is shown by the ordering energy's significant negative values and the chemical short range order parameter. It is possible that 1-1 type complexes (AuZn) exist in the liquid alloys based on the deep in concentration fluctuation at the long wave length limit and the bigger negative value of excess free energy of mixing at $c = 1/2$. This suggests that Au-Zn liquid alloys with symmetrical mixing properties belong to a system with strong interactions (Prasad & Singh, 1990). In the framework of QLT, the thermodynamic and microscopic behavior of Ag-Sn (Prasad et al., 1998), Mg-Zn (N. Jha et al., 2001), Bi-Pb (Novakovic et al., 2002), Ag-Cu, Ag-Ti and Cu-Ti (Novakovic et al., 2003) were explored. With particular attention paid to their bulk and surface properties, the energetics of molten alloys Ag-Zr and Cu-Zr have been examined. Additionally, the propensity of both systems to form glass at increasing Zr concentrations is suggested by the qualitative associative tendency between dissimilar constituent elements as reflected by microscopic functions (Novakovic et al., 2004). The QLT is also applied to Ag-Ti and Ag-Hf (Novakovic, Tanaka, et al., 2005), Sn-Ag, Sn-Bi, and Sn-In (Prasad & Jha, 2005), Al-Mg (A. K. Mishra & Milanarun, 2006), Cu-Sn, Sn-Ti and Cu-Ti (Novakovic et al., 2006) liquid melts to explore their characteristics on mixing.

Applying formulae derived using the quasi-lattice approximation, the energetics and its impact on the mixing behavior of the relevant binaries Al-Zn, Al-Sn, and Sn-Zn as well as ternary Al-Sn-Zn liquid have been explored. Through the use of the model developed by Chou & Wei (1997), the binary composition of the ternary Al-Sn-Zn was fixed using the same interaction energies that were used to describe the alloying behavior of the binaries discussed above. Theoretical findings are in good agreement with those of

the experiment (Kohler, 1960; Prasad & Mikula, 2006). The experimental results were reproduced by the theoretical analysis of the concerned binaries (Ag-Sn, Sn-Zn, and Ag-Sn) of the ternary Ag-Sn-Zn liquid alloys. Extended QLT has been used to explore both the bulk and surface properties of the Ag-Sn-Zn ternary liquid alloys, based on the results of the binary system (Prasad & Jha, 2007). The mixing functions of Cu-Bi and Bi-Zn (Akinlade et al., 1998), Ga-Sn, Al-Sn and Fe-Sn (Akinlade et al., 1999), In-Zn and Sn-Zn (Ilo-Okeke et al., 2005) Ga-Tl and Zn-Cd (Akinlade & Awe, 2006), Al-Zn and Bi-In, (Oduote et al., 2007), Cd-Ga (Sommer, 2007) Ni-Ti (Novakovic et al., 2008), Cd-Ga (Anusionwu, Madu, & Orji, 2009), Al-Nb and Nb-Ti (Novakovic, 2010), Fe-Si (Kumar et al., 2011), Al-Si (B. P. Singh et al., 2012), Sn-Tl (R. P. Koirala, Jha, et al., 2014) were explained with reference to QLT.

For Mg-Pb alloys at various temperatures, the excess free energy of mixing G_M^{XS} , concentration fluctuation in the long-range wave length limit $S_{cc}(0)$, and the chemical short-range order parameter α_1 were assessed. At $c_{Mg} = c_{Pb} = 0.5$, these properties were reported to be asymmetrical, and they exhibit a minimum at $c_{Mg} \cong 0.60$. Chemical compounds, such as Mg_2Pb , are thought to be the cause of the asymmetry. When Mg and Pb atoms tend to couple as nearest neighbors, there appears to be significant hetero-coordination, according to the $S_{cc}(0)$ and α_1 values (R. N. Singh & Arafin, 2015). The various properties of binary melts in conjunction with QLT were studied for Cd-Hg (I. Koirala et al., 2015), Mg-Sb and Cu-Sb (Ajayi & Ogunmola, 2018), Cu-Sn (Panthi et al., 2021), Ag-Sb (Panthi et al., 2020), Si-Ti (Yadav, Mehta, et al., 2020), Cu-Mg (Yadav, Gautam, & Adhikari, 2020), Na-Hg (Panthi et al., 2021), and Hg-Pb (Panthi et al., 2022) systems.

2.3.4 Regular associated solution model (RASM)

To calculate the complex concentration of an A_pB_q type cluster in a liquid alloy, Lele & Ramachandrarao (1981) developed a new approach. For this, the activity coefficient of the components at infinite dilution and activity values for any other composition were utilized. The equilibrium constant for cluster dissociation as well as the nature and magnitude of pairwise interaction energies between unassociated atoms and clusters are evaluated without making any assumptions. The model is then applied to molten Mg-Sn and In-Sb alloys, where excellent agreement with experimental data is observed. The model is modified and updated as regular associated solution model and used by many researchers to investigate the binary liquid mixture. The regular associated solution model (RASM) was used to examine the thermodynamic characteristics and microscopic functions of liquid Fe-Si alloys at 1873 K. The complex concentration in a regular associated solution of Fe, Si, and Fe_2Si was calculated using the model. The integral excess free energy of mixing, activity, concentration fluctuation in the long

wavelength limit, $S_{cc}(0)$, and the Warren-Cowley short range parameter, α_1 were all calculated using the complex concentration. According to the analysis, the hetero-coordination that results in the production of the complex Fe_2Si is likely to occur in the liquid due to its strong nature of interaction. Based on the model chosen, the observed asymmetry in the properties of mixing in Fe-Si alloys in the molten state is satisfactorily explained (Adhikari, Jha, & Singh, 2010). The similar investigation were done for Cu-Sn (Adhikari, Singh, et al., 2010), Ag-Al (Adhikari, Jha, & Singh, 2010), Cd-Na (Adhikari, Singh, et al., 2010), Ag-Sb (B. P. Singh et al., 2010), Mg-Tl (Adhikari, Jha, et al., 2011), Hg-Na (Adhikari, Singh, et al., 2011), Mg-Pb (Adhikari, 2011), Li-Mg (I. S. Jha et al., 2011), Na-Pb (B. P. Singh et al., 2011), Cd-Hg and Cd-Na (Adhikari et al., 2012a), In-Na and Na-Pb (I. S. Jha et al., 2012), Al-Fe (Adhikari et al., 2014), Tl-Na (Yadav et al., 2015b), In-Sn (Yadav et al., 2015a), In-Bi, Tl-Bi (Yadav et al., 2015b) and Pb-Tl (Yadav, Jha, & Adhikari, 2016) binary liquid alloys. Using the RASM, the thermodynamic properties of the Pb-Hg liquid alloy at 600 K have been calculated, including the free energy of mixing, heat of mixing, activity, and structural properties like concentration fluctuation in the long wave length limit and short range order parameter. To calculate the surface tension of the alloys at various temperatures, it was then correlated with a modified Butler model. At greater Pb concentrations, it is observed that the Pb-Hg system at 600 K is ordered (Yadav, Jha, Jha, et al., 2016). Further the mixing energetics of Ni-Al, (Yadav, Lamichhane, et al., 2016), Tl-Na (Yadav et al., 2017) and Al-Mg (Yadav et al., 2018) alloys are explained in the frame of regular associated solution model. Ramachandrarao et al. (1984) have elaborated on the linkages between $S_{cc}(0)$, the equilibrium phase diagram, the existence of chemical complex in the liquid state, and the formation of glasses. In a number of binary liquid alloys, G_M and the heat mixing H_M are composition-dependent asymmetric quantities. This asymmetry is frequently attributed to differences in the size, valency, and electronegativity of the liquid alloy's constituents. Despite the fact that these characteristics are also responsible for stimulating the formation of compounds or complexes in the alloy, asymmetry in the compositional dependency of these features does not necessarily imply complex formation. In this context, the use of $S_{cc}(0)$ is preferable to direct thermodynamic analysis for determining the extent of association in the liquid. The magnitude of $S_{cc}(0)$ in liquid solutions depends on the nature of the solution formed and can vary significantly from ideal to non-ideal solution. In a binary system, the concentration dependency of $S_{cc}(0)$ changes depending on the nature of the solution and the type of interaction between the species. $S_{cc}(0)$ has a magnitude of zero in strongly interacting systems, an intermediate value in weakly interacting systems, and a significant positive value in non-interacting systems. Extensive research by Bhatia and colleagues, (Bhatia & Hargrove, 1974) has revealed that the magnitude of $S_{cc}(0)$ may even tend to infinity (as in the case of Tl-Te), yet in strongly coupled or compound forming systems it may

approach zero at compositions equivalent to the complex or compound's stoichiometry. Figure 7 demonstrates the different behaviors exhibited by $S_{cc}(0)$. The full circles are for TeTl₂ at $T = 873$ K (Ivanov & Berezutski, 1996), the open circles are for In-Tl at $T = 723$ K (I. Koirala et al., 2014b), the dashed line represents ideal value of $S_{cc}(0)$, the solid line is for Cu-Sn at $T = 1373$ K from (Novakovic et al., 2006), the stars also represents $S_{cc}(0)$ values for Cu-Sn at $T = 1400$ K (Adhikari, Singh, et al., 2010) and the dotted line is for Bi-Pb alloys at $T = 623$ K (Novakovic et al., 2002).

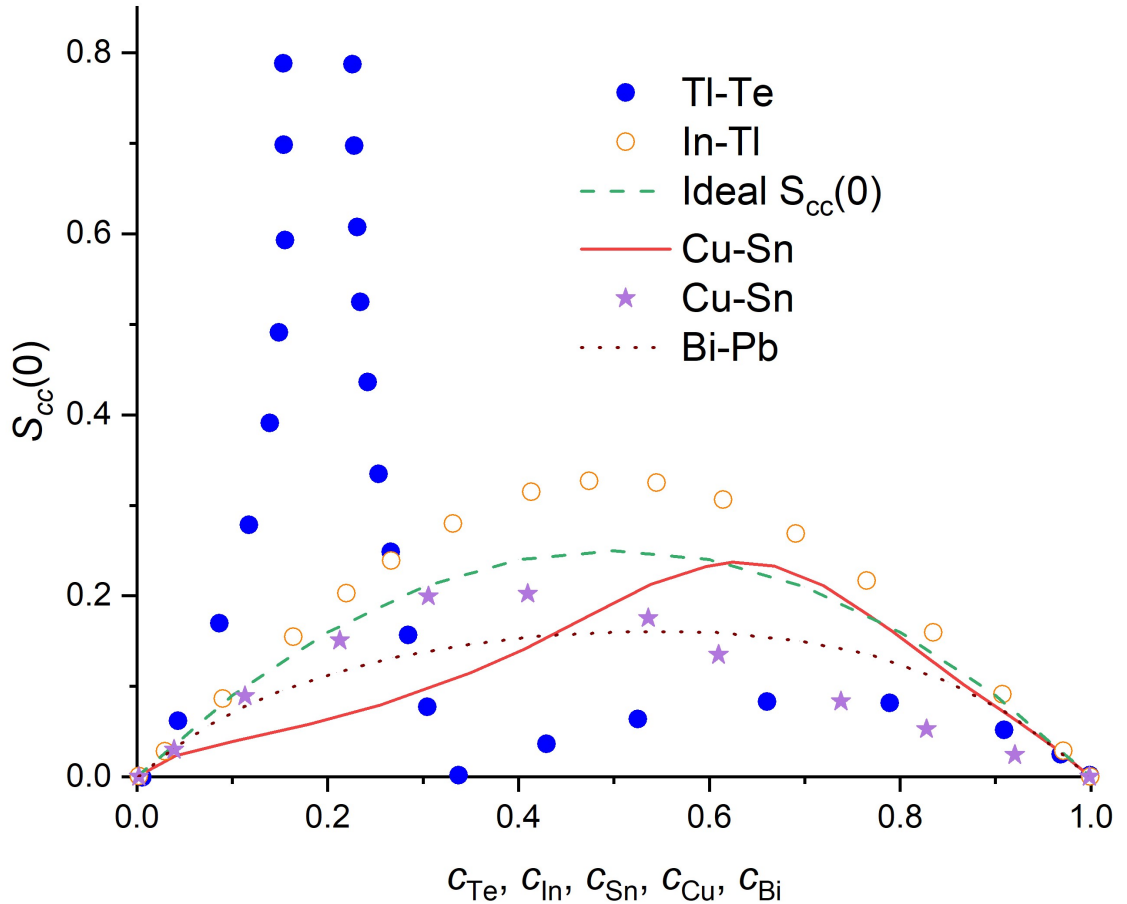


Figure 7: Different behaviors exhibited by $S_{cc}(0)$ (Ivanov & Berezutski, 1996; I. Koirala et al., 2014b; Novakovic et al., 2006; Adhikari, Singh, et al., 2010; Novakovic et al., 2002).

In several binary metallic systems, the range of compositions that can form glass is related to the composition dependence of $S_{cc}(0)$, which is the concentration-concentration fluctuation structure factor at its long wavelength limit. In the range of compositions that make glass, the $S_{cc}(0)$ reaches the possible ideal value as shown in Figure 8. This indicates that in the glass forming liquid alloys, a random distribution of constituent atoms and complexes prevails at the concentration corresponding to the ideal value of $S_{cc}(0)$. However, the tendency for complex formation is unrelated to the tendency for glass formation. Because the $S_{cc}(0)$ values in the glass forming composition range tend to be near their ideal magnitude, short-range order in these alloys is negligible

(Ramachandrarao et al., 1984). The composition range in which glass is formed typically lies a significant distance from the stoichiometric composition. Consequently, in the context of the CFM, one can conclude that the unassociated species (A and B atoms) and the complex A_uB_v mix in a random manner at that composition. This random mixture can hinder nucleation and promote glass formation. However, it appears that the ideal value of $S_{cc}(0)$ may not be adequate but is an essential requirement for creating glass from molten alloys. Many of the binary molten alloys that create compounds are excellent glass-makers, for instance, Al-La, Ca-Mg, Mg-Zn, Cu-Ti, etc. (R. N. Singh, 1987).

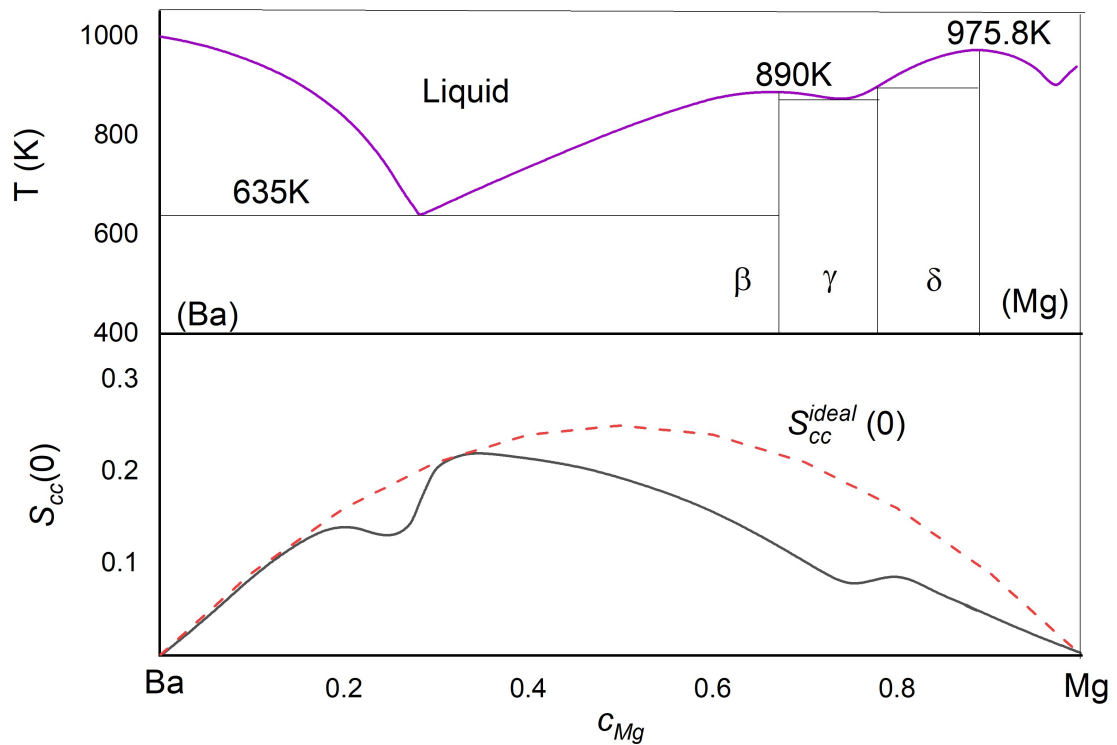


Figure 8: The phase diagram and the composition dependence of $S_{cc}(0)$ at 1054 K in the system Ba-Mg (Ramachandrarao et al., 1984).

Systems with $-G_M/RT > 3$ and an asymmetric concentration dependence of the thermodynamic function are known to have significant chemical interactions and form complexes in the liquid state. On the basis of the G_M/RT value, alloy systems can be classified as strongly interacting, moderately interacting, weakly interacting according to their propensity for complex formation (Ramachandrarao et al., 1984).

A model for the heat of mixing of two metals with differing lattice constants was proposed by (Gijzeman, 1985). It is demonstrated that the model adequately describes the heat of mixing as a function of composition. Ag-Pd, Cu-Ni, Cu-Pd, Ni-Pt, Ag-Au, Fe-Ni, Cu-Pt, and liquid Cu-Fe are shown as examples. $S_{cc}(0)$ in Li-Pb, Hg-K, Na-Ga, Ar-Kr, Na-Cs, Bi-Mg, and Na-Tl liquid alloys was investigated by Waseda et al. (1984). In

addition, the G_M , H_M , and S_M of Na-Ga liquid alloys were examined. The equations for calculating the Gibbs energy, enthalpy, and entropy of mixing were formulated by Schmid & Chang (1985). Asymmetric behavior and miscibility gap were examined with relation to Si-Te liquid alloys at 1100 K. For treating the thermodynamic properties of high polymer solutions, the Flory formula for the entropy of mixing was initially proposed. The study investigated the application of Flory's formula to a broader range of binary alloys and shows how the method can be used to accurately determine the mixing entropy of compound forming alloys. The updated Flory's formula for mixing entropy is used in the work, and appropriate results are produced. For compound forming alloys, it was observed that the results are better than in the hard sphere system (P. Singh et al., 1985). Experiments were done to figure out the activity of calcium in Ca-Al alloys. The concentration-concentration structure factor at zero wave vector has been calculated from the measured activity data. Regular associated solution model was used to learn further about thermodynamic properties (Jacob et al., 1988). The volume of mixing, the free energy, activity, and $S_{ij}(0)$ of liquid Hg-Na and Hg-K alloys were investigated by I. S. Jha et al. (1990). In all compositions, Hg-Na liquid alloys were shown to be more stable than Hg-K liquid alloys.

2.3.5 Simple statistical model (SSM)

To determine the conditional probability of nearby atoms appearing in molten alloys, a simple statistical mechanical model based on pair wise interaction has been taken into consideration. The analytical expressions for activity, free energy of mixing, concentration fluctuation in the long wave length limit, and chemical short range order parameter have been obtained by extending this by constructing a grand partition function. The ordering energy and concentration-dependent thermodynamic characteristics of Cu-Pb, K-Na, Li-Mg, and Cd-Mg are computed. The investigation demonstrates that Cu-Pb and K-Na exhibit self-coordination among their nearest neighbors, but Li-Mg and Cd-Mg exhibit hetero coordination (R. N. Singh & Mishra, 1988). For a similar study, the model is also used to Cd-based liquid alloys (Cd-Bi, Cd-Mg, and Cd-Ga) (R. N. Singh et al., 1990). Using the theoretical model developed by Prasad et al. (1994), Anusionwu et al. (1998) investigated size effects in the Na-Sn, Sa-Ga, Cu-Ni, Li-Ba, and Na-Te systems. The model was further extended to analyze surface $S_{cc}(0)$ in the systems specified. From $S_{cc}(0)$ measurements that were evaluated using literature-based activity data, Prasad & Mikula (2000a) determined the surface tension values of Al-Sn liquid alloy. The values for surface tension were also used to complete the work of adhesion (W) and interfacial tension between solid Al_2O_3 and liquid Al-Sn over the full concentration range. In 2013, I. Koirala et al. (2013) used the simple statistical model to investigate the thermal, transport and surface characteristics of liquid In-Pb alloys. Investigations into addi-

tional properties, such as diffusion coefficient, viscosity, surface tension, and surface concentration, have been conducted using the same energy parameters that have been used to fit thermodynamic properties. The research shows that the liquid In-Pb alloy is a phase-separating system with weak interactions. The model is also used to study the symmetric behavior in K-Na (I. Koirala et al., 2013), Ag-Cu (I. S. Jha et al., 2014), Cd-Bi (I. Koirala et al., 2014b), In-Tl (I. Koirala et al., 2014b), Cd-Pb (B. P. Singh et al., 2014), Al-Ga (I. Koirala et al., 2014a), Cd-Zn (I. Koirala et al., 2014), Al-Ge, Al-Fe (I. Koirala et al., 2016b), Al-Fe (I. Koirala et al., 2016a), and Ag-Au (I. Koirala, 2018).

On the basis of the free volume theory and the first approximation to the regular solutions, a thermodynamic model was created. The model has the ability to calculate the excess entropy produced by mixing of liquid binary alloys. The calculated outcomes were discussed and matched with the findings of the experiment. In the liquid systems of Ag-Zn, Au-Cu, Al-In, Al-Mg, Cd-Pb, Cd-Mg, Na-Tl, Na-Pb, Cu-Pb, Cu-Mg, Fe-Cu, Fe-Si, K-Pb, K-Tl, Hg-Na, and Hg-In, the model is used to get excess free energy, excess heat of formation, excess entropy, and excess activity. The relationship between ΔH^{XS} and ΔS^{XS} in an infinitely dilated solution of liquid binary alloys is also discussed using this model (T. Tanaka et al., 1990). The activity, the small-angle partial structural factors, the excess free energy of mixing, and the chemical short-range parameter have all been analytically expressed using the grand partition function. By assuming that the complex Al_3Mg_2 exists in the liquid phase, it has been used to explain the asymmetry in the properties of mixing of Al-Mg molten alloys (N. K. P. Singh et al., 1991). According to the findings of the structural analysis, Ag-Si is a segregating system, Al-Ge is chemically more ordered, and Ag-Ge experiences an inversion from order to segregation as a function of concentration (Sinha & Singh, 1991). Both the pseudo-isopiestic method and the Knudsen effusion-mass loss method have been used to measure the activity of barium in liquid Al-Br at 1373 K. Using thermodynamic information, the $S_{cc}(0)$ has been calculated. The thermodynamic behavior of liquid Al-Ba alloys has been described using the associated solution model with Al_5Ba_4 as the predominant complex (Srikanth & Jacob, 1991). An identical study was performed for Al-Sr alloys (Srikanth & Jacob, 1991).

2.3.6 Self-association model (SAM)

On the basis of the association model, Sommer (1990) described the concentration and temperature dependence of thermodynamic mixing functions. In order to investigate the enthalpy, entropy, and Gibbs's free energy of mixing in Li-Mg at 940 K, Al-Li at 973 K, Sn-Te at 1140 K, and Li-Pb at 1000 K, the model was employed. The author also studied into the mixing enthalpies of Ca-Si at 1600 K and $S_{cc}(0)$ in Li-Pb at 930 K. To evaluate the thermodynamic properties of mixing liquid alloys with miscibility gaps, R. N. Singh

& Sommer (1992a) suggested a model. The atoms of the constituent elements A and B are considered to be in the form of a polyatomic matrix, which produces a fraction of like-atom clusters or self-associates of the type A-A or B-B. In addition to explaining the positive divergence of the mixing property in the Bi-Zn system from Raoult's law, the model provides closed equations for a number of thermodynamic functions. The model is also used to understand the demixing in Cd-Ga and Bi-Ga alloys. The $S_{cc}(0)$ values for phase separation alloys are found to decrease with increasing temperature (R. N. Singh, Yu, & Sommer, 1993). The CFM and the SAM were both employed by Akinlade et al. (2001) to compare the surface and bulk properties of hetero-coordinating liquid alloys: Ga-Bi, Ga-In, and In-Bi. Using a simple statistical model developed by Singh and Sommer (R. N. Singh & Sommer, 1992a) the thermodynamic and surface properties of Na-Cs, Na-Bi, and Na-Sn have been examined. The concentration of the intermetallic compounds is related to the asymmetry and peaks in the surface tension computed for Na-Bi and Na-Sn (Anusionwu, 2003). Using a statistical model based on the association of like species, the segregation tendencies of In-Zn liquid alloy in the bulk and at the surface have been examined at temperatures of 692 K, 850 K, and 1000 K. With an increase in temperature, the strength of segregation in the majority of this alloy appears to decrease exponentially. Sn-Zn liquid alloys were also the subject of similar research at 650 K, 875 K, and 1123 K (Ilo-Okeke et al., 2005). The investigation for Bi-Cd, In-Pb, and Ni-Pd alloys was conducted similarly (Awe et al., 2005). The demixing tendency in binary melts were also studied in Al-Ga (R. P. Koirala, Adhikari, et al., 2013), Cd-Zn (R. P. Koirala, Singh, et al., 2013), Co-Fe and Fe-Pd (R. P. Koirala, Kumar, et al., 2014), In-Pb, In-Tl and In-Zn (R. P. Koirala et al., 2016). The self-association model was used to analyze the energetics of mixing and its impact on the bulk and surface properties of Al-Sn and Sn-Tl liquid alloys at 973 K and 723 K, respectively. The findings show that in Al-Sn and Sn-Tl liquid alloys, Sn and Tl atoms segregate to the surface at all bulk concentrations of Sn. However, it is anticipated that Al-Sn liquid alloys will exhibit more segregation than Sn-Tl. As the bulk concentration increases, the surface tension falls, indicating that Al-Sn and Sn-Tl liquid alloys are segregated systems in the bulk and at the surface across the whole concentration range. The $S_{cc}(0)$, α_1 and diffusion coefficients, (D_M/D_{id}) measurements of both systems agree with the surface tension observation (Odusote et al., 2016). The SAM is further applied to explore the thermophysical properties of Zn-Cd (Awe & Azeez, 2017), Cd-Pb and Cd-Sn (R. P. Koirala et al., 2018), Cr-Mo and Cr-Fe (Odusote & Popoola, 2017), In-Tl (Shrestha et al., 2018), Zn-Sn (Shrestha, Singh, Jha, Koirala, Singh, & Adhikari, 2017), Al-Sn (Shrestha, Singh, Jha, Singh, & Adhikari, 2017), Cu-Pb (Shrestha, Singh, Jha, & Koirala, 2017), Fe-Co and Fe-Mn (Ogundeji et al., 2021).

In order to identify the higher order atomic correlations in the nearest neighbor shell of

liquid binary alloys, a thermodynamic model based on a cluster of four atoms is taken into consideration. For Bi-Cd, Li-Mg, Cd-Mg, Cd-Ga, Cu-Pb, and K-Na, the values of order energy, activity, and chemical short range order parameter were estimated and presented (R. N. Singh, 1993). The model is adopted and employed to Au-Zn, K-Pb, Ni-In, Cu-In (Akinlade, 1997) and Al-In, Ag-In, In-Sb binary systems (Akinlade et al., 2003) to explain their thermophysical characteristics. To account for liquid binary metal alloys, the analytic pair potential model was expanded. The parameters of each case are calculated separately using the appropriate electron concentration and electron-ion interaction potential. The formalism is used to observe the concentration fluctuations and thermodynamic characteristics of the liquid binary alloys Li-Na, Na-K, and Na-Cs. The parameters so found are also used to calculate the resistivity values (Dalgiç et al., 1994). Due to the formation of unlike atom associations, the thermodynamic properties of binary liquid alloys of rare earth metals with copper and silver imply that these system possesses chemical short-range ordering. The calculated thermodynamic parameters, including the concentration correlation function, $S_{cc}(0)$, for Cu-Y, Cu-La, and Cu-Lu melts using the ideal associated solution model (IAS) are in good agreement with the experimental results. The charge transfer impact for Ag-La melts and the Faber-Ziman partial structural factors in the zero-wave vector limit were also assessed (Ivanov & Berezutski, 1994). The Khudsen effusion method was used to determine the concentration dependence of activity $a(c)$ in liquid Au-Gd alloys at 1623 K, and the results show a large ordering effect. For many metallic solutions with chemical short-range order (SRO), the percolation theory is proposed for analysis and calculation of activity data using concentration correlation function $S_{cc}(0)$. Experimental results and theoretical calculations of $a(c)$ from provided $S_{cc}(0)$ and vice versa agree satisfactorily. The activity and $S_{cc}(0)$ measurements in the ordered melts of Ag-Nd, Al-Au, Hg-Na, Ge-Ni, Ge-Cu, and Tl-Te were shown to be correctly interpreted and predicted using the percolation theory (Ivanov & Berezutski, 1996).

Expressions for various thermodynamic and microscopic structural functions for 4:3 inter-metallic compounds have been developed using a statistical mechanical theory in conjunction with a compound formation model. The data obtained show that Zn_4Sb_3 compound was present in the melt. Additionally, it has been noted that the propensity for inter-metallic interaction declines as temperature rises (Prasad & Mikula, 2000b). A model of an ideal associated solution was considered, which contained self-associates of various sizes and shapes. The thermodynamic and structural properties, as well as the liquidus lines for the Na-K system, were investigated (Shunyaev & Lisin, 2000). On the basis of experimental enthalpy of mixing data acquired at constant temperature, a relationship to estimate the composition and temperature dependence of the excess entropy of mixing, S^{XS} and the excess heat capacity, C_p^{XS} for the liquid binary alloys has

been introduced. Liquid alloys including Fe-C, Mn-Si, Co-B, Ag-Ge, Sb-Zn, Hg-Na, Ca-Mg, and Ni-Zr were subjected to the model's application (Witusiewicz & Sommer, 2000). Morachavskii & Erofeev (2001) conducted an analysis of the thermodynamic characteristics of liquid alloys in the Mg-Sn system. Using modified software, the excess molar Gibbs energy and mixing enthalpy's concentration dependency is characterized in terms of the ideal and regular solution model. From the thermodynamic conditions of liquid-vapor equilibrium, Shpil'rain et al. (2002) measured the activity coefficient of the Na-K binary system's constituents. Both experimental and theoretical literature data were found to be in satisfactory agreement with the reported findings. The probability that a bond is of the A-B type for a system of N sites with M neighbors surrounding each site is given by,

$$P_{AB} = \lim_{n \rightarrow \infty} \left(\frac{N_{AB}}{\frac{1}{2}MN} \right) \quad (2.16)$$

Here N_{AB} denotes the total number of A-B bonds. The total number of bonds in the system is represented by the denominator of equation 2.16. Considering that each site in the system is independently occupied by an A or B atom with probability P_A or P_B ($P_A + P_B = 1$), P_{AB} would be equal to $2P_AP_B$. Then, the following difference is used to calculate the nearest neighbor correlation parameter, Γ_{AB} .

$$\Gamma_{AB} = \frac{1}{2}P_{AB} - P_AP_B \quad (2.17)$$

The well-known Warren-Cowley SRO parameter is obtained by dividing Γ_{AB} by $-P_AP_B$.

$$\alpha_1 = 1 - \frac{P_{AB}}{2P_AP_B} \quad (2.18)$$

Depending on the sign of α_1 , the components will either prefer clustering $\alpha_1 > 0$ or A-B ordering $\alpha_1 < 0$. The normalized SRO parameter lies in the range such that $-1 \leq \alpha_1 \leq +1$; $\alpha_1 = 0$ for a perfect random alloy, that is, an alloy with no association (Müller, 2003).

The Mg-Nd system was presented with a self-consistent thermodynamic description. The association model for the liquid phase was put to the test and compared with the random solution model for the asymmetric shape of the liquidus in the binary phase diagram. For comparison with additional experimental investigations, the enthalpy of mixing in the liquid is computed using the two basic models. The optimization's results demonstrated that the association model, as compared to the random solution model, yields a higher agreement with experimental results (Gorsse et al., 2005).

The findings of experimental and analytical thermodynamic studies of the Ga-Bi system were reported. Quantitative differential analysis was used to get integral molar enthalpies of mixing. The Zang-Chou method for binary systems was used to calculate the activities of bismuth over the whole composition range and temperature range of 573 to 1073 K (Živković et al., 2005). The Gibbs-Duhem equation

$$\ln a_B = \ln c_B - c_{ACB}\alpha_A + \int_0^{c_A} \alpha_A dc_A \quad (2.19)$$

with

$$\alpha_A = \frac{\ln \gamma_A}{(1 - c_A)^2}$$

was used to calculate the activities of gallium (a_{Ga}). Where c is the mole fraction and γ is the activity coefficient. There is good agreement when experimental and computed results are compared to data from the literature.

Utilizing thermodynamic data collected over a wide temperature range, the Cu-Zr binary system was evaluated thermodynamically. The short-range ordering in the system is described using the associated solution model (Abe et al., 2006). The variational approach of the thermodynamic perturbation theory is used to compute the free energy of mixing in Fe-Ni alloys at various compositions and temperatures. The consistency with the existing experimental data is very good (Dubinin, 2009). Awe & Onifade (2012) worked within the context of two statistical theories QCA and SAM. By altering the surface coordination fraction u ($= 0.25, 0.5, 0.75$ and 1), the impacts of surface coordination on the surface (surface tension and surface concentration) and structural properties ($S_{cc}(0)$ and α_1) of Au-Zn, Na-Te, Ag-Cu, Cd-Ga, Bi-Cd, and Li-Mg liquid alloys was investigated. The results showed that a change in u does not significantly affect the c^s and σ for the segregating Ag-Cu and Cd-Ga system; and for the weakly interacting Bi-Cd and Li-Mg liquid alloys. On the other hand, this variables do significantly affect the short-range ordered Au-Zn and Na-Te liquid alloys. The $S_{cc}(0)$ has a considerable impact on the change in u values for the other alloys, it has no significant impact on the weakly interacting liquid alloys Bi-Cd and Li-Mg. However, the choice of u has a large impact on α_1 , for all alloys.

The phase diagram and thermodynamic properties of eleven important Mg-based binary systems, including Mg-Al, Mg-Zn, Mg-Mn, Mg-Ca, Mg-Sr, Mg-Y, Mg-Ni, Mg-Ce, Mg-Nd, Mg-Cu, and Mg-Sn, have been examined and critically evaluated. To provide a thorough knowledge of the systems, all the experimental data had been compiled and thoroughly evaluated. The optimized parameters were used to calculate the phase diagrams. According to experimental data, first-principles calculations, and CALPHAD

optimization, the heat of formation of intermetallic compounds is presented (Mezbahul-Islam et al., 2014). Based on the available experimental data, such as thermodynamic characteristics and phase equilibria data, thermodynamic assessments of the Mg-Pb and Mg-Bi systems were performed using the CALPHAD technique. Both the association model and the substitutional solution model were used to explain the liquid phase. In particular, for the liquid phase with the short range order behavior, it was discovered that the association model can more satisfactorily account for the experimental data than the substitutional solution one (Zhang et al., 2014). The free volume model (FVM) is used to examine the thermodynamic features of liquid Al-Cu and Al-Zn alloys. The experimental asymmetrical shape of mixing functions for liquid Al-Cu alloys is accurately reflected by the FVM data. The Warren-Cowley short range order parameter and concentration fluctuation $S_{cc}(0)$ in both binary alloys were investigated to better understand the local atomic arrangement. While Al-Zn alloy shows a tendency to phase separation, Al-Cu exhibits a high preference for hetero atomic nearest neighbors' bonds on the Cu rich side and weaker ones in the Al rich side part. Diffusivity has been investigated for both liquid alloys based on Darken's thermodynamic relationship (Trybuła et al., 2015).

2.3.7 Redlich-Kister polynomial method (RKPM)

It has been demonstrated that the exponential model for temperature (T) dependence of the excess Gibbs energy of liquid solutions within the Redlich-Kister polynomial (Redlich & Kister, 1948) is an effective tool for avoiding high- T artefacts such as an artificially inverted miscibility gap induced by the linear model. The exponential approach, however, can produce low- T artefacts. A low- T polynomial is introduced to address the low- T artefact and is matched with the exponential model at the system's lowest liquidus temperature (T^*). The low- T model is described by a four-parameter potential, which is derived analytically from the two fitted parameters of the exponential model. This ensures that the four excess functions (the excess Gibbs energy, the excess heat of mixing, the excess entropy, and the excess heat capacity) are continuous functions of T in the whole T -interval at any composition. When the complexity of the liquid alloy necessitates more than two semi-empirical parameters, it is recommended to utilize the combination linear-exponential model rather than the exponential model, with the same low- T potential. The latest assessment of the Mg-Si system demonstrates that the exponential model may be applied to this system without producing any artefacts (Kaptay, 2017). Recently, the exponential model has been utilized to eliminate artefacts in the various thermodynamic and structural properties of liquid alloys Cu-Si, Al-Mn, Al-Fe, Fe-Si, Al-Li and Li-Mg at higher temperatures (Gohivar, Koirala, et al., 2020; Gohivar, Yadav, et al., 2020; Gohivar, Yadav, Koirala, & Adhikari, 2021a; Gohivar, Yadav, Koirala, Shrestha, & Adhikari, 2021; Gohivar, Yadav, Koirala, & Adhikari, 2021b). Using square

well potential under the mean spherical model approximation, the Bhatia-Thronton (BT) correlation functions, specifically the number-number, concentration-concentration, and number-concentration correlation functions, are studied in liquid Al-Cu alloys. The concentration-concentration correlation function, $S_{cc}(0)$, which is used to describe the mixing behavior in binary melt, is a thermodynamically significant microscopic function that is analytically determined in the long wavelength limit. Through structural studies in the long wavelength limit, the Warren-Cowley chemical short range order parameter, α_1 is also calculated for liquid Al-Cu alloys as a function of Cu- content. The results obtained for the value of $S_{cc}(0)$ and α_1 provide evidence of the compound forming behavior in Al-Cu alloys. Using correlation functions in the binary mixture's long wavelength limit values, transport features also have been observed (Lalnehpuui et al., 2019).

CHAPTER 3

MATERIALS AND METHODOLOGY

To explain the thermodynamic characteristics of binary liquid alloys and to relate them to many other characteristics, a number of models and ideas have been put forth. Two different theories, such as the electronic theory of mixing and the statistical mechanical theory of mixing, can be used to study the alloying behavior of binary liquid alloys. In the first hypothesis, a liquid is said to be made up of an ion and electron system, and the charge transfer phenomenon is taken into consideration. In this method, the pseudo-potential theory (Hafner, 1977; R. N. Singh & Ali, 2006; Faruk & Bhuiyan, 2013) are typically used to address the problem. Although basic liquid metals and binary alloys were addressed in the application of the pseudo-potential theory, this cannot be used to learn about significant structural functions like $S_{cc}(0)$. On the other hand, workers turned their focus to alternative statistical techniques to get around this problem. By Bhatia and Hargrove (Bhatia et al., 1973), the Guggenheim (Guggenheim, 1952) conformal solution theory was updated and expanded as a complex formation model (CFM), which is helpful to analyze Gibbs free energy of mixing, enthalpy of mixing, entropy of mixing and $S_{cc}(0)$. However, there was no extension to determine the chemical short-range parameter, α_1 in terms of thermodynamic properties for binary liquid alloys.

Within the framework of the CFM, there are two approximations that make it possible to approach the hetero atomic interactions of atoms in the liquid state in a correct way. These approximations are the approximation for strongly (Westbrook, 1996) interactive systems and the approximation for weakly (Bhatia & Singh, 1984) interactive systems. The approach can be reduced to a quasi-chemical approximation (QCA) for regular solutions due to the absence of clusters in the mixture. The complex formation approach was simplified and presented under various titles, including simple statistical model

(SSM), self-association model (SAM), and quasi lattice theory (QLT). The SAM is used to explore the demixing propensity in liquid alloys, whereas the SSM only works for symmetric types of alloys. To detect chemical short range order parameter and diffusion coefficient, the complex formation model for thermodynamic characteristics and concentration fluctuation in zero wave vector has been expanded in the current work. To explore these features at high temperatures, the CFM is further expanded. Viscosity as a function of composition is investigated within the framework of the BBK (Budai-Benko-Kaptay) model (Budai et al., 2007), and surface features such as surface concentration and surface tension have been investigated by Kaptay's revision of the Butler model (Kaptay, 2019).

The complex formation model makes the assumption that compounds are very likely to exist in the liquid state at one or more stoichiometric compositions if they are formed at one or more stoichiometric compositions in the solid state. By assuming that complexes exist close to melting points, the alloying behavior of binary solution can be studied. The preferred association between the constituent species is a model presumption. The molten alloy is assumed to be made up of a ternary combination of A and B atoms, as well as a number of chemical complexes A_pB_q , which are all in chemical equilibrium with one another. In this context, p and q both are pairs of small integers represent the stoichiometric indices for the binary alloy.

3.1 Thermodynamic Properties

Thermodynamic properties are affected when components A and B are combined to form a binary A-B solution. Whether the chosen system forms compounds or segregates depends on changes in thermodynamic characteristics. The ternary mixture, also known as conformational solution, is assumed to consist of three species: A atom, B atom, and chemical complex A_pB_q . Let c be the atomic concentration of A atoms (the percentage contribution of A in the A-B ideal before mixing), and $(1-c)$ be the atomic concentration for B atoms (the percentage contribution of B in the A-B ideal before mixing). Due to the production of compounds in the melt, the amount of free atoms will decrease. Now, given n_1 gram of A , n_2 gram of B , and n_3 gram of A_pB_q atoms (Bhatia & Hargrove, 1974),

$$n_1 = c - pn_3, \quad n_2 = (1 - c) - qn_3 \quad (3.1)$$

and the total number of atoms,

$$n = n_1 + n_2 + n_3 = 1 - (p + q - 1)n_3 \quad (3.2)$$

In thermodynamics, the chemical potential of a species is a type of energy that can be taken in or given off during a chemical reaction or phase change when the number of particles in the species changes. The chemical potential of the species in a mixture is the rate at which the free energy of a thermodynamic system changes in relation to the change in the number of atoms or molecules of the species that are added to the system. So, it is a partial change in the free energy based on the amount of the species, while the concentration of all other species in the mixture stays the same. When both the temperature and the pressure remained the constant, the partial molar Gibb's free energy is the chemical potential. Fermi energy is the name for the chemical potential at 0 K in a semiconductor. Now, if we write the chemical potential per atom of species i ($i = 1, 2, 3$) in its unmixed (pure) form as $G_i^{(0)}$, we may write the free energy of mixing of the binary A-B mixture as (Bhatia & Hargrove, 1974),

$$G_M = G - \sum_i n_i G_i^{(0)}$$

$$G_M = G - NcG_1^{(0)} - N(1-c)G_2^{(0)} = -n_3\chi + G' \quad (3.3)$$

In the equation 3.3, G represents the total Gibbs free energy before mixing,

$$\chi = pG_1^{(0)} + qG_2^{(0)} - G_3^{(0)} \quad \text{and} \quad G' = G - (n_1G_1^{(0)} + n_2G_2^{(0)} + n_3G_3^{(0)})$$

where $-n_3\chi$ denotes a decrease in free energy caused by the formation of the compound, and χ denotes the energy required for the formation of the complex. The free energy of mixing of the ternary mixture of A, B, and A_pB_q is denoted by the symbol G' . Weak interactions are assumed to exist between n_1 , n_2 and n_3 for any given quantity of each respective atom.

The components of a mixture do not chemically react with one another in an ideal solution. The total volume is the same as the total of the individual volumes. For the solution to perform ideally, interactions between like and unlike molecules must be same. No heat is absorbed or created as a result of the mixing process in an ideal mixture since the components do not react with one another. When inter molecular forces between dissimilar molecules are weaker than those between like molecules, positive divergence from ideal behavior occurs. When inter molecular forces between dissimilar molecules are stronger than those between like molecules, the behavior deviates negatively from the ideal.

According to the statistical concept of entropy, $\Delta S = nR\ln V_2/V_1$. Now, for each gas, V_1 is the initial volume of gas and V_2 is the final volume, which is $V_A + V_B$ when both gases

are combined. So, for the two distinct components,

$$\Delta S_A = n_A R \ln \left(\frac{V_A + V_B}{V_A} \right) \quad \text{and} \quad \Delta S_B = n_B R \ln \left(\frac{V_A + V_B}{V_B} \right)$$

The overall entropy of mixing is,

$$\Delta S_{\text{mix}} = \Delta S_A + \Delta S_B = n_A R \ln \left(\frac{V_A + V_B}{V_A} \right) + n_B R \ln \left(\frac{V_A + V_B}{V_B} \right)$$

Recalling the ideal gas equation $PV = nRT$, we can see that the number of moles is precisely proportional to volume, allowing us to replace volume with the number of moles.

$$\Delta S_{\text{mix}} = n_A R \ln \left(\frac{n_A + n_B}{n_A} \right) + n_B R \ln \left(\frac{n_A + n_B}{n_B} \right)$$

$$\Delta S_{\text{mix}} = -n_A R \ln \left(\frac{n_A}{n} \right) - n_B R \ln \left(\frac{n_B}{n} \right)$$

where $n = n_A + n_B$

$$\Delta S_{\text{mix}} = -R \left(n_A \ln \left(\frac{n_A}{n} \right) + n_B \ln \left(\frac{n_B}{n} \right) \right)$$

$$\Delta S_{\text{mix}} = -R \sum n_i \ln \left(\frac{n_i}{n} \right) \quad (3.4)$$

Now the free energy that comes from mixing is, $\Delta G_{\text{mix}} = \Delta H_{\text{mix}} - T\Delta S_{\text{mix}}$

For an ideal solution, $\Delta H_{\text{mix}} = 0$

$$\Delta G_{\text{mix}} = RT \sum n_i \ln \left(\frac{n_i}{n} \right) \quad (3.5)$$

Consequently, in the event that the binary melt is an ideal solution,

$$G' = RT \sum n_i \ln \left(\frac{n_i}{n} \right) \quad (3.6)$$

The theory of regular solutions in the zeroth approximation (Guggenheim, 1952) or the conformal solution approximation (Longuet-Higgins, 1951) is valid if the effects of the different sizes of the mixture's constituents cannot be ignored and the interaction E_{ij} is minimal but not zero. Assign the interactions between two A components, E_{AA} , two B components, E_{BB} , and an A and a B , E_{AB} , in a solution made up of two atoms A and B . The ideal solution is achieved if the three interaction energies are equal. The solution's

thermodynamic behavior will not be ideal if they are not equal.

Assume that a solution was formed by combining n_A and n_B molecules of A and B atoms respectively. The number of AA interactions (n_{AA}), BB interactions (n_{BB}), and AB interactions (n_{AB}) determines the energy ($U(A,B)$) of such a solution.

$$U(A, B) = n_{AA}E_{AA} + n_{AB}E_{AB} + n_{BB}E_{BB} \quad (3.7)$$

This lattice-based solution theory is sometimes referred to as regular solution theory. The interactions between molecules in a regular solution are weak, and all molecules are roughly the same size. In the theory of regular solutions, the number of sites for a certain lattice position is an essential number. This can be compared to the number of neighbors a molecule of A or B has, which in this simple lattice model is z for A and B . Therefore, the number of neighbors surrounding n_A molecules is zn_A and can be written as the number of AA and AB contacts, n_{AA} and n_{AB} .

$$\begin{aligned} zn_A &= 2n_{AA} + n_{AB} \\ n_{AA} &= \frac{zn_A - n_{AB}}{2} \end{aligned} \quad (3.8)$$

There exists a similar equation for the number of neighbors surrounding B molecules.

$$\begin{aligned} zn_B &= 2n_{BB} + n_{AB} \\ n_{BB} &= \frac{zn_B - n_{AB}}{2} \end{aligned} \quad (3.9)$$

Substituting the equations 3.8 and 3.9 for equation 3.7

$$\begin{aligned} U(A, B) &= \left(\frac{zn_A - n_{AB}}{2}\right) E_{AA} + n_{AB}E_{AB} + \left(\frac{zn_B - n_{AB}}{2}\right) E_{BB} \\ &= \left(\frac{zE_{AA}}{2}\right) n_A + \left(\frac{zE_{BB}}{2}\right) n_B + \left(E_{AB} - \frac{E_{AA} + E_{BB}}{2}\right) n_{AB} \end{aligned} \quad (3.10)$$

The only unknown parameter in this equation is n_{AB} , as the number of AB contacts relies on the particular arrangement of A and B on the lattice. However, we may calculate this amount using statistics. The probability that a given A molecule has a B neighbor is

$$P_B = \frac{n_B}{n_A + n_B} = \frac{n_B}{n}$$

Therefore, the number of AB contacts equals the number of neighbors around $n_A A$ molecules multiplied by the probability that at least one of these neighbors is a B

molecule.

$$n_{AB} = z n_A P_B = \frac{z n_A n_B}{n}$$

The energy equation 3.10 now becomes

$$U(A, B) = \left(\frac{z E_{AA}}{2} \right) n_A + \left(\frac{z E_{BB}}{2} \right) n_B + \left(E_{AB} - \frac{E_{AA} + E_{BB}}{2} \right) \left(\frac{z n_A n_B}{n} \right)$$

$$U(A, B) = \left(\frac{z E_{AA}}{2} \right) n_A + \left(\frac{z E_{BB}}{2} \right) n_B + \beta RT \left(\frac{n_A n_B}{n} \right)$$

where

$$\beta = \frac{z}{RT} \left(E_{AB} - \frac{E_{AA} + E_{BB}}{2} \right)$$

The energy equation consists of three parts, which may be written as

$$U(A, B) = U(A) + U(B) + \Delta U_{\text{mix}}(A, B)$$

The energies of the separated components are represented by the first two terms. The third term results from the mixing of components.

$$\Delta U_{\text{mix}} = \beta RT \left(\frac{n_A n_B}{n} \right)$$

Remember also that $\Delta H = \Delta U + \Delta(PV) \approx \Delta U$ if the solution's pressure and volume remained the constant. Then, for a regular solution,

$$\Delta H_{\text{mix}} \approx \Delta U_{\text{mix}} = \beta RT \left(\frac{n_A n_B}{n} \right)$$

$A - B$ interactions are preferable than $A - A$ and $B - B$ interactions if $\beta < 0$, which means that mixing is exothermic. The mixing is endothermic if $\beta > 0$.

Let us define a parameter represented as Ψ_{AB} , which is an indicator of the interactions that occur between $A - B$ molecules relative to $A - A$ and $B - B$ molecules.

$$\Psi_{AB} = \beta RT$$

$$\Delta H_{\text{mix}} = \Psi_{AB} \left(\frac{n_A n_B}{n} \right)$$

For systems with multiple components, it is given by

$$\Delta H_{\text{mix}} = \sum \Psi_{ij} \left(\frac{n_i n_j}{n} \right) \quad (3.11)$$

The Gibbs free energy, enthalpy and entropy of mixing are related as

$$G' = \Delta H_{\text{mix}} - T\Delta S_{\text{mix}} \quad (3.12)$$

When equation 3.4 is combined with equations 3.11 and 3.12, we obtain the equation (3.13)

$$G' = RT \sum n_i \ln \left(\frac{n_i}{n} \right) + \sum \Psi_{ij} \left(\frac{n_i n_j}{n} \right) \quad (3.13)$$

This equation is also called conformal solution approximation. Where Ψ_{ij} ($= 0$ for $i = j$) are called interaction energies. By definition, Ψ_{ij} do not depend on concentration, but they may depend on temperature and pressure.

Substituting G' from equation 3.13 into equation 3.3, we obtain the expression for free energy of mixing G_M for binary alloys

$$G_M = -n_3\chi + RT \sum_{i=1}^3 n_i \ln \left(\frac{n_i}{n} \right) + \sum_{i<j} \sum \left(\frac{n_i n_j}{n} \right) \Psi_{ij} \quad (3.14)$$

If the value of (G_M/RT) falls between 0 and -1, the system interacts weakly; if it falls between -1 and -2, the system interacts moderately; and if it falls below -2.5, the system interacts strongly (Lele & Ramachandrarao, 1981). Since,

$$\Delta G = \Delta U + P\Delta V - T\Delta S = \Delta H - T\Delta S \quad (3.15)$$

In the case of mixing, equation 3.15 can be expressed as,

$$G_M = H_M - TS_M \quad (3.16)$$

Differentiating equation 3.16 with respect to temperature,

$$\frac{\partial G_M}{\partial T} = -S_M$$

Substituting S_M for equation 3.16

$$H_M = G_M - T \left(\frac{\partial G_M}{\partial T} \right)_P \quad (3.17)$$

This equation is called the Gibbs-Helmholtz equation.

We can use equation 3.17 in equation 3.14 to determine the expression for enthalpy of

mixing for a binary liquid system.

$$H_M = -n_3\chi + RT \sum_{i=1}^3 n_i \ln \left(\frac{n_i}{n} \right) + \sum_{i<j} \sum \left(\frac{n_i n_j}{n} \right) \Psi_{ij} - T \frac{\partial}{\partial T} \left[-n_3\chi + RT \sum_{i=1}^3 n_i \ln \left(\frac{n_i}{n} \right) + \sum_{i<j} \sum \left(\frac{n_i n_j}{n} \right) \Psi_{ij} \right] \quad (3.18)$$

$$H_M = -n_3\chi + RT \sum_{i=1}^3 n_i \ln \left(\frac{n_i}{n} \right) + \sum_{i<j} \sum \left(\frac{n_i n_j}{n} \right) \Psi_{ij} + n_3 T \frac{\partial \chi}{\partial T} - RT \sum_{i=1}^3 n_i \ln \left(\frac{n_i}{n} \right) - T \sum_{i<j} \sum \left(\frac{n_i n_j}{n} \right) \frac{\partial \Psi_{ij}}{\partial T} \quad (3.19)$$

$$H_M = -n_3 \left[\chi - T \left(\frac{\partial \chi}{\partial T} \right) \right] + \sum_{i<j} \sum \left(\frac{n_i n_j}{n} \right) \left[\Psi_{ij} - T \frac{\partial \Psi_{ij}}{\partial T} \right] \quad (3.20)$$

Substituting G_M and H_M from equations 3.14 and 3.20, respectively, into equation 3.16

$$S_M = n_3 \frac{\partial \chi}{\partial T} - R \sum_{i=1}^3 n_i \ln \frac{n_i}{n} - \sum_{i<j} \sum \frac{n_i n_j}{n} \frac{\partial \Psi_{ij}}{\partial T} \quad (3.21)$$

One of the fundamental assumptions of CFM is that the mixture of A atoms, B atoms, and chemical complexes of type $A_p B_q$ are in chemical equilibrium. This necessitates that, under constant temperature and pressure, G_M must be a minimum value that determines the number of chemical species in equilibrium. Consequently, the equilibrium value of chemical complexes, n_3 , at a particular pressure and temperature is calculated as follows (Bhatia & Hargrove, 1974):

$$\left(\frac{\partial G_M}{\partial n_3} \right)_{T,P,N,c} = 0 \quad (3.22)$$

Using equation (3.14) on (3.22)

$$\frac{\partial}{\partial n_3} \left[-n_3\chi + RT \sum_{i=1}^3 n_i \ln \left(\frac{n_i}{n} \right) + \sum_{i=j} \sum \left(\frac{n_i n_i}{n} \right) \Psi_{ij} \right] = 0$$

$$\frac{\partial}{\partial n_3} [t_1 + t_2 + t_3] = 0 \quad (3.23)$$

$$\frac{\partial t_1}{\partial n_3} = \frac{\partial(-n_3\chi)}{\partial n_3} = -\chi \quad (3.24)$$

Here,

$$\begin{aligned} \frac{\partial t_2}{\partial n_3} &= \frac{\partial}{\partial n_3} \left[\sum_{i=1}^3 n_i \ln \left(\frac{n_i}{n} \right) \right] \\ \frac{\partial t_2}{\partial n_3} &= \frac{\partial}{\partial n_3} \left[n_1 \ln \left(\frac{n_1}{n} \right) \right] + \frac{\partial}{\partial n_3} \left[n_2 \ln \left(\frac{n_2}{n} \right) \right] + \frac{\partial}{\partial n_3} \left[n_3 \ln \left(\frac{n_3}{n} \right) \right] \\ \frac{\partial t_2}{\partial n_3} &= \frac{\partial}{\partial n_3} (t_{21} + t_{22} + t_{23}) \end{aligned} \quad (3.25)$$

Now,

$$\begin{aligned} \frac{\partial t_{21}}{\partial n_3} &= \frac{\partial}{\partial n_3} \left[n_1 \ln \left(\frac{n_1}{n} \right) \right] = \ln \left(\frac{n_1}{n} \right) \frac{\partial n_1}{\partial n_3} + n_1 \frac{\partial \ln (n_1/n)}{\partial n_3} \\ &= \ln \left(\frac{n_1}{n} \right) \frac{\partial (c - pn_3)}{\partial n_3} + n_1 \frac{\partial \ln (n_1)}{\partial n_3} - n_1 \frac{\partial \ln (n)}{\partial n_3} \\ \frac{\partial t_{21}}{\partial n_3} &= -p \ln \left(\frac{n_1}{n} \right) - p + \frac{n_1}{n} (p + q - 1) \end{aligned} \quad (3.26)$$

and,

$$\begin{aligned} \frac{\partial t_{22}}{\partial n_3} &= \frac{\partial}{\partial n_3} \left[n_2 \ln \left(\frac{n_2}{n} \right) \right] = \ln \left(\frac{n_2}{n} \right) \frac{\partial n_2}{\partial n_3} + n_2 \frac{\partial \ln (n_2/n)}{\partial n_3} \\ &= \ln \left(\frac{n_2}{n} \right) \frac{\partial (1 - c - qn_3)}{\partial n_3} + n_2 \frac{\partial \ln (n_2)}{\partial n_3} - n_2 \frac{\partial \ln (n)}{\partial n_3} \\ \frac{\partial t_{22}}{\partial n_3} &= -q \ln \left(\frac{n_2}{n} \right) - q + \frac{n_2}{n} (p + q - 1) \end{aligned} \quad (3.27)$$

similarly,

$$\begin{aligned} \frac{\partial t_{23}}{\partial n_3} &= \frac{\partial}{\partial n_3} \left[n_3 \ln \left(\frac{n_3}{n} \right) \right] \\ &= \ln \left(\frac{n_3}{n} \right) + n_3 \frac{\partial \ln (n_3)}{\partial n_3} - n_3 \frac{\partial \ln (n)}{\partial n_3} \\ \frac{\partial t_{23}}{\partial n_3} &= \ln \left(\frac{n_3}{n} \right) + 1 + \frac{n_3}{n} (p + q - 1) \end{aligned} \quad (3.28)$$

Now using equations 3.26, 3.27 and 3.28 in 3.25

$$\begin{aligned}
\frac{\partial t_2}{\partial n_3} &= RT \left[-p \ln \left(\frac{n_1}{n} \right) - p + \frac{n_1}{n} (p+q-1) - q \ln \left(\frac{n_2}{n} \right) - q \right. \\
&\quad \left. + \frac{n_2}{n} (p+q-1) \ln \left(\frac{n_3}{n} \right) + 1 + \frac{n_3}{n} (p+q-1) \right] \\
&= RT \left[\ln \left(\frac{n_3}{n} \right) - \ln \left(\frac{n_1}{n} \right)^p - \ln \left(\frac{n_2}{n} \right)^q - (p+q-1) + (p+q+1) \frac{n_1+n_2+n_3}{n} \right] \\
&= RT \left[\ln \left(\frac{n_3}{n} \right) - \ln \left(\frac{n_1}{n} \right)^p - \ln \left(\frac{n_2}{n} \right)^q \right] \\
&= RT \left[\ln \left\{ \frac{n_3}{n} \left(\frac{n}{n_1} \right)^p \left(\frac{n}{n_2} \right)^q \right\} \right] \\
\frac{\partial t_2}{\partial n_3} &= RT \ln \left(n_3 n^{p+q-1} n_1^{-p} n_2^{-q} \right) \tag{3.29}
\end{aligned}$$

Again

$$\begin{aligned}
\frac{\partial t_3}{\partial n_3} &= \frac{\partial}{\partial n_3} \left[\sum_{i < j} \sum \left(\frac{n_i n_j}{n} \right) \Psi_{ij} \right] = \frac{\partial}{\partial n_3} \left[\frac{n_1 n_2}{n} \Psi_{12} + \frac{n_2 n_3}{n} \Psi_{23} + \frac{n_1 n_3}{n} \Psi_{13} \right] \\
\frac{\partial t_3}{\partial n_3} &= \frac{\partial}{\partial n_3} (t_{31} + t_{32} + t_{33}) \tag{3.30}
\end{aligned}$$

Now

$$\begin{aligned}
\frac{\partial t_{31}}{\partial n_3} &= \frac{\partial}{\partial n_3} \left(\frac{n_1 n_2}{n} \Psi_{12} \right) = \left[\frac{\partial n_1}{\partial n_3} \frac{n_2}{n} + \frac{\partial n_2}{\partial n_3} \frac{n_1}{n} + n_1 n_2 \frac{\partial}{\partial n_3} \left(\frac{1}{n} \right) \right] \Psi_{12} \\
&= \left[\frac{n_2}{n} (-u) + \frac{n_1}{n} (-v) + \frac{n_1 n_2}{n^2} (u+v-1) \right] \Psi_{12} \\
\frac{\partial t_{31}}{\partial n_3} &= \left[\frac{n_1 n_2}{n^2} (p+q-1) - p \frac{n_2}{n} - q \frac{n_1}{n} \right] \Psi_{12} \tag{3.31}
\end{aligned}$$

Again

$$\begin{aligned}
\frac{\partial t_{32}}{\partial n_3} &= \frac{\partial}{\partial n_3} \left(\frac{n_2 n_3}{n} \Psi_{23} \right) = \left[\frac{\partial n_2}{\partial n_3} \frac{n_3}{n} + \frac{\partial n_3}{\partial n_3} \frac{n_2}{n} + n_2 n_3 \frac{\partial}{\partial n_3} \left(\frac{1}{n} \right) \right] \Psi_{23} \\
&= \left[\frac{n_3}{n} (-q) + \frac{n_2}{n} + \frac{n_2 n_3}{n^2} (p+q-1) \right] \Psi_{23} \\
\frac{\partial t_{32}}{\partial n_3} &= \left[\frac{n_2 n_3}{n^2} (p+q-1) - q \frac{n_3}{n} + \frac{n_2}{n} \right] \Psi_{23} \tag{3.32}
\end{aligned}$$

Again

$$\begin{aligned}\frac{\partial t_{33}}{\partial n_3} &= \frac{\partial}{\partial n_3} \left(\frac{n_1 n_3}{n} \Psi_{13} \right) = \left[\frac{\partial n_1}{\partial n_3} \frac{n_3}{n} + \frac{\partial n_3}{\partial n_3} \frac{n_1}{n} + n_1 n_3 \frac{\partial}{\partial n_3} \left(\frac{1}{n} \right) \right] \Psi_{13} \\ &= \left[\frac{n_3}{n} (-p) + \frac{n_1}{n} + \frac{n_1 n_3}{n^2} (p+q-1) \right] \Psi_{13} \\ \frac{\partial t_{33}}{\partial n_3} &= \left[\frac{n_1 n_3}{n^2} (p+q-1) - p \frac{n_3}{n} + \frac{n_1}{n} \right] \Psi_{13}\end{aligned}\quad (3.33)$$

Substituting equations 3.31, 3.32 and 3.33 in 3.30

$$\begin{aligned}\frac{\partial t_3}{\partial n_3} &= \left[\frac{n_1 n_2}{n^2} (p+q-1) - p \frac{n_2}{n} - q \frac{n_1}{n} \right] \Psi_{12} + \left[\frac{n_2 n_3}{n^2} (p+q-1) - q \frac{n_3}{n} + \frac{n_2}{n} \right] \Psi_{23} \\ &+ \left[\frac{n_1 n_3}{n^2} (p+q-1) - p \frac{n_3}{n} + \frac{n_1}{n} \right] \Psi_{13}\end{aligned}\quad (3.34)$$

Now using equation, 3.24 together with equations 3.29 and 3.34 in equation 3.23

$$\begin{aligned}-\chi + RT \ln \left(n_3 n^{p+q-1} n_1^{-p} n_2^{-q} \right) + \left[\frac{n_1 n_2}{n^2} (p+q-1) - p \frac{n_2}{n} - q \frac{n_1}{n} \right] \Psi_{12} \\ + \left[\frac{n_2 n_3}{n^2} (p+q-1) - q \frac{n_3}{n} + \frac{n_2}{n} \right] \Psi_{23} + \left[\frac{n_1 n_3}{n^2} (p+q-1) - p \frac{n_3}{n} + \frac{n_1}{n} \right] \Psi_{13} = 0\end{aligned}$$

$$\begin{aligned}\ln \left(n_3 n^{p+q-1} n_1^{-p} n_2^{-q} \right) + \left[\frac{n_1 n_2}{n^2} (p+q-1) - p \frac{n_2}{n} - q \frac{n_1}{n} \right] \frac{\Psi_{12}}{RT} + \left[\frac{n_2 n_3}{n^2} (p+q-1) - q \frac{n_3}{n} + \frac{n_2}{n} \right] \frac{\Psi_{23}}{RT} \\ + \left[\frac{n_1 n_3}{n^2} (p+q-1) - p \frac{n_3}{n} + \frac{n_1}{n} \right] \frac{\Psi_{13}}{RT} = \frac{\chi}{RT}\end{aligned}$$

$$\ln \left(n_3 n^{p+q-1} n_1^{-p} n_2^{-q} \right) + Y = \frac{\chi}{RT}\quad (3.35)$$

where

$$\begin{aligned}Y = \left[\frac{n_1 n_2}{n^2} (p+q-1) - p \frac{n_2}{n} - q \frac{n_1}{n} \right] \frac{\Psi_{12}}{RT} + \left[\frac{n_2 n_3}{n^2} (p+q-1) - q \frac{n_3}{n} + \frac{n_2}{n} \right] \frac{\Psi_{23}}{RT} \\ + \left[\frac{n_1 n_3}{n^2} (p+q-1) - p \frac{n_3}{n} + \frac{n_1}{n} \right] \frac{\Psi_{13}}{RT}\end{aligned}$$

From equation 3.35

$$-\ln \left(n_3 n^{p+q-1} n_1^{-p} n_2^{-q} \right) - Y = -\frac{\chi}{RT}$$

$$\ln \left(n_3 n^{p+q-1} n_1^{-p} n_2^{-q} \right)^{-1} = Y - \frac{\chi}{RT}\quad (3.36)$$

$$\left(n_3 n^{p+q-1} n_1^{-p} n_2^{-q} \right)^{-1} = \exp \left(Y - \frac{\chi}{RT} \right) = \exp(Y) \exp \left(-\frac{\chi}{RT} \right) = k \exp(Y)$$

where $\exp(-\chi/RT) = k$.

$$n_1^p n_2^q = \left(n_3 n^{p+q-1} \right) k \exp(Y) \quad (3.37)$$

In complex formation model, equation 3.37 is called the equilibrium equation.

3.2 Structural Properties

The concentration-concentration structural factor $S_{cc}(0)$, which denotes concentration variation in the long wave length limit, has drawn a lot of interest (Ratti & Bhatia, 1975; Ramachandrarao et al., 1984). The partial structural factor's long-wavelength limit provides direct information regarding whether the mixture is ideal or not (Bhatia & March, 1975b). In a number of binary liquid alloys, G_M and the heat mixing H_M are compositionally asymmetric. This asymmetry is frequently attributed to differences in the size, valency, and electronegativity of the liquid alloy's constituents. Despite the fact that these characteristics are also responsible for stimulating the formation of compounds or complexes in the alloy, asymmetry in the compositional dependency of these features does not necessarily imply complex formation. In this context, the use of $S_{cc}(0)$ is preferable to direct thermodynamic analysis for determining the extent of association in the liquid. $S_{cc}(0)$ is proportional to the mean-square concentration fluctuation in the long wave length limit ($q \rightarrow 0$), and it is related to thermodynamic data via the curvature of the free energy G_M in the $G_M - c$ diagram i.e. $\partial^2 G_M / \partial c^2$. When using the standard statistical thermodynamic relation, one arrives at the following relationship between $S_{cc}(0)$ and the Darken stability function, $\partial^2 G_M / \partial c^2$ (Bhatia & Thornton, 1970):

$$S_{cc}(0) = RT \left(\frac{\partial^2 G_M}{\partial c^2} \right)_{T,P,N}^{-1} \quad (3.38)$$

We have from equation 3.14

$$\frac{\partial^2 G_M}{\partial c^2} = \frac{\partial^2}{\partial c^2} \left[-n_3 \chi + RT \sum_{i=1}^3 n_i \ln \left(\frac{n_i}{n} \right) + \sum_{i<j} \sum \left(\frac{n_i n_j}{n} \right) \Psi_{ij} \right]$$

$$\frac{\partial^2 G_m}{\partial c^2} = \frac{\partial^2 d_1}{\partial c^2} + RT \frac{\partial^2 d_2}{\partial c^2} + \frac{\partial^2 d_3}{\partial c^2} \quad (3.39)$$

Here

$$d_1 = -n_3 \chi, \quad d_2 = \sum_{i=1}^3 n_i \ln \left(\frac{n_i}{n} \right), \quad \text{and} \quad d_3 = \sum_{i<j} \sum \left(\frac{n_i n_j}{n} \right) \Psi_{ij}$$

Now,

$$\frac{\partial d_1}{\partial c} = \frac{\partial(-n_3\chi)}{\partial c} = -n'_3\chi$$

$$\frac{\partial^2 d_1}{\partial c^2} = -n''_3\chi \quad (3.40)$$

Again,

$$\frac{\partial d_2}{\partial c} = \frac{\partial}{\partial c} \left[\sum_{i=1}^3 n_i \ln \left(\frac{n_i}{n} \right) \right] = \frac{\partial}{\partial c} \left[n_1 \ln \left(\frac{n_1}{n} \right) + n_2 \ln \left(\frac{n_2}{n} \right) + n_3 \ln \left(\frac{n_3}{n} \right) \right]$$

$$\frac{\partial d_2}{\partial c} = \left(\frac{\partial d_{21}}{\partial c} + RT \frac{\partial d_{22}}{\partial c} + \frac{\partial d_{23}}{\partial c} \right) \quad (3.41)$$

Now,

$$\frac{\partial d_{21}}{\partial c} = \frac{\partial}{\partial c} (n_1 \ln n_1 - n_1 \ln n) = \frac{n_1 n'_1}{n_1} + n'_1 \ln n_1 - n'_1 \ln n - \frac{n_1 n'_1}{n}$$

$$\frac{\partial d_{21}}{\partial c} = n'_1 + n'_1 \ln n_1 - n'_1 \ln n - \frac{n_1 n'_1}{n} \quad (3.42)$$

and

$$\frac{\partial d_{22}}{\partial c} = \frac{\partial}{\partial c} (n_2 \ln n_2 - n_2 \ln n) = \frac{n_2 n'_2}{n_2} + n'_2 \ln n_2 - n'_2 \ln n - \frac{n_2 n'_2}{n}$$

$$\frac{\partial d_{22}}{\partial c} = n'_2 + n'_2 \ln n_2 - n'_2 \ln n - \frac{n_2 n'_2}{n} \quad (3.43)$$

Similarly,

$$\frac{\partial d_{23}}{\partial c} = \frac{\partial}{\partial c} (n_3 \ln n_3 - n_3 \ln n) = \frac{n_3 n'_3}{n_3} + n'_3 \ln n_3 - n'_3 \ln n - \frac{n_3 n'_3}{n}$$

$$\frac{\partial d_{23}}{\partial c} = n'_3 + n'_3 \ln n_3 - n'_3 \ln n - \frac{n_3 n'_3}{n} \quad (3.44)$$

Now using equations, 3.42, 3.43 and 3.44 in equation 3.41

$$\begin{aligned}\frac{\partial d_2}{\partial c} &= n'_1 + n'_1 \ln n_1 - n'_1 \ln n - \frac{n_1 n'}{n} + n'_2 + n'_2 \ln n_2 - n'_2 \ln n - \frac{n_2 n'}{n} + n'_3 + n'_3 \ln n_3 - n'_3 \ln n - \frac{n_3 n'}{n} \\ \frac{\partial d_2}{\partial c} &= n'_1 + n'_2 + n'_3 + n'_1 \ln n_1 + n'_2 \ln n_2 + n'_3 \ln n_3 - \ln n (n'_1 + n'_2 + n'_3) - \frac{n'}{n} (n_1 + n_2 + n_3) \\ \frac{\partial d_2}{\partial c} &= n' + n'_1 \ln n_1 + n'_2 \ln n_2 + n'_3 \ln n_3 - n' \ln n - n' \\ \frac{\partial d_2}{\partial c} &= -n' \ln n + n'_1 \ln n_1 + n'_2 \ln n_2 + n'_3 \ln n_3\end{aligned}\quad (3.45)$$

Again

$$\begin{aligned}\frac{\partial^2 d_2}{\partial c^2} &= -n'' \ln n - \frac{(n')^2}{n} + n''_1 \ln n_1 + \frac{(n'_1)^2}{n_1} + n''_2 \ln n_2 + \frac{(n'_2)^2}{n_2} + n''_3 \ln n_3 + \frac{(n'_3)^2}{n_3} \\ \frac{\partial^2 d_2}{\partial c^2} &= \frac{(n'_1)^2}{n_1} + \frac{(n'_2)^2}{n_2} + \frac{(n'_3)^2}{n_3} - \frac{(n')^2}{n} + n''_1 \ln n_1 + n''_2 \ln n_2 + n''_3 \ln n_3 - n'' \ln n \\ \frac{\partial^2 d_2}{\partial c^2} &= \left[\sum_1^3 \frac{(n'_i)^2}{n_i} - \frac{(n')^2}{n} \right] + n''_1 \ln n_1 + n''_2 \ln n_2 + n''_3 \ln n_3 - n'' \ln n\end{aligned}\quad (3.46)$$

Now the term, $n''_1 \ln n_1 + n''_2 \ln n_2 + n''_3 \ln n_3 - n'' \ln n$ in equation 3.46 is

$$\begin{aligned}&= -pn''_3 \ln n_1 - qn''_3 \ln n_2 + n''_3 \ln n_3 + (p + q - 1)n''_3 \ln n \\ &= -n''_3 \ln n_1^p - n''_3 \ln n_2^q + n''_3 \ln n_3 + n''_3 \ln n^{(p+q-1)} \\ &= n''_3 \ln \left[\frac{n_3 n^{(p+q-1)}}{n_1^p n_2^q} \right] \\ &= n''_3 \ln \left[\frac{n_3 n^{(p+q-1)}}{n_3 n^{(p+q-1)} k e^Y} \right] \\ &= -n''_3 \ln (k e^Y) = -n''_3 \ln (k) - n''_3 Y = \frac{n''_3 \chi}{RT} - n''_3 Y\end{aligned}$$

Substituting this expression in equation 3.46, one obtains,

$$RT \frac{\partial^2 d_2}{\partial c^2} = RT \sum_{i=1}^3 \left(\frac{(n'_i)^2}{n_i} - \frac{(n')^2}{n} \right) + n''_3 \chi - n''_3 Y RT \quad (3.47)$$

Now,

$$\frac{\partial d_3}{\partial c} = \frac{\partial}{\partial c} \left(\sum_{i=j} \sum \left(\frac{n_i n_i}{n} \right) \Psi_{ij} \right) = \frac{\partial}{\partial c} \left(\frac{n_1 n_2}{n} \Psi_{12} \right) + \frac{\partial}{\partial c} \left(\frac{n_2 n_3}{n} \Psi_{23} \right) + \frac{\partial}{\partial c} \left(\frac{n_1 n_3}{n} \Psi_{13} \right)$$

$$\frac{\partial d_3}{\partial c} = \frac{\partial d_{31}}{\partial c} + \frac{\partial d_{32}}{\partial c} + \frac{\partial d_{33}}{\partial c} \quad (3.48)$$

Again,

$$\frac{\partial d_{31}}{\partial c} = \frac{\partial}{\partial c} \left(\frac{n_1 n_2}{n} \Psi_{12} \right) = \left(\frac{n'_1 n_2}{n} + \frac{n_1 n'_2}{n} - \frac{n_1 n_2 n'}{n^2} \right) \Psi_{12}$$

$$\frac{\partial d_{31}}{\partial c} = \left[\frac{(1 - p n'_3) n_2}{n} + \frac{(-1 - q n'_3) n_1}{n} + \frac{(p + q - 1) n_1 n_2 n'_3}{n^2} \right] \Psi_{12}$$

$$\frac{\partial d_{31}}{\partial c} = \left[-\frac{n_1}{n} + \frac{n_2}{n} + \left\{ \frac{n_1 n_2}{n^2} (p + q - 1) - p \frac{n_2}{n} - q \frac{n_1}{n} \right\} n'_3 \right] \Psi_{12} \quad (3.49)$$

and

$$\frac{\partial d_{32}}{\partial c} = \frac{\partial}{\partial c} \left(\frac{n_2 n_3}{n} \Psi_{23} \right) = \left(\frac{n'_2 n_3}{n} + \frac{n_2 n'_3}{n} - \frac{n_2 n_3 n'}{n^2} \right) \Psi_{23}$$

$$\frac{\partial d_{32}}{\partial c} = \left[\frac{(-1 - q n'_3) n_3}{n} + \frac{n_2 n'_3}{n} + \frac{(p + q - 1) n_2 n_3 n'_3}{n^2} \right] \Psi_{23}$$

$$\frac{\partial d_{32}}{\partial c} = \left[-\frac{n_3}{n} + \left\{ \frac{n_2 n_3}{n^2} (p + q - 1) - q \frac{n_3}{n} + \frac{n_2}{n} \right\} n'_3 \right] \Psi_{23} \quad (3.50)$$

and

$$\frac{\partial d_{33}}{\partial c} = \frac{\partial}{\partial c} \left(\frac{n_1 n_3}{n} \Psi_{13} \right) = \left(\frac{n'_1 n_3}{n} + \frac{n_1 n'_3}{n} - \frac{n_1 n_3 n'}{n^2} \right) \Psi_{13}$$

$$\frac{\partial d_{33}}{\partial c} = \left[\frac{(1 - p n'_3) n_3}{n} + \frac{n_1 n'_3}{n} + \frac{(p + q - 1) n_1 n_3 n'_3}{n^2} \right] \Psi_{13}$$

$$\frac{\partial d_{33}}{\partial c} = \left[\frac{n_3}{n} + \left\{ \frac{n_1 n_3}{n^2} (p + q - 1) - p \frac{n_3}{n} + \frac{n_1}{n} \right\} n'_3 \right] \Psi_{13} \quad (3.51)$$

Substituting the corresponding values from equation 3.49, 3.50 and 3.51 in equation 3.48

$$\begin{aligned}
\frac{\partial d_3}{\partial c} &= \left[-\frac{n_1}{n} + \frac{n_2}{n} + \left\{ \frac{n_1 n_2}{n^2} (p+q-1) - u \frac{n_2}{n} - v \frac{n_1}{n} \right\} n_3' \right] \Psi_{12} \\
&+ \left[-\frac{n_3}{n} + \left\{ \frac{n_2 n_3}{n^2} (p+q-1) - q \frac{n_3}{n} + \frac{n_2}{n} \right\} n_3' \right] \Psi_{23} \\
&+ \left[\frac{n_3}{n} + \left\{ \frac{n_1 n_3}{n^2} (p+q-1) - p \frac{n_3}{n} + \frac{n_1}{n} \right\} n_3' \right] \Psi_{13} \\
&= \left(-\frac{n_1}{n} + \frac{n_2}{n} \right) \Psi_{12} - \frac{n_3}{n} \Psi_{23} + \frac{n_3}{n} \Psi_{13} + n_3' \text{RT} \left[\left\{ \frac{\Psi_{12}}{\text{RT}} \left(\frac{n_1 n_2}{n^2} (p+q-1) - p \frac{n_2}{n} - q \frac{n_1}{n} \right) \right. \right. \\
&+ \left. \frac{\Psi_{23}}{\text{RT}} \left\{ \frac{n_2 n_3}{n^2} (p+q-1) - q \frac{n_3}{n} + \frac{n_2}{n} \right\} + \frac{\Psi_{13}}{\text{RT}} \left\{ \frac{n_1 n_3}{n^2} (p+q-1) - p \frac{n_3}{n} + \frac{n_1}{n} \right\} \right. \\
\frac{\partial d_3}{\partial c} &= \left(-\frac{n_1}{n} + \frac{n_2}{n} \right) \Psi_{12} - \frac{n_3}{n} \Psi_{23} + \frac{n_3}{n} \Psi_{13} + n_3' \text{RTY} \tag{3.52}
\end{aligned}$$

Now,

$$\frac{\partial^2 d_3}{\partial c^2} = \left[\left(\frac{n_2}{n} \right)' - \left(\frac{n_1}{n} \right)' \right] \Psi_{12} - \left(\frac{n_3}{n} \right)' \Psi_{23} + \left(\frac{n_3}{n} \right)' \Psi_{13} + n_3'' \text{RTY} + n_3' \text{RTY}' \tag{3.53}$$

Here the last term of equation 3.53 is $n_3' \text{RTY}'$. To find Y' , we have from equation 3.36,

$$Y = Y_1 \frac{\Psi_{12}}{\text{RT}} + Y_2 \frac{\Psi_{23}}{\text{RT}} + Y_3 \frac{\Psi_{13}}{\text{RT}} \tag{3.54}$$

Here,

$$Y_1 = \left[\frac{n_1 n_2}{n^2} (p+q-1) - p \frac{n_2}{n} - q \frac{n_1}{n} \right]$$

$$Y_2 = \left[\frac{n_2 n_3}{n^2} (p+q-1) - q \frac{n_3}{n} + \frac{n_2}{n} \right]$$

$$Y_3 = \left[\frac{n_1 n_3}{n^2} (p+q-1) - p \frac{n_3}{n} + \frac{n_1}{n} \right]$$

Now

$$\frac{\partial Y_1}{\partial c} = \left[(p+q-1) \left(\frac{n_1}{n} \right)' \left(\frac{n_2}{n} \right) + (p+q-1) \left(\frac{n_1}{n} \right) \left(\frac{n_2}{n} \right)' - p \left(\frac{n_2}{n} \right)' - q \left(\frac{n_1}{n} \right)' \right]$$

Multiplying with n_3'

$$n_3' \frac{\partial Y_1}{\partial c} = n_3' \left[(p+q-1) \left(\frac{n_1}{n} \right)' \left(\frac{n_2}{n} \right) + (p+q-1) \left(\frac{n_1}{n} \right) \left(\frac{n_2}{n} \right)' - p \left(\frac{n_2}{n} \right)' - q \left(\frac{n_1}{n} \right)' \right] \tag{3.55}$$

From equations 3.1 and 3.2, we get,

$$\begin{aligned}
n'_1 &= 1 - pn'_3 \\
pn'_3 &= 1 - n'_1 \\
n'_2 &= -1 - qn'_3 \\
qn'_3 &= -1 - n'_2, \\
n' &= -(p + q - 1)n'_3
\end{aligned} \tag{3.56}$$

Applying equation 3.56 in equation 3.55, we get,

$$n'_3 \frac{\partial Y_1}{\partial c} = -n' \left(\frac{n_1}{n}\right)' \left(\frac{n_2}{n}\right) - n' \left(\frac{n_1}{n}\right) \left(\frac{n_2}{n}\right)' - (1 - n'_1) \left(\frac{n_2}{n}\right)' - (-1 - n'_2) \left(\frac{n_1}{n}\right)' \tag{3.57}$$

$$n'_3 \frac{\partial Y_1}{\partial c} = -\left(\frac{n_2}{n}\right)' + \left(\frac{n_1}{n}\right)' - n' \frac{n_2}{n} \left(\frac{n_1}{n}\right)' - n' \frac{n_1}{n} \left(\frac{n_2}{n}\right)' + n'_1 \left(\frac{n_2}{n}\right)' + n'_2 \left(\frac{n_1}{n}\right)' \tag{3.58}$$

Again,

$$\frac{\partial Y_2}{\partial c} = \left[(p + q - 1) \left(\frac{n_2}{n}\right)' \left(\frac{n_3}{n}\right) + (p + q - 1) \left(\frac{n_2}{n}\right) \left(\frac{n_3}{n}\right)' - q \left(\frac{n_3}{n}\right)' - \left(\frac{n_2}{n}\right)' \right]$$

Multiplying with n'_3 and proceeding in similar way

$$n'_3 \frac{\partial Y_2}{\partial c} = n'_3 \left[(p + q - 1) \left(\frac{n_2}{n}\right)' \left(\frac{n_3}{n}\right) + (p + q - 1) \left(\frac{n_2}{n}\right) \left(\frac{n_3}{n}\right)' - q \left(\frac{n_3}{n}\right)' + \left(\frac{n_2}{n}\right)' \right]$$

$$n'_3 \frac{\partial Y_2}{\partial c} = -n' \left(\frac{n_2}{n}\right)' \left(\frac{n_3}{n}\right) - n' \left(\frac{n_2}{n}\right) \left(\frac{n_3}{n}\right)' - (-1 - n'_2) \left(\frac{n_3}{n}\right)' + n'_3 \left(\frac{n_2}{n}\right)'$$

$$n'_3 \frac{\partial Y_2}{\partial c} = \left(\frac{n_3}{n}\right)' - n' \frac{n_3}{n} \left(\frac{n_2}{n}\right)' - n' \frac{n_2}{n} \left(\frac{n_3}{n}\right)' + n'_2 \left(\frac{n_3}{n}\right)' + n'_3 \left(\frac{n_2}{n}\right)' \tag{3.59}$$

Again,

$$\frac{\partial Y_3}{\partial c} = \left[(p + q - 1) \left(\frac{n_1}{n}\right)' \left(\frac{n_3}{n}\right) + (p + q - 1) \left(\frac{n_1}{n}\right) \left(\frac{n_3}{n}\right)' - p \left(\frac{n_3}{n}\right)' + \left(\frac{n_1}{n}\right)' \right]$$

Multiplying with n'_3 and following the similar procedure as above,

$$n'_3 \frac{\partial Y_3}{\partial c} = n'_3 \left[(u + v - 1) \left(\frac{n_1}{n}\right)' \left(\frac{n_3}{n}\right) + (u + v - 1) \left(\frac{n_1}{n}\right) \left(\frac{n_3}{n}\right)' - u \left(\frac{n_3}{n}\right)' + \left(\frac{n_1}{n}\right)' \right]$$

$$= -n' \left(\frac{n_1}{n}\right)' \left(\frac{n_3}{n}\right) - n' \left(\frac{n_1}{n}\right) \left(\frac{n_3}{n}\right)' - (1 - n'_1) \left(\frac{n_3}{n}\right)' + n'_3 \left(\frac{n_1}{n}\right)'$$

$$= -\left(\frac{n_3}{n}\right)' - n' \frac{n_3}{n} \left(\frac{n_1}{n}\right)' - n' \frac{n_1}{n} \left(\frac{n_3}{n}\right)' + n_1' \left(\frac{n_3}{n}\right)' + n_3' \left(\frac{n_1}{n}\right)' \quad (3.60)$$

Employing equations 3.58, 3.59 and 3.60 in equation 3.54, we have,

$$\begin{aligned} n_3' RTY' &= \Psi_{12} \left[-\left(\frac{n_2}{n}\right)' + \left(\frac{n_1}{n}\right)' - n' \frac{n_2}{n} \left(\frac{n_1}{n}\right)' - n' \frac{n_1}{n} \left(\frac{n_2}{n}\right)' + n_1' \left(\frac{n_2}{n}\right)' + n_2' \left(\frac{n_1}{n}\right)' \right] \\ &+ \Psi_{23} \left[\left(\frac{n_3}{n}\right)' - n' \frac{n_3}{n} \left(\frac{n_2}{n}\right)' - n' \frac{n_2}{n} \left(\frac{n_3}{n}\right)' + n_2' \left(\frac{n_3}{n}\right)' + n_3' \left(\frac{n_2}{n}\right)' \right] \\ &+ \Psi_{13} \left[-\left(\frac{n_3}{n}\right)' - n' \frac{n_3}{n} \left(\frac{n_1}{n}\right)' - n' \frac{n_1}{n} \left(\frac{n_3}{n}\right)' + n_1' \left(\frac{n_3}{n}\right)' + n_3' \left(\frac{n_1}{n}\right)' \right] \end{aligned}$$

Substituting the value of $n_3' RTY'$ in equation 3.53 we get

$$\begin{aligned} \frac{\partial^2 d_3}{\partial c^2} &= \left\{ \left(\frac{n_2}{n}\right)' - \left(\frac{n_1}{n}\right)' \right\} \Psi_{12} - \left(\frac{n_3}{n}\right)' \Psi_{23} + \left(\frac{n_3}{n}\right)' \Psi_{13} + n_3'' RTY \\ &\Psi_{12} \left[-\left(\frac{n_2}{n}\right)' + N \left(\frac{n_1}{n}\right)' - n' \frac{n_2}{n} \left(\frac{n_1}{n}\right)' - n' \frac{n_1}{n} \left(\frac{n_2}{n}\right)' + n_1' \left(\frac{n_2}{n}\right)' + n_2' \left(\frac{n_1}{n}\right)' \right] \\ &+ \Psi_{23} \left[\left(\frac{n_3}{n}\right)' - n' \frac{n_3}{n} \left(\frac{n_2}{n}\right)' - n' \frac{n_2}{n} \left(\frac{n_3}{n}\right)' + n_2' \left(\frac{n_3}{n}\right)' + n_3' \left(\frac{n_2}{n}\right)' \right] \\ &+ \Psi_{13} \left[-\left(\frac{n_3}{n}\right)' - n' \frac{n_3}{n} \left(\frac{n_1}{n}\right)' - n' \frac{n_1}{n} \left(\frac{n_3}{n}\right)' + n_1' \left(\frac{n_3}{n}\right)' + n_3' \left(\frac{n_1}{n}\right)' \right] \end{aligned}$$

$$\begin{aligned} \frac{\partial^2 d_3}{\partial c^2} &= n_3'' RTY + \Psi_{12} \left[\left(-\frac{n' n_2}{n} + n_2'\right) \left(\frac{n_1}{n}\right)' + \left(-\frac{n' n_1}{n} + n_1'\right) \left(\frac{n_2}{n}\right)' \right] \\ &\Psi_{23} \left[\left(-\frac{n' n_3}{n} + n_3'\right) \left(\frac{n_2}{n}\right)' + \left(-\frac{n' n_2}{n} + n_2'\right) \left(\frac{n_3}{n}\right)' \right] \\ &+ \Psi_{13} \left[\left(-\frac{n' n_3}{n} + n_3'\right) \left(\frac{n_1}{n}\right)' + \left(-\frac{n' n_1}{n} + n_1'\right) \left(\frac{n_3}{n}\right)' \right] \end{aligned}$$

$$\frac{\partial^2 d_3}{\partial c^2} = n_3'' RTY + \Psi_{12} d_{31} + \Psi_{23} d_{32} + \Psi_{13} d_{33} \quad (3.61)$$

Here,

$$\begin{aligned} d_{31} &= \left(-\frac{n' n_2}{n} + n_2'\right) \left(\frac{n_1}{n}\right)' + \left(-\frac{n' n_1}{n} + n_1'\right) \left(\frac{n_2}{n}\right)' \\ &= \left(-\frac{n' n_2}{n} + n_2'\right) \left(\frac{n_1'}{n} - \frac{n_1 n_1'}{n^2}\right) + \left(-\frac{n' n_1}{n} + n_1'\right) \left(\frac{n_2'}{n} - \frac{n_2 n_2'}{n^2}\right) \end{aligned}$$

$$\begin{aligned}
&= -\frac{n'n_1n_2}{n^2} + \frac{(n')^2 n_1n_2}{n^3} + \frac{n'n'_2}{n} - \frac{n'n_1n'_2}{n^2} - \frac{n'n_1n'_2}{n^2} + \frac{(n')^2 n_1n_2}{n^3} + \frac{n'n'_2}{n} - \frac{n'n_1n_2}{n^2} \\
&= 2 \left[\frac{n'n'_2}{n} - \frac{n'n_1n_2}{n^2} - \frac{n'n_1n'_2}{n^2} + \frac{(n')^2 n_1n_2}{n^3} \right]
\end{aligned}$$

Similarly,

$$d_{32} = 2 \left[\frac{n'_2n'_3}{n} - \frac{n'n'_2n_3}{n^2} - \frac{n'n_2n'_3}{n^2} + \frac{(n')^2 n_2n_3}{n^3} \right]$$

$$d_{33} = 2 \left[\frac{n'_1n'_3}{n} - \frac{n'n'_1n_3}{n^2} - \frac{n'n_1n'_3}{n^2} + \frac{(n')^2 n_1n_3}{n^3} \right]$$

Substituting the values of d_{31} , d_{32} and d_{33} in equation (3.61)

$$\begin{aligned}
\frac{\partial^2 d_3}{\partial c^2} &= n_3'' RTY + 2\Psi_{12} \left[\frac{n'_1n'_2}{n} - \frac{n'n'_1n_2}{n^2} - \frac{n'n_1n'_2}{n^2} + \frac{(n')^2 n_1n_2}{n^3} \right] \\
&+ 2\Psi_{23} \left[\frac{n'_2n'_3}{n} - \frac{n'n'_2n_3}{n^2} - \frac{n'n_2n'_3}{n^2} + \frac{(n')^2 n_2n_3}{n^3} \right] \\
&+ 2\Psi_{13} \left[\frac{n'_1n'_3}{n} - \frac{n'n'_1n_3}{n^2} - \frac{n'n_1n'_3}{n^2} + \frac{(n')^2 n_1n_3}{n^3} \right]
\end{aligned}$$

$$\begin{aligned}
\frac{\partial^2 d_3}{\partial c^2} &= n_3'' RTY + 2n\Psi_{12} \left\{ \frac{n'_1n'_2}{n^2} - \frac{n'n'_1n_2}{n^3} - \frac{n'n_1n'_2}{n^3} + \frac{(n')^2 n_1n_2}{n^4} \right\} \\
&+ 2n\Psi_{23} \left\{ \frac{n'_2n'_3}{n^2} - \frac{n'n'_2n_3}{n^3} - \frac{n'n_2n'_3}{n^3} + \frac{(n')^2 n_2n_3}{n^4} \right\} \\
&+ 2n\Psi_{13} \left\{ \frac{n'_1n'_3}{n^2} - \frac{n'n'_1n_3}{n^3} - \frac{n'n_1n'_3}{n^3} + \frac{(n')^2 n_1n_3}{n^4} \right\}
\end{aligned}$$

$$\begin{aligned}
\frac{\partial^2 d_3}{\partial c^2} &= n_3'' RTY + 2n\Psi_{12} \left(\frac{n'_1}{n} - \frac{n_1n'_1}{n^2} \right) \left(\frac{n'_2}{n} - \frac{n_2n'_2}{n^2} \right) \\
&+ 2n\Psi_{23} \left(\frac{n'_2}{n} - \frac{n_2n'_2}{n^2} \right) \left(\frac{n'_3}{n} - \frac{n_3n'_3}{n^2} \right) \\
&+ 2n\Psi_{13} \left(\frac{n'_1}{n} - \frac{n_1n'_1}{n^2} \right) \left(\frac{n'_3}{n} - \frac{n_3n'_3}{n^2} \right)
\end{aligned}$$

$$\frac{\partial^2 d_3}{\partial c^2} = n_3'' RTY + 2n \left[\Psi_{12} \left(\frac{n_1}{n} \right)' \left(\frac{n_2}{n} \right)' + \Psi_{23} \left(\frac{n_2}{n} \right)' \left(\frac{n_3}{n} \right)' + \Psi_{13} \left(\frac{n_1}{n} \right)' \left(\frac{n_3}{n} \right)' \right]$$

$$\frac{\partial^2 d_3}{\partial c^2} = n_3'' RTY + 2n \sum_{i < j} \sum \Psi_{ij} \left(\frac{n_i}{n} \right)' \left(\frac{n_j}{n} \right)' \quad (3.62)$$

Substituting equations 3.40, 3.47 and 3.62 for 3.39

$$\frac{\partial^2 G_M}{\partial c^2} = -n_3'' \chi + RT \sum_{i=1}^3 \left(\frac{(n_i')^2}{n_i} - \frac{(n')^2}{n} \right) + n_3'' \chi - n_3'' YRT + n_3'' RTY + 2n \sum_{i < j} \sum \Psi_{ij} \left(\frac{n_i}{n} \right)' \left(\frac{n_j}{n} \right)'$$

$$\frac{\partial^2 G_M}{\partial c^2} = RT \sum_{i=1}^3 \left(\frac{(n_i')^2}{n_i} - \frac{(n')^2}{n} \right) + 2n \sum_{i < j} \sum \Psi_{ij} \left(\frac{n_i}{n} \right)' \left(\frac{n_j}{n} \right)' \quad (3.63)$$

Now equation 3.63 and 3.38 yield

$$S_{cc}(0) = \frac{RT}{RT \sum_{i=1}^3 \left(\frac{(n_i')^2}{n_i} - \frac{(n')^2}{n} \right) + 2n \sum_{i < j} \sum \Psi_{ij} \left(\frac{n_i}{n} \right)' \left(\frac{n_j}{n} \right)'}$$

$$S_{cc}(0) = \frac{1}{\sum_{i=1}^3 \left(\frac{(n_i')^2}{n_i} - \frac{(n')^2}{n} \right) + \frac{2n}{RT} \sum_{i < j} \sum \Psi_{ij} \left(\frac{n_i}{n} \right)' \left(\frac{n_j}{n} \right)'}$$

$$S_{cc}(0) = \frac{1 / \sum_{i=1}^3 \left(\frac{(n_i')^2}{n_i} - \frac{(n')^2}{n} \right)}{1 + \frac{2n}{RT} \sum_{i < j} \sum \Psi_{ij} \left(\frac{n_i}{n} \right)' \left(\frac{n_j}{n} \right)' \frac{1}{\sum_{i=1}^3 \left(\frac{(n_i')^2}{n_i} - \frac{(n')^2}{n} \right)}}$$

$$S_{cc}(0) = \frac{S_{cc}}{1 + DS_{cc}} \quad (3.64)$$

where,

$$S_{cc} = \frac{1}{\sum_{i=1}^3 \left(\frac{(n_i')^2}{n_i} - \frac{(n')^2}{n} \right)} = \left[\sum_{i=1}^3 \left(\frac{(n_i')^2}{n_i} - \frac{(n')^2}{n} \right) \right]^{-1} \quad (3.65)$$

And

$$D = \frac{2n}{RT} \sum_{i < j} \sum \Psi_{ij} \left(\frac{n_i}{n} \right)' \left(\frac{n_j}{n} \right)' \quad (3.66)$$

Equation 3.64 along with the equation 3.65 and 3.66 can be used to calculate $S_{cc}(0)$ in

any types of the binary liquid alloys. When considering ideal solutions, the expression for G_M is as follows (Hultgren et al., 1973):

$$G_M^{\text{ideal}} = RT (c \ln c + (1 - c) \ln (1 - c)) \quad (3.67)$$

The use of equation 3.67 in equation 3.38 results in

$$S_{cc}^{(\text{ideal})}(0) = c(1 - c) \quad (3.68)$$

Any divergence of $S_{cc}(0)$ from the ideal value $S_{cc}^{(\text{ideal})}(0)$ is interesting in terms of representing the degree of interaction in the mixture. If $S_{cc}(0) \gg S_{cc}^{(\text{ideal})}(0)$ at a particular composition, there is a trend toward segregation or phase separation, whereas $S_{cc}(0) \ll S_{cc}^{(\text{ideal})}(0)$ indicates strong association or the presence of chemical complexes in the solution.

Using the formulation provided by Bhatia & Thornton (1970), McAlister & Turner (1972) investigated the zero wave vector partial structural factors for Na-K alloys at 373 K and K-Hg alloys at 573 K. The partial structure factors showed noticeable fluctuation at zero wave vector, despite the fact that they do not vary much for large wave vectors. The ratio between the vapor pressure of the species in the mixture and the vapor pressure of the substance in its pure form when both are at the same temperature was described by the authors as the activity of a species (a_i). It is also suggested that the mole fractions of the species and their activity might be used to calculate the $S_{cc}(0)$ (McAlister & Turner, 1972).

$$S_{CC}(0) = c_2 \left[\frac{1}{a_1} \left(\frac{\partial a_1}{\partial c_1} \right)_{T,P} \right]^{-1} = c_1 \left[\frac{1}{a_2} \left(\frac{\partial a_2}{\partial c_2} \right)_{T,P} \right]^{-1} \quad (3.69)$$

Here, a_1 and a_2 are used to signify the thermodynamic activity of species 1 and 2, respectively. Experimental values of $S_{cc}(0)$ are the values determined by utilizing equation 3.69 by taking the experimental values of the component activities from literature.

For the purpose of describing the chemical short range order (SRO) and connecting it to different features, a number of models and ideas had been put forth. However, it is generally quite difficult to directly separate the portion of a single observed scattering intensity that is modulated by SRO. Neutron diffraction is only able to directly examine SRO scattering for a few rare alloys. For the first neighbor shell, the short range-order parameter (α_1) (Warren, 1990; Cowley, 1950) is usually described in terms of the conditioned probability [A/B] (Ruppersberg & Egger, 1975), i.e.

$$[A/B] = c(1 - \alpha_1) \quad (3.70)$$

In the case of a random distribution, $[A/B]$ is just c , and $\alpha_1 = 0$. Where $[A/B]$ specifies the probability that a specific B atom at site 1 has a nearest neighbor A atom at site 2. Therefore, equation 3.70 offers immediate insight into the local arrangement of atoms inside the mixture. In the similar way, $[B/A]$ can be written as,

$$[B/A] = (1 - c)(1 - \alpha_1) \quad (3.71)$$

Equations 3.70 and 3.71 allow us to have

$$[A/B] = \frac{c}{1 - c} [B/A]$$

A-B pairings of atoms are preferred over A-A or B-B pairs as nearest neighbors if $\alpha_1 < 0$; if $\alpha_1 > 0$, the opposite is true. Using a probabilistic technique, the limiting values of α_1 can be easily demonstrated to be within the range,

$$-\frac{c}{1 - c} \leq \alpha_1 \leq 1 \text{ for } (c \leq 1/2)$$

$$-\frac{(1 - c)}{c} \leq \alpha_1 \leq 1 \text{ for } (c \geq 1/2)$$

One has $-1 \leq \alpha_1 \leq 1$ for binary liquid alloys. While the highest value $\alpha_1^{(\max)} = 1$ denotes complete segregation by the A-A and B-B pairings in the melt. The complete ordering of A-B pairings in the melt is shown by $\alpha_1^{(\min)} = -1$, which is the minimum value.

Equation 3.70 can alternatively be expressed in terms of generalized probability, X_{AB} , which indicates that an A-atom occupies one lattice site and a B-atom occupies the other in a nearest neighbor pair.

$$X_{(AB)} = (1 - c) [A/B]$$

Consequently, again from equation 3.70

$$X_{(AB)} = c(1 - c) [1 - \alpha_1]$$

On the basis of fundamental thermodynamic relationships, $S_{cc}(0)$ and α_1 are directly connected. For a melt where size effects are insignificant, there is an exact relationship between $S_{cc}(0)$ and α_1 for different shells (March et al., 1976; Ruppertsberg & Egger, 1975).

$$\frac{S_{cc}(0)}{c_A c_B} = \frac{1 + \alpha_1}{1 - (z - 1)\alpha_1} \quad (3.72)$$

In its expanded version, this equation 3.72 can be stated as

$$\frac{S_{cc}(0)}{c_A c_B} = 1 + \sum_l z_l \alpha_1$$

where z_l denotes the coordination number of the l^{th} shell (l varies from first-neighbor shells to higher shells). Later on, Bhatia and Singh (1982) utilized the lattice model theory to get the expressions for α_1 and $S_{cc}(0)$, i.e.

$$\alpha_1 = \frac{S - 1}{S + 1} \quad (3.73)$$

and

$$S_{cc}(0) = \frac{c_A c_B}{1 + \frac{1}{2}z(1/S - 1)} \quad (3.74)$$

with

$$S = [1 + 4c_A c_B (\exp(2\Psi/zk_B T) - 1)]^{1/2}$$

The zero value of $\Psi/k_B T$ implies $\alpha_1 = 0$, i.e., a random distribution in the alloy resulting in ideal mixing. If $\Psi/k_B T > 0$, α_1 is positive, indicating that like atoms A-A or B-B tend to pair as nearest neighbors, but if $\Psi/k_B T < 0$, α_1 is negative, indicating that unlike atoms (A-B) prefer to pair in the alloy.

Since it is difficult to get α_1 from scattering experiments, the easy link between α_1 and thermophysical properties is of very importance. In the nearest neighbor shell ($l=1$), α_1 can be calculated from $S_{cc}(0)$ using equation 3.72 (Bhatia & Singh, 1984), i.e.

$$\alpha_1 = \frac{S^* - 1}{S^* (z - 1) + 1}, \quad S^* = \frac{S_{cc}(0)}{c_A c_B} \quad (3.75)$$

As the unit value of the long-range order parameter indicates a completely ordered state, the unit value of the short-range order parameter indicates a perfectly disordered state (Bhatia & Thornton, 1970).

3.3 Transport Properties

The study of the dynamic properties of the alloys can help one to understand the mixing of the two atomic species in a binary liquid alloy very well at the microscopic level. In order to investigate the transport properties of binary systems in the context of the thermodynamic construct $S_{cc}(0)$, one might investigate properties such as diffusion coefficient. Based on the research of Darken (1948), the intrinsic diffusion coefficient

(D_A or D_B) can be expressed in terms of the observed tracer diffusion coefficient (D_A^* or D_B^*), (R. N. Singh & Sommer, 1997) i.e.

$$D_A = D_A^* \frac{\partial \ln a_A}{\partial \ln c_A} \quad (3.76)$$

$$D_B = D_B^* \frac{\partial \ln a_B}{\partial \ln c_B} \quad (3.77)$$

Darken analysis is applicable to experiments in which the tracer diffusion coefficients are directly measured by monitoring the evolving concentration profile of a diluted radioactive isotope A^* or B^* . Owing to the Gibbs–Duhem relationship, we have (R. N. Singh & Sommer, 1997)

$$\frac{\partial \ln a_A}{\partial \ln c_A} = \frac{\partial \ln a_B}{\partial \ln c_B}$$

Now, the chemical diffusion coefficient, also known as mutual diffusion or interdiffusion coefficient, is given by

$$\begin{aligned} D_M &= c_A D_B + c_B D_A \\ D_M &= (c_A D_B^* + c_B D_A^*) \frac{\partial \ln a_A}{\partial \ln c_A} \\ D_M &= (c_A D_B^* + c_B D_A^*) \frac{\partial \ln a_A}{\partial a_A} \left(\frac{1}{\frac{\partial \ln c_A}{\partial c_A}} \right) \frac{\partial a_A}{\partial c_A} = (c_A D_B^* + c_B D_A^*) \frac{c_A}{a_A} \frac{\partial a_A}{\partial c_A} \\ D_M &= (c_A D_B^* + c_B D_A^*) \frac{c_A c_B}{\frac{\partial a_A}{\partial c_A}} = (c_A D_B^* + c_B D_A^*) \frac{S_{cc}^{(ideal)}(0)}{S_{cc}(0)} \end{aligned} \quad (3.78)$$

For ideal alloys,

$$S_{cc}(0) = S_{cc}^{(ideal)}(0) = c_A c_B \text{ and } D_M = c_A D_B + c_B D_A = c_A D_B^* + c_B D_A^* = D_{id}$$

It should be emphasized that equations 3.76 and 3.77 ensure that the intrinsic diffusion coefficient D_i and the tracer diffusion coefficient, D_i^* (determined for the dilute solution limit) are same for an ideal mixture. As a result, equation 3.78 becomes

$$\frac{D_M}{D_{id}} = \frac{S_{cc}^{(ideal)}(0)}{S_{cc}(0)} \quad (3.79)$$

The viscosity of liquid metals and alloys is one of the technologically significant transport

parameters required to create and optimize metallurgical technologies, such as through the use of computer software. These computer programs need the dynamic viscosity value as a function of temperature and composition (Seetharaman & Sichen, 1994). For the modeling and design of metallurgical processes, it's essential to have accurate viscosity information of high temperature metallic melts as well as ionic melts. For instance, knowing the kinetics of reactions related to process metallurgy as well as for processes like casting and welding requires knowledge of the viscosity of metallic melts and slags (Kaptay, 2005b). Despite the fact that numerous theoretical and experimental measurements have been made. Viscosity data is still in short supply when compared to the demands of modern technologies. The viscosity data for binary alloys are scarce when compared to metallic systems, where the viscosities of numerous pure liquid metals have been reported. The viscosities of liquids are highly dependent on the movements of species and, by extension, the bonding and arrangement of species in the liquid. On the other hand, thermodynamic parameters such as molar Gibb's energy, enthalpy, entropy, and volume of mixing are also connected to the nature and strength of the bonds between species and their distribution in a liquid with respect to order-disorder phenomena. Thus, connections between viscosity and thermodynamic parameters could be anticipated. The dependency of both viscosity and enthalpy of mixing on the binding and arrangement of species in liquids makes it possible to develop a mathematical link between these two properties.

Since the thermodynamic characteristics of complex systems at high temperatures have been widely researched, the relationship between viscosity and thermodynamic property would be a valuable tool for estimating viscosity values utilizing the huge quantity of accessible thermodynamic data.

Various formulas are used to predict the viscosity of pure liquid metals at their melting point and the temperature dependence of this property. Andrade's equation (Andrade, 1934) is fairly effective in predicting the viscosities at the melting point of pure liquid metals using a single empirically valid parameter. However, there is no known equation similar to Andrade's equation that can predict the temperature dependence of the viscosity of pure liquid metals using one or more generally valid semi empirical constants. Furthermore, the literature describes the temperature dependence of the viscosity of liquid metals using two opposing concepts: the activation energy concept and the free volume concept. A generally valid unified equation for viscosity was derived by combining the activation energy concept and the free volume concept with Andrade's equation. The equation may predict the melting point viscosity values and temperature dependency of pure liquid metals using only two semi-empirical coefficients that are generally valid (Kaptay, 2005b). Andrade (1934) used the idea that momentum is transferred within atoms, which are in touch with surrounding layers via their vibrational displacement,

to describe the melting point viscosity of liquids. Andrade (1934) derived the equation with the assumption that the characteristic vibrational frequencies of normal liquid and solid metals at their melting temperatures are roughly the same.

$$\eta_i = \frac{C_A M_i^{\frac{1}{2}} T_{m,i}^{\frac{1}{2}}}{V_i^{\frac{2}{3}}} \quad (3.80)$$

where $T_{m,i}$ is the melting point of pure liquid metal i in Kelvin, V_i (m^3/mol) is the molar volume of liquid metal i at its melting point, and η_i (Pa.S) is the dynamic viscosity of pure liquid metal i at its melting point. According to Andrade's theoretical derivation, the coefficient C_A is equal to $1.655 \times 10^{-7} (\text{J/K mol}^{1/3})^{1/2}$. Despite having a slightly different value for the coefficient C_A , equation (3.80) is acknowledged as the most successful equation for estimating the melting point viscosities of pure liquid metals. The best semi-empirical estimate of C_A from various measurements of viscosity values is found to be around $1.8 \times 10^{-7} (\text{J/K mol}^{1/3})^{1/2}$ (Battezzati & Greer, 1989; Guthrie & Iida, 1993).

In the first approximation, Andrade recommended using the Arrhenius equation to determine how the viscosity of pure liquid metals changes with temperature (Andrade, 1934).

$$\eta_i = C_1 \exp\left(\frac{E_i}{RT}\right) \quad (3.81)$$

where C_1 is a semi-empirical coefficient, E_i (J/mol) denotes the activation energy of viscous flow for pure liquid i and R denotes the universal gas constant (8.3 J/K mol) respectively.

Eyring, in 1936, obtained the following simplified equation based on his concept of the rate theory (Eyring, 1936).

$$\eta_i = \frac{h N_{AV}}{V_i} \left(\frac{E_i}{RT}\right) \quad (3.82)$$

where h is the Planck's constant and N_{AV} is the Avogadro number. It should be mentioned that Eyring himself devised a variety of models to forecast the viscosity of liquids starting in 1936 and later working with other co-authors on the kinetics of chemical reactions, viscosity, diffusion and electrochemical phenomena (Eyring et al., 1941). Equation 3.82 was used to obtain one of the modifications of as follows:

$$\eta_i = \frac{d_i}{v_i} (2\pi M_i RT)^{\frac{1}{2}} \exp\left(\frac{E_i}{RT}\right) \quad (3.83)$$

where d_i (m) is the diameter of the space that an atom occupies. The following equation (equation 3.84) can be developed by taking equations 3.80 and 3.81 and by assuming that the atomic diameter d_i is proportional to $V_i^{\frac{1}{3}}$ in equation 3.83.

$$\eta_i = \mu \frac{M_i^{\frac{1}{2}} T^{\frac{1}{2}}}{V_i^{\frac{2}{3}}} \exp\left(\frac{E_i}{RT}\right) \quad (3.84)$$

The activation energy of viscous flow, in a physical sense, is a small part of the cohesion energy that must be supplied for each atomic displacement of viscous flow between neighboring liquid layers:

$$E_i = -\frac{\Delta z_i}{z_i} \Delta_c U_i \quad (3.85)$$

where z_i represents the average coordination number found in liquid metals, Δz_i represents the number of broken bonds that occur during viscous flow, and $\Delta_c U_i$ represents the cohesion energy of the liquid metal. Although the vaporization enthalpy is typically employed to assess cohesion energy, using the example of surface tension, it has been demonstrated that cohesion energy correlates better with the melting point of common metals (Kaptay et al., 2003).

$$\Delta_c U_i = -\Phi RT_{m,i} \quad (3.86)$$

where the semi-empirical parameter Φ is found to be $\Phi \cong 25.4 \pm 2$ (Kaptay, 2005a). Substituting equation (3.86) into equation (3.84) and assuming that the ratio of $\Delta z_i/z_i$ is roughly constant for all liquid metals, a constant ν can be introduced as follows:

$$\nu = \Phi \frac{\Delta z_i}{z_i} \quad (3.87)$$

The following equation (which includes the temperature-dependent portion of the activation energy in parameter μ) is eventually obtained by substituting equations 3.84 through 3.87 into equation 3.83:

$$\eta_i = \mu \frac{M_i^{\frac{1}{2}} T^{\frac{1}{2}}}{V_i^{\frac{2}{3}}} \exp\left(\nu \frac{T_{m,i}}{T}\right) \quad (3.88)$$

At the melting point of metal equation (3.88) reduces to the Andrade equation, equation 3.80, and the parameters C_A , μ , and ν have the following relationships:

$$C_A = \mu \exp(\nu) \quad (3.89)$$

Seetharaman & Sichen (1994) used the free volume idea to construct the same equation as equation 3.88, which was then defined as the unified equation for the viscosity of pure liquid metals. The values of semi-empirical parameter μ and ν are estimated using the numerous literature data and provided the average value as the best value:

$$\mu = (1.80 \pm 0.39) \times 10^{-8} \left(J/K \text{mol}^{1/3} \right)^{\frac{1}{2}} \quad (3.90)$$

and

$$\nu = 2.34 \pm 0.20 \quad (3.91)$$

As the binary and multi component extension of equation (3.88), Budai et al. (2007) derives a new equation known as the Budai-Benko-Kaptay (BBK) model. The following relation extends the molar mass, molar volume, and cohesion energy of pure liquid metals i in equation 3.88 to multi-component alloys.

$$M = \sum_i c_i M_i \quad (3.92)$$

$$V = \sum_i c_i V_i + \Delta V^E \quad (3.93)$$

$$\Delta_c U_i = -\Phi R \sum_i c_i T_{m,i} + H_M \quad (3.94)$$

Results from different experiments or theories can be used to determine the excess molar volume (ΔV^E) and the integral heat of mixing H_M , which are concentration and temperature dependent quantities. The following unified equation for the viscosity of multi-component liquid alloys can be obtained by substituting equation 3.92-3.94 into equation 3.88 (Budai et al., 2007).

$$\eta = \frac{\mu \left(\sum_i (c_i M_i) \right)^{\frac{1}{2}}}{\left(\sum_i c_i V_i + \Delta V_E \right)^{\frac{2}{3}}} T^{\frac{1}{2}} \exp \left[\frac{\nu}{T} \left(\sum_i c_i T_{m,i} - \frac{H_M}{\Phi R} \right) \right] \quad (3.95)$$

3.4 Surface Properties

One of the most significant physical characteristics of liquid alloys is surface tension, which is known to govern a variety of interfacial phenomena in metallurgical processes. Even the calculated surface tension in the alloys from the thermodynamic database

would be of enormous significance because the literature's value of surface tension in liquid alloys are few and widely dispersed (T. Tanaka & Iida, 1994). It is possible to consider the surface of a multicomponent solution to be a "phase." The chemical potential of each component in the surface phase is equivalent to the chemical potential of the corresponding component in the bulk solution plus the surface energy of the components in the surface phase and the bulk phase are in thermodynamic equilibrium. Butler (1932) demonstrated that by first assuming that the partial surface areas of alloy components in the alloy are equal to the molar surface areas of pure elements, and then taking into account the equilibrium between a bulk phase and a mono layer at the surface, which is regarded as an individual phase, one can obtain the following thermodynamic equation for surface tension σ of a liquid binary A-B alloy.

$$\sigma = \sigma_A + \frac{RT}{S_A} \ln \frac{a_A^s}{a_A^b} = \sigma_B + \frac{RT}{S_B} \ln \frac{a_B^s}{a_B^b} \quad (3.96)$$

where σ , σ_A , and σ_B represent the surface tension of the solution, pure component A, and pure component B, respectively; S_i , the monolayer surface area of component i ($i = A$ or B); a_i^b , the activity of component i in the bulk phase; a_i^s , the activity of component i in the surface phase; R, the gas constant; and T, the absolute temperature. The standard states for the bulk and surface phases must be defined correctly for equation 3.96 to be valid. Equation 3.96 can be written as the following by substituting an activity with the product of the mole fraction and activity coefficient (T. Tanaka & Iida, 1994).

$$\begin{aligned} \sigma &= \sigma_A + \frac{RT}{S_A} \ln \left(\frac{1 - c_B^s}{1 - c_B^b} \right) + \frac{RT}{S_A} \ln \left(\frac{Y_A^s}{Y_A^b} \right) \\ &= \sigma_B + \frac{RT}{S_B} \ln \frac{c_B^s}{c_B^b} + \frac{RT}{S_B} \ln \left(\frac{Y_B^s}{Y_B^b} \right) \end{aligned} \quad (3.97)$$

where Y_i^b and Y_i^s represent the activity coefficient of component i in the bulk and surface phases, respectively, and c_B^b and c_B^s represent the mole fractions of component B in the bulk and surface phases, respectively. Using a quasi-chemical model, the activity coefficient for the bulk phase was determined by Fowler & Guggenheim (1965), and it is as follows:

$$\ln Y_A = \frac{z}{2} \ln \left(\frac{(\zeta - 1 + 2c_B)}{c_B (\zeta + 1)} \right) \quad (3.98)$$

and

$$\ln \Upsilon_B = \frac{z}{2} \ln \left(\frac{(\zeta + 1 - 2c_B)}{(1 - c_B)(\zeta + 1)} \right), \quad (3.99)$$

respectively with

$$\zeta = \left[4c_B (1 - c_B) e^{\frac{2\omega}{k_B T}} + (1 - 2c_B)^2 \right]^{\frac{1}{2}}.$$

In the equations 3.98 and 3.99, k_B is the Boltzmann's constant, z is the coordination number of the atoms in the bulk phase, and ω is the pair-wise interaction energy given as,

$$\omega = \frac{E_{AB} - (E_{AA} + E_{BB})}{2}$$

Here, the energy attributed to the $i - j$ bonds is denoted by the symbol E_{ij} . For equation 3.96, the value for S_i is found as (T. Tanaka & Iida, 1994)

$$S_i = b N_{AV}^{\frac{1}{3}} V_i^{\frac{2}{3}} \quad (3.100)$$

where N_{AV} is Avogadro's number, V_i is the component's molar volume, which can be estimated from its density, and b ($= 1.091$ for a closed lattice) is the geometric factor.

The operating temperature (T) for the alloys and the temperature (T_i^0) at which surface tension data for the components are available may differ. In these cases, the necessary data at required temperature (T) were estimated from available data at certain temperature.

$$\sigma_i(T) = \sigma_i^0 + (T - T_i^0) \frac{\partial \sigma_i}{\partial T}$$

where $\partial \sigma_i / \partial T$ represent temperature coefficients of surface tension for the components of the metal alloys. In terms of partial excess free energy in bulk ($G_i^{XS,b}$) and surface ($G_i^{XS,s}$) of the components equation 3.97 can be expressed as shown below in equation 3.101 (T. Tanaka & Iida, 1994)

$$\begin{aligned} \sigma &= \sigma_A + \frac{RT}{S_A} \ln \left(\frac{1 - c_B^S}{1 - c_b^B} \right) + \frac{1}{S_A} (G_A^{XS,s} - G_A^{XS,b}) \\ &= \sigma_B + \frac{RT}{S_B} \ln \left(\frac{c_B^S}{c_b^B} \right) + \frac{1}{S_B} (G_B^{XS,s} - G_B^{XS,b}) \end{aligned} \quad (3.101)$$

T. Tanaka & Iida (1994) reported the relationship between a component's partial excess Gibb's energy in the surface phase and that in the bulk phase

$$\frac{G_i^{XS,s}}{G_i^{XS,b}} = \frac{z^s}{z^b} = \lambda \quad (3.102)$$

Equation 3.102 indicates that $G_i^{XS,s}$, which has the same formula as $G_i^{XS,b}$, can be produced by substituting the mole fraction of the bulk phase c^b with the mole fraction of the surface phase c^s and then multiplying $G_i^{XS,b}$ by λ . Where z^s and z^b are, respectively, the surface phase and bulk phase co-ordination numbers. Using the least squares regression method, T. Tanaka & Iida (1994) determined $\lambda = 0.83$ for liquid alloys and $\lambda = 0.94$ for ionic melts including oxide mixtures. Additionally, the authors show that the value of b in relation 3.100 is 1.091 for liquid metal alloys under the assumptions of a closed packed structure and $b = 1$ for the fused salt.

Surface tension of solutions and surface adsorption of their components are two important aspects of colloid chemistry. The combination of the two Butler equations provides a valuable tool for estimating equilibrium surface composition and surface tension of solution. In Butler's equation, the partial surface tensions of the components are defined improperly. Since the Butler equation was derived by assuming a surface monolayer, its applicability is limited (Kaptay, 2019). Without using the idea of partial surface tensions, Kaptay (2019) gave a better derivation of the Butler equation from the fundamental Gibbs equations. Both the equilibrium surface composition and the equilibrium surface tension of a liquid solution can be calculated using the resulting equation. It is only assumed that the surface region can be characterized with an average composition, ignoring the composition gradients, in order to derive the new equations. These equations are derived without making any assumptions on the structure or thickness of the surface region. In comparison to the original Butler equations, which were calculated by assuming a surface monolayer, it has a wider range of applicability. The improved Butler equation that was derived is (Kaptay, 2019),

$$\begin{aligned} \sigma &= \frac{S_A^\circ}{S_A} \sigma_A + \frac{RT}{S_A} \ln \left(\frac{c_A^s}{c_A} \right) + \frac{1}{S_A} (G_A^{XS,s} - G_A^{XS,b}) \\ &= \frac{S_B^\circ}{S_B} \sigma_B + \frac{RT}{S_B} \ln \left(\frac{c_B^s}{c_B} \right) + \frac{1}{S_B} (G_B^{XS,s} - G_B^{XS,b}) \end{aligned} \quad (3.103)$$

When the entire system is made up of only one component i , S_i° (m^2/mole) represents the standard molar surface area of component i . It can be defined as $S_i^\circ = bN_{AV}^{\frac{1}{3}} (\Delta V^E)^{\frac{2}{3}}$ same

as S_i is defined. The partial molar volume of the component is often replaced by the standard molar volume of the same pure component and vice versa if the excess molar volume of the solution is negligible or unknown.

CHAPTER 4

RESULTS AND DISCUSSION

Two Bi-based and two In-based binary liquid systems are treated in this chapter using the theoretical framework introduced in Chapter 3. Within the context of a complex formation model, the diffusion coefficients of liquid Bi-Mg, Bi-Pb, Cu-In, and In-Pb alloys with regard to their bulk composition at a certain temperature are investigated, together with their structural and thermodynamic features. Energetics derived from their experimental thermodynamic data are utilized to analyze surface characteristics using the Buttler equation and viscosity using the BBK model.

4.1 Thermodynamic Properties

To study thermodynamic and structural properties, the complex formation model first needs to know the stoichiometry of the complex. To do this, we assume that in the liquid state of the alloy, there is a chemical complex with the form A_pB_q . The number of complexes, n_3 , was calculated using equations 3.1, 3.2 and equation 3.37 by selecting the values of p and q from the phase diagram and determining the initial values of energy parameters χ and Ψ_{ij} as described by Bhatia et al. (1973). The value of p and q determined from phase diagram are given in Table 1 (Hultgren et al., 1973). Using these p , q , χ , Ψ_{ij} and n_3 values, we continue to fit the experimental values of alloy mixing free energy by adjusting the energy parameters χ and Ψ_{ij} . Once χ and Ψ_{ij} are fixed, their values do not change during the calculation of the diffusion coefficients, structural properties and other thermodynamic properties.

The concentration dependence of the equilibrium values of chemical complexes, n_3 , is seen to exhibit its greatest value at the compound-forming composition, $c_c = p/p + q$. The mixing functions, or the Gibbs free energy (Figure 9), are negative for all alloys at all bulk compositions. It displays a flat minimum of -3.3542 at the composition, $c_{Bi} = 0.444$ for Bi-Mg, signifying a considerable propensity for compounds to form as presented in

Figure 9(a). The fact that G_M/RT is less than -3 (i.e., -3.3265) even at the value of $c_c = 0.4$ indicates the strong tendency of chemical ordering toward stoichiometric composition in Bi-Mg alloys.

Compounds do not exist as distinct thermodynamic phases in the liquid state. Liquid compounds can be identified by their distinctive physical behavior around particular proportions, which we will refer to as stoichiometric or compound-forming compositions by definition. These behaviors include extremes and minima in the free energy of mixing (G_m), Heat of formation (H_m), entropy of mixing (S_m), chemical short range order parameter (α_1) ratio of mutual to intrinsic diffusion coefficient (D_M/D_{id}), and Darken stability function ($\partial^2 G_M/\partial c^2$). For liquid alloys made of Bi-Pb, Cu-In, and In-Pb, the stoichiometric compositions are 0.25, 0.67, and 0.5, respectively (Figure 9 (b, c, d)). In the region of the compound forming concentration, the minimum G_M/RT value for Bi-Pb is -0.9041 at $c_{Bi} = 0.5$ and for Cu-In, it is -0.9408 at $c_{Cu} = 0.6$. The lowest negative G_M/RT value for In-Pb alloys, which is -0.5865 at $c_{In} = 0.5$, suggests that In-Pb is the least strong of the four alloys in terms of association.

Calculations of the enthalpy of formation H_M , mixing entropy S_M , concentration-concentration fluctuation at the long wavelength limit $S_{cc}(0)$, and mutual diffusivities D_M/D_{id} will be done using the set of energy parameters that propagate the computed values of the free energy of mixing of liquid alloys to a reasonable extent. Table 1 contains the p and q values along with the interaction energy parameters that were used in the calculation. The formation of intermetallic compounds of the type Bi_2Mg_3 in the solid phase is depicted by the phase diagram for Bi-Mg (Hultgren et al., 1973). Therefore, we assume that the compound will continue to be stable, remain in the liquid phase, and reasonably influence the liquid alloy's thermodynamic properties. The choice of p and q corresponding to the $BiPb_3$, Cu_2In , and $InPb$ complexes are able to reasonably reproduce the stated free energy of the mixing values of the alloy in the case of the liquid alloys Bi-Pb, Cu-In, and In-Pb. Figure 9 depicts the plot of G_M/RT with the corresponding bulk concentration for the liquid alloys Bi-X (X = Mg, Pb) and In-Y (Y = Cu, Pb).

Table 1: Stoichiometric indices and interaction parameters.

System	p	q	χ/RT	Ψ_{12}/RT	Ψ_{23}/RT	Ψ_{13}/RT
Bi-Mg	2	3	16.28	0.000	-3.320	-2.520
Bi-Pb	1	3	1.880	-0.887	-0.714	0.519
Cu-In	2	1	2.221	0.235	0.140	1.165
In-Pb	1	1	0.730	0.480	1.376	1.230

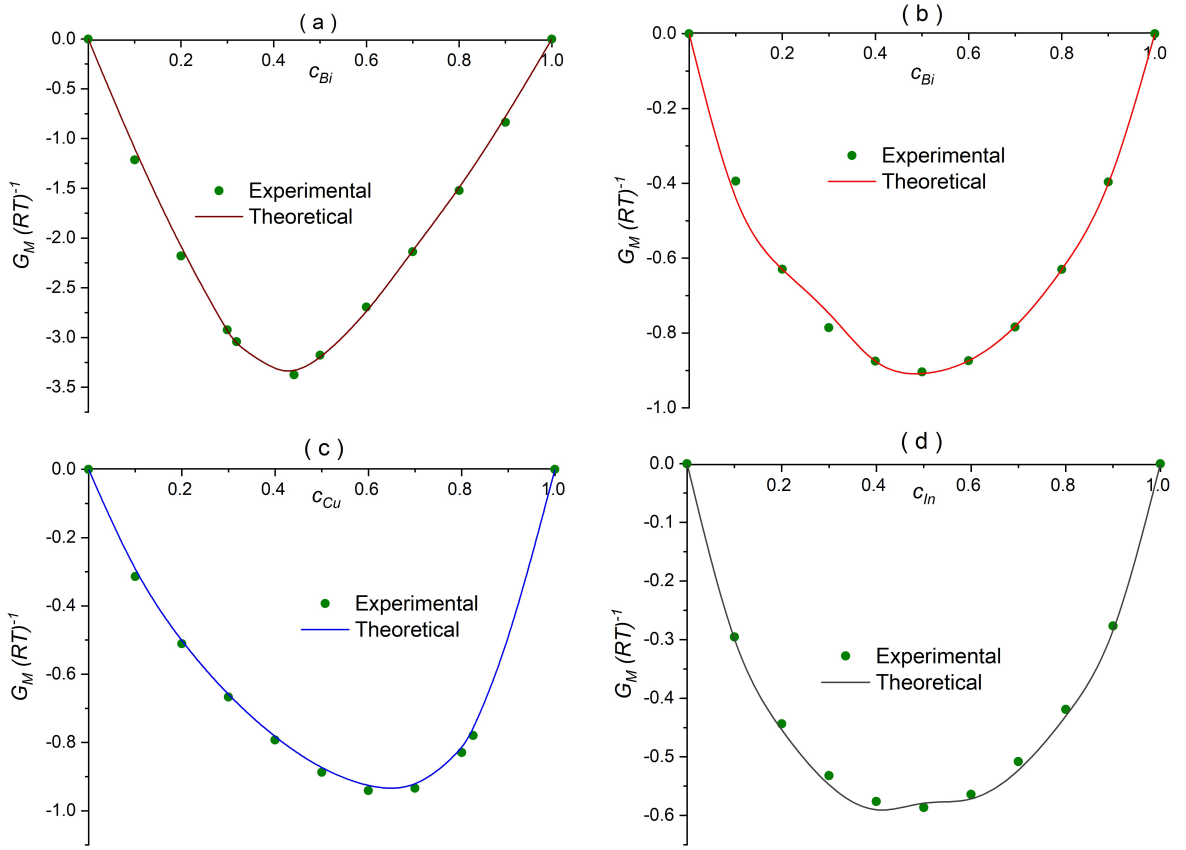


Figure 9: Free energy of mixing ($G_M(RT)^{-1}$) versus bulk concentration for (a) Bi-Mg, (b) Bi-Pb, (c) Cu-In, and (d) In-Pb alloys at 975 K, 700 K, 1073 K and 673 K respectively.

The lines represent calculated values at 975K for Bi-Mg, 700 K for Bi-Pb, 975 K for Cu-In, and 673 K for In-Pb alloy systems. The points represent experimental data from Hultgren et al. (1973). Table 1 shows the energy inputs parameters that were used for the calculation. It should be noted that certain factors, such as the coordination number (z) and the order energy parameters, χ , Ψ_{ij} do not depend on concentration within the context of the models discussed above. The thermodynamic parameters of liquid alloys computed using the R-K polynomial contained artifacts, which were removed using the exponential dependency of the interaction energies with temperature (Gohivar, Yadav, et al., 2020). However, utilizing a complex formation model, we were unable to detect any artifacts that would have allowed us to employ the linear relationship between interaction energies and temperature (Bhandari, Koirala, & Adhikari, 2021). The order energy parameters are fitted using the thermodynamic data, and the value of z is chosen from the structural data.

Calculations using $p = 2$ and $q = 3$ for Bi-Mg, $p = 1$ and $q = 3$ for Bi-Pb, $p = 2$ and $q = 1$ for Cu-In, and $p = 1$ and $q = 1$ for In-Pb complexes are shown in Figure 9. These complexes are most likely to form in the liquid phase of the alloy, according to the observed free energy of mixing liquid alloys. The aforementioned complexes exhibit an

excellent fit for the free energy values at the specified temperatures illustrate the validity of the model chosen. Equation 3.20 and experimental H_M values from Hultgren et al. (1973) were used to fit the H_M vs concentration graph. The temperature coefficient values for the interaction parameters that best fit the experimental H_M data are displayed in Table 2. The $\partial\Psi_{ij}/\partial T$ values also remain constant throughout the whole calculation once they have been fitted.

Table 2: Temperature coefficient values for the interaction parameter

System	$\frac{1}{R} \frac{\partial\chi}{\partial T}$	$\frac{1}{R} \frac{\partial\Psi_{12}}{\partial T}$	$\frac{1}{R} \frac{\partial\Psi_{13}}{\partial T}$	$\frac{1}{R} \frac{\partial\Psi_{23}}{\partial T}$
Bi-Mg	1.571	2.510	-3.200	-1.400
Bi-Pb	1.580	-0.150	0.500	0.900
Cu-In	1.160	-1.461	1.500	0.171
In-Pb	1.110	9.500	0.650	0.500

If energy parameters are assumed to be temperature independent, the values of H_m and S_M are found to be in poor agreement with the experiment. In order to calculate heat and entropy of formation that agrees with observed values, we have consequently assumed that these quantities vary with temperature. In all alloy systems, Figure 10 shows that there is good agreement between the experimental and predicted values of H_M/RT .

The fact that the H_M/RT values for the Bi-Mg and Bi-Pb systems are negative over the entire concentration further supports that these alloys are chemically favorable systems. Based on the positive to negative H_M/RT values for the Cu-In system, this alloy goes through a phase separating to ordering transformation with regard to bulk composition. The positive H_M/RT values for In-Pb, on the other hand, indicate that it is much more weaker in complexes formation than earlier systems.

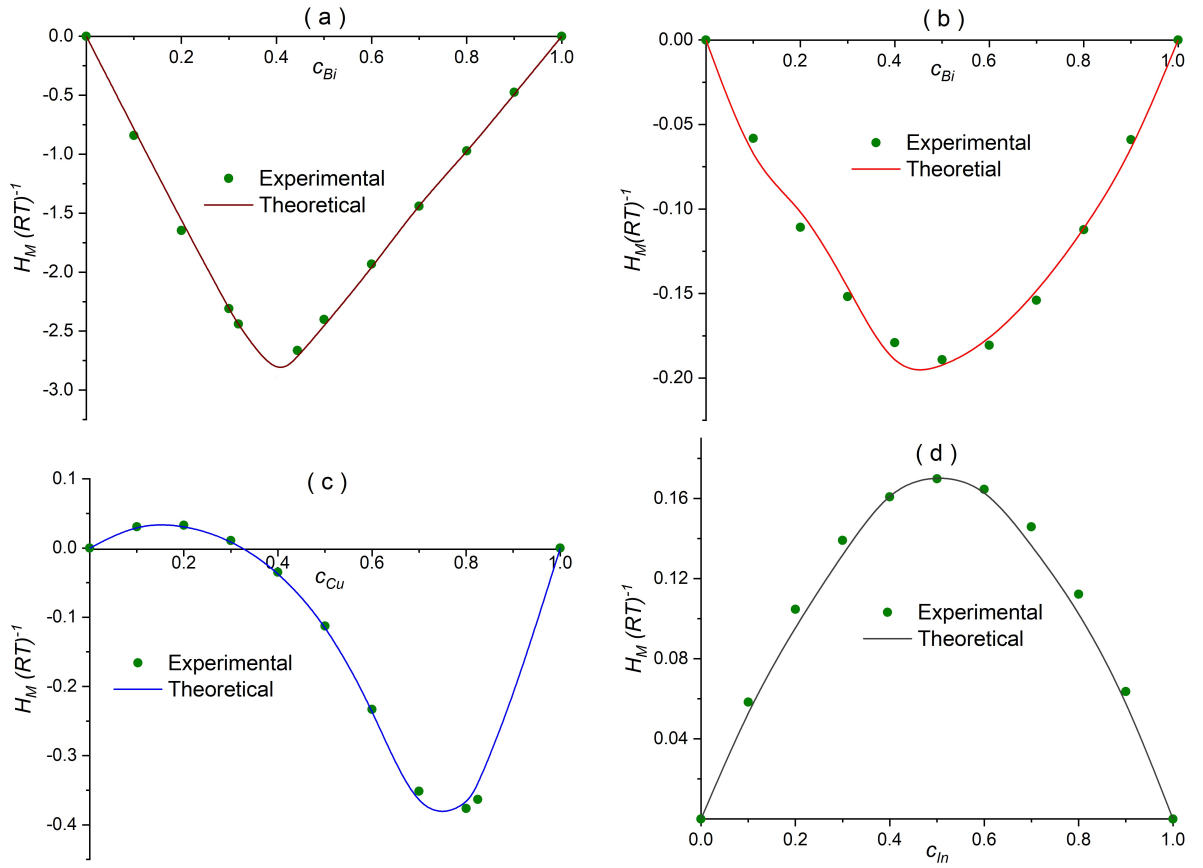


Figure 10: Heat of mixing ($H_M(RT)^{-1}$) versus bulk concentration for a) Bi-Mg, b) Bi-Pb, c) Cu-In and d) In-Pb alloys at 975 K, 700 K, 1073 K and 673 K respectively.

Equation 3.21 is used to compute S_M/R using the same interaction parameters that were used to calculate the values of G_M and H_M . Figure 11 illustrates the fair agreement between estimated values and experimental values of S_M for the systems under consideration. Theoretical data for the liquid alloy of Bi-Mg at $c = 0.4$ shows a substantial fall in S_M/R value to 0.4340, which implies a higher degree of complex formation behavior at that composition.

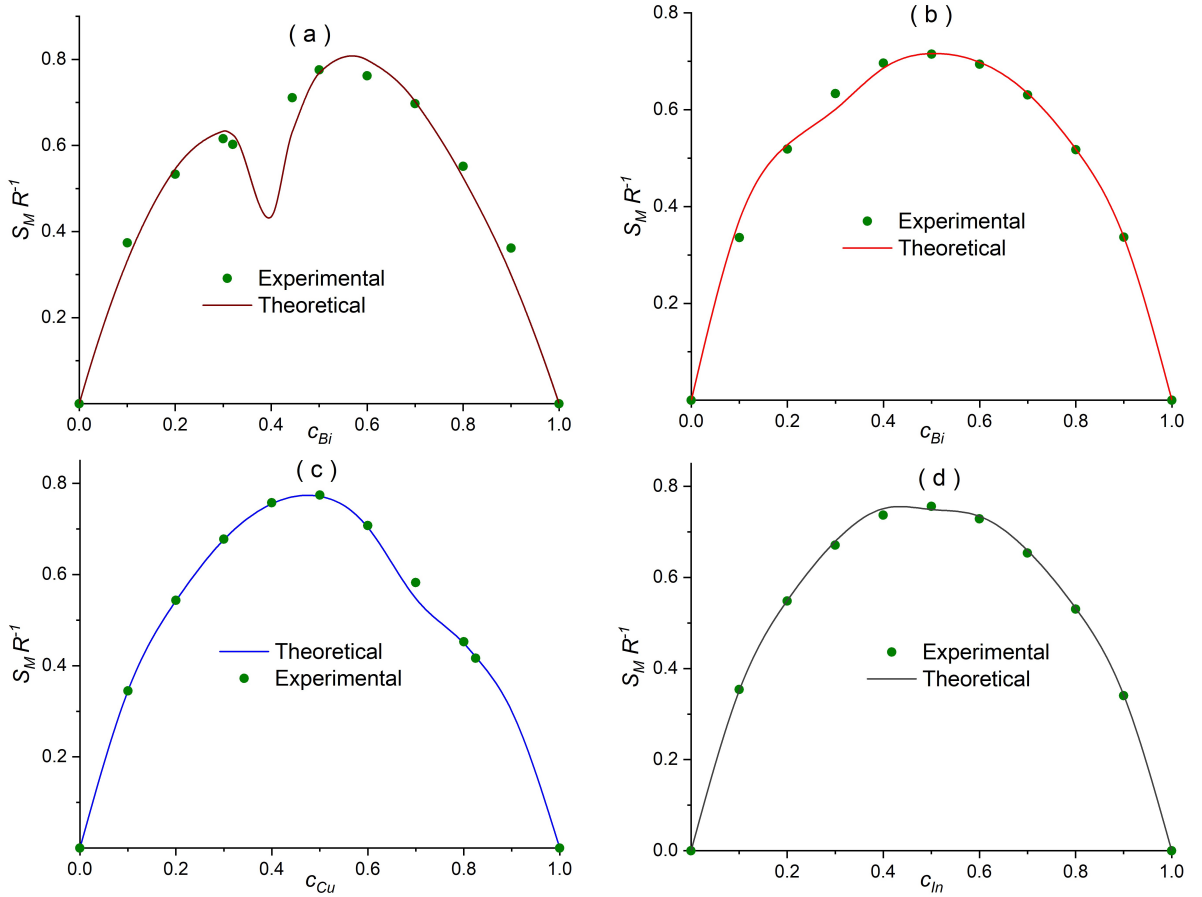


Figure 11: Entropy of mixing ($S_M R^{-1}$) versus bulk concentration for a) Bi-Mg, b) Bi-Pb, c) Cu-In and d) In-Pb alloys at 975 K, 700 K, 1073 K and 673 K respectively.

4.2 Structural Properties

Because diffraction experiments are difficult, the theoretical estimation of concentration fluctuations in the long wavelength limit $S_{cc}(0)$ is very important when trying to figure out how atoms interact in the melt. In the case of liquid solutions, the size of $S_{cc}(0)$ depends on how the solution is made and can vary from an ideal solution to a non-ideal solution. In a binary system, the dependence of $S_{cc}(0)$ on concentration also depends on the nature of the solution and how the species interact with each other. In strongly interacting systems, the magnitude of $S_{cc}(0)$ goes to zero; in weakly interacting systems, it has an intermediate value; and in non-interacting systems, it has significant large positive values. Using the estimated energy parameters from our earlier calculations, we computed $S_{cc}(0)$ and the Warren-Cowley short-range order parameter (α_1). Any divergence of $S_{cc}(0)$ from its ideal value is of great significance to anyone attempting to visualize the extent of interaction in the mixture. $S_{cc}(0) \ll S_{cc}^{(ideal)}(0)$ is a sign of strong association or the presence of chemical complexes in the mixture. If for a certain composition $S_{cc}(0) \gg S_{cc}^{(ideal)}(0)$ then there is a tendency of segregation or phase separation. The ideal value of $S_{cc}(0)$, which is related to ideal mixing, is $S_{cc}^{(ideal)}(0)$.

Figure 12 depicts the plots of $S_{cc}(0)$ for the complexes of Bi-Mg, Bi-Pb, Cu-In, and In-Pb.

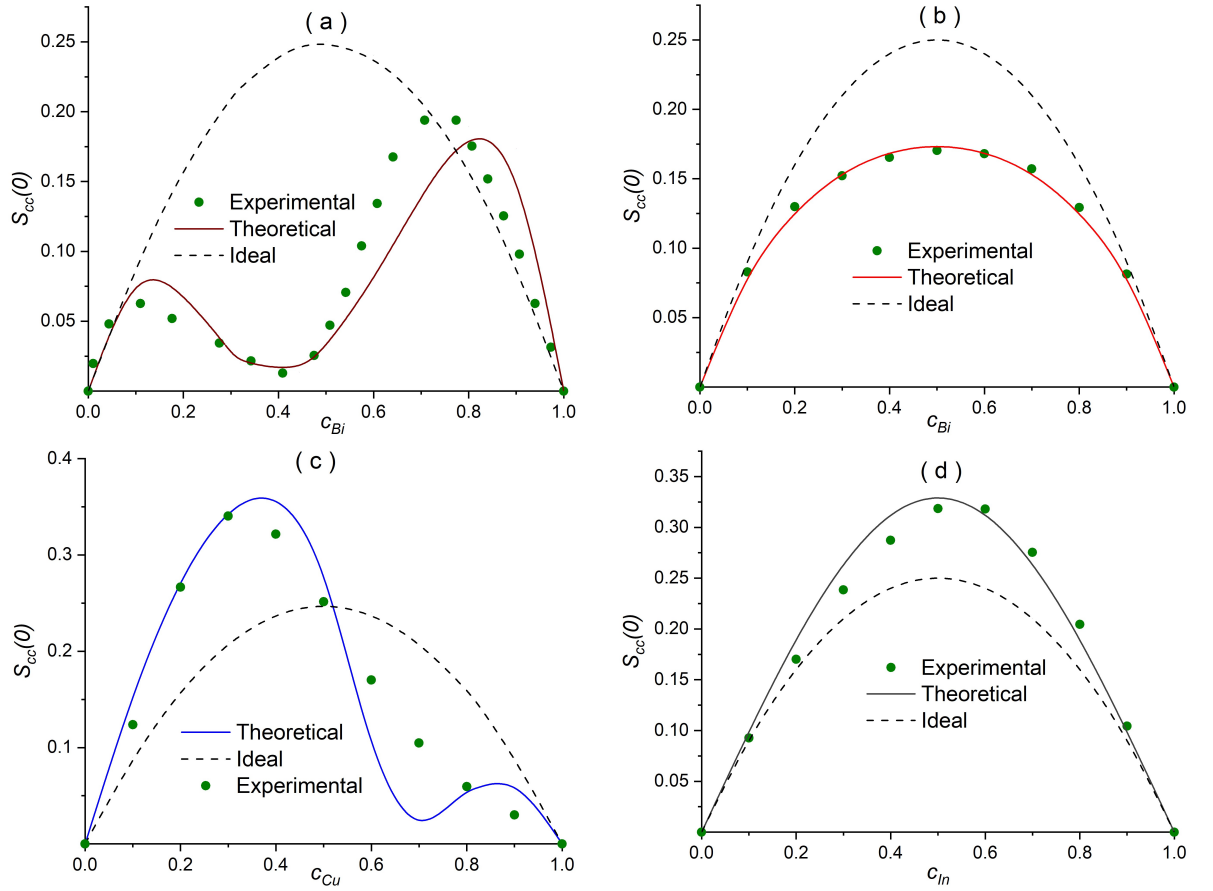


Figure 12: Concentration fluctuation at long wavelength limit $S_{cc}(0)$ versus bulk concentration for a) Bi-Mg, b) Bi-Pb, c) Cu-In and d) In-Pb alloys at 975 K, 700 K, 1073 K and 673 K respectively.

The points represent experiment results, whilst the lines represent calculated values. The experimental data for Bi-Mg are taken from Bhatia & Hargrove (1974). The experimental values for Bi-Pb, Cu-In, and In-Pb were computed using equation 3.69 utilizing the experimental activity data shown in Table 3. And in Figure 12, the dashed line represents the ideal values of $S_{cc}(0)$ as determined by equation 3.68.

Table 3: Input activity data for the calculation of experimental $S_{cc}(0)$ (Hultgren et al., 1973) .

$c_{\text{Bi, Cu, In}}$	Bi-Pb		Cu-In		In-Pb	
	a_{Bi}	a_{Pb}	a_{Cu}	a_{In}	a_{In}	a_{Pb}
0	0	1	0	1	0	1
0.1	0.052	0.897	0.096	0.916	0.133	0.900
0.2	0.115	0.782	0.151	0.848	0.259	0.805
0.3	0.195	0.657	0.192	0.783	0.375	0.712
0.4	0.293	0.527	0.233	0.706	0.48	0.624
0.5	0.406	0.404	0.282	0.603	0.576	0.538
0.6	0.530	0.292	0.349	0.462	0.662	0.454
0.7	0.656	0.196	0.453	0.283	0.745	0.366
0.8	0.779	0.116	0.620	0.107	0.825	0.268
0.825	–	–	0.680	0.072	–	–
0.9	0.895	0.052	–	–	0.908	0.151
1	1	0	1	0	1	0

According to our theoretical analysis, the maximum deviation of $S_{cc}(0)$ from the ideal value, $S_{cc}^{(\text{ideal})}(0)$, for Bi-Mg liquid alloys occurs at stoichiometric composition, or at $c_c = 0.4$. This suggests that c_c is the concentration at which the tendency to form compounds is strongest. Bi-Pb liquid alloys have a favorable tendency to compound formation at all compositions because the computed $S_{cc}(0)$ values are smaller than the ideal values $S_{cc}^{(\text{ideal})}(0)$. Cu-In liquid alloys, on the other hand, exhibit ordering features for $c > 0.6$ while having a tendency to phase separate for $c < 0.6$. Despite this, liquid systems including Bi-Mg and Cu-In have shown a tendency to form glasses. The mixture that forms glass is that composition at which the observed $S_{cc}(0)$ value reaches the ideal $S_{cc}(0)$ ideal value. Therefore, the theoretical observation shows that the glass-forming compositions for the Bi-Mg and Cu-In systems are 0.52 and 0.772, respectively, which are quite near to the values of 0.5 and 0.72 that are shown by experimental observation. It has also been seen from Figure 12(c) that In-Pb undergo phase segregation as it has larger $S_{cc}(0)$ values in the whole concentration range.

A measurement of the degree of compound formation in the liquid alloy is also provided by the chemical short-range order parameter (α_1). The minimum value of α_1 is -1, which denotes total ordering in a liquid alloy, while the greatest value of α_1 is 1, which depicts complete separation of alloy components. The investigation of chemical short range order parameter also provides support for the mixing pattern seen in terms of $S_{cc}(0)$. The fact that the α_1 value less than -0.65 value and approaching -1 near the stoichiometric composition clearly suggests that the Bi-Mg binary melt has a tendency toward hetero-coordination. α_1 values for the Bi-Pb complex likewise appear to be stronger, with a minimum depth of $\alpha_1 = -0.0425$ at equiatomic composition. In the situation of Cu-In liquid alloy, a α_1 value smaller than -0.4 near the stoichiometric composition indicates a favorable tendency for compound formation. However, the presence of positive values

across the full composition range of In-Pb alloys indicates that the alloy segregates throughout the whole concentration zone. The behavior of α_1 in four different liquid alloys indicates that the ordering tendency diminishes from Bi-Mg to Cu-In, Bi-Pb, and In-Pb.

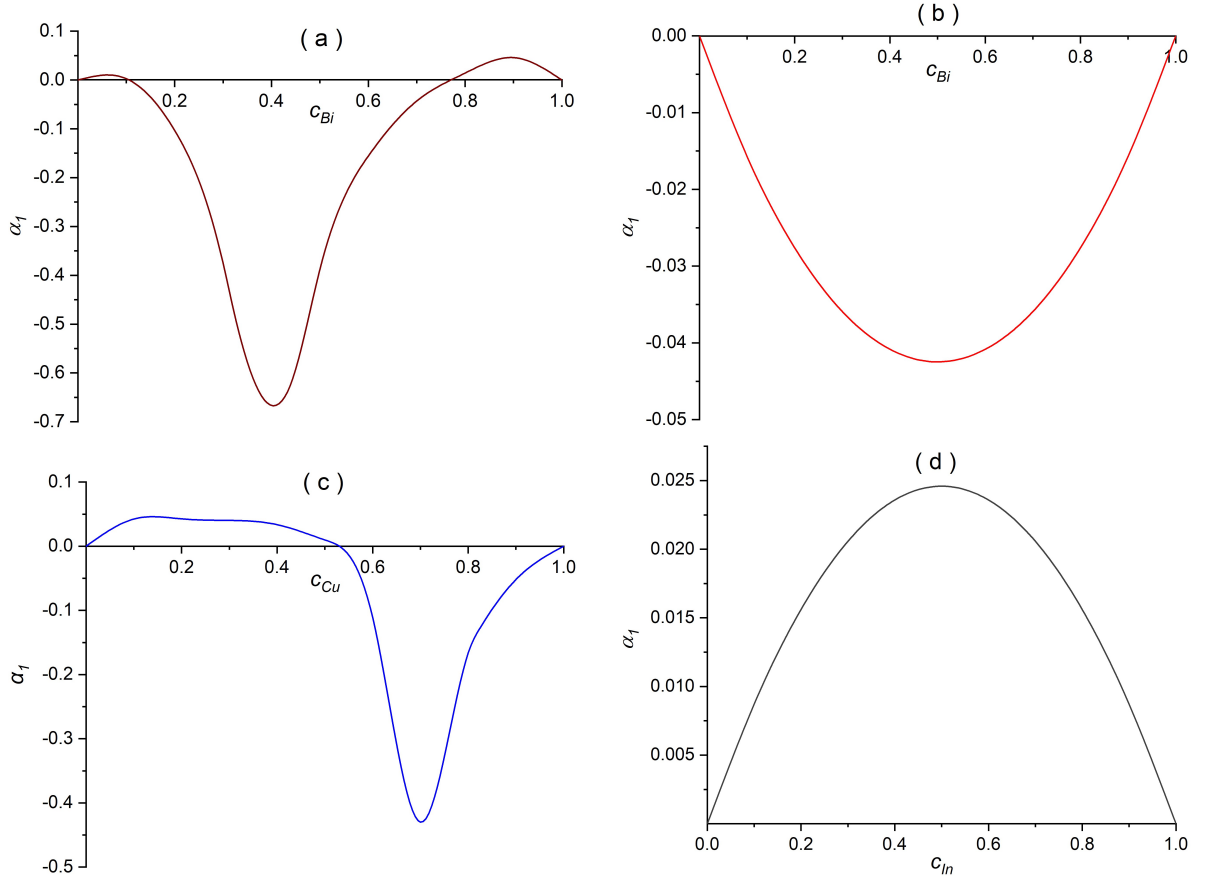


Figure 13: Chemical short range order (α_1) versus bulk concentration for a) Bi-Mg, b) Bi-Pb, c) Cu-In and d) In-Pb alloys at 975 K, 700 K, 1073 K and 673 K, respectively.

4.3 Transport Properties

Using equation 3.79, the obtained values of $S_{cc}(0)$ can also be utilized to assess the ratio of mutual and intrinsic diffusivities (D_M/D_{id}) as functions of composition. It should be noted that the level of order in a liquid binary alloy can also be determined using this ratio of mutual to intrinsic diffusivities. The alloy having a random combination of components that leads to the ideal distribution if $D_M/D_{id} = 1$. $D_M/D_{id} > 1$ therefore, exhibits a propensity toward hetero-coordination, whereas $D_M/D_{id} < 1$ exhibits a tendency toward homo-coordination. Figure 14 displays the plots of D_M/D_{id} versus concentration for all selected binary liquid alloys.

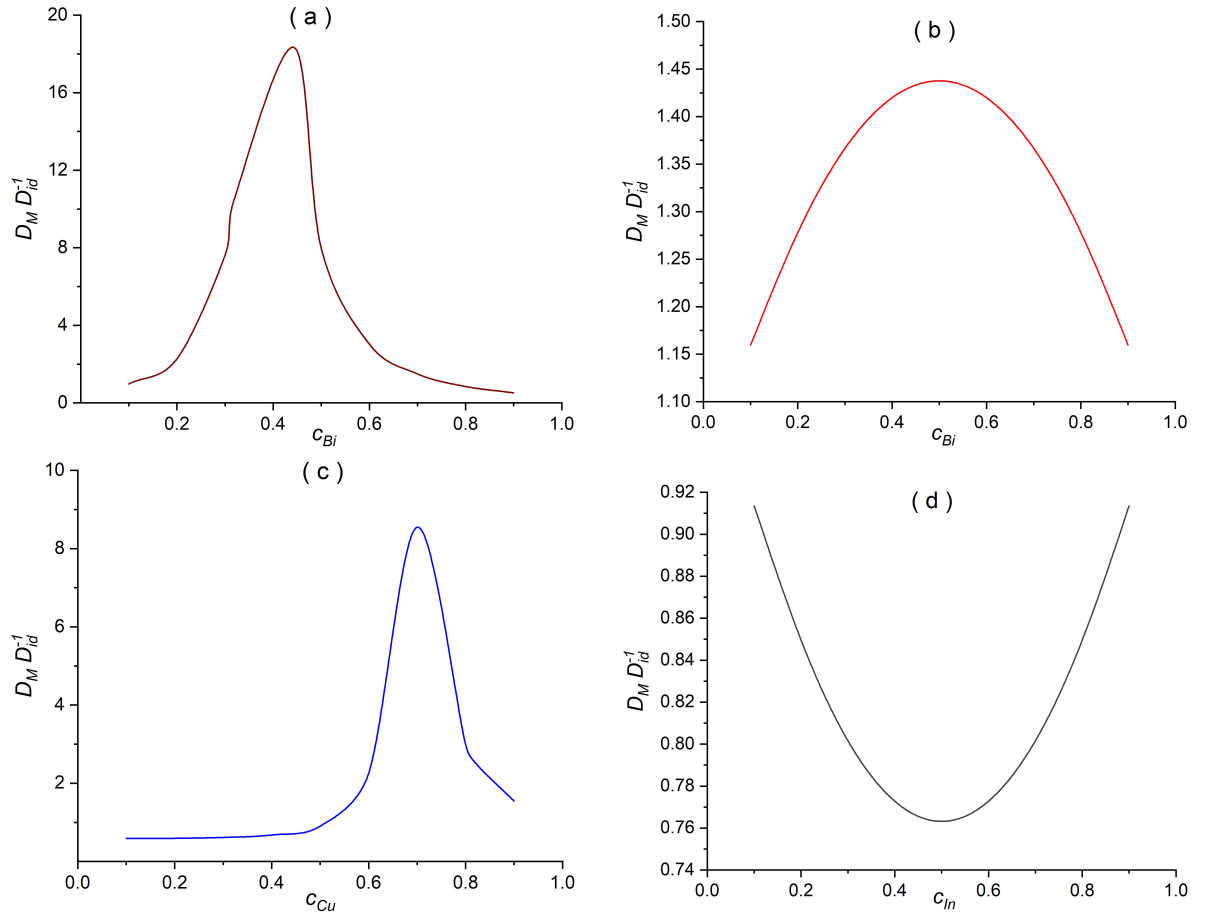


Figure 14: Ratio of mutual and intrinsic diffusion coefficients ($D_M D_{id}^{-1}$) versus bulk concentration for a) Bi-Mg, b) Bi-Pb, c) Cu-In and d) In-Pb alloys at 975 K, 700 K, 1073 K and 673 K respectively.

In the composition range of 0.2 to 0.7, it is observed that the values of D_M/D_{id} obtained for Bi-Mg are positive and greater than one (Figure 14(a)). At the compound forming concentration, the value is at its highest point (being more than 18.33). Because this value is so high, the theoretical analysis of the presence of the strong chemical order in the liquid state of Bi-Mg alloy at 975 K is further clarified by this finding. At a temperature of 1073 K, the values for D_M/D_{id} are found to be less than one up to the bulk composition $c_{Cu} = 0.5$, which implies that there is a phase separation in Cu-In system around that composition range. The D_M/D_{id} value is at its greatest (= 8.54), which occurs around the compound forming concentration. This also provides evidence that the liquid Cu-In alloys exhibit significant degree of ordering around compound forming concentration. The values of D_M/D_{id} for the liquid Bi-Pb alloy based on the energy parameters related to the $BiPb_3$ complex indicated values that fall in the range of 1.1 to 1.45 all over the whole concentration range. This demonstrated further that the Bi-Pb alloy is capable of good compound formation throughout the full concentration range, despite having a lower level of strength compared to the Cu-In and Bi-Mg systems. It has been reported that the D_M/D_{id} values, when measured for In-Pb at 673 K, decrease initially to the

increasing bulk composition. Stoichiometric composition yields the smallest possible value for D_M/D_{id} , which is equal to 0.76. The D_M/D_{id} values steadily grow with the relevant bulk concentration after the stoichiometric composition. The fact that the value of D_M/D_{id} is less than unity throughout the entire composition range in In-Pb liquid alloys suggests segregation throughout the whole of the composition range and, as a result, provides further support for the very weak tendency of compound formation in the In-Pb alloy.

The equation $\rho_i(T) = \rho_i^0 + (T - T_i^0)\partial\rho/\partial T$ is used to optimize the density values at necessary temperature (T) utilizing the density values of component elements given at melting temperature (T_i^0). The atomic volumes of the components are calculated using the density values at the necessary temperature combined with the atomic masses. The relevant quantities in the expression for viscosity are then evaluated using the equation 3.92 and equation 3.93. Finally, the equation 3.95 is employed to determine the viscosity of particular liquid binary alloys. As shown in Table 3, the additional required input values are taken from Brandes & Brook (2013). Figure 15 illustrates how the viscosity of all systems is dependent on composition. Over the whole compositional range, the viscosities obtained for Bi-Mg alloys are higher than the ideal values. Positive departure from ideality increases until $c_{Bi} = 0.4$, where it reaches its maximum value ($= 0.001427$).

Table 4: Input parameters for calculation of viscosity (Brandes & Brook, 2013).

Element	Atomic Mass M_i (kg/mol)	Melting Temperature T_i^0 (K)	Density at T_i^0 (kg/m ³)	Temperature coefficient of density $\frac{\partial\rho}{\partial T}$ (kg/m ³ K)
Bi	0.2090	544.0	10068	-1.3300
Mg	0.0243	924.0	1590.0	-0.2647
In	0.1148	429.6	7023.0	-0.6798
Pb	0.2072	600.0	10678	-1.3174
Cu	0.0635	1356	8000.0	-0.8010

As seen in Figure 15 (c), the value of viscosity in the case of Cu-In melt drops to its lowest point ($=0.008207$) when c_{Cu} is equal to 0.2, while it reaches its highest point (0.008522) when c_{Cu} is equal to 0.8. The value of viscosity for Bi-Pb first rises with the bulk composition, and then it reaches its highest point when it has an equiatomic composition. When there is a further increase in the concentration of bismuth, it goes down. It is observed that the viscosity values for Bi-Pb have a higher value than the corresponding ideal values. At a c_{Bi} value of 0.9, the deviation from ideal values is found to be the greatest (0.003214). It is reported that the viscosity measured for Bi-Pb and In-Pb show opposing behaviors when compared to one another. For the In-Pb system, the viscosity isotherm almost perfectly demonstrates symmetrical behavior, with minima

located at $c_{In} = 0.5$. In contrast to the behavior observed in the Bi-Mg and Bi-Pb values, it was found that the viscosity values for the In-Pb values initially decreased when the corresponding composition increased. After equiatomic composition, viscosity values are observed to increase as concentration increases.

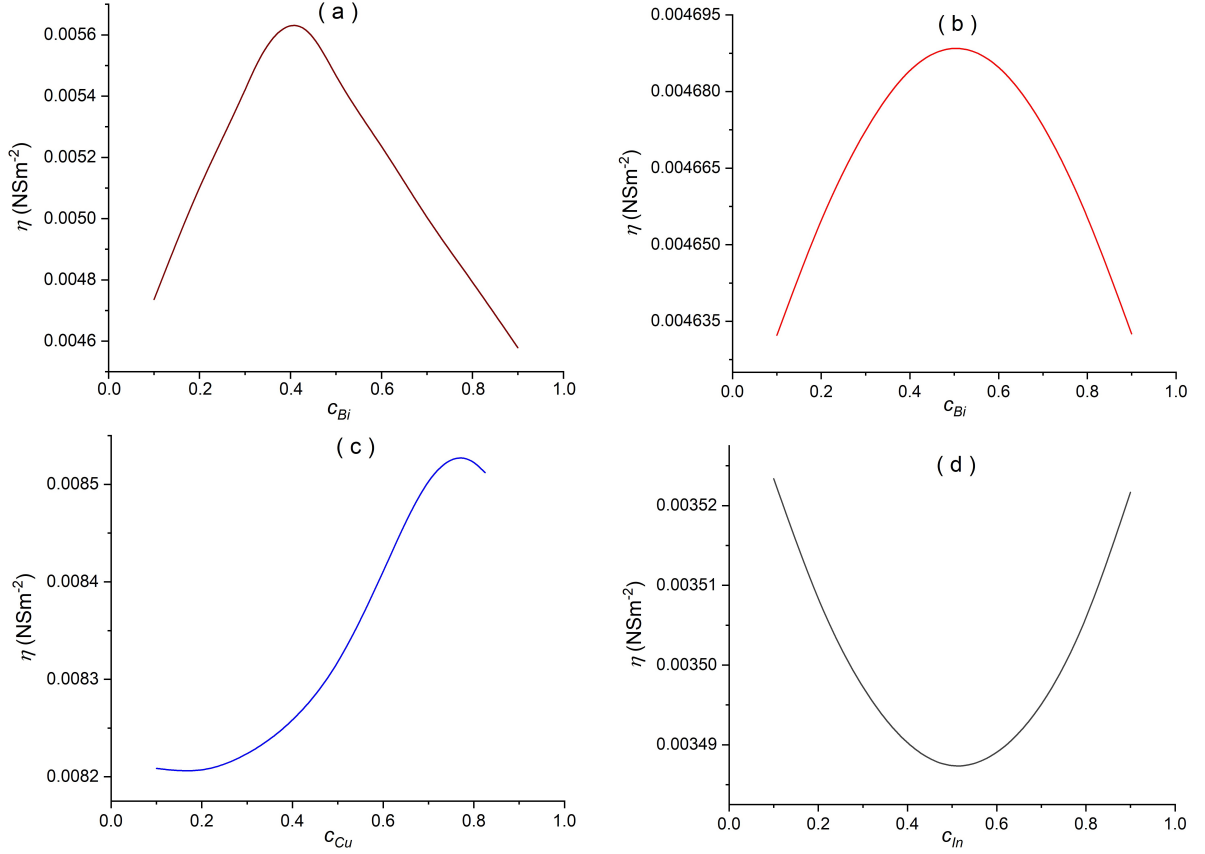


Figure 15: Viscosity (η) versus bulk concentration for a) Bi-Mg, b) Bi-Pb, c) Cu-In and d) In-Pb alloys at 975 K, 700 K, 1073 K and 673 K respectively.

4.4 Surface Properties

The surface concentrations of components and the surface tension values for the liquid alloys Bi-Mg, Bi-Pb, Cu-In, and In-Pb are calculated numerically using the formulae in the equation 3.103. As shown in Table 5, the partial excess free energy in bulk ($G_i^{XS,b}$) for Bi, Mg, Pb, Cu, and In in corresponding alloys are extracted from reference Hultgren et al. (1973). Additionally, equation 3.102 is used to determine the partial excess free energy in the surface ($G_i^{XS,s}$) of the components Bi, Mg, Pb, Cu, and In in the respective alloys.

Table 5: Excess bulk free energies of the components of the alloys in corresponding alloys (Hultgren et al., 1973) .

c	Bi-Mg		Bi-Pb		Cu-In		In-Pb	
	$G_{Bi}^{XS,b}$	$G_{Mg}^{XS,b}$	$G_{Bi}^{XS,b}$	$G_{Pb}^{XS,b}$	$G_{Cu}^{XS,b}$	$G_{In}^{XS,b}$	$G_{In}^{XS,b}$	$G_{Pb}^{XS,b}$
0.1	-16531	-282	-915	-5	-92	37	381	1
0.2	-14426	-892	-772	-31	-605	125	346	8
0.3	-11726	-2064	-601	-88	-953	239	300	23
0.32	-11134	-2386	–	–	–	–	–	–
0.4	–	–	-432	-179	-1155	346	249	53
0.444	-1850	-9023	–	–	–	–	–	–
0.5	-814	-10148	-290	-295	-1224	399	188	98
0.6	-86	-11423	-173	-437	-1154	306	131	168
0.7	-86	-11986	-91	-590	-930	-125	84	265
0.8	-2	-13006	-37	-752	-544	-1325	38	386
0.825	–	–	–	–	-413	-1892	–	–
0.9	-2	-14343	-8	-915	–	–	10	551

The surface tensions (σ_i^0) and densities (ρ_i^0) of the components of the alloy system at a constant temperature (T_i^0) were obtained from reference Brandes & Brook (2013), (where i represent Bi, Mg, Cu, In, and Pb) and are provided in Table 6. To achieve surface tension at working temperatures (T) of 975 K, 700 K, 1073 K, and 675 K for Bi-Mg, Bi-Pb, Cu-In, and In-Pb respectively, the temperature dependence of the surface tension of the liquid metals is given by $\sigma_i(T) = \sigma_i^0 + (T - T_i^0) \partial\sigma_i/\partial T$. Here $\partial\sigma_i/\partial T$ is the temperature coefficient of surface tension, and T is the working temperature in Kelvin for the component of the alloys. The area of the monoatomic surface layer for the component i can be calculated using the formula 3.100.

Table 6: Input parameters for calculation of surface tension (Brandes & Brook, 2013).

Element	Melting Temperature T_i^0 (K)	Surface tension (σ_i^0) at T_i^0 (N/m)	Temperature coefficient of surface tension $\partial\sigma/\partial T$ (N/m K)
Bi	544.0	0.378	-7.0×10^{-5}
Mg	924.0	0.559	-3.5×10^{-4}
In	429.6	0.556	-9.0×10^{-5}
Pb	600.0	0.468	-1.3×10^{-4}
Cu	1356	1.285	-1.3×10^{-4}

Figures 16(a), 16(b), 16(c), and 16(d), respectively demonstrate the surface concentration of Bi (c_{Bi}^s) versus bulk concentration of Bi (c_{Bi}) in Bi-Mg liquid alloy at 975 K, surface concentration of Bi (c_{Bi}^s) versus bulk concentration of Bi (c_{Bi}) in Bi-Pb liquid alloy at 700 K, surface concentration of Cu (c_{Cu}^s) versus bulk concentration of Cu (c_{Cu}) in Cu-In

liquid alloy at 1073 K and surface concentration of In (c_{In}^s) versus bulk concentration of In (c_{In}) in In-Pb liquid alloy at 673 K. Bi surface concentration curve in liquid Bi-Mg and Bi-Pb alloys deviate positively from ideality. In contrast, the surface concentrations of Cu and In in liquid Cu-In and In-Pb alloys deviate negatively from their ideal values. The surface concentrations of Bi in Bi-Mg, Bi in Bi-Pb, Cu in Cu-In, and In in In-Pb liquid alloys increase as the respective bulk concentrations increase. In liquid Bi-Mg alloy, the surface concentration of Bi is greater than its bulk concentration, but the surface concentration of Mg is lower than its bulk concentration. In liquid Bi-Pb alloy, the surface concentration of Bi is greater than its bulk concentration, whereas the surface concentration of Pb is lower than its bulk concentration. However, it is observed that the surface concentration of Cu is lower than its bulk concentration and the surface concentration of In is higher than its bulk concentration in the Cu-In liquid alloy. The surface concentration of In is found to be less than its bulk concentration, while the surface concentration of Pb is found to be greater than its bulk concentration in the In-Pb liquid alloy. The conclusion that can be drawn from this is that the Bi atoms in the Bi-Mg alloy, the Bi atoms in the Bi-Pb alloy, the In atoms in the Cu-In alloy, and the Pb atoms in the In-Pb alloy segregate along the surface of the alloy. In each binary system, the component that has greater surface concentrations values relative to its own bulk concentration values is the one that segregates tremendously over the surface.

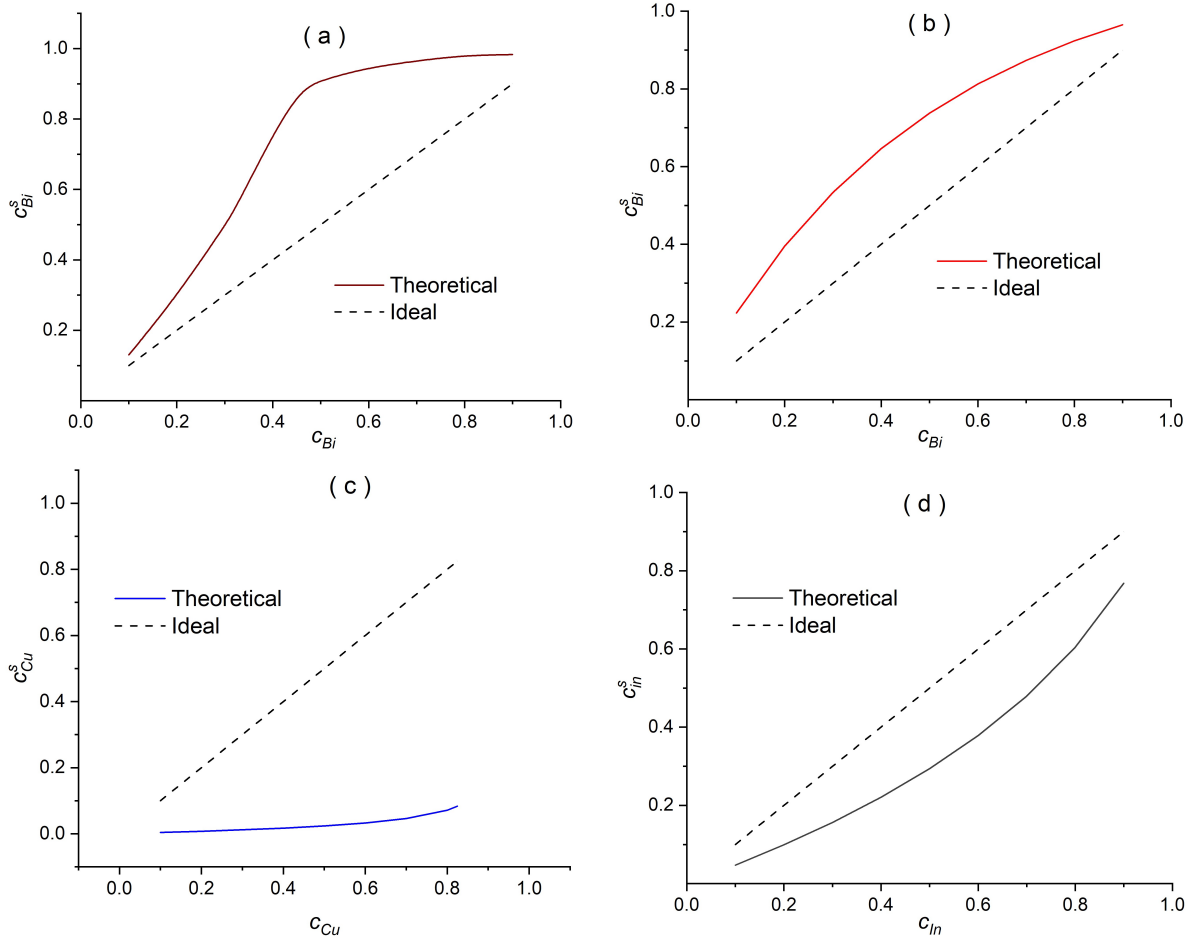


Figure 16: a) c_{Bi}^s versus c_{Bi} in Bi-Mg liquid alloy at 975 K. b) c_{Bi}^s versus c_{Bi} in Bi-Pb liquid alloy at 700 K. c) c_{Cu}^s versus c_{Cu} in Cu-In liquid alloy at 1073 K. d) c_{In}^s versus c_{In} in In-Pb liquid alloy at 673 K.

In order to calculate the surface tension, the values of the surface composition with respect to concentration are once again used into the same equations (equation 3.103). An intriguing behavior is displayed by the surface tension isotherm when Bi-Mg is considered. It has been noticed that the positive deviation from ideality ($\sigma_{ideal} = c\sigma_A + (1 - c)\sigma_B$) occurs when c is between 0 and 0.4, while the negative divergence occurs when c is between 0.4 and 1. The surface tension behavior of the Bi_2Mg_3 melt clearly suggests that the Bi-Mg alloy is most stable at stoichiometric content $c_c = 0.4$. The remaining three alloys, Bi-Pb, Cu-In, and In-Pb, all deviate negatively from ideality. It is found that the observed theoretical values are lower than the equivalent ideal values. When there is an increase concentration of copper in the bulk, there is a corresponding increase in the surface tension values of Cu-In. Because indium has lower surface tension than copper, indium atoms segregate on the surface of the Cu-in system. Adding a small number of bismuth atoms reduces the surface tension values of Bi-Pb. Bi has a lower surface tension compared to lead. As illustrated in Figure 17 (b), as the majority of bismuth atoms migrate to the surface and populate it, the surface tension of the alloy decreases from the surface tension value of lead and approaches the surface tension

value of pure bismuth as the bismuth bulk concentration increases. For In–Pb, a rise in surface tension was found with increasing Indium concentration. The surface tension values grow with the bulk concentration and reach a maximum of around 0.5211 at an indium concentration of 0.9 atomic fraction, which is near to the surface tension of the individual indium component. The surface tension values of the above binary systems vary between the surface tension values of the individual components with the bulk concentration of a component. The highest surface tension value of the alloy system is close to the surface tension value of the component having larger surface tension. The smallest surface tension value of the alloy system is close to the surface tension value of a component having lower surface tension.

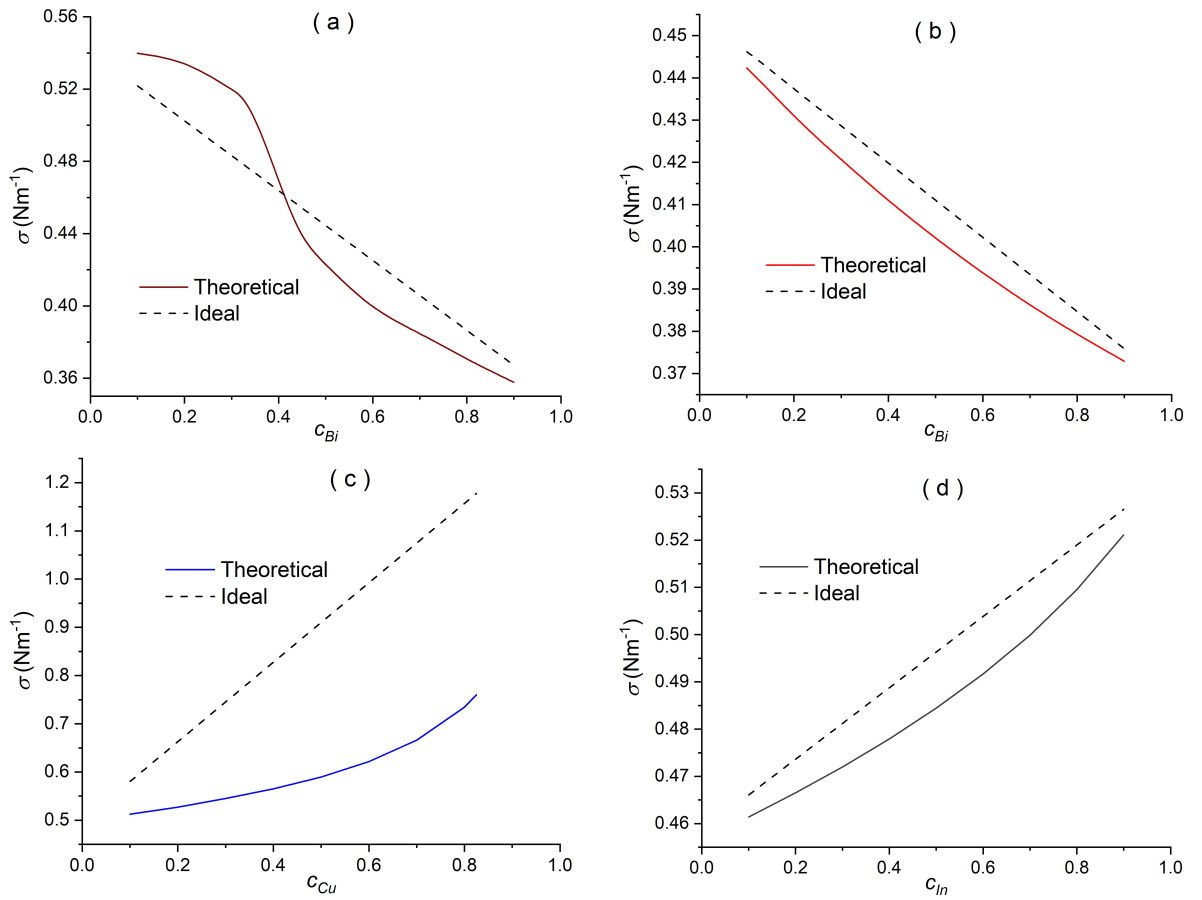


Figure 17: Surface tension (σ) versus bulk concentration for a) Bi-Mg, b) Bi-Pb, c) Cu-In and d) In-Pb alloys at 975K, 700K, 1073K and 673K respectively.

4.5 Temperature Dependent Behavior of Binary Liquid Alloys

Here, we have shown the outcomes of an expansion of the current models to higher temperatures. By applying their values at the particular temperature, the interaction energy parameters at the necessary temperature can be computed.

$$\Psi_{ij}(T_R) = \Psi_{ij}(T) + (T - T_R) \partial \Psi_{ij} / \partial T, \text{ Here, } T_R = 900 \text{ K, } 1100 \text{ K, } 1300 \text{ K and } 1500 \text{ K}$$

Using the values of the interaction energy parameters at 700K and associated temperature coefficients, the interaction energy parameters at 900 K, 1100 K, 1300 K, and 1500 K are now determined for Bi-Pb liquid alloys, as shown in Table 7.

Table 7: Interaction energy parameters at higher temperatures.

Interaction Energies	Temperatures			
	900 K	1100 K	1300 K	1500 K
Ψ_{12}/RT	-0.724	-0.619	-0.547	-0.494
Ψ_{13}/RT	-0.444	-0.272	-0.154	-0.066
Ψ_{23}/RT	0.604	0.658	0.695	0.722
χ/RT	1.814	1.771	1.742	1.720

From equation 3.14, the variation of G_M with temperature is obtained by using these interaction parameters at various temperatures (Figure 18). When temperatures are between 700 K and 1500 K, the maximum value of G_M/RT at equiatomic composition increases from -0.9084 to -0.8058 and exhibits a tendency toward phase separation.

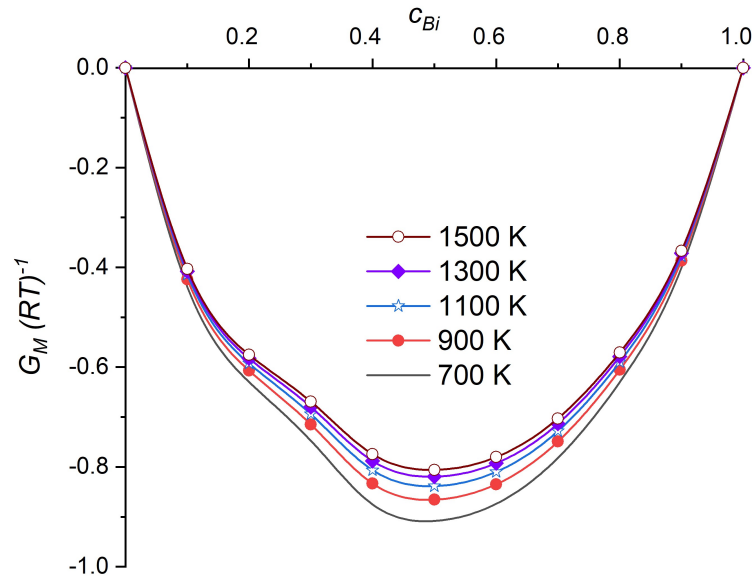


Figure 18: Compositional dependence of free energy of mixing ($G_M(RT)^{-1}$) in liquid Bi-Pb alloy at different temperatures.

Using the same interaction parameters from Table 7 in equation 3.64, the value of $S_{cc}(0)$ has been computed at various temperatures as depicted in Figure 19. The value of $S_{cc}(0)$ increases from 0.1732 to 0.2005 at equiatomic composition as the temperature rises from 700 K to 1500 K, narrowing the gap between $S_{cc}(0)$ values and their ideal values. This also suggests that as temperature rises, the alloy's propensity to form compounds decreases.

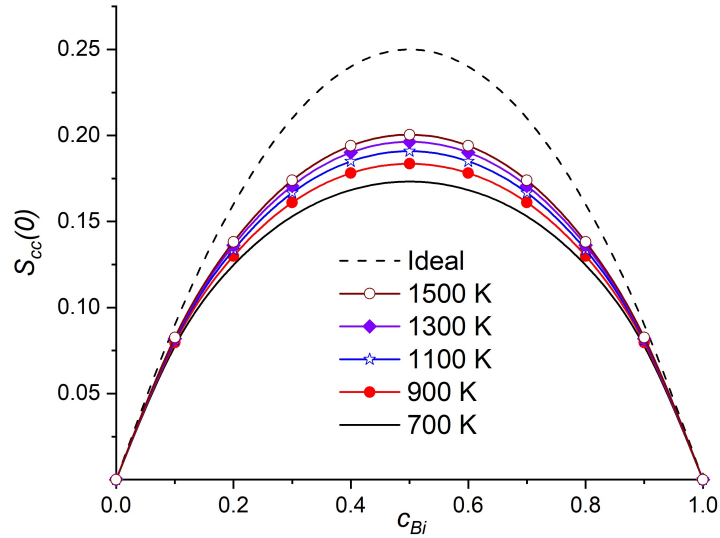


Figure 19: Compositional dependence of $S_{cc}(0)$ in liquid Bi-Pb alloy at different temperatures.

As is well known, the propensity for heterocordination in a binary melt system is represented by a rising -ve value of the chemical short range order parameter. Here, we see that the value of α_1 rises from -0.0425 at 700 K to -0.0241 at 1500 K. In terms of α_1 , Figure 20 also demonstrates the phase separation in the Bi-Pb system as a function of temperature.

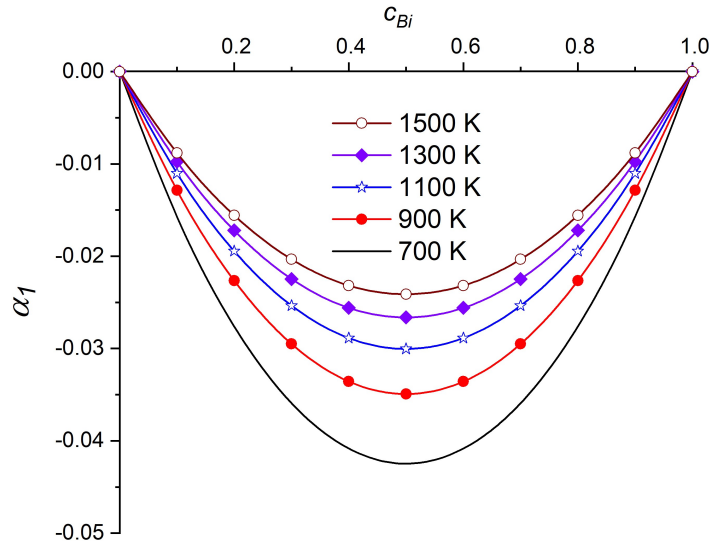


Figure 20: Compositional dependence of SRO parameter (α_1) in liquid Bi-Pb alloy at different temperatures.

Equation 3.79 is then applied to the $S_{cc}(0)$ value computed at various temperatures to determine the D_M/D_{id} values for that temperature, as shown in Figure 21. The trend toward phase separation of the system with temperature rise, as shown by G_M/RT , $S_{cc}(0)$ and α_1 , is further supported by the decreasing value of D_M/D_{id} (from 1.4435 to 1.247) with rise in temperature from 700 K to 1500 K.

Figure 22 depicts the compositional relationship between viscosity and temperature. Plotting η at various temperatures against c_{Bi} reveals that η tends to decrease as temperature rises and that the difference is greatest (0.002464) at the stoichiometric composition.

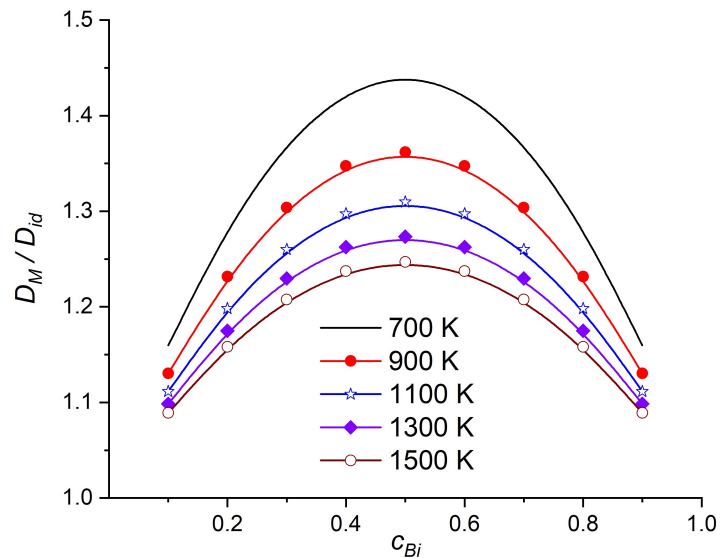


Figure 21: Compositional dependence of ratio of mutual and intrinsic diffusion coefficients (D_M/D_{id}) versus concentration of Bismuth (c_{Bi}) in the liquid Bi-Pb alloy at different temperatures.

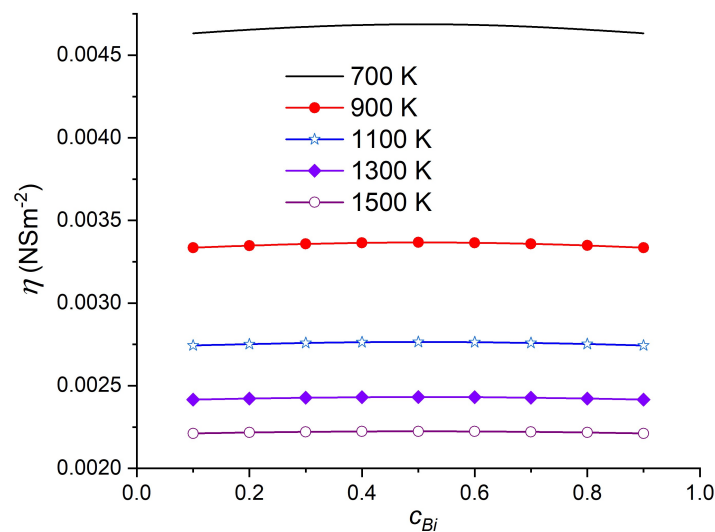


Figure 22: Compositional dependence of viscosity (η) of liquid Bi-Pb alloy at different temperatures.

Figure 23 shows the calculated values of surface concentration of Bi for molten Bi-Pb alloys at 700 K and at various temperatures. With an increase in temperature, it is observed that the surface concentration of Bi decreases. The propensity for surface composition to decrease as temperature increases from 700 K to 1500 K is greatest ($=0.1916$) at $c_{Bi} = 0.4$ and least ($=0.0425$) at $c_{Bi} = 0.9$. This indicates that the lowering tendency of surface composition with regard to temperature initially increases with an

increase in bulk composition up to $c_{Bi}=0.4$ and then reduces gradually up to $c_{Bi}=0.9$. The surface tension of Bi-Pb alloy with respect to bulk concentration of Bi at different temperatures are plotted in Figure 24. It has been noticed that the surface tension of the alloy reduces with increase in temperature, showing that the selected alloy's stability decreases with rise in temperature. The difference in surface tension values from 700 K to 1500 K is greatest ($= 0.0949$) at $c_{Bi}= 0.1$ and smallest ($=0.0577$) at $c_{Bi} = 0.9$. This indicates that $\sigma_{700K} - \sigma_{1500K}$ is found to have a decreasing relationship with increasing bulk composition of Bi.

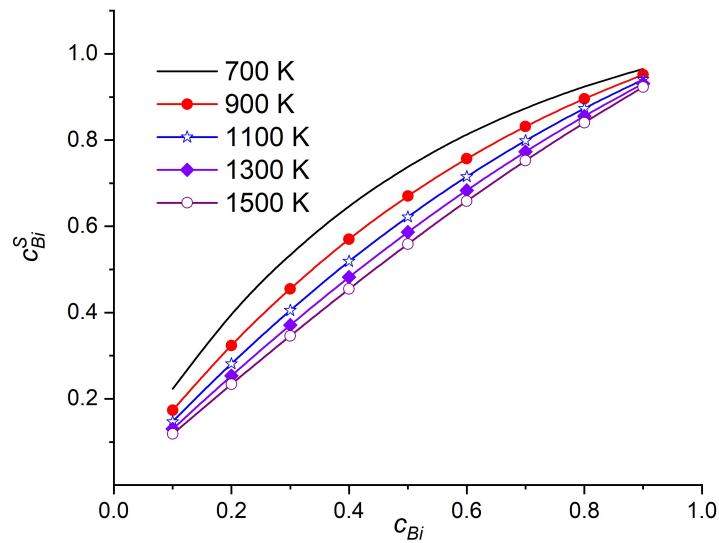


Figure 23: Compositional dependence of surface concentration of Bismuth (c_{Bi}^s) versus concentration of Bismuth (c_{Bi}) in the liquid Bi-Pb alloy at different temperatures.

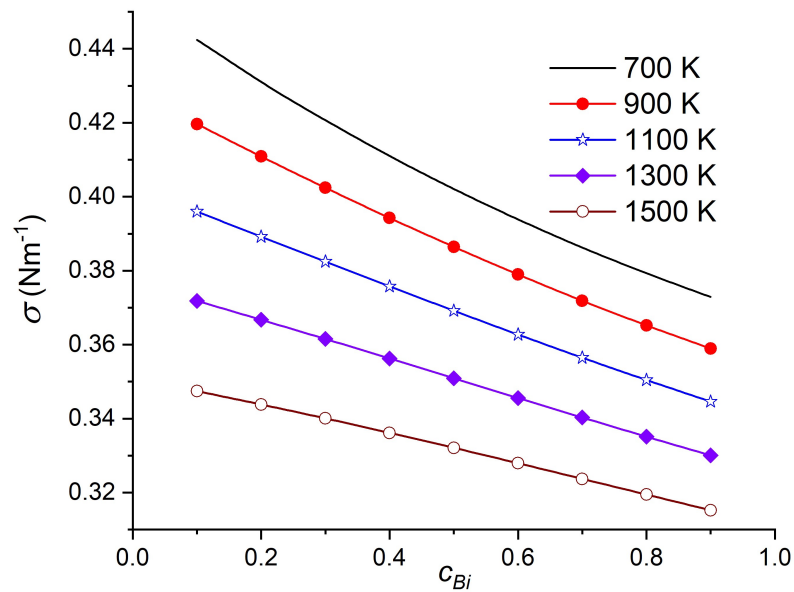


Figure 24: Compositional dependence of surface tension (σ) of liquid Bi-Pb alloy at different temperatures.

CHAPTER 5

CONCLUSION AND RECOMMENDATIONS

5.1 Conclusion

The primary focus of the work that has been given is the investigation of the mixing behavior of a few binary liquid alloys, including Bi-Mg, Bi-Pb, Cu-In, and In-Pb. The thermodynamic properties of the aforementioned liquid alloys, such as the free energy of mixing (G_M), heat of mixing (H_M), and entropy of mixing (S_M); microscopic structural properties of the aforementioned liquid alloys, such as concentration fluctuation in long wave length limit ($S_{cc}(0)$), chemical short range order parameter (α_1), and the ratio of diffusion coefficient (D_M/D_{id}) in the context of complex formation model. Assuming the complex is of type A_pB_q , modeling formulations for these thermodynamic and structural functions have also been derived. Here, the values of the two small indices p and q rely on the stoichiometric concentration at which the majority of intermetallic compounds are formed. The phase diagram of the relevant alloy in the solid state is used to obtain the values of p and q . With the use of experimental values for the free energy of mixing, the model fit parameters, such as interaction energies (Ψ_{12} , Ψ_{23} , Ψ_{13}) and formation energies (χ), have been calculated for all preferred binary liquid alloys. When (Ψ_{ij}) has a positive value, it means that species i and j are attracted to one another and vice versa. The equilibrium equation and other modeling equations used in the framework of the complex formation model are used to calculate the compositional dependency of the number of unassociated atoms A (n_1), B (n_2), and A_pB_q (n_3) complexes for all systems. In the recommended model, all interaction parameters are taken to be temperature dependent and concentration independent. With the help of experimental heat of mixing values for the various liquid alloys, the modeling equations have been used to derive the temperature coefficients of the interaction energy parameters ($\partial\Psi_{12}/\partial T$, $\partial\Psi_{23}/\partial T$, $\partial\Psi_{13}/\partial T$). For Bi-Mg liquid alloys at 975 K,

compositional dependence of the number of complexes reveals (n_3) that the maximum association occurs at 40 at.% of Bi, while for Bi-Pb liquid alloys at 700 K, compositional dependence of the number of complexes reveals that the maximum association occurs at 25 at.% of Bi. The maximum association occurs at 67 at.% of Cu in liquid Cu-In alloys at 1073 K, according to theoretically calculated values of the number of complexes as a function of concentration. The maximum value of n_3 at 50 at.% of In in liquid In-Pb alloys at 673 K demonstrate the maximum interaction in this alloy at that composition.

Comparison of the computed values of the thermodynamic and structural parameters with the experimental values has established the validity of the proposed statistical model. The Budai-Benko-Kaptay (BBK) model has been used to calculate and study the transport property as viscosity. The renovated Butler model has been used to investigate surface attributes like surface concentrations (c_i^s) and surface tensions (σ). Later, the Complex Formation Model was expanded to examine the structural, thermodynamic, and diffusion coefficients at various temperatures. The liquid alloys chosen for this investigation cover a broad spectrum of mixing behavior, ranging from symmetric to asymmetric in terms of thermodynamic and structural characteristics. Additionally, as described in Chapter 1, these alloys have a wide range of uses in the different sectors.

In the absence of experimental data, the theoretical prediction of the thermodynamic, structural, transport, and surface properties for the relevant systems at various temperatures will serve as the database. The liquid Bi-Pb alloy has been examined at temperatures of 700 K, 900 K, 1100 K, 1300 K, and 1500 K. It has been noted that as temperature rises, the propensity for compounds to form diminishes. At higher temperatures, it is possible to study additional binary liquid alloys in a similar manner.

Theoretical analysis reveals that all alloys have a negative free energy of mixing. The calculated values and the experimental values have a very good agreement. Bi-Mg liquid alloys exhibit the strongest tendency for compound formation at 975 K, as indicated by the maximum negative values of free energy of mixing. As we approach Cu-In at 1073 K, Bi-Pb at 700 K, and In-Pb at 673 K, the tendency becomes less pronounced. About equiatomic compositions, the free energy of mixing curves are found to be asymmetric. The nature and extent of the atomic bonds that develop between the elements of liquid mixtures to create complexes are better understood through the study of the heat of mixing of binary liquid alloys. While homo-coordinating liquid alloys are typically defined by low negative or positive values of heat of mixing, hetero-coordinating liquid alloys are typically characterized by substantial negative heat of mixing. Both the observed and computed values of H_M/RT as a function of concentration are reported to be negative throughout the full concentration in the cases of Bi-Mg liquid alloy at 975 K and Bi-Pb liquid alloy at 700 K. These systems are discovered to be asymmetric in terms of H_M . H_M values for Cu-In liquid alloys at 1073 K are found to be positive for

$c_{Cu} = 0.1, 0.2,$ and $0.3,$ but negative for the remaining concentrations up to $c_{Cu} = 0.9.$ This means that at $1073\text{ K},$ the liquid Cu-In alloy transitions from phase separation to ordering with respect to bulk concentration. The homo-coordinating tendency in In-Pb liquid alloys is demonstrated by the theoretically obtained as well as the experimental values of H_M/RT as a function of concentration at 673 K being positive over the whole concentration range. The comparative examination of heat of mixing of the favored liquid alloys in this research reveals that Bi-Mg is the most interactive system, followed by Cu-In, Bi-Pb, and In-Pb.

To maintain consistency, we computed the entropy of mixing (S_M) of the liquid alloys that were the subject of this investigation using the same set of interaction energy parameters that were used to estimate the above-mentioned thermodynamic properties. The study of S_M of binary liquid alloys provides information about the mixture's stability and aids in the analysis of the ordering tendency of the initial melt at the equilibrium state. The computed and experimental S_M/R values for the liquid alloys of Bi-Mg, Bi-Pb, Cu-In, and In-Pb are well agreed upon as a function of concentration. For all alloys, it has been observed that the S_M values have positive values across the whole concentration range.

Understanding the nature of atomic association or local arrangement of the atoms in the early melt is made easier by the study of structural characteristics. We calculated the concentration fluctuation in the long wavelength limit ($S_{cc}(0)$) and chemical short range order parameter (α_1) of the chosen alloys at their different melting temperatures to clarify and comprehend the structural features. We used the same set of interaction energy parameters that we used to compute thermodynamic properties to estimate structural properties. Throughout concentration range, the compositional dependency of $S_{cc}(0)$ is less than the ideal values for Bi-Pb system. At all concentrations for In-Pb, the compositional dependence of $S_{cc}(0)$ is greater than the ideal values. The $S_{cc}(0)$ values at $c_{Bi} = 0.1, 0.8,$ and 0.9 for Bi-Mg are higher than the corresponding ideal values. At other concentration values the computed $S_{cc}(0)$ values of Bi-Mg are less than the ideal values. The estimated $S_{cc}(0)$ value at the stoichiometric composition is considerably less than the ideal values. Up to a concentration of $c_{Cu} = 0.5,$ it is found that the estimated $S_{cc}(0)$ values for Cu-In liquid alloy are higher than the corresponding ideal values. These values are lower than the respective ideal values above this concentration. At stoichiometric composition, the lowest $S_{cc}(0)$ values are seen. Theoretical analysis of $S_{cc}(0)$ reveals that the liquid alloys of Bi-Mg and Cu-In have strong compound-forming tendencies at stoichiometric composition, Bi-Pb has good compound-formation tendencies across the entire concentration range, whereas the In-Pb system experiences phase separation across the entire concentration range. In the case of the liquid alloy Bi-Mg, a significant negative value of the chemical short range order parameter (α_1) is observed to be present around the stoichiometric composition. Liquid alloys of Cu-In

and Bi-Pb come next. In contrast, In-Pb alloys have been found to have positive values of α_1 throughout the concentration range. The α_1 observation supports the same tendency in mixing behavior of preferred systems as the concentration fluctuation at the long wave length limit.

The viscosity (η) and the ratio of mutual to intrinsic diffusion coefficients (D_M/D_{id}) are explored in the research of the transport properties of the liquid alloys mentioned above. The viscosities value initially rises up to a specific composition, $c_{Bi} = 0.44$ for Bi-Mg and $c_{Bi} = 0.50$ for Bi-Pb liquid alloys. The viscosity values for both alloys are observed to be dropping beyond that compositions. The viscosity of the liquid In-Pb alloy initially declines with regard to the bulk composition of indium up to the concentration of 0.5, in contrast to the cases of Bi-Mg and Bi-Pb systems. The viscosity values gradually rise after this composition. However, the s-shaped viscosity isotherm has been seen in the case of liquid Cu-In alloy. At $c_{Cu} = 0.8$ the value of η reaches its maximum, and at $c_{Cu} = 0.2$, its smallest value has been recorded. The large positive values of (D_M/D_{id}) in Bi-Mg liquid alloys, followed by Cu-In and Bi-Pb systems, show a diminishing compound formation tendency as we go away from the Bi-Mg system and toward the Cu-In and Bi-Pb systems. However, extremely low values of (D_M/D_{id}) throughout the whole concentration range in the In-Pb system support the homo-coordinating tendency as demonstrated by previous investigations.

The study of surface properties enables one to comprehend the nature of the atomic arrangement on the liquid mixture's surface layer. As a result, the analysis of surface phenomena can provide information regarding the kinetics of phase transformation, the catalytic activities of alloy catalysts, wettability, annealing conditions, and other thermophysical properties of liquid alloys. By computing the compositional dependency of surface tension (σ) and surface concentration (c_i^s) of constituent atoms within the framework of the renovated Butler model, the surface properties of the chosen liquid alloys have been described. In both Bi-Mg and Bi-Pb liquid alloys, the compositional dependence of the surface concentration of Bi (c_{Bi}^s) is greater than the corresponding ideal values across the whole concentration range, showing that these atoms segregate along the surface of the respective alloys. However, the surface concentrations of copper (c_{Cu}^s) and Indium (c_{In}^s) in the Cu-In and In-Pb liquid alloys are lower than the corresponding ideal values over the whole concentration range, indicating that the atoms remain in the bulk. As a result, indium atoms concentrate on the surface of the copper-indium system, and lead atoms shift from the bulk to the surface of the indium-lead system. For Bi-Mg and Bi-Pb liquid alloys, the compositional dependence of the estimated value of surface tension (σ) diminishes as the corresponding bulk concentration rises. However, it is observed that the values for Cu-In and In-Pb are rising as the corresponding bulk concentration rises. Theoretical surface tension (σ) values

for the Bi-Mg liquid alloy are greater than the ideal values for the concentration range $0 < c < 0.4$ and smaller than the ideal values for the concentration range $0.4 < c < 1$, respectively. However, across the whole concentration range, the theoretical values of surface tension (σ) for the binary alloys Bi-Pb, Cu-In, and In-Pb are lower than the corresponding ideal values.

Using the extended complex formation model, the interaction energy parameters for the Bi-Pb liquid alloys are determined for high temperatures. Thermodynamic, structural, transport, and surface properties of the liquid Bi-Pb alloy are determined using the interaction energy parameter that has been optimized for higher temperatures. The hetero-coordinating tendency in binary liquid alloys is shown to decrease with an increase in temperature by the increasing value of the free energy of mixing (G_M/RT), the concentration fluctuation at the long wavelength limit ($S_{cc}(0)$), and the chemical short range order parameter (α_1), and the decreasing value of the ratio of mutual to intrinsic diffusion coefficients (D_M/D_{id}). In addition, it is revealed that when the temperature increases, the viscosity (η), surface tension (σ) of the alloy and surface concentration of bismuth in Bi-Pb liquid alloys all decrease.

5.2 Recommendations for Future Work

In this thesis, it has been established that a formalism that considers both thermodynamic and dynamical features within the context of the Complex Formation Model (CFM) is appropriate for describing the alloying behaviors of liquid binary alloys. Through the analysis of their thermodynamic and microscopic functions, the CFM for highly interacting systems was used to explore ordering and glass forming tendencies in binary alloys of Bi-Mg and Cu-In. The model presented here has been successful in elucidating the thermodynamic characteristics of the alloys Bi-Mg, Bi-Pb, Cu-In, and In-Pb. Through this study, it has also been demonstrated that the experimental $S_{cc}(0)$ values acquired through component activity are comparable to the theoretical values. At higher temperatures, thermodynamic and structural data are collected that can be compared to certain crucial outcomes of upcoming experiments. The method is applicable to various binary liquid alloys, which is useful in the absence of data at constant and elevated temperatures. Binary liquid alloys are of practical value in current manufacturing practice from a technological standpoint. As a result of the complications and difficulties associated with high-temperature experiments, a good theoretical understanding of the energetics of the interrelationship between thermodynamic and structural behavior of these materials are an important task for the current scientific investigations.

Future research should focus on locating binary liquid alloys for which there are currently no thermodynamic data available in the literature. Since multi-component alloys

significantly rely on their constituent binary systems, the current study can also be used to determine the thermodynamic parameters of ternary and quaternary systems. In future studies, it would also be highly desirable to extend the current understanding of concentration-concentration fluctuations in the long-wavelength limits, $S_{cc}(0)$, the chemical short-range order parameter, α_1 and the ratio of mutual to intrinsic diffusion coefficients, D_M/D_{id} in explaining the energetics in terms of chemical ordering and phase separation to ternary and quaternary liquid alloys. Due to their potential use in industrial applications, higher component liquid alloys have recently received increased attention.

With a major rise in activity in this growing area of research, it is expected that our understanding of the electrical, structural, and thermodynamic properties of ternary and quaternary liquid alloys, which are still in their early phases, will continue to evolve in the coming years.

CHAPTER 6

SUMMARY

6.1 Summary

The mixing behavior of two metals that combine to form binary alloys is a consequence of the interaction between energetic and structural reorganization of the constituent atoms. When A and B atoms are combined, they may prefer to remain self-coordinated, establishing A-A or B-B pairings, or they may generate a strong interaction between constituent atoms, resulting in hetero-coordinated A-B pairings. On the basis of their deviations from the additive rule of mixing (Raoult's law), all liquid binary alloys can be divided into two major categories: segregating (positive deviation) and ordering or short-range ordered (negative deviation) alloys. To create new alloys and enhance current ones, a comprehensive understanding of the thermodynamic variables of the constituent systems is required. To fully comprehend the observed behaviors, a comprehensive theoretical knowledge of the structural adjustments and energy preferences of atoms in binary liquid metallic systems may be required.

Analytical formulas were used to evaluate how mixing properties in the binary liquid systems of Bi-Mg, Cu-In, Bi-Pb, and In-Pb depended on concentration at the certain temperatures, keeping in mind that the mixing qualities of favored systems are not fully explained in the literature. The interaction parameters were obtained using the complex formation model (CFM), which are believed to be invariant in all calculations. A theoretical approach is used to investigate the bulk and dynamic properties of Bi-Mg, Bi-Pb, Cu-In, and In-Pb liquid alloys, with a focus on their bulk thermodynamic properties such as free energy of mixing (G_M), heat of mixing (H_M), entropy of mixing (S_M), concentration fluctuations in the long-wavelength limit ($S_{cc}(0)$), chemical short range order parameter (α_1), and the concentration dependence of diffusion (D_M/D_{id}). In the framework of the Budai-Benko-Kaptay (BBK) model, the viscosity of the chosen alloys is investigated. Viscosity isotherms have shown that Bi-Pb and In-Pb liquid alloys

behave symmetrically with respect to composition. However, the viscosity curve of the liquid Bi-Mg alloy at 975 K displays asymmetries. The updated Butler model has made estimates about the surface concentrations (c_i^s) and surface tension (σ) values.

The experimental data obtained at 975 K from literature support the theoretical examination of Bi-Mg liquid alloy. The microscopic functions $S_{cc}(0)$ and SRO (α_1) have been used to evaluate the ordering in the Bi-Pb and Cu-In liquid phases. Bi-Pb, Cu-In, and Bi-Mg are hetero-coordinated liquid alloys that are at temperatures of 700 K, 1073 K, and 975 K, respectively. The latter exhibits a higher degree of chemical order than the former. The liquid miscibility gap or segregation in the melt is indicated by the computed values of these functions in the In-Pb liquid alloy. On the basis of the theory given in Chapter 3, the bulk, thermodynamic, and dynamic properties of the four liquid alloys have been reasonably explained.

Although a large heat of mixing (H_M) is always present during compound formation, this property may not necessarily give a reliable indication of the stoichiometric composition. Concentration fluctuation at long wavelength limits has been added as a crucial parameter because of this. The minimum in the plot of compositional dependency of $S_{cc}(0)$ provides us enough about the stoichiometric composition. With regard to Bi-Mg and Cu-In liquid alloys, it is noted that computed $S_{cc}(0)$ almost approach ideal values in the glass forming composition range, which is typically far from the stoichiometric composition, consequently in the framework of the complex formation model, one infers that the unassociated species (A and B atoms) and the complex (A_pB_q) mix randomly. Such a random mixing may prevent nucleation and aid in the creation of glass. However, it appears that the ideal value of $S_{cc}(0)$ may not be adequate but is an essential requirement for creating glass from molten alloys. Many of the binary molten alloys that form compounds are excellent glass-formers. However, the likelihood for complex formation is not directly related to the tendency for glass formation.

It is found that different factors, including size difference and electronegativity difference, are responsible for the asymmetric behavior of binary liquid alloys. These variables, however, are insufficient to explain the observed asymmetry in the liquid alloys of Bi-Mg and Cu-In. As a result, it is suggested that the asymmetry in the aforementioned alloys is caused by the development of complexes like Bi_2Mg_3 in the liquid alloy of Bi-Mg and Cu_2In in the liquid alloy of Cu-In. This implies that asymmetry around stoichiometric composition is created in any complexes where stoichiometric composition lies at a specific composition other than equiatomic composition. Despite the fact that the CFM used in the study of microscopic functions of binary liquid alloys has been reported to have some shortcomings when applied to strongly interacting alloys such as in $S_{cc}(0)$ of Bi-Mg and Cu-In liquid alloys, the model as used here has successfully explained thermodynamic and other structural properties.

The model parameters that were fitted for the experimental data of mixing free energy have been optimized for higher temperatures using temperature coefficients derived from experimental data of mixing enthalpy. The higher temperature investigation is performed with reference to the Bi-Pb system, and the study can be expanded to additional alloys to obtain data for a variety of binary liquid alloys at various temperatures. The higher temperature investigation of Bi-Pb liquid alloy reveals that the system's phase separating behavior increases with increasing temperature.

The results of this work show or confirm that this theoretical approach can be used to describe the mixing properties of binary liquid alloys in the right way.

REFERENCES

- Abe, T., Shimono, M., Ode, M., & Onodera, H. (2006). Thermodynamic modeling of the undercooled liquid in the Cu-Zr system. *Acta Materialia*, 54(4), 909–915.
- Adedipe, A. M., Odusote, Y. A., Ndukwe, I. C., & Madu, C. A. (2019). Energetics of compound formation in liquid Bi-Sb, Bi-Sn, and Sb-Sn binary alloys. *Physics Journal*, 3, 37–48.
- Adhikari, D. (2011). Inhomogeneity in structure of MgPb liquid alloy. *Physica B: Condensed Matter*, 406(3), 445–448.
- Adhikari, D. (2018). *Regular associated solution model for the properties of binary liquid alloys* (Unpublished doctoral dissertation).
- Adhikari, D., Jha, I. S., & Singh, B. P. (2010). Structural asymmetry in liquid Fe-Si alloys. *Philosophical Magazine*, 90(20), 2687–2694.
- Adhikari, D., Jha, I. S., Singh, B. P., & Kumar, J. (2011). Thermodynamic and structural investigations of liquid magnesium–thallium alloys. *Journal of Molecular Structure*, 985(1), 91–94.
- Adhikari, D., Singh, B. P., & Jha, I. S. (2012a). Energetics of Cd-based binary liquid alloys. *Journal of Non-Crystalline Solids*, 358(11), 1362–1367.
- Adhikari, D., Singh, B. P., & Jha, I. S. (2012b). Phase separation in Na-K liquid alloy. *Phase Transitions*, 85(8), 675–680.
- Adhikari, D., Singh, B. P., Jha, I. S., & Singh, B. K. (2010). Thermodynamic properties and microscopic structure of liquid Cd-Na alloys by estimating complex concentration in a regular associated solution. *Journal of Molecular Liquids*, 156(2-3), 115–119.
- Adhikari, D., Singh, B. P., Jha, I. S., & Singh, B. K. (2011). Chemical ordering and thermodynamic properties of HgNa liquid alloys. *Journal of Non-Crystalline Solids*, 357(15), 2892–2896.

- Adhikari, D., Yadav, S. K., & Jha, L. N. (2014). Thermo-physical properties of Al-Fe melt. *Journal of the Chinese Advanced Materials Society*, 2(3), 149–158.
- Ajayi, A. A., & Ogunmola, E. D. (2018). Investigation on compound formation in Mg-Sb and Cu-Sb liquid alloys. *International Journal of Advanced Materials Research*, 4(2), 29–34.
- Akasofu, T., Kusakabe, M., & Tamaki, S. (2020). An interpretation on the thermodynamic properties of liquid Pb-Te alloys. *High Temperature Materials and Processes*, 39(1), 297–303.
- Akimoto, T., Ueno, T., Tsutsumi, Y., Doi, H., Hanawa, T., & Wakabayashi, N. (2018). Evaluation of corrosion resistance of implant-use Ti-Zr binary alloys with a range of compositions. *Journal of Biomedical Materials Research Part B: Applied Biomaterials*, 106(1), 73–79.
- Akinlade, O. (1994). Thermodynamics of molten K-Te alloys. *Journal of Physics: Condensed Matter*, 6(25), 4615–4624.
- Akinlade, O. (1996). Thermodynamic investigation of atomic order in molten K-Bi alloys. *Physics and Chemistry of Liquids*, 32(3), 159–168.
- Akinlade, O. (1997). Higher order conditional probabilities and thermodynamics of binary molten alloys. *Modern Physics Letters B*, 11(02n03), 93–106.
- Akinlade, O. (1998). Energetic effects in some molten alloys of arsenic. *Physica B: Condensed Matter*, 245(4), 330–336.
- Akinlade, O., Ali, I., & Singh, R. N. (2001). Correlation between bulk and surface phenomena in Ga-(Bi, In) and In-Bi liquid alloys. *International Journal of Modern Physics B*, 15(22), 3039–3053.
- Akinlade, O., & Awe, O. E. (2006). Bulk and surface properties of liquid Ga-Tl and Zn-Cd alloys. *International Journal of Materials Research*, 97(4), 377–381.
- Akinlade, O., & Boyo, A. O. (2004). Thermodynamics and surface properties of Fe-V and Fe-Ti liquid alloys. *International Journal of Materials Research*, 95(5), 387–395.
- Akinlade, O., Boyo, A. O., & Ijaluola, B. R. (1999). Demixing tendencies in some Sn-based liquid alloys. *Journal of Alloys and Compounds*, 290(1-2), 191–196.
- Akinlade, O., Hussain, L. A., & Awe, O. E. (2003). Thermodynamics of liquid Al-In, Ag-In and In-Sb alloys from a four-atom cluster model. *International Journal of Materials Research*, 94(12), 1276–1279.

- Akinlade, O., & Singh, R. N. (2002). Bulk and surface properties of liquid In-Cu alloys. *Journal of Alloys and Compounds*, 333(1-2), 84–90.
- Akinlade, O., Singh, R. N., & Sommer, F. (1998). Thermodynamic investigation of viscosity in Cu-Bi and Bi-Zn liquid alloys. *Journal of Alloys and Compounds*, 267(1-2), 195–198.
- Akinlade, O., Singh, R. N., & Sommer, F. (2000). Thermodynamics of liquid Al-Fe alloys. *Journal of Alloys and Compounds*, 299(1-2), 163–168.
- Alcock, C. B., Sridhar, R., & Svedberg, R. C. (1969). A mass spectrometric study of the binary liquid alloys, Ag-In and Cu-Sn. *Acta Metallurgica*, 17(7), 839–844.
- Alonso, J. A., & Gallego, L. J. (1985). A note on the entropy of mixing of liquid sodium-caesium and other binary alkali alloys. *Journal of Physics F: Metal Physics*, 15(7), L185–L188.
- Alonso, J. A., & March, N. H. (1982). Concentration fluctuations in simple metallic liquid alloys. *Physica B + C*, 114(1), 67–70.
- Amore, S., Giuranno, D., Novakovic, R., Ricci, E., Nowak, R., & Sobczak, N. (2014). Thermodynamic and surface properties of liquid Ge-Si alloys. *Calphad*, 44, 95–101.
- Andrade, E. d. C. (1934). Xli. a theory of the viscosity of liquids—part i. *The London, Edinburgh, and Dublin Philosophical Magazine and Journal of Science*, 17(112), 497–511.
- Angelo, P. C., & Subramanian, R. (2008). *Powder metallurgy: science, technology and applications*. PHI Learning Pvt. Ltd.
- Anusionwu, B. C. (2000). Concentration fluctuations and chemical complexes in the Zn-Au liquid alloy. *Physics and Chemistry of Liquids*, 38(6), 671–682.
- Anusionwu, B. C. (2002). A theoretical investigation of chemical association in Li-Mg liquid alloy. *Physica B: Condensed Matter*, 311(3-4), 272–278.
- Anusionwu, B. C. (2003). Surface properties of some sodium-based binary liquid alloys. *Journal of Alloys and Compounds*, 359(1-2), 172–179.
- Anusionwu, B. C. (2004). Thermodynamic and surface properties of Ge-Ga and Ge-Sb liquid alloys. *Physics and Chemistry of Liquids*, 42(3), 245–259.
- Anusionwu, B. C. (2006). Thermodynamic and surface properties of Sb-Sn and In-Sn liquid alloys. *Pramana*, 67(2), 319–330.

- Anusionwu, B. C., & Adebayo, G. A. (2001). Quasi-chemical studies of ordering in the Cu-Zr and Cu-Si melts. *Journal of Alloys and Compounds*, 329(1-2), 162–167.
- Anusionwu, B. C., Adebayo, G. A., & Madu, C. A. (2009). Thermodynamics and surface properties of liquid Al-Ga and Al-Ge alloys. *Applied Physics A*, 97(3), 533–541.
- Anusionwu, B. C., Akinlade, O., & Hussain, L. A. (1998). Assessment of size effect on the surface properties of some binary liquid alloys. *Journal of Alloys and Compounds*, 278(1-2), 175–181.
- Anusionwu, B. C., Madu, C. A., & Orji, C. E. (2009). Theoretical studies of mutual diffusivities and surface properties in Cd-Ga liquid alloys. *Pramana*, 72(6), 951–967.
- Anusionwu, B. C., Ogundare, F. O., & Orji, C. E. (2003). A theoretical study of compound formation in liquid Cu-Hf alloys at high temperatures. *Journal of the Physical Society of Japan*, 72(1), 117–121.
- Arzpeyma, G., Gheribi, A. E., & Medraj, M. (2013). On the prediction of gibbs free energy of mixing of binary liquid alloys. *The Journal of Chemical Thermodynamics*, 57, 82–91.
- Ashcroft, N. W., & Stroud, D. (1978). Theory of the thermodynamics of simple liquid metals. In *Solid state physics* (Vol. 33, pp. 1–81). Elsevier.
- Attri, K. S., Ahluwalia, P. K., & Sharma, K. C. (1995). Concentration dependent interaction energies and thermodynamic properties of mercury indium liquid alloy. *Physics and Chemistry of Liquids*, 29(2), 117–128.
- Attri, K. S., Ahluwalia, P. K., & Sharma, K. C. (1996). Two-compound formation in liquid binary alloys: Temperature dependence of thermodynamic functions in mercury indium alloy. *Physics and Chemistry of Liquids*, 31(4), 231–244.
- Awe, O. E., Akinlade, O., & Hussain, L. A. (2003). Thermodynamic properties of liquid Te-Ga and Te-Tl alloys. *Journal of Alloys and Compounds*, 361(1-2), 227–233.
- Awe, O. E., Akinlade, O., & Hussain, L. A. (2005). Thermodynamic investigations of Bi-Cd, In-Pb, and Ni-Pd liquid alloys. *International Journal of Materials Research*, 96(1), 89–93.
- Awe, O. E., & Azeez, A. A. (2017). Temperature dependence of the bulk and surface properties of liquid Zn-Cd alloys. *Applied Physics A*, 123(5), 1–10.

- Awe, O. E., Odusote, Y. A., Akinlade, O., & Hussain, L. A. (2008). Thermodynamic properties of some gallium-based binary alloys. *Physica B: Condensed Matter*, 403(17), 2629–2633.
- Awe, O. E., Odusote, Y. A., Hussain, L. A., & Akinlade, O. (2011). Temperature dependence of thermodynamic properties of Si-Ti binary liquid alloys. *Thermochimica Acta*, 519(1-2), 1–5.
- Awe, O. E., & Onifade, A. (2012). Effects of surface coordination of atoms on the surface properties of some liquid binary alloys. *Physics and Chemistry of Liquids*, 50(5), 579–595.
- Awe, O. E., & Oshakuade, O. M. (2016). Computation of infinite dilute activity coefficients of binary liquid alloys using complex formation model. *Physica B: Condensed Matter*, 487, 13–17.
- Baran, G., & Woodland, E. C. (1981). Forming of cast precious metal alloys. *Journal of Dental Research*, 60(10), 1767–1772.
- Barbin, N., Terentiev, D., Alexeev, S., & Barbina, T. (2013). Thermodynamic modeling of the Pb + Bi melt evaporation under various pressures and temperatures. *Computational Materials Science*, 66, 28–33.
- Battezzati, L., & Greer, A. (1989). The viscosity of liquid metals and alloys. *Acta Metallurgica*, 37(7), 1791–1802.
- Bauccio, M., et al. (1993). *Asm metals reference book*. ASM international.
- Bergman, C., Castanet, R., Said, H., Gilbert, M., & Mathieu, J.-C. (1982). Configurational entropy and the regular associated model for compound-forming binary systems in the liquid state. *Journal of the Less Common Metals*, 85, 121–135.
- Bhandari, I. B., Koirala, I., & Adhikari, D. (2021). Temperature-dependent mixing behaviours of Bi-Mg liquid alloys. *Physics and Chemistry of Liquids*, 59(6), 918–931.
- Bhandari, I. B., Panthi, N., Gaire, S., & Koirala, I. (2021). Effect of temperature on mixing behavior and stability of liquid Al-Fe alloys. In *Journal of physics: Conference series* (Vol. 2070, pp. 012025–11pp).
- Bhandari, I. B., Panthi, N., & Koirala, I. (2019). Thermodynamics of liquid Gallium-Zinc alloy. *Himalayan Physics*, 8, 33–38.
- Bhandari, I. B., Panthi, N., & Koirala, I. (2021a). Investigation on thermo-physical properties of liquid In-Tl alloy. *BBECHANNA*, 18(1), 149–158.

- Bhandari, I. B., Panthi, N., & Koirala, I. (2021b). Temperature-dependent mixing behavior of Pb-Sb alloys in liquid state. *International Journal of Computational Materials Science and Engineering*, 10(3), 2150018–20pp.
- Bhandari, I. B., Panthi, N., Koirala, I., & Adhikari, D. (2021). Phase segregating and complex forming Pb-based (= X-Pb) liquid alloys. *Phase Transitions*, 94(5), 338–352.
- Bhatia, A. B., & Gupta, O. P. (1969). Electrical resistivities of dilute alloys and deviations from matthiessen's rule. *Physics Letters A*, 29(6), 358–359.
- Bhatia, A. B., & Hargrove, W. H. (1974). Concentration fluctuations and thermodynamic properties of some compound forming binary molten systems. *Physical Review B*, 10(8), 3186-3196.
- Bhatia, A. B., Hargrove, W. H., & March, N. H. (1973). Concentration fluctuations in conformal solutions and partial structure factor in alloys. *Journal of Physics C: Solid State Physics*, 6(4), 621–630.
- Bhatia, A. B., & March, N. H. (1972). Liquidus curves for eutectic systems. *Physics Letters A*, 41(5), 397–399.
- Bhatia, A. B., & March, N. H. (1975a). Eutectic type liquidus curves in compound forming systems. *Physics and Chemistry of Liquids*, 4(4), 279–283.
- Bhatia, A. B., & March, N. H. (1975b). Size effects, peaks in concentration fluctuations and liquidus curves of Na-Cs. *Journal of Physics F: Metal Physics*, 5(6), 1100–1106.
- Bhatia, A. B., & March, N. H. (1978). Surface tension, compressibility, and surface segregation in liquid binary alloys. *The Journal of Chemical Physics*, 68(10), 4651–4656.
- Bhatia, A. B., & March, N. H. (1979). Statistical mechanical theory of liquid surface tension. *Physics and Chemistry of Liquids*, 9(1), 1–9.
- Bhatia, A. B., March, N. H., & Rivaud, L. (1974). Liquid curves of eutectic system Na-K under pressure. *Physics Letters A*, 47(3), 203–204.
- Bhatia, A. B., March, N. H., & Tosi, M. P. (1980). Theory of surface tension in liquid mixtures. *Physics and Chemistry of Liquids*, 9(3), 229–244.
- Bhatia, A. B., & Ratti, V. K. (1975). Structure factors of compound forming liquid mixtures. *Physics Letters A*, 51(7), 386–388.

- Bhatia, A. B., & Ratti, V. K. (1977). Number-concentration structure factors and their long wavelength limit in multicomponent fluid mixtures. *Physics and Chemistry of Liquids*, 6(3), 201–213.
- Bhatia, A. B., & Singh, R. N. (1980). Volume of mixing of compound forming molten alloys. *Physics Letters A*, 78(5-6), 460–462.
- Bhatia, A. B., & Singh, R. N. (1982a). Short range order and concentration fluctuations in regular and compound forming molten alloys. *Physics and Chemistry of Liquids*, 11(4), 285–313.
- Bhatia, A. B., & Singh, R. N. (1982b). Thermodynamic properties of compound forming molten alloys in a weak interaction approximation. *Physics and Chemistry of Liquids*, 11(4), 343–351.
- Bhatia, A. B., & Singh, R. N. (1984). A quasi-lattice theory for compound forming molten alloys. *Physics and Chemistry of Liquids*, 13(3), 177–190.
- Bhatia, A. B., & Thornton, D. E. (1970). Structural aspects of the electrical resistivity of binary alloys. *Physical Review B*, 2(8), 3004–3012.
- Bhatia, A. B., & Thornton, D. E. (1971). Structural aspects of the electrical resistivity of binary alloys. ii. long-wavelength limit of the structure factors for a solid alloy. *Physical Review B*, 4(8), 2325–2328.
- Boyo, A. O. (2005). The study of thermodynamic properties of liquid NaCs alloys. *African Journal of Science, Technology, Innovation and Development*, 6, 73–80.
- Brandes, E. A., & Brook, G. B. (2013). *Smithells metals reference book*. Elsevier.
- Brillo, J., Bytchkov, A., Egry, I., Hennet, L., Mathiak, G., Pozdnyakova, I., . . . Zanghi, D. (2006). Local structure in liquid binary Al-Cu and Al-Ni alloys. *Journal of Non-Crystalline Solids*, 352(38-39), 4008–4012.
- Budai, I., Benkő, M. Z., & Kaptay, G. (2005). Analysis of literature models on viscosity of binary liquid metallic alloys on the example of the Cu-Ag system. In *Materials science forum* (Vol. 473, pp. 309–314).
- Budai, I., Benkő, M. Z., & Kaptay, G. (2007). Comparison of different theoretical models to experimental data on viscosity of binary liquid alloys. In *Materials science forum* (Vol. 537, pp. 489–496).
- Butler, J. A. V. (1932). The thermodynamics of the surfaces of solutions. *Proceedings of the Royal Society of London. Series A, Containing Papers of a Mathematical and Physical Character*, 135(827), 348–375.

- Callister, W. D., & Rethwisch, D. G. (2018). *Materials science and engineering: an introduction* (Vol. 9). Wiley New York.
- Campbell, F. C. (2011). *Joining: understanding the basics*. ASM International.
- Chatterjee, S. K., Prasad, L. C., & Bhattarai, A. (2011). Microscopic structure of NaCd compound forming binary molten alloys. *Materials Sciences and Applications*, 2(06), 605–608.
- Chou, K.-C., & Wei, S.-K. (1997). A new generation solution model for predicting thermodynamic properties of a multicomponent system from binaries. *Metallurgical and Materials Transactions B*, 28(3), 439–445.
- Chunju, N. I. U., Changrong, L. I., Zhenmin, D. U., Cuiping, G. U. O., & Yongjuan, J. I. N. G. (2012). Thermodynamic assessment of the Bi-Mg binary system. *Acta Metallurgica Sinica (English Letters)*, 25(1), 19–28.
- Clarke, J., & Sarkar, A. D. (1979). Wear characteristics of as-cast binary aluminium-silicon alloys. *Wear*, 54(1), 7–16.
- Cowley, J. M. (1950). An approximate theory of order in alloys. *Physical Review*, 77(5), 669–675.
- Cretu, C., & Van Der Lingen, E. (1999). Coloured gold alloys. *Gold Bulletin*, 32(4), 115–126.
- Dalgiç, S., Dalgiç, S., Dereli, G., & Tomak, M. (1994). Thermodynamics and structure of liquid binary alloys calculated using an analytic pair potential. *Physical Review B*, 50(1), 113–117.
- Davis, J. R., et al. (2001). *Copper and copper alloys*. ASM international.
- Deloffre, P., Balbaud-Célérier, F., & Terlain, A. (2004). Corrosion behaviour of aluminumized martensitic and austenitic steels in liquid Pb–Bi. *Journal of Nuclear Materials*, 335(2), 180–184.
- Delsante, S., Borzone, G., & Novakovic, R. (2019). Experimental thermodynamics, surface and transport properties of liquid Ag-Ge alloys. *Thermochimica Acta*, 682, 1–10.
- Dossett, J. L., & Boyer, H. E. (2006). *Practical heat treating*. Asm International.
- Dubin, N. (2009). Thermodynamics of liquid Fe-Ni alloys: calculations at different temperatures. In *Journal of physics: Conference series* (Vol. 144, pp. 012115–4pp).

- Durham, P. J., & Greenwood, D. A. (1976). The structure and electronic properties of metal/molten salt solutions. *Philosophical Magazine*, 33(3), 427–440.
- Egami, T., & Waseda, Y. (1984). Atomic size effect on the formability of metallic glasses. *Journal of Non-Crystalline Solids*, 64(1-2), 113–134.
- Equey, S., Houriet, A., & Mischler, S. (2011). Wear and frictional mechanisms of copper-based bearing alloys. *Wear*, 273(1), 9–16.
- Eyring, H. (1936). Viscosity, plasticity, and diffusion as examples of absolute reaction rates. *The Journal of chemical physics*, 4(4), 283–291.
- Eyring, H., Glasstone, S., & Laidler, K. J. (1941). *The theory of rate processes: the kinetics of chemical reactions, viscosity, diffusion and electrochemical phenomena*. McGraw-Hill Book Company.
- Faber, T. E., & Ziman, J. M. (1965). A theory of the electrical properties of liquid metals: Iii. the resistivity of binary alloys. *Philosophical Magazine*, 11(109), 153–173.
- Fang, D., Sun, Z., Li, Y., & Cheng, X. (2016). Preparation, microstructure and thermal properties of MgBi alloys as phase change materials for thermal energy storage. *Applied Thermal Engineering*, 92, 187–193.
- Faruk, M. M., & Bhuiyan, G. M. (2013). Investigation of segregation for Al_xIn_{1-x} liquid binary alloys. *Physica B: Condensed Matter*, 422, 56–63.
- Fowler, R. H., & Guggenheim, E. A. (1965). *Statistical thermodynamics, theory of the properties of matter in equilibrium*. Cambridge University Press: New York.
- Fratesi, R., Roventi, G., Maja, M., & Penazzi, N. (1984). Electrodeposition of lead alloys from fluoborate baths. *Journal of Applied Electrochemistry*, 14(4), 505–510.
- Friauf, J. B. (1927). The crystal structures of two intermetallic compounds. *Journal of the American Chemical Society*, 49(12), 3107–3114.
- Gallego, L. J., López, J. M., & Alonso, J. A. (1983). Concentration dependence of the heat of formation of binary liquid alloys. *Physica B + C*, 122(1), 23–27.
- Ganesan, S., Speiser, R., & Poirier, D. R. (1987). Viscosities of aluminum-rich Al- Cu liquid alloys. *Metallurgical Transactions B*, 18(2), 421–424.
- Ghali, E. (2010). *Corrosion resistance of aluminum and magnesium alloys: understanding, performance, and testing*. John Wiley & Sons.
- Gijzeman, O. L. (1985). Surface composition of binary metal alloys; applicability of bulk parameters to surfaces. *Surface Science*, 150(1), 1–13.

- Giuranno, D., & Novakovic, R. (2020). Surface and transport properties of liquid Bi-Sn alloys. *Journal of Materials Science: Materials in Electronics*, 31(7), 5533–5545.
- Givan, D. A. (2014). *5 - precious metal alloys for dental applications*. Elsevier.
- Godbole, R. P., Jha, S. A., Milanarun, M., & Mishra, A. K. (2004). Thermodynamics of liquid Cu-Mg alloys. *Journal of Alloys and Compounds*, 363(1-2), 187–193.
- Gohivar, R. K., Koirala, R. P., Yadav, S. K., & Adhikari, D. (2020). Temperature dependence of interaction parameters of Cu-Si liquid alloy. *AIP Advances*, 10(8), 085121–7pp.
- Gohivar, R. K., Yadav, S. K., Koirala, R. P., & Adhikari, D. (2020). Artifacts in Al-Mn liquid alloy. *Physica B: Condensed Matter*, 595, 412348–6pp.
- Gohivar, R. K., Yadav, S. K., Koirala, R. P., & Adhikari, D. (2021a). Assessment of thermo-structural properties of Al-Fe and Fe-Si alloys at high temperatures. *Physics and Chemistry of Liquids*, 59(5), 679–689.
- Gohivar, R. K., Yadav, S. K., Koirala, R. P., & Adhikari, D. (2021b). Study of artifacts in thermodynamic and structural properties of Li-Mg alloy in liquid state using linear and exponential models. *Heliyon*, 7(3), e06613–9pp.
- Gohivar, R. K., Yadav, S. K., Koirala, R. P., Shrestha, G. K., & Adhikari, D. (2021). Temperature dependence of interaction parameters for Al-Li liquid alloy. *Philosophical Magazine*, 101(2), 179–192.
- Gorsse, S., Hutchinson, C. R., Chevalier, B., & Nie, J.-F. (2005). A thermodynamic assessment of the Mg-Nd binary system using random solution and associate models for the liquid phase. *Journal of Alloys and Compounds*, 392(1-2), 253–262.
- Guggenheim, E. A. (1952). *Mixtures: the theory of the equilibrium properties of some simple classes of mixtures, solutions and alloys*. Clarendon Press.
- Guthrie, R. I. L., & Iida, T. (1993). *The physical properties of liquid metals*. Oxford, Clarendon Press.
- Habashi, F. (2008). *Alloys: preparation, properties, applications*. John Wiley & Sons.
- Hafner, J. (1977). Structure and thermodynamics of liquid metals and alloys. *Physical Review A*, 16(1), 351–364.
- Harner, L. L. (1994). Selecting controlled expansion alloys. *Advanced Materials & Processes*, 146(4), 19–23.

- Hasegawa, R. (2001). Applications of amorphous magnetic alloys in electronic devices. *Journal of Non-Crystalline Solids*, 287(1-3), 405–412.
- Huijben, M. J., Van Der Lugt, W., Reimert, W. A. M., De Hosson, J. T. M., & Van Dijk, C. (1979). Investigations on the structure of liquid Na-Cs alloys. *Physica B + C*, 97(4), 338–364.
- Hultgren, R., Desai, P. D., Hawkins, D. T., Gleiser, M., & Kelley, K. K. (1973). *Selected values of the thermodynamic properties of the elements* (Tech. Rep.). National Standard Reference Data System.
- Ichikawa, K., Granstaff Jr, S. M., & Thompson, J. C. (1974). Chemical potentials and related thermodynamics of liquid Na-Cs alloys. *The Journal of Chemical Physics*, 61(10), 4059–4062.
- Ilinčev, G. (2002). Research results on the corrosion effects of liquid heavy metals Pb, Bi and Pb-Bi on structural materials with and without corrosion inhibitors. *Nuclear Engineering and Design*, 217(1-2), 167–177.
- Ilo-Okeke, E. O., Anusionwu, B. C., & Popoola, O. (2005). Thermodynamic evaluation of viscosity in In-Zn and Sn-Zn liquid alloys. *Physics and Chemistry of Liquids*, 43(4), 333–342.
- Ivanov, M. I., & Berezutski, V. V. (1994). Short-range ordering in binary liquid alloys of rare earth metals with copper and silver. *Journal of Alloys and Compounds*, 210(1-2), 165–170.
- Ivanov, M. I., & Berezutski, V. V. (1996). Thermodynamics of Au-Gd melts and percolation theory application for compound-forming liquid alloys. *Journal of Alloys and Compounds*, 234(1), 119–124.
- Jacob, K. T., Srikanth, S., & Waseda, Y. (1988). Activities, concentration fluctuations and complexing in liquid Ca-Al alloys. *Transactions of the Japan Institute of Metals*, 29(1), 50–59.
- Jank, W., & Hafner, J. (1988). The electronic structure of liquid germanium. *Europhysics Letters*, 7(7), 623–628.
- Jha, I. S., Adhikari, D., Kumar, J., & Singh, B. P. (2011). Anomaly in mixing properties of lithium–magnesium liquid alloy. *Phase Transitions*, 84(11-12), 1075–1083.
- Jha, I. S., Adhikari, D., & Singh, B. P. (2012). Mixing behaviour of sodium-based liquid alloys. *Physics and Chemistry of Liquids*, 50(2), 199–209.

- Jha, I. S., Khadka, R., Koirala, R. P., Singh, B. P., & Adhikari, D. (2016). Theoretical assessment on mixing properties of liquid Tl-Na alloys. *Philosophical Magazine*, 96(16), 1664–1683.
- Jha, I. S., Koirala, I., Singh, B. P., & Adhikari, D. (2014). Concentration dependence of thermodynamic, transport and surface properties in Ag-Cu liquid alloys. *Applied Physics A*, 116(3), 1517–1523.
- Jha, I. S., & Singh, B. P. (2005). Thermodynamic properties of CdNa alloys. *Indian Journal of Physics*, 79, 635–637.
- Jha, I. S., Singh, R. N., Srivastava, P. L., & Mitra, N. R. (1990). Stability of HgNa and HgK liquid alloys. *Philosophical Magazine B*, 61(1), 15–24.
- Jha, N., Mishra, A. K., & Rafique, S. M. (2001). Thermodynamic properties and electrical resistivity of liquid MgZn alloys. *Indian Journal of Physics*, 75(5), 519–523.
- Johnson, M. W., March, N. H., Parrinello, M., Tosi, M. P., & Page, D. I. (1975). Wavenumber-dependent concentration fluctuations in liquid mixtures. *Journal of Physics C: Solid State Physics*, 8(6), 751–760.
- Jovanović, M. T., Lukić, B., Mišković, Z., Bobić, I., Cvijović, I., & Dimčić, B. (2007). Processing and some applications of nickel, cobalt and titanium-based alloys. *Association of Metallurgical Engineers of Serbia*, 91–106.
- Jung, I.-H., Kang, D.-H., Park, W.-J., Kim, N. J., & Ahn, S. (2007). Thermodynamic modeling of the Mg-Si-Sn system. *Calphad*, 31(2), 192–200.
- Kaban, I., Hoyer, W., Il'inskii, A., Slukhovskii, O., & Slyusarenko, S. (2003). Short-range order in liquid silver-tin alloys. *Journal of Non-Crystalline Solids*, 331(1-3), 254–262.
- Kang, Y.-B., Pelton, A. D., Chartrand, P., & Fuerst, C. D. (2008). Critical evaluation and thermodynamic optimization of the Al-Ce, Al-Y, Al-Sc and Mg-Sc binary systems. *Calphad*, 32(2), 413–422.
- Kaptay, G. (2005a). Modelling interfacial energies in metallic systems. In *Materials science forum* (Vol. 473, pp. 1–10).
- Kaptay, G. (2005b). A unified equation for the viscosity of pure liquid metals. *International Journal of Materials Research*, 96(1), 24–31.
- Kaptay, G. (2017). The exponential excess gibbs energy model revisited. *Calphad*, 56, 169–184.

- Kaptay, G. (2019). Improved derivation of the butler equations for surface tension of solutions. *Langmuir*, 35(33), 10987–10992.
- Kaptay, G., Csicsovszki, G., & Yaghmaee, M. S. (2003). An absolute scale for the cohesion energy of pure metals. In *Materials science forum* (Vol. 414, pp. 235–240).
- Klement Jr, W. (1963). Hexagonal close-packed structures in Bi-Pb alloys and the polymorphism of lead at high pressure. *The Journal of Chemical Physics*, 38(2), 298–299.
- Kleppa, O. J., & Thalmayer, C. E. (1959). An emf investigation of binary liquid alloys rich in zinc. *The Journal of Physical Chemistry*, 63(11), 1953–1958.
- Knosp, H., Holliday, R. J., & Corti, C. W. (2003). Gold in dentistry: alloys, uses and performance. *Gold bulletin*, 36(3), 93–102.
- Kobatake, H., Brillo, J., Schmitz, J., & Pichon, P.-Y. (2015). Surface tension of binary Al-Si liquid alloys. *Journal of Materials Science*, 50(9), 3351–3360.
- Kohler, F. (1960). Estimation of the thermodynamic data for a ternary system from the corresponding binary systems. *Monatsh. Chem*, 91(4), 738–740.
- Koirala, I. (2018). Chemical ordering of Ag-Au alloys in the molten state. *Journal of Institute of Science and Technology*, 22(2), 191–201.
- Koirala, I., Jha, I. S., Singh, B. P., & Adhikari, D. (2013). Thermodynamic, transport and surface properties in In-Pb liquid alloys. *Physica B: Condensed Matter*, 423, 49–53.
- Koirala, I., Singh, B. P., & Jha, I. S. (2014). Transport and surface properties of molten Cd-Zn alloys. *Journal of Institute of Science and Technology*, 19(1), 14–18.
- Koirala, I., Singh, B. P., & Jha, I. S. (2014a). Study of segregating nature in liquid Al-Ga alloys. *Scientific World*, 12(12), 14–20.
- Koirala, I., Singh, B. P., & Jha, I. S. (2014b). Theoretical assessment on segregating nature of liquid In-Tl alloys. *Journal of Non-Crystalline Solids*, 398, 26–31.
- Koirala, I., Singh, B. P., & Jha, I. S. (2016a). Theoretical investigation of mixing behavior of Al-Fe alloys in molten stage. *The African Review of Physics*, 10, 329–335.
- Koirala, I., Singh, B. P., & Jha, I. S. (2016b). Thermodynamic and structural investigations on mixing behavior of hetero-coordinated Al-based alloys in the fusion state. *BIBECHANA*, 13, 87–93.

- Koirala, I., Singh, B. P., Jha, I. S., & Mallik, A. K. (2015). Theoretical investigation of energetic and its effect on Cd-Hg amalgam. *Journal of Nepal Physical Society*, 3(1), 60–66.
- Koirala, R. P., Adhikari, D., Jha, I. S., & Singh, B. P. (2013). Thermodynamic and structural behaviour of liquid Al-Ga alloys. *Advanced Materials Letters*, 4(4), 283–287.
- Koirala, R. P., Jha, I. S., Singh, B. P., & Adhikari, D. (2014). Structural study of liquid Sn-Tl alloys. *BIBECHANA*, 11, 46–52.
- Koirala, R. P., Koirala, I., & Adhikari, D. (2018). Energetics of mixing and transport phenomena in Cd-X (X= Pb, Sn) melts. *Bibechana*, 15, 113–120.
- Koirala, R. P., Kumar, J., Singh, B. P., & Adhikari, D. (2014). Bulk and surface properties of Co-Fe and Fe-Pd liquid alloys. *Journal of Non-Crystalline Solids*, 394, 9–15.
- Koirala, R. P., Singh, B. P., Jha, I. S., & Adhikari, D. (2013). Thermodynamic, structural and surface properties of liquid Cd-Zn alloys. *Journal of Molecular Liquids*, 179, 60–66.
- Koirala, R. P., Singh, B. P., Jha, I. S., & Adhikari, D. (2016). Energetics and local order in In-based liquid alloys. *BIBECHANA*, 13, 60–71.
- Kostrivas, A., & Lippold, J. C. (1999). Weldability of li-bearing aluminium alloys. *International Materials Reviews*, 44(6), 217–237.
- Kresse, G., & Hafner, J. (1993). Ab initio molecular dynamics for liquid metals. *Physical Review B*, 47(1), 558–561.
- Kumar, A., Jha, I. S., & Singh, B. P. (2011). Quasi-lattice model for the thermodynamic properties and microscopic structure of molten Fe-Si alloy. *Physica B: Condensed Matter*, 406(23), 4338–4341.
- Kumar, A., Rafique, S. M., & Jha, N. (2006). Study of glass forming tendency of Ca-Mg binary alloy and its physical properties: Pseudomolecule formation model. *Physica B: Condensed Matter*, 373(1), 169–176.
- Kumar, A., Rafique, S. M., Jha, N., & Mishra, A. K. (2005). Structure, thermodynamic, electrical and surface properties of Cu-Mg binary alloy: complex formation model. *Physica B: Condensed Matter*, 357(3-4), 445–451.
- Kurata, Y., Futakawa, M., Kikuchi, K., Saito, S., & Osugi, T. (2002). Corrosion studies in liquid Pb-Bi alloy at jaeri: R & d program and first experimental results. *Journal of Nuclear Materials*, 301(1), 28–34.

- Lalneihpuii, R., Shrivastava, R., Lalnuntluanga, C., & Mishra, R. K. (2019). Bhatia-Thornton fluctuations, transport and ordering in partially ordered Al-Cu alloys. *Journal of Statistical Mechanics: Theory and Experiment*, 2019(5), 053202–13pp.
- Laty, P., Joud, J. C., Mathieu, J. C., & Desre, P. (1978). Influence of the short-range chemical order effect on the partial interference functions of a dilute binary liquid alloy. *Philosophical Magazine B*, 38(1), 1–13.
- Lee, Y. W., & Aaronson, H. I. (1980). Surface concentration profile and surface energy in binary alloys. *Surface Science*, 95(1), 227–244.
- Lele, S., & Ramachandrarao, P. (1981). Estimation of complex concentration in a regular associated solution. *Metallurgical Transactions B*, 12(4), 659–666.
- Liu, H. S., Cui, Y., Ishida, K., Liu, X. J., Wang, C. P., Ohnuma, I., . . . Jin, Z. P. (2002). Thermodynamic assessment of the Cu-In binary system. *Journal of Phase Equilibria*, 23(5), 409–415.
- Longuet-Higgins, H. C. (1951). The statistical thermodynamics of multicomponent systems. *Proceedings of the Royal Society of London. Series A. Mathematical and Physical Sciences*, 205(1081), 247–269.
- March, N. H., Parrinello, M., & Tosi, M. P. (1976). Structure factors of liquids containing chemical complexes. *Physics and Chemistry of Liquids*, 5(1), 39–43.
- Marrocco, T., Driver, L. C., Harris, S., & McCartney, D. G. (2006). Microstructure and properties of thermally sprayed Al-Sn-based alloys for plain bearing applications. *Journal of Thermal Spray Technology*, 15(4), 634–639.
- Matson, M., & Orbaek, A. W. (2013). *Inorganic chemistry for dummies*. John Wiley & Sons.
- McAlister, S. P., & Turner, R. (1972). The partial structure factors at zero wave vector for binary liquid alloys. *Journal of Physics F: Metal Physics*, 2(3), L51–L54.
- Mekler, C., & Kaptay, G. (2008). Calculation of surface tension and surface phase transition line in binary Ga-Tl system. *Materials Science and Engineering: A*, 495(1-2), 65–69.
- Mezbahul-Islam, M., Mostafa, A., & Medraj, M. (2014). Essential magnesium alloys binary phase diagrams and their thermochemical data. *Journal of Materials*, 2014, 1–33.
- Mills, A. P. (1922). *Materials of construction: Their manufacture and properties*. John Wiley & sons, Incorporated.

- Minic, D., Zivkovic, D., & Zivkovic, Z. (2001). Calorimetric investigation of the Pb-In binary system. *Thermochimica Acta*, 372(1-2), 85–91.
- Mishra, A. K. (2007). Thermodynamic properties, surface properties and volume of mixing of liquid Cd-Na alloys-complex formation model incorporating volume interaction terms. *High Temperature Materials and Processes*, 26(3), 201–208.
- Mishra, A. K., & Milanarun, M. (2005). Thermodynamic properties of liquid Cd-Mg and Cd-Ga alloys. *High Temperature Materials and Processes*, 24(1), 47–56.
- Mishra, A. K., & Milanarun, M. (2006). Thermodynamic properties of liquid AlMg alloys. *Indian Journal of Physics*, 80, 55–59.
- Mishra, A. K., Singh, R. N., Rukhaiyar, A. K., & Sahay, B. B. (1994). Electrical and thermodynamic properties of HgNa and HgK liquid alloys. *physica status solidi (a)*, 144(2), 335–342.
- Mishra, A. K., Singh, R. N., & Sahay, B. B. (1990). Electrical resistivity and entropy of mixing of liquid lithium-lead and sodium-lead alloys. *Physica B: Condensed Matter*, 167(1), 7–18.
- Mishra, P. P., Milanarun, M., Jha, N., & Mishra, A. K. (2002). Thermodynamic properties of liquid glass-forming Ca-Mg alloys. *Journal of Alloys and Compounds*, 340(1-2), 108–113.
- Monteiro, W. A. (2014). *Light metal alloys applications*. BoD–Books on Demand.
- Morachavskii, A. G., & Erofeev, K. B. (2001). Modeling of thermodynamic properties of liquid alloys in the system magnesium-tin. *Russian Journal of Applied Chemistry*, 74(6), 930–932.
- Muktinatalapati, N. R. (2011). *Advances in gas turbine technology* (Vol. 23). InTech.
- Müller, S. (2003). Bulk and surface ordering phenomena in binary metal alloys. *Journal of Physics: Condensed Matter*, 15(34), R1429–R1500.
- Nakamura, M. (1995). Fundamental properties of intermetallic compounds. *Mrs Bulletin*, 20(8), 33–39.
- Neale, F. E., & Cusack, N. E. (1982). Thermodynamic properties of liquid sodium-caesium alloys. *Journal of Physics F: Metal Physics*, 12(12), 2839–2850.
- Novakovic, R. (2010). Thermodynamics, surface properties and microscopic functions of liquid Al-Nb and Nb-Ti alloys. *Journal of Non-Crystalline Solids*, 356(31-32), 1593–1598.

- Novakovic, R., & Brillo, J. (2014). Thermodynamics, thermophysical and structural properties of liquid Fe–Cr alloys. *Journal of Molecular Liquids*, 200, 153–159.
- Novakovic, R., Giuranno, D., Caccia, M., Amore, S., Nowak, R., Sobczak, N., . . . Ricci, E. (2016). Thermodynamic, surface and structural properties of liquid Co–Si alloys. *Journal of Molecular Liquids*, 221, 346–353.
- Novakovic, R., Giuranno, D., Ricci, E., Delsante, S., Li, D., & Borzone, G. (2011). Bulk and surface properties of liquid Sb–Sn alloys. *Surface Science*, 605(1-2), 248–255.
- Novakovic, R., Giuranno, D., Ricci, E., & Lanata, T. (2008). Surface and transport properties of In–Sn liquid alloys. *Surface Science*, 602(11), 1957–1963.
- Novakovic, R., Giuranno, D., Ricci, E., Tuissi, A., Wunderlich, R., Fecht, H.-J., & Egry, I. (2012). Surface, dynamic and structural properties of liquid Al–Ti alloys. *Applied Surface Science*, 258(7), 3269–3275.
- Novakovic, R., Muolo, M. L., & Passerone, A. (2004). Bulk and surface properties of liquid X–Zr (X= Ag, Cu) compound forming alloys. *Surface Science*, 549(3), 281–293.
- Novakovic, R., Ricci, E., Giuranno, D., & Gnecco, F. (2002). Surface properties of Bi–Pb liquid alloys. *Surface Science*, 515(2-3), 377–389.
- Novakovic, R., Ricci, E., Giuranno, D., Lanata, T., & Amore, S. (2009). Thermodynamics and surface properties of liquid Bi–In alloys. *Calphad*, 33(1), 69–75.
- Novakovic, R., Ricci, E., Giuranno, D., & Passerone, A. (2005). Surface and transport properties of Ag–Cu liquid alloys. *Surface Science*, 576(1-3), 175–187.
- Novakovic, R., Ricci, E., & Gnecco, F. (2006). Surface and transport properties of Au–In liquid alloys. *Surface science*, 600(23), 5051–5061.
- Novakovic, R., Ricci, E., Muolo, M. L., Giuranno, D., & Passerone, A. (2003). On the application of modelling to study the surface and interfacial phenomena in liquid alloy-ceramic substrate systems. *Intermetallics*, 11(11-12), 1301–1311.
- Novakovic, R., & Tanaka, T. (2006). Bulk and surface properties of Al–Co and Co–Ni liquid alloys. *Physica B: Condensed Matter*, 371(2), 223–231.
- Novakovic, R., Tanaka, T., Muolo, M. L., Lee, J., & Passerone, A. (2005). Bulk and surface properties of liquid Ag–X (X= Ti, Hf) compound forming alloys. *Surface science*, 591(1-3), 56–69.
- Novakovic, R., & Zivkovic, D. (2005). Thermodynamics and surface properties of liquid Ga–X (X= Sn, Zn) alloys. *Journal of Materials Science*, 40(9), 2251–2257.

- Odusote, Y. A. (2008). Thermodynamics of compound forming molten Cu-In alloys. *International Journal of Modern Physics B*, 22(27), 4833–4844.
- Odusote, Y. A. (2014). Thermodynamic and dynamical properties of liquid Al-X (X= Sn, Ge, Cu) systems. *Journal of Non-Crystalline Solids*, 402, 96–100.
- Odusote, Y. A., Hussain, L. A., & Awe, O. E. (2007). Bulk and dynamic properties in Al-Zn and Bi-In liquid alloys using a theoretical model. *Journal of Non-Crystalline Solids*, 353(11-12), 1167–1171.
- Odusote, Y. A., & Popoola, A. I. (2017). Thermodynamic and surface properties of Cr-X,(X= Mo, Fe) liquid alloys. *American Journal of Condensed Matter Physics*, 7(3), 57–66.
- Odusote, Y. A., & Popoola, A. I. (2019). Thermodynamic prediction of the free energy of mixing and activities of some gold based binary liquid alloys. *Nigeria Journal of Pure and Applied Physics*, 9(1), 11–16.
- Odusote, Y. A., Popoola, A. I., & Oluyamo, S. S. (2016). Bulk and surface properties of demixing liquid Al-Sn and Sn-Tl alloys. *Applied Physics A*, 122(2), 1–9.
- Ogundeji, S. O., Awe, O. E., Madu, C. A., & Anusionwu, B. C. (2021). Fe-Co and Fe-Mn liquid alloys: A study of bulk and transport properties. *Journal of Molecular Liquids*, 328, 115393–8pp.
- Ortiz-Corona, J., & Rodriguez-Gomez, F. (2019). Role of copper in tarnishing process of silver alloys in sulphide media. *Transactions of Nonferrous Metals Society of China*, 29(12), 2646–2657.
- Paliwal, M., & Jung, I.-H. (2009). Thermodynamic modeling of the Mg-Bi and Mg-Sb binary systems and short-range-ordering behavior of the liquid solutions. *Calphad*, 33(4), 744–754.
- Panthi, N., Bhandari, I. B., Jha, I. S., & Koirala, I. (2021). Complex formation behavior of Copper-Tin alloys at its molten state. *Advanced Materials Letters*, 12(1), 1–7.
- Panthi, N., Bhandari, I. B., & Koirala, I. (2020). Theoretical assessment on hetero-coordination of alloys silver-antimony at molten state. *Himalayan Journal of Science and Technology*, 3-4, 68–73.
- Panthi, N., Bhandari, I. B., & Koirala, I. (2022). Thermophysical behavior of mercury-lead liquid alloy. *Papers in Physics*, 14, 140005–11pp.
- Passerone, A., Muolo, M. L., Valenza, F., & Novakovic, R. (2009). Thermodynamics and surface properties of liquid Cu-B alloys. *Surface Science*, 603(17), 2725–2733.

- Pelton, A. D., & Blander, M. (1986). Thermodynamic analysis of ordered liquid solutions by a modified quasichemical approach—application to silicate slags. *Metallurgical Transactions B*, 17(4), 805–815.
- Polak, M., & Rubinovich, L. (2000). The interplay of surface segregation and atomic order in alloys. *Surface Science Reports*, 38(4-5), 127–194.
- Pollock, D. D. (2018). *Thermocouples: theory and properties*. Routledge.
- Polmear, I. (2005). *Light alloys: from traditional alloys to nanocrystals*. Elsevier.
- Porter, F. C. (1994). *Corrosion resistance of zinc and zinc alloys*. CRC Press.
- Praiphruk, S., Lothongkum, G., Nisaratanaporn, E., & Lohwongwatana, B. (2013). Investigation of supersaturated silver alloys for high hardness jewelry application. *Journal of Metals, Materials and Minerals*, 23(2), 67–73.
- Prasad, L. C., Chatterjee, S. K., & Jha, R. K. (2007). Atomic order and interionic pair potentials in Cu-Sn liquid alloys. *Journal of Alloys and Compounds*, 441(1-2), 43–51.
- Prasad, L. C., Chatterjee, S. K., & Singh, V. N. (1996). Intermetallic associations in AlMg liquid alloys. *Physica B: Condensed Matter*, 217(3-4), 285–291.
- Prasad, L. C., & Jha, R. K. (2005). Surface tension and viscosity of Sn -based binary liquid alloys. *Physica Status Solidi (a)*, 202(14), 2709–2719.
- Prasad, L. C., & Jha, R. K. (2007). Correlation between bulk and surface properties of ternary Ag-Sn-Zn liquid alloys and concerned binaries. *Physics and Chemistry of Liquids*, 45(2), 149–167.
- Prasad, L. C., & Mikula, A. (2000a). Concentration fluctuations and interfacial adhesion at the solid-liquid interface between Al_2O_3 and Al-Sn liquid alloys. *High Temperature Materials and Processes*, 19(1), 61–69.
- Prasad, L. C., & Mikula, A. (2000b). Effect of temperature on inter-metallic associations in Sb-Zn liquid alloys. *Journal of Alloys and Compounds*, 299(1-2), 175–182.
- Prasad, L. C., & Mikula, A. (2006). Thermodynamics of liquid Al-Sn-Zn alloys and concerned binaries in the light of soldering characteristics. *Physica B: Condensed Matter*, 373(1), 64–71.
- Prasad, L. C., & Singh, R. N. (1990). A quasi-lattice model for the thermodynamic properties of Au-Zn liquid alloys. *Physics and Chemistry of Liquids*, 22(1-2), 1–9.

- Prasad, L. C., Singh, R. N., & Singh, G. P. (1994). The role of size effects on surface properties. *Physics and Chemistry of Liquids*, 27(3), 179–185.
- Prasad, L. C., Singh, R. N., Singh, V. N., & Chatterjee, S. K. (1995). Compound formation in Sn-based liquid alloys. *Physica B: Condensed Matter*, 215(2-3), 225–232.
- Prasad, L. C., Singh, R. N., Singh, V. N., & Singh, G. P. (1998). Correlation between bulk and surface properties of AgSn liquid alloys. *The Journal of Physical Chemistry B*, 102(6), 921–926.
- Predel, B. (1976). Thermodynamic properties and structure of liquid alloys. *Berichte der Bunsengesellschaft für physikalische Chemie*, 80(8), 695–704.
- Rafique, S. M., & Kumar, A. (2007). Thermodynamic properties and alloying behaviour of liquid binary alloy: CdZn. *Indian Journal of Physics*, 81, 35–39.
- Ramachandrarao, P., Singh, R. N., & Lele, S. (1984). Role of concentration fluctuations in metallic glass formation. *Journal of Non-Crystalline Solids*, 64(3), 387–398.
- Rapson, W. S. (1990). The metallurgy of the coloured carat gold alloys. *Gold Bulletin*, 23(4), 125–133.
- Ratti, V. K., & Bhatia, A. B. (1975). Electrical properties of compound forming molten systems: Mg-Bi and Tl-Te. *Journal of Physics F: Metal Physics*, 5(5), 893–902.
- Ratti, V. K., & Bhatia, A. B. (1977). Structural aspects of energy in binary alloys. *Journal of Physics F: Metal Physics*, 7(4), 647–653.
- Ratti, V. K., & Bhatia, A. B. (1978). Concentration fluctuations and structure factors of alloys. *Il Nuovo Cimento B (1971-1996)*, 43(1), 1–12.
- Redlich, O., & Kister, A. (1948). Algebraic representation of thermodynamic properties and the classification of solutions. *Industrial & Engineering Chemistry*, 40(2), 345–348.
- Reed, R. C. (2008). *The superalloys: fundamentals and applications*. Cambridge university press.
- Rukhaiyar, A. K., Singh, V. N., & Mishra, A. K. (2001). Electronic properties and compound formation in LiPb molten alloys. *Indian Journal of Physics*, 75(1), 73–75.
- Ruppersberg, H., & Egger, H. (1975). Short-range order in liquid Li-Pb alloys. *The Journal of Chemical Physics*, 63(10), 4095–4103.

- Ruzankina, J. S., & Vasiliev, O. S. (2016). Study on possibility for the improvement of corrosion resistance of metals using laser-formed oxide surface structure. In *Journal of physics: Conference series* (Vol. 735, pp. 012050–6pp).
- Salmon, P. S. (1992). The structure of molten and glassy 2: 1 binary systems: an approach using the Bhatia—Thornton formalism. *Proceedings of the Royal Society of London. Series A: Mathematical and Physical Sciences*, 437(1901), 591–606.
- Schmid, R., & Chang, Y. A. (1985). A thermodynamic study on an associated solution model for liquid alloys. *Calphad*, 9(4), 363–382.
- Schwartz, M. (2002). *Encyclopedia of materials, parts and finishes*. CRC press.
- Schwartz, M. (2014). *Soldering: understanding the basics*. ASM International.
- Seetharaman, S. D. J. M., & Sichen, D. (1994). Estimation of the viscosities of binary metallic melts using Gibbs energies of mixing. *Metallurgical and Materials Transactions B*, 25(4), 589–595.
- Semlitsch, M., & Willert, H. G. (1980). Properties of implant alloys for artificial hip joints. *Medical and Biological Engineering and Computing*, 18(4), 511–520.
- Sharma, N., Thakur, A., & Ahluwalia, P. K. (2013). Thermodynamic, surface and transport properties of liquid Hg-Pb and Hg-In amalgams. *Journal of Molecular Liquids*, 188, 104–112.
- Shiga, M. (1996). Invar alloys. *Current Opinion in Solid State and Materials Science*, 1(3), 340–348.
- Shih, C.-C., Lin, S.-J., Chung, K.-H., Chen, Y.-L., & Su, Y.-Y. (2000). Increased corrosion resistance of stent materials by converting current surface film of polycrystalline oxide into amorphous oxide. *Journal of Biomedical Materials Research*, 52(2), 323–332.
- Shokrollahi, H. (2009). The magnetic and structural properties of the most important alloys of iron produced by mechanical alloying. *Materials & Design*, 30(9), 3374–3387.
- Shokrollahi, H., & Janghorban, K. (2007). Soft magnetic composite materials (smcs). *Journal of Materials Processing Technology*, 189(1-3), 1–12.
- Shpil'rain, E. E., Shkermontov, V. I., Skovorod'ko, S. N., & Mozgovoï, A. G. (2002). Activity of the components of binary alloys of alkali metals: Na-K system. *High Temperature*, 40(1), 33–43.

- Shrestha, G. K., Jha, I. S., & Singh, B. K. (2018). Theoretical investigations on temperature dependence of thermodynamic properties and concentration fluctuations of In-Tl binary liquid alloys by optimization method. *BIBECHANA*, 15, 11–23.
- Shrestha, G. K., Singh, B. K., Jha, I. S., & Koirala, I. (2017). Theoretical study of thermodynamic properties of Cu-Pb liquid alloys at different temperature by optimization method. *Journal of Institute of Science and Technology*, 22(1), 25–33.
- Shrestha, G. K., Singh, B. K., Jha, I. S., Koirala, I., Singh, B. P., & Adhikari, D. (2017). Theoretical investigations on thermodynamic properties and concentration fluctuations of Zn-Sn binary liquid alloys at different temperatures by optimization method. *Journal of the Chinese Advanced Materials Society*, 5(3), 186–203.
- Shrestha, G. K., Singh, B. K., Jha, I. S., Singh, B. P., & Adhikari, D. (2017). Optimization method for the study of the properties of Al-Sn binary liquid alloys. *Physica B: Condensed Matter*, 514, 1–7.
- Shunyaev, K., & Lisin, V. (2000). Calculation of thermodynamic properties and of liquidus line positions for Na-K alloys. *Journal of Thermal Analysis and Calorimetry*, 60(3), 851–856.
- Singh, B. P., Adhikari, D., & Jha, I. S. (2010). Concentration dependence of the structure and thermodynamic properties of silver–antimony alloys. *Journal of non-crystalline solids*, 356(33-34), 1730–1734.
- Singh, B. P., Adhikari, D., & Jha, I. S. (2012). Short range order in molten Al-Si alloys. *Physics and Chemistry of Liquids*, 50(6), 697–704.
- Singh, B. P., Koirala, I., Jha, I. S., & Adhikari, D. (2014). The segregating nature of Cd-Pb liquid binary alloys. *Physics and Chemistry of Liquids*, 52(4), 457–470.
- Singh, B. P., Kumar, J., Jha, I. S., & Adhikari, D. (2011). Concentration dependence of thermodynamic properties of NaPb liquid alloy. *World Journal of Condensed Matter Physics*, 1(3), 97–100.
- Singh, N. K. P., Singh, R. N., & Choudhary, R. B. (1991). Thermodynamic investigation of atomic order in AlMg liquid alloys. *Journal of Physics: Condensed Matter*, 3(20), 3635–3644.
- Singh, P., Pal, C., & Khanna, K. N. (1985). Entropy of mixing of compound forming liquid binary alloys using flory's formula. *Physics and Chemistry of Liquids*, 14(4), 297–302.

- Singh, R. N. (1981). Free energy and heat of mixing of alloys. *Journal of Physics F: Metal Physics*, 11(2), 389–396.
- Singh, R. N. (1987). Short-range order and concentration fluctuations in binary molten alloys. *Canadian Journal of Physics*, 65(3), 309–325.
- Singh, R. N. (1993). Higher order conditional probabilities and short range order in molten alloys. *Physics and Chemistry of Liquids*, 25(4), 251–267.
- Singh, R. N., & Ali, I. (2006). Structure-induced order-disorder transformation in Cd-Na liquid alloys. *International Journal of Materials Research*, 97(4), 382–387.
- Singh, R. N., & Arafin, S. (2015). Chemical short range order in MgPb alloys. *Physics and Chemistry of Liquids*, 53(1), 38–45.
- Singh, R. N., & Bhatia, A. B. (1984). Flory's formula for the entropy of mixing of NaCs alloy. *Journal of Physics F: Metal Physics*, 14(10), 2309–2314.
- Singh, R. N., Jha, I. S., & Pandey, D. K. (1993). Thermodynamics of liquid Mg-Sn alloys. *Journal of Physics: Condensed Matter*, 5(16), 2469–2478.
- Singh, R. N., & Mishra, I. K. (1988). Conditional probabilities and thermodynamics of binary molten alloys. *Physics and Chemistry of Liquids*, 18(4), 303–319.
- Singh, R. N., Mishra, I. K., & Singh, V. N. (1990). Local order in Cd-based liquid alloys. *Journal of Physics: Condensed Matter*, 2(42), 8457–8462.
- Singh, R. N., Pandey, D. K., Sinha, S., Mitra, N. R., & Srivastava, P. L. (1987). Thermodynamic properties of molten LiMg alloy. *Physica B + C*, 145(3), 358–364.
- Singh, R. N., & Sommer, F. (1992a). A simple model for demixing binary liquid alloys. *International Journal of Materials Research*, 83(7), 533–540.
- Singh, R. N., & Sommer, F. (1992b). Temperature dependence of the thermodynamic functions of strongly interacting liquid alloys. *Journal of Physics: Condensed Matter*, 4(24), 5345–5358.
- Singh, R. N., & Sommer, F. (1997). Segregation and immiscibility in liquid binary alloys. *Reports on Progress in Physics*, 60(1), 57–150.
- Singh, R. N., & Sommer, F. (1998). Thermodynamic investigation of viscosity and diffusion in binary liquid alloys. *Physics and Chemistry of Liquids*, 36(1), 17–28.
- Singh, R. N., & Sommer, F. (2012). Viscosity of liquid alloys: generalization of andrade's equation. *Monatshefte für Chemie-Chemical Monthly*, 143(9), 1235–1242.

- Singh, R. N., Yu, S. K., & Sommer, F. (1993). Concentration fluctuations and thermodynamic properties of demixing liquid binary alloys. *Journal of Non-Crystalline Solids*, 156, 407–411.
- Sinha, S. K., & Singh, R. N. (1991). Small-angle structure and atomic order in Ge-and Si-based liquid alloys. *Journal of Physics: Condensed Matter*, 3(44), 8745–8750.
- Smith, R. C. (1970). *Materials of construction*. Tokyo.
- Soltwisch, M., Quitmann, D., Ruppertsberg, H., & Suck, J. B. (1983). Dynamics of concentration fluctuations in a heterocoordinated binary liquid alloy. *Physical Review B*, 28(10), 5583–5598.
- Sommer, F. (1990). Thermodynamic properties of compound-forming liquid alloys. *Journal of Non-Crystalline Solids*, 117, 505–512.
- Sommer, F. (2007). Thermodynamics of liquid alloys. *Journal of Non-Crystalline Solids*, 353(32-40), 3709–3716.
- Srikanth, S., & Jacob, K. T. (1991). Thermodynamics of aluminum-barium alloys. *Metallurgical Transactions B*, 22(5), 607–616.
- Strnat, K. J., & Strnat, R. M. (1991). Rare earth-cobalt permanent magnets. *Journal of Magnetism and Magnetic Materials*, 100(1-3), 38–56.
- Suryanarayana, C., & Inoue, A. (2017). *Bulk metallic glasses*. CRC press.
- Swamy, K. N., Kahol, P. K., Chaturvedi, D. K., & Pathak, K. N. (1977). Dynamical structure factors in binary liquids. ii. liquid Na-K alloy. *Journal of Physics C: Solid State Physics*, 10(21), 4191–4196.
- Tamaki, S., Wadeda, Y., Takeda, S., & Tsuchiya, Y. (1982). A compound-forming effect in liquid Hg-Na alloys. *Journal of Physics F: Metal Physics*, 12(6), 1101–1109.
- Tanaka, R. (2000). Research and development of ultra-high temperature materials in japan. *Materials at High Temperatures*, 17(4), 457–464.
- Tanaka, T., Gokcen, N. A., & Morita, Z. (1990). Relationship between enthalpy of mixing and excess entropy in liquid binary alloys. *Zeitschrift für Metallkunde*, 81(1), 49–54.
- Tanaka, T., & Iida, T. (1994). Application of a thermodynamic database to the calculation of surface tension for iron-base liquid alloys. *Steel Research*, 65(1), 21–28.
- Tanaka, Y., Ohtomo, N., & Arakawa, K. (1983). Statistical thermodynamics of liquid alkali alloys. *Journal of the Physical Society of Japan*, 52(6), 2093–2101.

- Trybuła, M., Jakse, N., Gašior, W., & Pasturel, A. (2015). Thermodynamics and concentration fluctuations of liquid Al-Cu and Al-Zn alloys. *Archives of Metallurgy and Materials*, 60, 649–655.
- Van Humbeeck, J. (1999). Non-medical applications of shape memory alloys. *Materials Science and Engineering: A*, 273, 134–148.
- Van Humbeeck, J. (2001). Shape memory alloys: a material and a technology. *Advanced Engineering Materials*, 3(11), 837–850.
- Vera, J. H., Sayegh, S. G., & Ratcliff, G. A. (1977). A quasi lattice-local composition model for the excess Gibbs free energy of liquid mixtures. *Fluid Phase Equilibria*, 1(2), 113–135.
- Vinarcik, E. J. (2002). *High integrity die casting processes*. John Wiley & Sons.
- Von Fraunhofer, J. A. (2013). *Dental materials at a glance*. John Wiley & Sons.
- Wang, L., Makhlof, M., & Apelian, D. (1995). Aluminium die casting alloys: alloy composition, microstructure, and properties-performance relationships. *International Materials Reviews*, 40(6), 221–238.
- Warren, B. E. (1990). *X-ray diffraction*. Courier Corporation.
- Waseda, Y., Jacob, K. T., & Tamaki, S. (1984). Current views on the microscopic thermodynamics of liquid alloys. *High Temperature Materials and Processes*, 6(3), 119–141.
- Westbrook, J. H. (1977). Intermetallic compounds: Their past and promise. *Metallurgical Transactions A*, 8(9), 1327–1360.
- Westbrook, J. H. (1996). Applications of intermetallic compounds. *MRS Bulletin*, 21(5), 26–29.
- Witusiewicz, V. T., & Sommer, F. (2000). Estimation of the excess entropy of mixing and the excess heat capacity of liquid alloys. *Journal of Alloys and Compounds*, 312(1-2), 228–237.
- Wright, R. N. (2011). *Relevant aspects of copper and copper alloy metallurgy*. Elsevier.
- Yadav, S. K., Gautam, M., & Adhikari, D. (2020). Mixing properties of Cu-Mg liquid alloy. *AIP Advances*, 10(12), 125320–8pp.
- Yadav, S. K., Jha, L. N., & Adhikari, D. (2015a). Segregating to ordering transformation in In-Sn melt. *Physics and Chemistry of Liquids*, 53(4), 443–454.
- Yadav, S. K., Jha, L. N., & Adhikari, D. (2015b). Thermodynamic and structural behaviour of Tl-Na liquid alloy. *BIBECHANA*, 12, 20–29.

- Yadav, S. K., Jha, L. N., & Adhikari, D. (2016). Thermodynamic, structural, transport and surface properties of Pb-Tl liquid alloy. *BIBECHANA*, *13*, 100–113.
- Yadav, S. K., Jha, L. N., & Adhikari, D. (2017). Theoretical modeling to predict the thermodynamic, structural, surface and transport properties of the liquid Tl-Na alloys at different temperatures. *Journal of Nepal Physical Society*, *4*(1), 101–110.
- Yadav, S. K., Jha, L. N., Dhungana, A., Mehta, U., & Adhikari, D. (2018). Thermo-physical properties of Al-Mg alloy in liquid state at different temperatures. *Materials Sciences and Applications*, *9*(10), 812–828.
- Yadav, S. K., Jha, L. N., Jha, I. S., Singh, B. P., Koirala, R. P., & Adhikari, D. (2016). Prediction of thermodynamic and surface properties of Pb-Hg liquid alloys at different temperatures. *Philosophical Magazine*, *96*(18), 1909–1925.
- Yadav, S. K., Lamichhane, S., Jha, L. N., Adhikari, N. P., & Adhikari, D. (2016). Mixing behaviour of Ni-Al melt at 1873 K. *Physics and Chemistry of Liquids*, *54*(3), 370–383.
- Yadav, S. K., Mehta, U., Gohivar, R. K., Dhungana, A., Koirala, R. P., & Adhikari, D. (2020). Reassessments of thermo-physical properties of Si-Ti melt at different temperatures. *BIBECHANA*, *17*, 146–153.
- Yao, C., & Ma, Y. (2021). Superconducting materials: Challenges and opportunities for large-scale applications. *iScience*, *24*(6), 102541–46pp.
- Yu, J., Zhang, Y., Zu, F.-Q., Xi, Y., Li, X.-F., Xu, W., & Liu, H.-M. (2006). The abnormal changes of electrical resistivity in liquid Pb-In alloys. *Physics and Chemistry of Liquids*, *44*(4), 401–408.
- Zhang, F., Tang, Y., Hu, B., Liu, S., Du, Y., & Zhang, Y. (2014). Thermodynamic assessment of the Mg-Pb and Mg-Bi systems using substitutional solution and associate models for liquid phase. *Journal of Mining and Metallurgy, Section B: Metallurgy*, *50*(2), 115–115.
- Živković, D., Manasijević, D., & Živković, Ž. (2005). Comparative thermodynamic investigation of binary Ga-Bi system; experimental determination of enthalpies of mixing and activity estimation for liquid Ga-Bi alloys. *Journal of Thermal Analysis and Calorimetry*, *79*(1), 71–77.

APPENDIX

Academic Activities

A. Attended courses offered by IoST

In first semester:

PHS 911, Philosophy of Science (Cr. Hrs. 3)

RM 912, Research Methodology (Cr. Hrs. 3)

Sem 913, Seminar (Cr. Hrs. 3)

In second semester:

PHY 951, Advanced Research Methodology (Cr. Hrs. 3)

PHY 960, Material Thermodynamics B (Cr. Hrs. 3)

PHY 952, Seminar (Cr. Hrs. 3)

B. Paper publications

International

- 1) Bhandari, I. B., Koirala, I., & Adhikari, D. (2021). Temperature-dependent mixing behaviours of Bi-Mg liquid alloys. *Physics and Chemistry of Liquids*, 59(6), 918-931.
- 2) Panthi, N., B Bhandari, I., Jha, I. S., & Koirala, I. (2021). Complex formation behavior of Copper-Tin alloys at its molten state. *Advanced Materials Letters*, 12(1), 1-7.
- 3) Panthi, N., Bhandari, I. B., Rai, R. K., & Koirala, I. (2021). Thermophysical Behavior of Sodium Lead Alloy at Different Temperature. *Advanced Studies in Theoretical Physics*, 15(4), 153-165.
- 4) Bhandari, I. B., Panthi, N., Koirala, I., & Adhikari, D. (2021). Phase segregating and complex forming Pb-based (= X-Pb) liquid alloys. *Phase Transitions*, 94(5), 338-352.
- 5) Bhandari, I. B., Panthi, N., & Koirala, I. (2021). Temperature-dependent mixing behavior of Pb-Sb alloys in liquid state. *International Journal of Computational Materials Science and Engineering*, 10(3), 2150018–20pp.
- 6) Panthi, N., Bhandari, I. B., & Koirala, I. (2021). Complex formation of sodium-mercury alloy at molten state. *Journal of Physics Communications*, 5(8), 085005–11pp.

- 7) Bhandari, I. B., Panthi, N., Gaire, S., & Koirala, I. (2021, November). Effect of temperature on mixing behavior and stability of liquid Al-Fe alloys. *Journal of Physics: Conference Series*, 2070(1), 012025–12pp.
- 8) Panthi, N., Bhandari, I., & Koirala, I. (2022). Thermophysical behavior of mercury-lead liquid alloy. *Papers in Physics*, 14, 140005–11pp.
- 9) Panthi, N., Bhandari, I. B., & Koirala, I. (2022). High Temperature Stability of K-Pb Liquid Alloy. *Defect and Diffusion Forum*, 419, 147-154.

National

- 1) Bhandari, I. B., Panthi, N., & Koirala, I. (2019). Thermodynamics of liquid Gallium-Zinc alloy. *Himalayan Physics*, 8, 33-38.
- 2) Panthi, N., Bhandari, I. B., Pangeni, R. C., & Koirala, I. (2020). High Temperature Assessment of K-Tl Binary Liquid Alloy. *Journal of Nepal Physical Society*, 6(2), 20-25.
- 3) Panthi, N., Bhandari, I. B., & Koirala, I. (2020). Theoretical assessment on hetero-coordination of Alloys Silver-Antimony at Molten State. *Himalayan Journal of Science and Technology*, 3-4, 68-73.
- 4) Bhandari, I. B., Panthi, N., & Koirala, I. (2021). Investigation on thermo-physical properties of liquid In-Tl alloy. *BIBECHANA*, 18(1), 149-158.
- 5) Kafle, J., Thakur, B. K., & Bhandari, I. B. (2021). Visualization, formulation and intuitive explanation of iterative methods for transient analysis of series RLC circuit. *BIBECHANA*, 18(2), 9-17.
- 6) Panthi, N., Bhandari, I. B., Pangeni, R. C., & Koirala, I. (2021). Comparison of Thermo-physical Properties of Mg-Ga and Mg-Pb Alloys at 1000 K. *Journal of Institute of Science and Technology*, 26(1), 51-56.
- 7) Kafle, J., Thakur, B. K., & Bhandari, I. B. (2021). Application of Numerical Methods for the Analysis of Damped Parallel RLC Circuit. *Journal of Institute of Science and Technology*, 26(1), 28-34.

C. Participation

- 1) Participated in “International conference on nanosciences and high energy physics(ICNHEP-2019)”, held in Central Department of Physics, Kirtipur, Nepal during February 4-6, 2019.
- 2) Oral Presentation entitled “Thermodynamics of Liquid Gallium-Zinc Alloy” in the “36th General Meeting of Nepal Physical Society" held in Central Department of Physics, Kirtipur, Nepal in November 8, 2019.

- 3) Participated in “Workshop on Low-dimensional materials: experiment, theory, application”, organized by Organized by University of Aveiro, Portugal in July 6, 2021.
- 4) Oral Presentation entitled “Temperature-dependent mixing behaviors of Bi-Mg liquid alloys” in the “4th International Conference on Nanomaterials Science and Mechanical Engineering (ICNMSME2021)” Organized by University of Aveiro, Portugal during 6-9 July, 2021.
- 5) Oral Presentation entitled “Effect of temperature on mixing behavior and stability of liquid Al-Fe alloys” in the “2nd International Conference on Advances on Physical Sciences and Materials (ICAPSM-2021) held at SNS College of Technology, Coimbatore, Tamil Nadu, India during 12 -13, August 2021.

PAPER • OPEN ACCESS

Effect of temperature on mixing behavior and stability of liquid Al-Fe alloys

To cite this article: I B Bhandari *et al* 2021 *J. Phys.: Conf. Ser.* **2070** 012025

View the [article online](#) for updates and enhancements.

You may also like

- [The interface of heterogeneous nucleation on single crystal substrates](#)
L Yang, M Xia and J Li
- [Spatial heterogeneity in liquid–liquid phase transition](#)
Yun-Rui Duan, , Tao Li et al.
- [Bhatia–Thornton fluctuations, transport and ordering in partially ordered Al–Cu alloys](#)
R Lalneihpuii, Ruchi Shrivastava, C Lalnuntluanga et al.



The Electrochemical Society
Advancing solid state & electrochemical science & technology

241st ECS Meeting

May 29 – June 2, 2022 Vancouver • BC • Canada

Abstract submission deadline: Dec 3, 2021

Connect. Engage. Champion. Empower. Accelerate.
We move science forward



Submit your abstract



Effect of temperature on mixing behavior and stability of liquid Al-Fe alloys

I B Bhandari^{1,2,*}, N Panthi¹, S Gaire³ and Ishwar Koirala¹

¹Central Department of Physics, Tribhuvan University, Kirtipur, Nepal

²Department of Applied Sciences, Purwanchal Campus, Tribhuvan University, Dharan, Nepal

³Everest Engineering College, Pokhara University, Lalitpur, Nepal

E-mail: bhandari.indra@gmail.com

Abstract. A theoretical model based on the assumption of compound formation in binary liquid alloy has been used to investigate the thermodynamic properties (free energy of mixing, enthalpy of mixing and entropy of mixing), microscopic properties (concentration fluctuation in long wavelength limit and chemical short range order parameter), surface properties (surface tension and surface composition) and dynamic properties (viscosity and diffusion coefficient). All the properties of Al₂Fe binary melt have been measured using the same energy parameters configured for experimental values of free energy of mixing. The energy parameters are detected as independent of concentration, but depend on temperature. The findings are well consistent with the experimental standards.

Keywords: Bulk properties; Ordering; Surface tension; Positive deviation

1. INTRODUCTION

The development of lightweight, energy-efficient materials is critical for mitigating the global energy crisis [1]. Aluminum alloys are intensively researched in the automotive and aerospace sectors as test specimens, structural components, and massive metal surfaces. Aluminum alloys are the most often utilized light alloys for structural component weight reduction. At room temperature, these materials are often distinguished by their low density, high thermal conductivity, and good corrosion resistance [2–5]. Because of the extent to which its microstructure may be changed, the Al - Fe alloy system is particularly appealing for aeronautical constructions [6]. Al-Fe alloys have good oxidation properties, a high melting point, and a cheap material cost, making them an economically attractive material for industrial use [7,8]. Al-Fe alloys are also significant in powder metallurgy and spray forming [7,9]. They are the primary components of metal-matrix composites. Additionally, by changing the composition and thermal treatments of Al-Fe alloys, especially when coupled with additional elements like Mg, Si, Cu, and Zn, stronger Al-Fe alloys can be produced [10]. When the thermodynamic characteristics of a binary liquid alloy deviate significantly from ideality, the theoretical models used to analyze it provide vital information. These deviations induce asymmetry in thermodynamic characteristics away from equiatomic composition. The asymmetry in the thermodynamic characteristics of binary melt is mostly due to the size effect [11] and the electronegativity difference [12]. The size ratio (≈ 1.4) and electronegativity difference (≈ 0.22) for Al - Fe liquid alloy are too small to produce significant asymmetry in thermodynamic characteristics. The phase diagram [13] shows that the Al - Fe alloy has many stable phases, including Al₃Fe, which has a complex end – centered monoclinic structure, Al₃Fe₂, which has an end – centered orthorhombic structure, AlFe, which has an ordered bcc (B₂) structure isotypic with CsCl, AlFe₃, which has an ordered bcc (D0₃)



structure isotypic with BiF_3 , and Al_2Fe having a complex rhombohedral structure. Among these phases, the presence of Al_2Fe complex in the liquid state has been considered in this investigation, and its thermodynamic and microscopic characteristics at 1873 K have been calculated using the complex formation model [14]. The Moelwyn–Hughes method [15] has been used to investigate the viscosity of the selected alloy, whereas the Prasad model [16,17] was used to investigate the surface characteristics. Due to the lack of long-range atomic order, researching the characteristics of alloys in liquid form is challenging. As a result, theorists have used several models [18–24] to better explain the characteristics of binary liquid alloys. Theoreticians have previously studied the Al_3Fe alloy in its liquid form at a constant temperature of 1873K [12]. The energetics of Al_2Fe alloy at various temperatures have been investigated in this study utilizing a complex formation model [14]. To demonstrate the correctness of this technique in thermodynamic and structural description of the provided binary system, the results are examined and compared with published data [25].

2. Formulation

2.1 Thermodynamic Properties

To investigate the mixing behavior of Al - Fe compounds, the complex formation model has been used. According to this model, the Al-Fe alloy will be a ternary combination of three species: Al atoms, Fe atoms, and the chemical complex Al_2Fe , all of which will be in chemical equilibrium with one another. Conformal solution is another name for this ternary combination. $N_{\text{Al}} = x$ number of Al atoms and $N_{\text{Fe}} = (1 - x)$ number of Fe atoms make up the total number of atoms in the provided binary system, which equals $N = N_{\text{Al}} + N_{\text{Fe}}$. The thermodynamic characteristics of components Al and Fe are altered when they are combined to produce a binary Al-Fe solution. Because of compound formation in the melt, the quantity of free atoms will decrease. For n_1 g, n_2 g and n_3 g atoms of Al, Fe and Al_2Fe respectively,

$$n_1 = x - 2n_3 \text{ and } n_2 = 1 - x - n_3 \quad (1)$$

After mixing, the total number of atoms is

$$n = n_1 + n_2 + n_3 = 1 - 2n_3 \quad (2)$$

The free energy loss due to compound formation is given by $-n_3\psi$; the complex formation energy is denoted by ψ ; and the ternary mixture mixing free energy is denoted by G' . Then the binary mixture's free energy of mixing may be expressed as [14],

$$G_M = G' - n_3\psi \quad (3)$$

In the case of the ternary ideal solution,

$$G' = \frac{RT}{n} \sum_{i=1}^3 (n_i \ln n_i) \quad (4)$$

Where the implications of the size differences in the mixture are not to be neglected and the interaction between species is limited, but not zero, the zeroth approximation of regular solutions [26] or conformal solution approximation [27] must be valid. In this approximation, G' in terms of interaction energy parameter, V_{ij} can be expressed as,

$$G' = \frac{RT}{n} \sum_{i=1}^3 (n_i \ln n_i) + \frac{1}{n} \sum_{i<j} n_i n_j V_{ij} \quad (5)$$

The free energy of mixing for compound forming and regular binary alloys is now expressed as

$$G_M = \frac{RT}{n} \sum_{i=1}^3 (n_i \ln n_i) + \frac{1}{n} \sum_{i<j} n_i n_j V_{ij} - n_3\psi \quad (6)$$

The equilibrium state at a particular pressure and temperature may be used to calculate the value of n_3 .

$$\left(\frac{\partial G_M}{\partial n_3} \right)_{T,P,N,x} = 0 \quad (7)$$

Substituting G_M from equation 6 and doing some algebraic calculations, we get

$$\ln(n_3 n^2 n_1^{-2} n_2^{-1}) + \chi = \frac{\psi}{RT} \quad (8)$$

Which is the equilibrium equation, where

$$\chi = \left(\frac{2n_1 n_2}{n} - 2n_2 - n_1 \right) \frac{V_{12}}{nRT} + \left(\frac{2n_2 n_3}{n} - n_3 + n_2 \right) \frac{V_{23}}{nRT} + \left(\frac{2n_1 n_3}{n} - 2n_3 + n_1 \right) \frac{V_{13}}{nRT} \quad (9)$$

The heat of mixing H_M can be expressed as follows [14]:

$$H_M = G_M - T \left(\frac{\partial G_M}{\partial T} \right)_P \quad (10)$$

Using the value of G_M from equation 6, we obtain

$$H_M = -n_3 \left[\psi - T \left(\frac{\partial \psi}{\partial T} \right)_P \right] + \frac{1}{n} \sum_{i<j} \sum n_i n_j \left[V_{ij} - T \left(\frac{\partial V_{ij}}{\partial T} \right)_P \right] \quad (11)$$

The entropy of mixing expression, S_M , may be written as

$$S_M = \frac{(H_M - G_M)}{T} = n_3 \frac{\partial \psi}{\partial T} - R \sum_{i=1}^3 n_i \ln \frac{n_i}{n} - \frac{1}{n} \sum_{i<j} \sum n_i n_j \frac{\partial V_{ij}}{\partial T} \quad (12)$$

2.2 Structural Properties

Any variation from the ideal value $S_{cc}^{id}(0)$ is crucial in understanding the nature of ordering and phase separation in molten alloys, therefore the concentration fluctuation at the long wavelength limit is of great importance. The free energy of mixing is linked to concentration variation at long wavelength limits by the formula [28],

$$S_{cc}(0) = RT \left(\frac{\partial^2 G_M}{\partial x^2} \right)^{-1} \quad (13)$$

Differentiating G_M twice with respect to x

$$\begin{aligned} \frac{\partial^2 G_M}{\partial x^2} &= RT \sum_{i=1}^3 \left(\frac{n_i'^2}{n_i} - \frac{n_i'^2}{n} \right) + 2n \sum_{i<j} \sum V_{ij} \left(\frac{n_i}{n} \right)' \left(\frac{n_j}{n} \right)' \\ S_{cc}(0) &= \left[\sum_{i=1}^3 \left(\frac{n_i'^2}{n_i} - \frac{n_i'^2}{n} \right) + \frac{2n}{RT} \sum_{i<j} \sum V_{ij} \left(\frac{n_i}{n} \right)' \left(\frac{n_j}{n} \right)' \right]^{-1} \end{aligned} \quad (14)$$

In terms of composition, the prime on the n 's refers to their first derivative. By using the following formula, the theoretically predicted values of $S_{cc}(0)$ may be compared to observed values computed from constituent element activity at different compositions.

$$S_{cc}(0) = x_{Fe} a_{Al} \left(\frac{\partial a_{Al}}{\partial x_{Al}} \right)_{T,P,N}^{-1} = x_{Al} a_{Fe} \left(\frac{\partial a_{Fe}}{\partial x_{Fe}} \right)_{T,P,N}^{-1} \quad (15)$$

$S_{cc}^{id}(0)$ represent the ideal value as,

$$S_{cc}^{id}(0) = x_{Al} x_{Fe} \quad (16)$$

In the following equation, α_1 indicates Warren – Cowley chemical short range order parameter which measures the degree of local order within the binary melt [29,30].

$$\alpha_1 = \frac{s-1}{s(z-1)+1} \text{ here, } s = \frac{S_{cc}(0)}{x_{Al}x_{Fe}} \quad (17)$$

In equation 17, z is coordination number.

2.3 Transport Properties

The molten alloy's mixing behavior can even be examined at the fundamental level in terms of diffusion coefficient. With the aid of Darken's equation [31], the mutual diffusion coefficient (D_M) of binary liquid alloys may be described in terms of activity (a_i) and self- diffusion coefficient (D_{id}) of individual component.

$$D_M = x_i D_{id} \frac{d \ln a_i}{dx_i} \quad (18)$$

with $D_M = x_{Al}D_{Fe} + x_{Fe}D_{Al}$

Where D_{Al} and D_{Fe} are the self – diffusion coefficients of Al and Fe respectively. In terms of $S_{cc}(0)$, the ratio of mutual diffusion coefficient (D_M) to self – diffusion coefficient (D_{id}) can be expressed as

$$\frac{D_M}{D_{id}} = \frac{S_{cc}^{id}(0)}{S_{cc}(0)} \quad (19)$$

The microscopic mixing behavior of liquid alloys may also be described in terms of viscosity. The Moelwyn – Hughes equation for liquid alloy viscosity is

$$\eta = (x_{Al}\eta_{Al} + x_{Fe}\eta_{Fe}) \left(1 - 2x_{Al}x_{Fe} \frac{H_M}{RT} \right) \quad (20)$$

Here η_i is the viscosity of individual elements Al and Fe. This value can be optimized for required temperature (T) as [32],

$$\eta_i = \eta_{i0} \exp \left(\frac{E}{RT} \right) \quad (21)$$

Here η_{i0} is a constant in the unit of viscosity and E is the activation energy.

2.4 Surface Properties

The surface characteristics of the liquid solution reveal metallurgical phenomena including crystal development, welding, gas absorption, and gas bubble nucleation [33]. The surface tension equations provided by Prasad et al., [16, 17], have been simplified using the zeroth approximation as

$$\tau = \tau_{Al} + \frac{k_B T}{\xi} \ln \frac{x_{Al}^s}{x_{Al}} + \frac{\psi}{\xi} \left[p(x_{Fe}^s)^2 + (q-1)x_{Fe}^2 \right] \quad (22)$$

$$\tau = \tau_{Fe} + \frac{k_B T}{\xi} \ln \frac{x_{Fe}^s}{x_{Fe}} + \frac{\psi}{\xi} \left[p(x_{Al}^s)^2 + (q-1)x_{Al}^2 \right] \quad (23)$$

Where τ_i represents the surface tensions of pure Al and Fe, x_i and x_i^s denote the bulk and surface concentrations of alloy components while p and q represent the coordination fractions. These are the fraction of an atom's nearest neighbors generated within its own layer and those created by the next layer. The connection between the coordination fractions p and q is $p + 2q = 1$. For present

calculation, we assume the closed packed structure for which the p and q values are 0.5 and 0.25 respectively.

The mean atomic surface area (ξ) of the compound can be expressed in terms of component surface area (ξ_i) as,

$$\xi = \sum x_i \xi_i \quad (24)$$

Here

$$\xi_i = 1.102 \left(\frac{\Omega_i}{N_A} \right)^{2/3} \quad (25)$$

Where Ω_i is the component i 's molar volume and N_A is the Avogadro's number. Equations (22) and (23) may be solved for x_i^s as the function of x_i and hence surface tension compositional dependency can be examined.

3. RESULTS AND DISCUSSION

3.1 Thermodynamic Properties

The order energy values for the Al-Fe liquid phase were calculated using known experimental data on thermodynamic characteristics [25] as well as phase diagram information [13]. The mixing functions, i.e. the Gibbs free energy and the enthalpy of mixing (figure 1), are negative for all compositions and have a flat minimum of -1.4770 and -1.2775 at equiatomic composition, $x_c = 0.5$, showing the compositional site of an energetically favorable compound, the Al - Fe. The preferred configurations of Al and Fe component atoms facilitate the production of Al₂Fe complexes ($\mu=2$ and $\nu=1$) in liquid alloys. All calculations were performed at $T = 1873$ K, taking into account the Al - Fe phase diagram [13] and the existence of the liquid phase across the entire concentration range. At $T = 1873$ K, the interaction energy parameters ψ , V_{12} , V_{13} and V_{23} as well as their temperature derivatives, were calculated using the Gibbs energy of mixing, G_M , of liquid Al - Fe alloys and the enthalpy of mixing, H_M [25]. The interaction energy parameters' values were tweaked to produce concentration dependences of G_M that closely matched the thermodynamic data. $V_{12} = -3.095RT$, $V_{13} = -0.851RT$, $V_{23} = -1.970RT$ and $\psi = 2.552RT$ are the estimated interaction energy parameters for liquid Al - Fe alloys, and they remain constant throughout all computations. The number of complexes, n_3 , was calculated using equations (8-9) and equations (1-2). The concentration dependence of the equilibrium values of chemical complexes, n_3 , reaches a maximum value of around 0.261 at the compound forming composition, $x_c = 0.667$.

If energy parameters are assumed to be temperature independent, the values of H_M and S_M are found to be in poor agreement with the experiment. As a result, we looked at how these parameters changed with temperature to see how heat and entropy of formation changed with observed values [25]. At $T = 1873$ K, the temperature-dependent energies are $\partial V_{12} / \partial T = 0.980R$, $\partial V_{13} / \partial T = 2.591R$, $\partial V_{23} / \partial T = 2.984R$ and $\partial \psi / \partial T = 0.212R$. Equations (11) and (12) have been used to calculate the enthalpy of mixing, H_M and the entropy of mixing, S_M and have been compared to existing experimental data [25]. A comparison of the anticipated values of H_M and S_M computed at $T = 1873$ K with published data of liquid Al - Fe alloys reveals a reasonable agreement (figure 1).

The temperature-dependent fluctuation of interaction energy parameters can be written as

$$V_{ij}(T_R) = V_{ij}(T) + (T - T_R) \frac{\partial V_{ij}}{\partial T} \quad (26)$$

Here $T_R = 2073\text{K}, 2273\text{K}, 2473\text{K}$ and 2673K

Equation (26) was used to derive the interaction energy parameters at 2073K, 2273K, 2473K, and 2673K using the values of interaction energy parameters at 1873K and their temperature derivatives (figure 2). Table 1 shows the optimized values of interaction parameters at elevated temperatures.

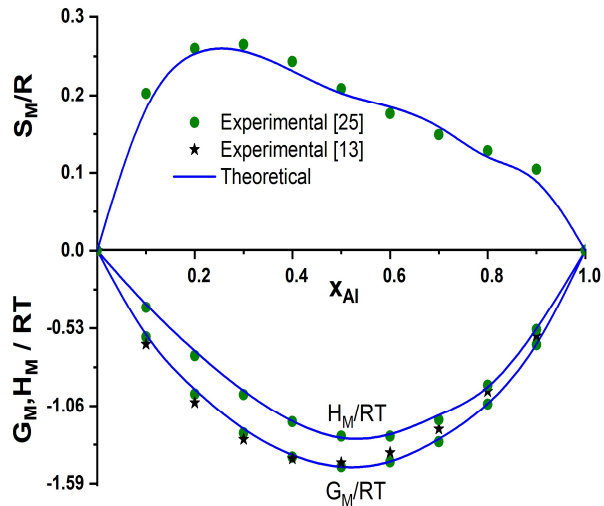


Figure 1. Gibb’s free mixing energy (G_M/RT), heat of mixing (H_M/RT) and entropy of mixing (S_M/R) vs. concentration of aluminum (x_{Al}) in the liquid Al - Fe alloy at 1873K.

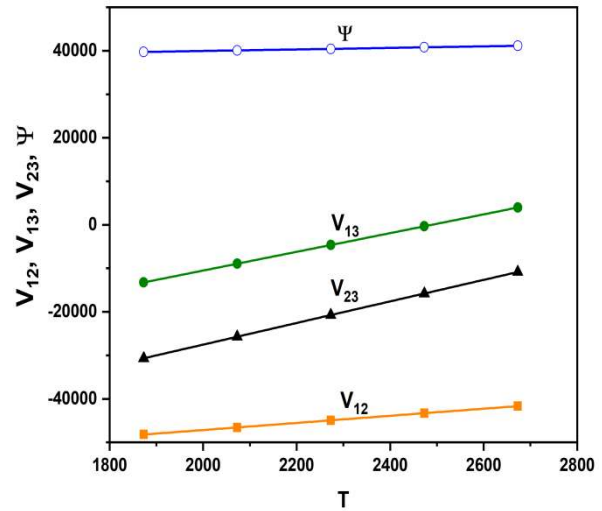


Figure 2. Temperature (T) effects on the interaction parameters (V_{ij} and ψ)

Table 1. Temperature-dependent optimization of the interaction energy parameters.

Parameter/ T	2073K	2273K	2473K	2673K
V_{12}/RT	-2.702	-2.378	-2.106	-1.875
V_{13}/RT	-0.519	-0.245	-0.016	0.179
V_{23}/RT	-1.492	-1.098	-0.768	-0.487
ψ/RT	2.326	2.140	1.984	1.852

The linear fit $V_{ij}(T) = a + bT$ for the temperature dependence of interaction energy parameters is excellent. Table 2 summarizes the a and b values for interaction parameters.

Table 2. Coefficient’s values for linear fit of interaction parameters.

Coefficients	V_{12}	V_{13}	V_{23}	ψ
a (Joule)	-63456.4	-53599.2	-77144.3	36438.8
b (Joule K^{-1})	8.14772	21.5416	24.8090	1.76257

Equation (6) is used to obtain the variation of G_M with temperature using these interaction parameters at various temperatures (figure 3). When temperature rises from 1873K to 2673K, the maximum value of G_M/RT at equiatomic composition increases from -1.4770 to -1.0947, indicating a phase separation tendency at higher temperatures.

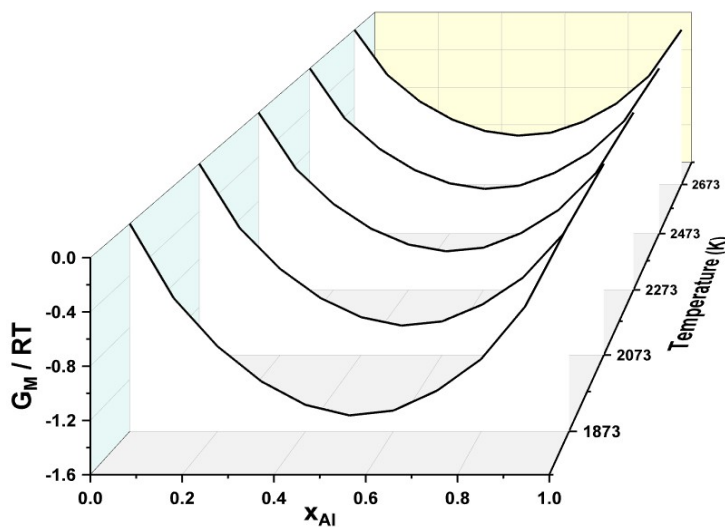


Figure 3. Temperature effects on G_M / RT with respect to bulk composition of Al.

3.2 Structural Properties

Concentration fluctuations in the long-wavelength limit, $S_{cc}(0)$, and chemical short-range order parameter, α_1 , as functions of bulk concentration, have been used to investigate the ordering processes in the Al - Fe liquid phase. Equations (14) and (16) are used to derive the $S_{cc}(0)$ values and the values that characterize ideal mixing $S_{cc}^{id}(0)$ in weak approximation. Figure 4 plots these values along with the observed values from equation (15) using activity data. At $x_c=0.5$, the largest difference between theoretical and ideal concentration fluctuations in the long-wavelength limit is 0.1519. This means that x_c is the concentration at which the chemical can form [28]. As can be observed, $S_{cc}(0)$ is lower than $S_{cc}^{id}(0)$, showing that chemical order exists across the whole concentration range. With increasing temperature, the value of $S_{cc}(0)$ decreases, reducing the gap between ideal and theoretical values, indicating the tendency of similar atom pairing, leading to homo co-ordination (figure 5). As the temperature rises, the solution approaches its optimum state. At $T \approx 7788\text{K}$, the regular solution becomes fully ideal, and $S_{cc}(0)$ is defined by the equation (16). The negative values of the Warren–Cowley parameter, α_1 over the whole concentration range support this conclusion (figure 4). The phase separating tendency is supported by the variation of α_1 with temperature, as evidenced by the variation of free energy of mixing with temperature.

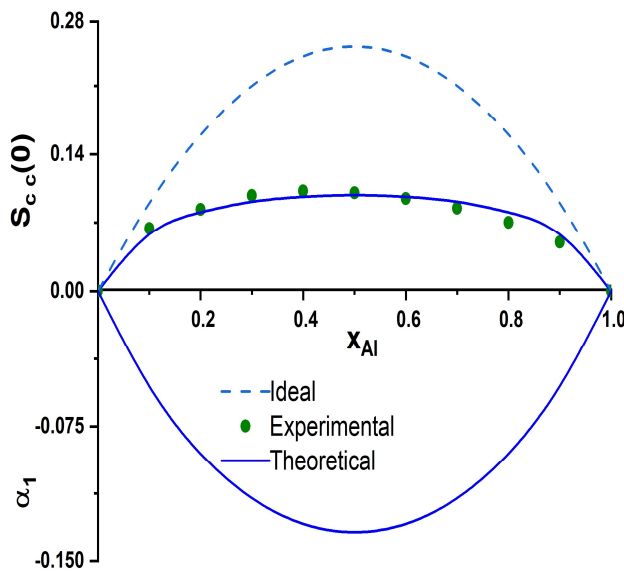


Figure 4. Concentration fluctuation at long wavelength limit ($S_{cc}(0)$) and chemical short range order (α_1) vs. concentration of aluminum (x_{Al}) in the liquid Al - Fe alloy at 1873K

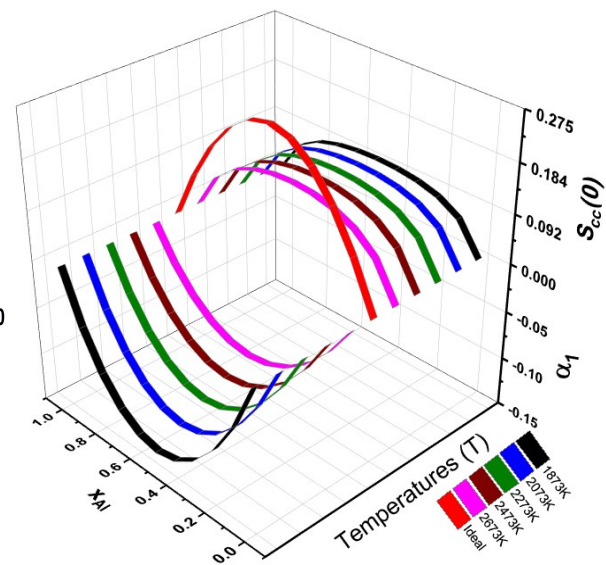


Figure 5. Temperature effects on $S_{cc}(0)$ and chemical short range order (α_1) of liquid Al - Fe alloy with respect to bulk composition of Al.

3.3 Transport Properties

The viscosities of the constituent elements, η_{i0} and the related activation energies at a fixed temperature were obtained from the literature [32]. Equation (21) is used to optimize these values for the temperature of research. Equation (20) is then used to calculate the viscosity of the liquid Al - Fe alloy at 1873K. Figure 6 depicts the viscosity's compositional dependence as well as the ideal value. Over the whole compositional range, the obtained viscosities are higher than ideal values. Up to $x_{Al} = 0.4$, the positive departure from ideality grows at which the deviation is maximum ($= 0.001866$) but sharply decreases below $x_{Al} = 0.7$. The plot of η at different temperature with respect to x_{Al} (figure 7.) shows that there is decreasing tendency of η as temperature increases.

At the fundamental level, the mixing tendency of the liquid alloy is investigated by determining the ratio of mutual and intrinsic diffusion coefficients (D_M/D_{id}). $D_M/D_{id} > 1$ denotes the likelihood of compound formation; $D_M/D_{id} < 1$ denotes phase separation; and $D_M/D_{id} = 1$ denotes the solution's ideality. The values of D_M/D_{id} are found to be positive and greater than unity throughout the compositions using equation (19) (figure 6). At the equiatomic composition, the maximum value ($=2.5475$) occurs. The theoretical examination of the presence of chemical order in the liquid state of Al-Fe alloy at 1873 K is now even clearer. Figure 8 shows that when the temperature raises, the amount of D_M/D_{id} decreases. The maximum difference ($=0.6098$) in D_M/D_{id} values for the temperatures 2673K and 1873K at equiatomic composition, $x_{Al} = 0.5$ again support high ordering tendency at that composition.

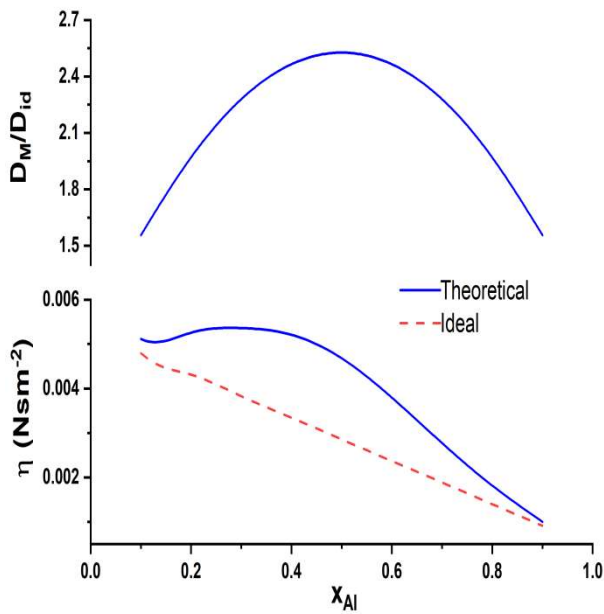


Figure 6. The mutual-to-intrinsic diffusion coefficient ratio (D_M/D_{id}) and viscosity (η) vs. concentration of aluminum (x_{Al}) in the liquid Al - Fe alloy at 1873K.

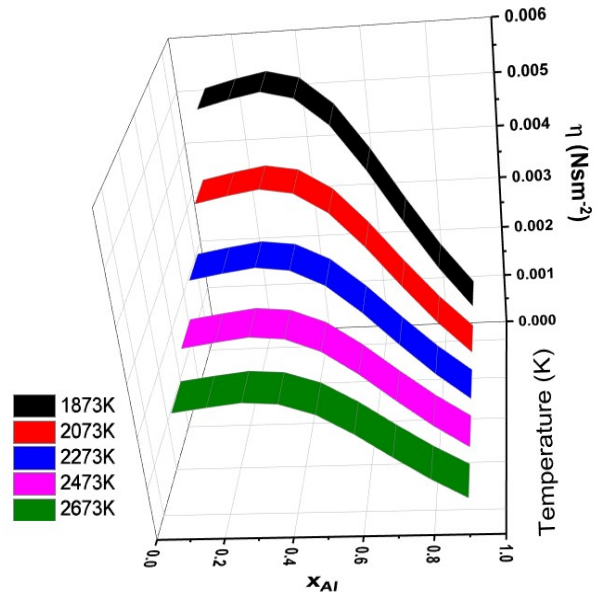


Figure 7. Temperature effects on viscosity (η) of liquid Al - Fe alloy with respect to bulk composition of Al.

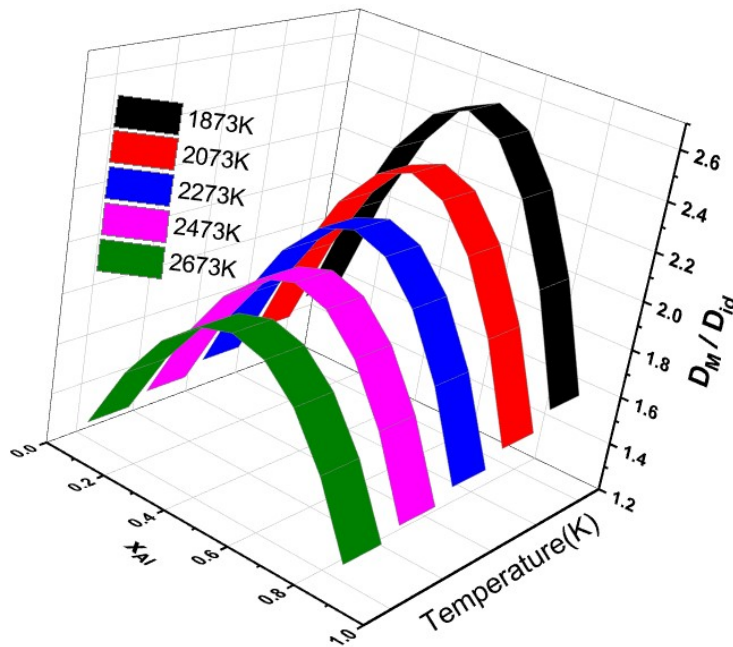


Figure 8. Temperature effects on the mutual-to-intrinsic diffusion coefficient ratio (D_M/D_{id}) of liquid Al - Fe alloy with respect to bulk composition of Al.

3.4 Surface Properties

The Prasad model [16,17] was used to compute the surface composition, x_{Al}^s , and surface tension, τ , of liquid Al₂Fe alloy as functions of bulk composition at various temperatures (T = 1873K, 2073K, 2273K, and 2473K). The surface composition values, x_{Al}^s , with regard to bulk concentration of Al, have been numerically solved using the expression derived by subtracting equation (23) from equation (22) (figure 9). Aluminum surface concentration in Al-Fe alloys is observed to rise as the bulk concentration of Al increases. The surface composition of Al deviates from ideality in a positive way. The surface compositions vs. concentration values were then utilized in the same equations to calculate the surface tension (figure 9). The same interaction energy parameters, surface coordination fractions ($p = 0.5$ and $q = 0.25$), mean atomic surface area, and surface tension data of pure components are used in both sets of equations (equations 24-25). The surface tensions of pure components at given temperatures, as well as the essential inputs for calculating mean atomic surface area and pure component element densities at fixed temperatures, were obtained from the literature [32]. Using the following formulas, these values have been evaluated at working temperature (T).

$$\rho_i(T) = \rho_i^0 + (T - T_i^0)\Delta\rho_i \tag{27}$$

$$\tau_i(T) = \tau_i^0 + (T - T_i^0)\Delta\tau_i \tag{28}$$

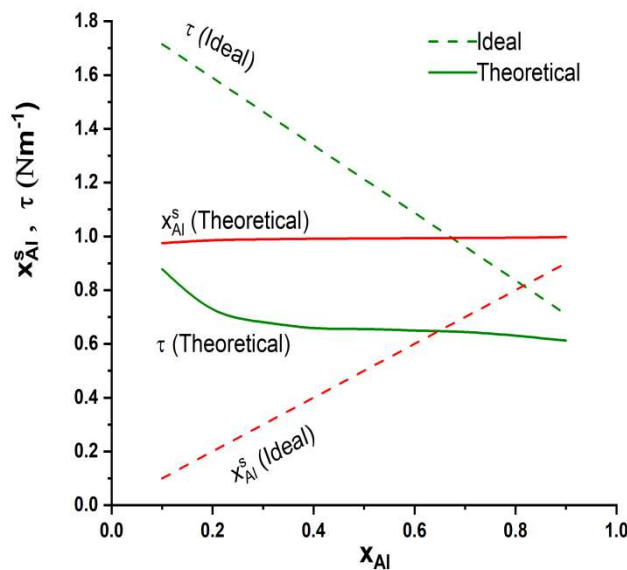


Figure 9. Surface concentration of aluminum (x_{Al}^s) and surface tension (τ) vs. bulk concentration of aluminum (x_{Al}) in the liquid Al - Fe alloy at 1873K.

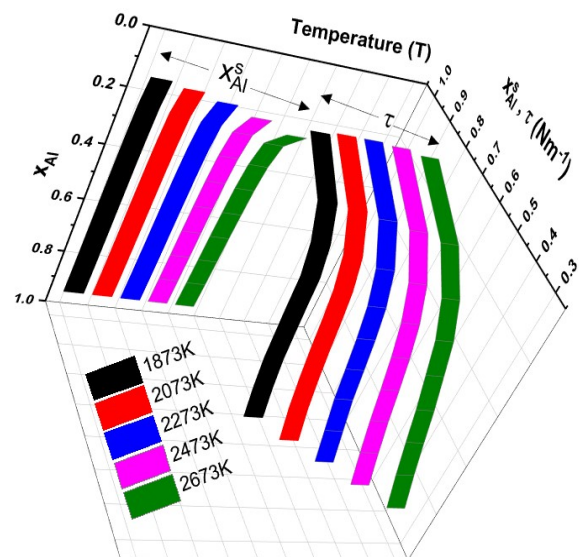


Figure 10. Compositional dependence of surface concentration of aluminum (x_{Al}^s) and surface tension (τ) in liquid Al - Fe alloy at different temperatures.

For the component metals of the alloys, $\Delta\rho_i$ and $\Delta\tau_i$ denote temperature coefficient of density and surface tension, respectively. Figure 10 shows the estimated surface concentration values for molten Al - Fe alloys at 1873 K and various temperatures. With increasing temperature, the surface concentration likewise decreases. The decreasing tendency of surface concentration with rise in temperature from 1873K to 2673K is maximum (=0.1310) at $x_{Al} = 0.1$ and minimum (=0.0060) at $x_{Al} = 0.9$. This implies the decreasing tendency of surface composition with respect to temperature, increases with decrease in bulk composition x_{Al} .

Furthermore, as shown in figure 9, the surface tension isotherm derived by the CFM for the regular solution deviates negatively from that calculated by the ideal solution model ($\tau_{ideal} = \tau_{Al}x_{Al} + \tau_{Fe}x_{Fe}$) with regard to surface composition of Al. This strongly suggests that liquid alloys with negative excess Gibbs energy in the bulk have negative surface tension departures from their ideal solution [34]. Figure 10 shows the surface tensions of Al-Fe alloys as a function of Al content at various temperatures. The surface tension of the alloy has been found to decrease as the temperature rises. At temperatures ranging from 1873K to 2673K, the difference in surface tension values is greatest (=0.2732) at $x_{Al} = 0.9$ and smallest (=0.0217) at $x_{Al} = 0.1$. This means that as the bulk composition of Al increases, $\tau_{2673K} - \tau_{1873K}$ increases as well.

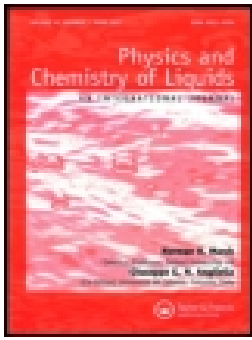
4. CONCLUSIONS

Different theoretical models have proven effective in explaining the thermodynamic, microscopic, transport, and surface characteristics of Al-Fe alloys. At all concentrations, the theoretical study of thermodynamic characteristics reveals a propensity for dissimilar atom pairing or ordering in liquid Al - Fe alloys. The energy parameters are found to be negative, suggesting that the component elements are attracted to one other. The interaction parameters are also discovered to be temperature dependent and concentration independent. With the exception of the formation energy parameter, the negativity of the rest of the interaction parameter diminishes as temperature increases. At all temperatures investigated, symmetry is seen in the free energy of mixing and the heat of mixing. For entropy of mixing, however, asymmetry is found about $x_{Al}=0.2$. The CSRO and concentration fluctuation studies reveal that there is a propensity for hetero co-ordination in liquid Al - Fe alloy. Viscosity isotherms show a positive divergence from Rault's law. At all compositions, the ratio of diffusion coefficients, $D_M / D_{id} > 1$, shows that there is a tendency for complex formation across the entire range of concentrations. The surface tension of the liquid alloy decreases as the bulk concentration of Al in the alloy increases at all temperatures studied. The surface tension of the Al-Fe alloy is found to be less than that of ideal solution. In the setting of varying temperatures, as the temperature of the investigation rises, it falls. Metals with lower surface tension tend to segregate on the surface of molten alloys, according to this research. The compound formation propensity of Al - Fe liquid alloy diminishes as temperature increases, according to temperature variation researches of all characteristics.

REFERENCES

- [1]. Srivastava S and Mohan S 2011 *Tribol. Ind.* **33** 128
- [2]. Bel'tyukov A L, Menshikova S G and Lad'yanov V I 2015 *J. Non. Cryst. Solids.* **410** 1. DOI: 10.1016/j.jnoncrysol.2014.11.028.
- [3]. Il'inskii A, Slyusarenko S, Slukhovskii O, Kaban I and Hoyer W 2002 *Mater. Sci. Eng. A.* **325** 98. DOI: 10.1016/S0921-5093(01)01457-5
- [4]. Audebert F 2005 *Prop. Appl. Nanocrystalline Alloy. from Amorph. Precursors.* 301. DOI: 10.1007/1-4020-2965-9_27.
- [5]. Dobromyslov A V and Taluts N I 2017 *Phys. Met. Metallogr.* **118** 564. DOI: 10.1134/S0031918X17060023.
- [6]. Cotton J D and Kaufman M J 1991 *Metall. Trans. A.* **22** 927. DOI: 10.1007/BF02659002.
- [7]. Egrý I, Brillo J, Holland-Moritz D and Plevachuk Y 2008 *Mater. Sci. Eng. A.* **495** 14. DOI: 10.1016/j.msea.2007.07.104.
- [8]. Rosas G, Esparza R, Bedolla-Jacuinde A and Pérez R 2009 *J. Mater. Eng. Perform.* **18** 57. DOI: 10.1007/s11665-008-9254-0.
- [9]. Xue Y, Shen R, Ni S, Song M and Xiao D 2015 *J. Alloys Compd.* **618**) 537. DOI: 10.1016/j.jallcom.2014.09.009.
- [10]. Cubero-Sesin J M and Horita Z 2012 *Metall. Mater. Trans. A Phys. Metall. Mater. Sci.* **43**

5182. DOI: 10.1007/s11661-012-1341-z.
- [11]. Singh R N 1987 *Can. J. Phys.* **65** 309. DOI: 10.1139/p87-038.
- [12]. Akinlade O, Singh R N and Sommer F 2000 *J. Alloys Compd.* **299** 163. DOI: 10.1016/S0925-8388(99)00682-9.
- [13]. Hultgren R, Desai P D, Hawkins D T, Gleiser M and Kelley K K 1973 *Selected values of the thermodynamic properties of the elements* National Standard Reference Data System
- [14]. Bhatia A B and Hargrove W H 1974 *Phys. Rev. B.* **10** 3186. DOI: 10.1103/PhysRevB.10.3186
- [15]. Moelwyn-Hughes E A. 1967 *A short course of physical chemistry* American Elsevier Publishing Company
- [16]. Prasad L C and Singh R N 1991 *Phys. Rev. B.* **44** 768. DOI: 10.1103/PhysRevB.44.13768
- [17]. Prasad L C, Singh R N, Singh V N and Singh G P 1998 *J. Phys. Chem. B.* **102** 921. DOI: 10.1021/jp9710421.
- [18]. Adhikari D, Singh B P, Jha I S and Singh B K 2011 *J. Non. Cryst. Solids.* **357** 2892. DOI: 10.1016/j.jnoncrysol.2011.03.029.
- [19]. Anusionwu B C 2003 *J. Alloys Compd.* **359** 172. DOI: 10.1016/S0925-8388(03)00213-5
- [20]. Awe O E 2019 *Phys. Chem. Liq.* **57** 296. DOI: 10.1080/00319104.2018.1443453.
- [21]. Jha I S, Koirala I, Singh B P and Adhikari D 2014 *Appl. Phys. A.* **116** (2014) 1517. DOI: 10.1007/s00339-014-8282-x
- [22]. Koirala I, Jha I S, Singh B P and Adhikari D 2013 *Phys. B Condens. Matter.* **423** 49. DOI: 10.1016/j.physb.2013.04.051.
- [23]. Novakovic R, Giuranno D, Ricci E, Delsante S, Li D and Borzone G 2011 *Surf. Sci.* **605** 248. DOI: 10.1016/j.susc.2010.10.026.
- [24]. Singh B P, Koirala I, Jha I S and Adhikari D 2014 *Phys. Chem. Liq.* **52** 457. DOI: 10.1080/00319104.2013.871668.
- [25]. Desai P D 1987 *J. Phys. Chem. Ref. Data.* **16** 109. DOI: 10.1063/1.555788.
- [26]. Guggenheim E A 1952 *Mixtures: The theory of The Equilibrium Properties of Some Simple Classes of Mixture Solutions and Alloys.* Clarendon Press
- [27]. Longuet-Higgins H C 1951 *Proc. R. Soc. London. Ser. A. Math. Phys. Sci.* **205** 247. DOI: 10.1098/rspa.1951.0028.
- [28]. Bhatia A B and Thornton D E 1970 *Phys. Rev. B.* **2** 3004. DOI: 10.1103/PhysRevB.2.3004.
- [29]. Warren B E 1990 *X-ray diffraction* New York Dover Publication
- [30]. Cowley J M 1950 *Phys. Rev.* **77** 669. DOI: 10.1103/PhysRev.77.669.
- [31]. Darken L S, Gurry R W and Bever M B 1953 *Physical chemistry of metals* McGraw-Hill.
- [32]. Brandes E A, Brook G B 1998 *Smithells metals reference book.* Oxford ; Boston: Butterworth-Heinemann 7
- [33]. Butler J A V *R. Soc. A.* 348. DOI: 10.1098/rspa.1983.0054.
- [34]. Westbrook J H and Fleischer R L 1995. *Intermetallic compounds: principles and practice.* Chichester New York Wiley 3 p



Temperature-Dependent Mixing behaviours of Bi - Mg Liquid Alloys

I. B. Bhandari , I. Koirala & D. Adhikari

To cite this article: I. B. Bhandari , I. Koirala & D. Adhikari (2020): Temperature-Dependent Mixing behaviours of Bi -Mg Liquid Alloys, Physics and Chemistry of Liquids, DOI: [10.1080/00319104.2020.1863402](https://doi.org/10.1080/00319104.2020.1863402)

To link to this article: <https://doi.org/10.1080/00319104.2020.1863402>



Published online: 24 Dec 2020.



Submit your article to this journal [↗](#)



View related articles [↗](#)



View Crossmark data [↗](#)



Temperature-Dependent Mixing behaviours of Bi -Mg Liquid Alloys

I. B. Bhandari^{a,b}, I. Koirala^a and D. Adhikari ^c

^aCentral Department of Physics, Tribhuvan University, Kirtipur, Nepal; ^bDepartment of Applied Sciences, Institute of Engineering, Tribhuvan University, Kathmandu, Nepal; ^cDepartment of Physics, M.M.A.M.C., Tribhuvan University, Biratnagar, Nepal

ABSTRACT

Bi – Mg is a strongly interacting system (the free energy of mixing $G_M > 3$ RT at equiatomic composition), the compositional dependence of the thermodynamic properties (free energy of mixing, heat of mixing and entropy of mixing) exhibits asymmetric behaviour about equiatomic composition and are in well agreement with experimental data literature. Such an interesting feature is explained here through complex formation model on the basis that a complex of the form Bi_2Mg_3 exists in the bulk phase. Its energetics is used to investigate the structural properties (concentration fluctuation in long wavelength limit and chemical short-range order parameter) and the transport property (ratio of mutual diffusion coefficient to intrinsic diffusion coefficient). The mixing behaviour of Bi – Mg system is further explored through the study of coefficient of viscosity, surface composition and surface tension. Our study indicates that the surface is enormously rich with Bismuth concentrations throughout the composition of the alloys.

ARTICLE HISTORY

Received 3 November 2020
Accepted 9 December 2020

KEYWORDS

Surface properties; strong interaction; deviation; mixing behaviour

1. Introduction

A number of researchers have employed different theoretical models [1–8] to study the thermodynamic properties of binary liquid alloys. The departure of the properties from ideal mixing is described in terms of interaction parameters. On the basis of deviation of their properties from the ideal properties the alloys can be classified as compound forming (unlike atoms pairing) or segregating (like atoms pairing). In thermodynamic properties this departure induces asymmetry away from the equiatomic composition. The asymmetry of binary alloy's thermodynamic properties is primarily related to the size effects and disparity in electronegativity of constituent elements [4]. One of the fundamental benefits of using such a thermodynamic model is that it can be easily applied to study structural properties (concentration fluctuation in long wavelength limit, $S_{cc}(0)$ [3] and chemical short-range order parameter, α_1 [9]), diffusion coefficients [10], surface tension and surface composition [11].

Bi-Mg system is interesting from a theoretical point of view, since the system exhibits the formation of stable intermetallic compound Bi_2Mg_3 [3,12]. System which forms compounds shows negative deviation from Raoult's law. The deviation ought to be larger; more stable is the intermetallic compounds. A strong tendency to short-range-ordering in the liquid occurs in binary systems in which the electro-negativities of the components are very different. In the liquid solutions of Bi- Mg, a maximum ordering has been observed at the stoichiometric composition (i.e. the composition corresponding to the ratio of chemical valences of the components). Evidence

for this ordering has come from thermodynamic studies as well as from the microscopic, transport and surface properties. Liquid Bi- Mg solutions exhibit a strong ordering tendency in the liquid solutions at Bi_2Mg_3 compositions.

Liquid Bi_2Mg_3 is one of the classical examples of a liquid semiconductor having-conductivity up to $45 \Omega^{-1}\text{cm}^{-1}$. Binary Bi-Mg system is also interesting systems for high-temperature Mg alloys. Magnesium alloys currently gained a great deal of interest in the automotive and aeronautical industries because of their low density relative to aluminium and steel alloy.

Alloying elements such as Sn, Si, Sb and Bi are being considered in order to produce new Mg alloys for high-temperature applications [13,14]. The Bi-Mg alloy also has an interesting application as phase change materials for thermal energy storage [15]. The thermodynamics of Bi-Mg binary system was also explored by using associate model integrated with substitutional model [16]. The authors described α - Bi_2Mg_3 phase and β - Bi_2Mg_3 with their crystal structure and critically evaluated the phase diagram of Bi-Mg binary system.

The thermodynamic (Free energy of mixing) and microscopic properties (concentration fluctuation in long wavelength limit) of the liquid Bi- Mg system showing very strong ordering tendency, are successfully explained using the complex formation model [3]. To the best of our knowledge, for the first time, in this paper, we have extended the model for the investigation of enthalpy of mixing, entropy of mixing, chemical short-range order parameter and the diffusion coefficients. The surface properties are explored through Butlers equation [17] and the transport properties like viscosity have been investigated through Molewyman – Hughes equation [18].

The layout of our paper is as follows: in the first part of the next section, we present the basic formalism used in the complex formation model. In the second part, we present results and discussions on G_M . In the second part of Section 3 we present results and discussions on surface properties, concentration fluctuations in the long-wavelength limit, $S_{cc}(0)$, and the Warren–Cowley short-range order parameter, α_1 , in addition, we make a comparative study of experimental vs. theoretical H_M , S_M and $S_{cc}(0)$ values, where they exist. In the last part of Section 3 we present the discussion of the results for transport phenomena, essentially, for diffusion coefficient and viscosity. We end the paper with a summary of concluding remarks.

2. Formalism

2.1 Thermodynamic properties

The complex formation model has been implemented to Bi-Mg compound-forming alloys to explain their mixing behaviour with regard to the Bi_2Mg_3 intermediate phase which is observed as energetically favoured [12]. In this framework the Bi – Mg alloy is anticipated to be ternary mixture of three species; Bi atoms, Mg atoms and chemical complex Bi_2Mg_3 , all in chemical equilibrium with another. Since the strong interactions in the mixture are incorporated through the formation of complexes, ternary mixture constituents can be considered to interact poorly with one another. The Gibbs free energy of the binary mixture, G_M , can be expressed as [3]

$$G_M = -x_3w + G' \quad (1)$$

In Equation (1), the first term $-x_3w$ stands for free energy diminution due to formation of complex Bi_2Mg_3 ; w is the formation energy of complex, G' is the Gibbs free energy of mixing of the ternary mixture of Bi, Mg and Bi_2Mg_3 , expressed as

$$G' = RT \sum_{i=1}^3 x_i \ln \left(\frac{x_i}{x} \right) + \sum V_{ij} \left(\frac{x_i x_j}{x} \right) \quad (2)$$

Let the binary alloy contain respectively c atoms of Bi atoms and $(1 - c)$ atoms of Mg atoms, c being the atomic fraction of the Bi atoms. We are assuming that only one kind of Bi_2Mg_3 chemical

complex is formed. If there are x_1 g moles of Bi atoms, x_2 g moles of Mg atoms and x_3 g moles of Bi_2Mg_3 complexes in the ternary mixture, then we have from conservation of atoms

$$x_1 = c - px_3, x_2 = (1 - c) - qx_3 \text{ and } x = x_1 + x_2 + x_3 = 1 - (p + q - 1)x_3 \quad (3)$$

Where p and q are small integers determined from the stoichiometry of energetically favoured compound. From Equations (1) and (2), the Gibbs energy of mixing, G_M , for compound forming binary alloys becomes:

$$G_M = -x_3w + RT \sum_{i=1}^3 x_i \ln\left(\frac{x_i}{x}\right) + \sum V_{ij}\left(\frac{x_i x_j}{x}\right) \quad (4)$$

The other thermodynamic functions can be obtained [3,9], using the standard thermodynamic relationship and after some algebra. The heat of mixing(H_M)and entropy of mixing(S_M)can be expressed as

$$H_M = -x_3 \left[w - T \left(\frac{\partial w}{\partial T} \right) \right] + \sum_{i < j} \sum \left(\frac{x_i x_j}{x} \right) \left[V_{ij} - T \left(\frac{\partial V_{ij}}{\partial T} \right) \right] \quad (5)$$

$$S_M = x_3 \frac{\partial w}{\partial T} - R \sum_{i=1}^3 x_i \ln \frac{x_i}{x} - \sum_{i < j} \sum \left(\frac{x_i x_j}{x} \right) \frac{\partial V_{ij}}{\partial T} \quad (6)$$

The value of x_3 can be calculated at a given pressure and temperature from the equilibrium state of free mixing energy, G_M , as

$$\left(\frac{\partial G_M}{\partial x_3} \right)_{T,P,c} = 0 \quad (7)$$

Keeping in mind Equation (3) and combining Equations (4) and (7) one gets

$$(x_3 x^{p+q-1} x_1^{-p} x_2^{-q})^{-1} = \exp\left(\psi - \frac{w}{RT}\right) \quad (8)$$

Where

$$\begin{aligned} \psi = & \left[(p + q - 1) \frac{x_1 x_2}{x^2} - p \frac{x_2}{x} - q \frac{x_1}{x} \right] \frac{V_{12}}{RT} + \left[(p + q - 1) \frac{x_2 x_3}{x^2} - q \frac{x_3}{x} + \frac{x_2}{x} \right] \frac{V_{23}}{RT} + \\ & \left[(p + q - 1) \frac{x_1 x_3}{x^2} - p \frac{x_3}{x} + \frac{x_1}{x} \right] \frac{V_{13}}{RT} \end{aligned} \quad (9)$$

Centred on the assumption of a monatomic surface layer, Butler's method [17]to evaluate surface tension, σ , of liquid solution can be expressed as.

$$\sigma = \frac{\Phi_A^s - \Phi_A^b}{\alpha_A} = \frac{\Phi_B^s - \Phi_B^b}{\alpha_B} = \dots = \frac{\Phi_i^s - \Phi_i^b}{\alpha_i} \quad (10)$$

Where Φ_i^s , Φ_i^b and α_i indicate the chemical potential of the hypothetical surface, the chemical potential of the bulk and molar surface area of pure element i respectively. Equation (10) provides the expression for surface tension in terms of partial excess free energy of mixing in bulk (G_i^b), partial excess free energy of mixing at the surface (G_i^s), bulk concentration (c) and surface concentration (c^s) as

$$\sigma = \sigma_A + \frac{G_A^s - G_A^b}{\alpha_A} + \frac{RT}{\alpha_A} \ln\left(\frac{c^s}{c}\right) = \sigma_B + \frac{G_B^s - G_B^b}{\alpha_B} + \frac{RT}{\alpha_B} \ln\left(\frac{1 - c^s}{1 - c}\right) \quad (11)$$

Where σ_A and σ_B are the surface tensions of pure components A and B respectively.

The monatomic surface area for each component is

$$\alpha_i = 1.091N_A^{1/3}\Omega_i^{2/3} \quad (12)$$

Where Ω_i is the molar volume of the component i can be determined from its molar mass and density and N_A stands for Avogadro number.

The concentration fluctuations in the long-wavelength limit, $S_{cc}(0)$, indicate the preference for homo-coordination or hetero-coordination that defines the essence of mixing in liquid alloys in terms of chemical order and segregation. The concentration fluctuation at long wavelength limit is associated with free energy of mixing by the expression [19].

$$S_{cc}(0) = \left(\frac{1}{RT} \frac{\partial^2 G_M}{\partial c^2} \right)^{-1} \quad (13)$$

Theoretically computed values of $S_{cc}(0)$ can be compared with the observed values assessed from activity of constituent element at different compositions by the expression,

$$S_{cc}(0) = \frac{c_{Mg} a_{Bi}}{\left(\frac{\partial a_{Bi}}{\partial c_{Bi}} \right)_{T,P,N}} = \frac{c_{Bi} a_{Mg}}{\left(\frac{\partial a_{Mg}}{\partial c_{Mg}} \right)_{T,P,N}} \quad (14)$$

Combining Equations (4) and (12) and after some algebra one obtains:

$$S_{cc}(0) = RT \left[\sum_{i=1}^3 \left(\frac{(x'_i)^2}{x_i} - \frac{(x')^2}{x} \right) + 2x \sum_{i < j} V_{ij} \left(\frac{x_i}{x} \right)' \left(\frac{x_j}{x} \right)' \right]^{-1} \quad (15)$$

Where the prime on x denotes its first differentiation with respect to c .

In strong interaction approximation [20], the $S_{cc}(0)$ is given by

$$S_{cc}(0) = \frac{\xi}{1 + \chi\xi} \quad (16)$$

Here for $0 < c \leq c_c$

$$\xi = \frac{c}{p} [p - c(p + q - 1)][p - c(p + q)], \chi = -2 \left(\frac{V_{23}}{p^2 x^3 RT} \right) \text{ and } x = \left[1 - \frac{c}{p}(p + q - 1) \right] \quad (17)$$

and for $c \leq c_c < 1$

$$\begin{aligned} \xi &= \frac{(1-c)}{q} [q - (1-c)(p + q - 1)][q - (1-c)(p + q)], \chi = -2 \left(\frac{V_{13}}{q^2 x^3 RT} \right) \text{ and } x \\ &= \left[1 - \frac{(1-c)}{q}(p + q - 1) \right] \end{aligned} \quad (18)$$

For ideal mixture the interaction parameters become zero and Equation (14) will be reduced to

$$S_{cc}^{id}(0) = c_A c_B \quad (19)$$

In order to measure the degree of order in the liquid alloy, we can calculate the Warren-Cowley short-range order parameter (α_1) [21,22]. Experimentally, α_1 can be determined on the basis of knowledge of the concentration-concentration $S_{cc}(q)$ and the number-number structure factors, $S_{NN}(q)$. However, in most diffraction experiments, these quantities are not readily measurable. From the knowledge of nearest neighbour contacts of unlike atoms in the melt, one can simply obtain an expression [5] for α_1 . Knowledge of α_1 provides a direct insight into the nature of the local arrangement of atoms in the mixture. $\alpha_1 = 0$ corresponds to a random distribution, $\alpha_1 < 0$ refers to unlike

atoms pairing as nearest neighbours whereas $\alpha_1 > 0$ corresponds to like atoms pairing in the first coordination shell. From a simple probabilistic method it can be demonstrated that the limiting values of α_1 for equiatomic composition lie in the range $-1 \leq \alpha_1 \leq +1$. The minimum possible value of α_1 is $\alpha_{\min} = -1$ indicates complete ordering. On the other hand, the maximum value $\alpha_{\max} = +1$ implies total segregation leading to phase separation. Singh et al. [23] have recommended that α_1 can be estimated from $S_{cc}(0)$.

$$\alpha_1 = \frac{S - 1}{S(z - 1) + 1}, \quad S = \frac{S_{cc}(0)}{S_{cc}^{id}(0)} \quad (20)$$

Here z is the coordination number of the alloy. It is taken as 10 for the present calculations, and the α_1 values are estimated.

The mixing behaviour of binary melt can also be understood at microscopic level by means of viscosity. The Moelwyn – Hughes equation for viscosity of liquid alloy [18] is

$$\eta = (c_A \eta_A + c_B \eta_B) \times \left(1 - 2c_A c_B \frac{H_M}{RT} \right) \quad (21)$$

Where η_i is the viscosity of pure component i . At temperature T , it is given by [24]

$$\eta_i = \eta_{i0} \exp\left(\frac{Q}{RT}\right) \quad (22)$$

Here η_{i0} is a constant in the unit of viscosity and Q is the activation energy.

The mixing behaviour of the binary liquid alloy can even be explored at the microscopic level in terms of diffusion coefficient. The mutual diffusion coefficient (D_M) of liquid alloys can be expressed in terms of activity (a_i) and self-diffusion coefficient (D_{id}) of individual component with the help of Darken's equation [25],

$$D_M = c_i D_{id} \frac{d \ln a_i}{dc_i} \quad (23)$$

with

$$D_M = cD_B + (1 - c)D_A \quad (24)$$

Where D_A and D_B are the self-diffusion coefficients of pure components A and B respectively. The ratio of mutual diffusion coefficient (D_M) to self-diffusion coefficient (D_{id}) is also related to concentration fluctuation in long-wavelength limit ($S_{cc}(0)$) as

$$\frac{D_M}{D_{id}} = \frac{c_A c_B}{S_{cc}(0)} \quad (25)$$

3. Results and discussion

3.1 Thermodynamic properties: free energy, enthalpy and entropy of mixing

The available experimental data on the thermodynamic properties as well as phase diagram information [12] have been used for the calculation of the order energy parameters for the Bi – Mg liquid phase indicating the compositional location of an energetically favoured compound. The Bi – Mg, thus, in the liquid alloys, the preferential arrangements of Bi and Mg constituent atoms favour the formation of Bi_2Mg_3 complexes ($p=2$ and $q=3$). Keeping in mind the Bi – Mg phase diagram [12] and the presence of the liquid phase over the whole concentration range, all calculations have been done at $T = 975$ K. The data set of the Gibbs energy of mixing, G_M , of liquid Bi-Mg alloys together with the enthalpy of mixing, H_M , have been used to calculate the interaction

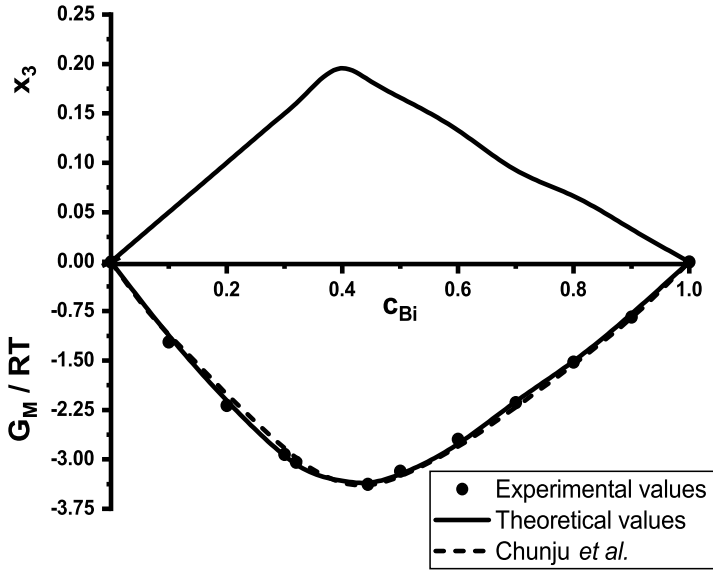


Figure 1. Number of complexes (x_3) and Free energy of mixing (G_M/RT) vs. concentration of bismuth (c_{Bi}) in the liquid Bi -Mg alloy at 975 K.

energy parameters, i.e. w , V_{12} , V_{13} and V_{23} and their temperature derivatives at $T = 975$ K. The values of the interaction energy parameters were adjusted to give the concentration dependences of G_M (Figure 1) that fit well with the corresponding thermodynamic data. The calculated interaction energy parameters for liquid Bi - Mg alloys are $V_{12} = 0$, $V_{13} = -3.32RT$, $V_{23} = -2.52RT$, $w = 16.28RT$ and remain constant in all calculations. Figure 1 shows the excellent agreement of computed free energy of mixing by the presented model with the experimental data [12] and the previous work [16].

Equations (8–9) along with Equation (3) were used to compute the number of complexes, x_3 . At the compound forming composition, $c_c = 0.4$, the concentration dependence of the equilibrium values of chemical complexes, x_3 , exhibits the maximum value of 0.1956 (Figure 1). For all compositions the mixing functions, i.e. the Gibbs free energy (Figure 1), are negative and exhibit a flat minimum of -3.3542 at the composition, $c = 0.444$ indicating strong compound forming tendency. Even at the $c_c = 0.4$ the value of G_M/RT is less than -3 (i.e. -3.3265) shows the large tendency of chemical ordering about stoichiometric composition.

The temperature-dependent energies at $T = 975$ K are $\partial V_{12}/\partial T = 2.510$ R, $\partial V_{13}/\partial T = -3.200$ R, $\partial V_{23}/\partial T = -1.400$ R and $\partial w/\partial T = 1.571$ R. The enthalpies of mixing, H_M and entropies of mixing, S_M have been evaluated by Equations (5) and (6), respectively, and compared with available experimental data [12]. The calculated enthalpies and entropies of mixing are in good agreement with experimental data, however little discrepancy is observed for observed enthalpies of mixing with literature data [16] as presented in Figure 2.

The heat of mixing (H_M/RT) shows a minimum of -2.8925 at $c_c = 0.4$. The values of H_M and S_M are found to be in poor agreement with the experiment if energy parameters are taken as being temperature independent. Therefore, we have considered the variation of these parameters with temperature to ascertain the variation of heat and entropy of formation with observed values. The variation of interaction energy parameters with temperature can be expressed as

$$V_{ij}(T_R) = V_{ij}(T) + (T - T_R) \frac{\partial V_{ij}}{\partial T} \quad (26)$$

Here $T_R = 1175$ K, 1375 K, 1575 K and 1775 K

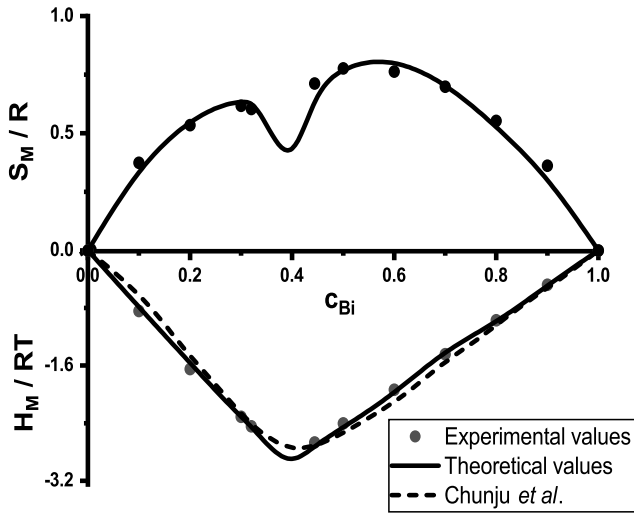


Figure 2. Heat of mixing (H_M/RT) and entropy of mixing (S_M/R) vs. concentration of bismuth (c_{Bi}) in the liquid Bi – Mg alloy at 975 K.

Now the values of interaction energy parameters at 975 K and their temperature derivatives were used in Equation (26) to obtain the interaction energy parameters at 1175 K, 1375 K, 1575 K and 1775 K. The temperature dependence of interaction energy parameters excellently follows linear fit $V_{ij} = a + bT$, a and b are constants having different values for different interaction parameters. These interaction parameters at different temperatures are used in Equation (4) to obtain the variation of G_M with temperature (Figure 3). The maximum value of G_M/RT at equiatomic composition increases from -3.3265 to -2.9228 when temperature ranges from 975 K to 1775 K showing phase separation tendency with increase in temperatures.

3.2 Surface properties: surface composition and surface tension

Surface composition, c^s , and surface tension, σ , of liquid Bi_2Mg_3 alloy have been calculated as functions of bulk composition at different temperatures ($T = 975$ K, 1175 K, 1375 K, 1575 K and

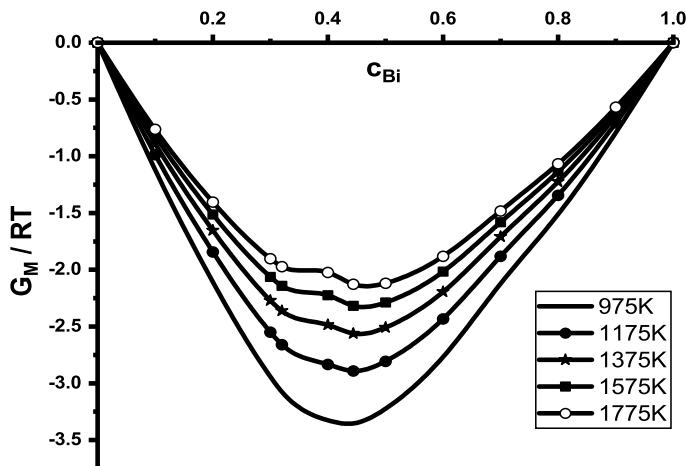


Figure 3. Compositional dependence of G_M/RT of liquid Bi – Mg alloy at different temperatures.

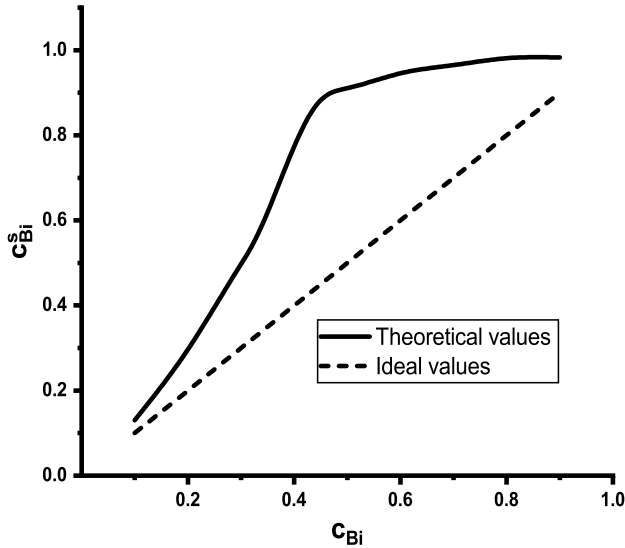


Figure 4. Surface concentration of bismuth c_{Bi}^s vs. bulk concentration of aluminium (c_{Bi}) in the liquid Bi – Mg alloy at 975 K.

1775 K), under the framework of the Butlers model [17]. Equation (11) is numerically solved, giving the surface composition values, c^s with respect to bulk concentration of Bi (Figure 4). Surface concentration of Bismuth in Bi-Mg alloys is found to increase with the increase of bulk concentration of Bi. There is positive deviation of surface composition of Bi from ideality. The values of surface composition with respect to concentration were further used in the same equations to obtain the surface tension (Figure 5). The surface tension isotherm shows an interesting behaviour. The positive deviation from ideality ($\sigma_{ideal} = c\sigma_A + (1 - c)\sigma_B$) is observed for $0 < c < 0.4$ and the negative deviation has been observed for $0.4 < c < 1$. This behaviour for surface tension of Bi_2Mg_3 melt strongly suggests that the Bi – Mg alloy has maximum stability around stoichiometric

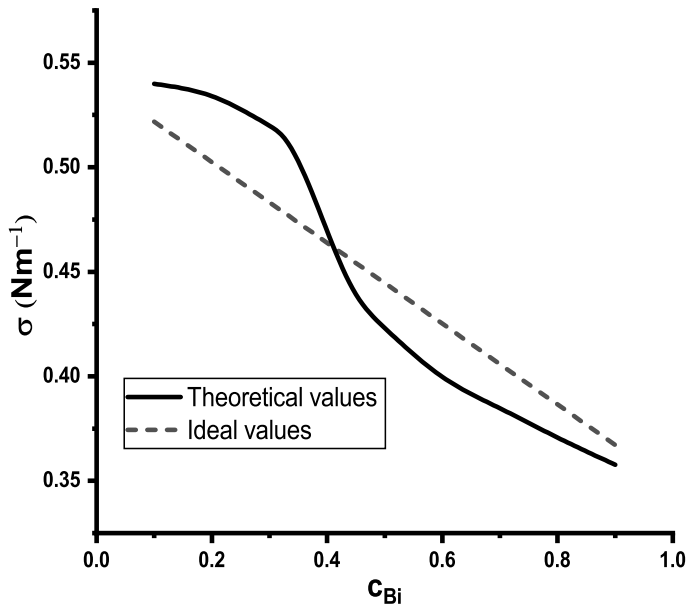


Figure 5. Surface tension (σ) vs. bulk concentration of bismuth (c_{Bi}) in the liquid Bi – Mg alloy at 975 K.

composition $c_c=0.4$. The surface tensions of pure components at fixed temperature and the necessary inputs to evaluate mean atomic surface area, the densities of pure component element at certain temperature are taken from Ref [24]. These values have been optimised at working temperature (T) by using the expressions,

$$\sigma_i(T) = \sigma_i^0 + (T - T_i^0)\Delta\sigma_i \quad (27)$$

$$\rho_i(T) = \rho_i^0 + (T - T_i^0)\Delta\rho_i \quad (28)$$

Here $\Delta\rho_i$ and $\Delta\sigma_i$ represent temperature coefficient of density and surface tension, respectively, for the component metal of the alloys. The computed values of surface concentration for molten Bi – Mg alloys at 975 K and at varying temperatures are depicted in Figure 6. The surface concentration is found to decrease with increase in temperature. The decreasing tendency of surface composition with rise in temperature from 975 K to 1775 K is maximum ($=0.366$) at $c_{Bi}=0.444$ and minimum ($=0.042$) at $c_{Bi}=0.9$. This implies the decreasing tendency of surface composition with respect to temperature, first increases with increase in bulk composition up to $c_{Bi}=0.444$ and then decreases slowly up to $c_{Bi}=0.9$.

The surface tensions of Bi-Mg alloy with respect to bulk concentration of Bi at different temperatures are plotted in Figure 7. It has been observed that the surface tension of the alloy decreases with increase in temperature showing the decreasing stability of the selected alloy with rise in temperature. The difference in surface tension values at the temperatures of 975 K to 1775 K is maximum ($=0.2609$) at $c_{Bi}=0.1$ and minimum ($=0.0576$) at $c_{Bi}=0.9$. This means $\sigma_{1775K} - \sigma_{975K}$ is found to be decreasing with increasing bulk composition of Bi.

3.3 Structural properties: concentration fluctuation in long wave length limit and Warren – Cowley parameter

The ordering phenomena in the Bi – Mg liquid phase have been analysed by concentration fluctuations in the long-wavelength limit, $S_{cc}(0)$, and chemical short-range order parameter, α_1 , as

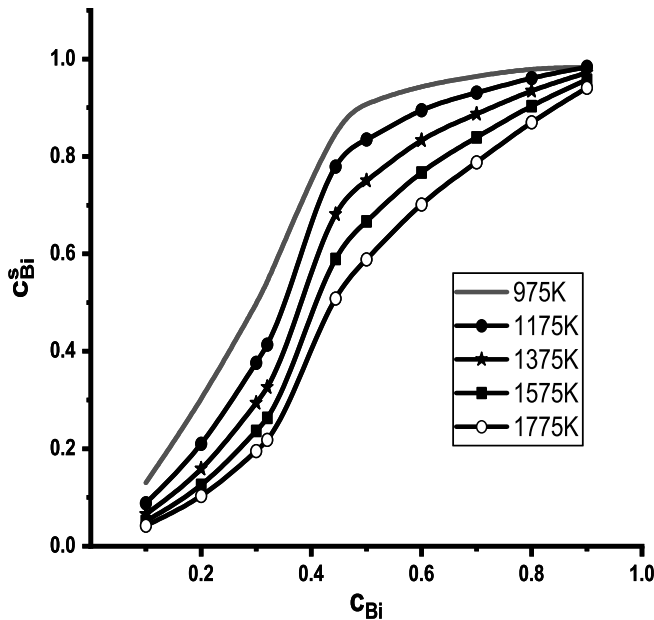


Figure 6. Compositional dependence of surface concentration of bismuth (c_{Bi}^s) in liquid Bi – Mg alloy at different temperatures.

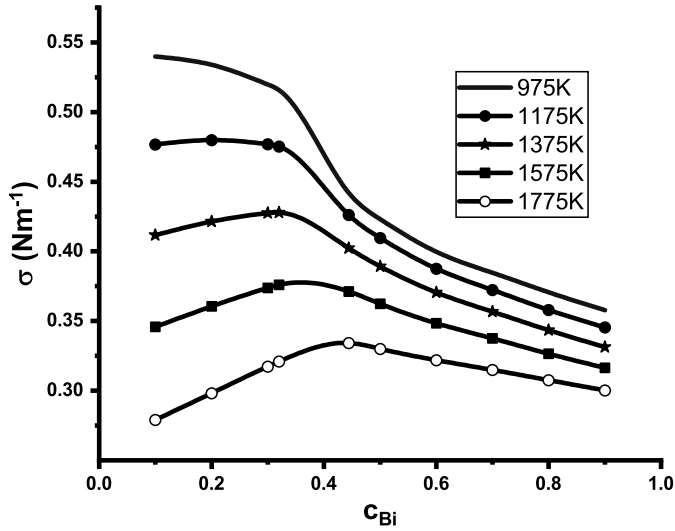


Figure 7. Compositional dependence of surface tension (σ) of Bi – Mg alloy at different temperatures.

functions of bulk composition. The $S_{cc}(0)$ values and the values that characterise ideal mixing, $S_{cc}^{id}(0)$, are calculated in strong interaction approximation by Equations (15) and (19), respectively. These values along with the observed values reproduced from Ref. [3] are plotted in Figure 8. At a given composition, for $S_{cc}(0) < S_{cc}^{id}(0)$, ordering in liquid alloy is expected and if $S_{cc}(0) > S_{cc}^{id}(0)$, there is tendency of phase separation. Our theoretical analysis shows that the deviation of $S_{cc}(0)$ from the ideal value, $S_{cc}^{id}(0)$, is maximum at stoichiometric composition, i.e. at $c_c = 0.4$. This implies that c_c is the concentration at which there is strongest tendency of compound formation [18].

This observation can be further justified by the negative values of the Warren–Cowley parameter, α_1 , over the concentration range 0.2 to 0.7 (Figure 8). The α_1 value near the stoichiometric composition is smaller than -0.6 and approaching towards -1 , strongly suggests the heterocoordinating tendency of Bi – Mg binary melt.

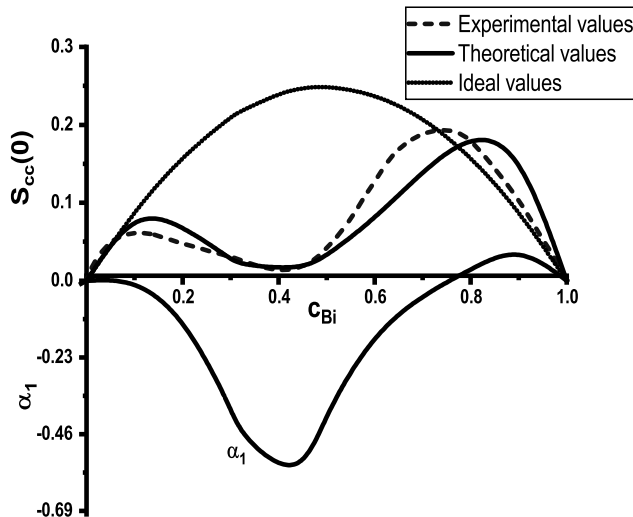


Figure 8. Concentration fluctuation at long wavelength limit ($S_{cc}(0)$) and chemical short-range order (α_1) vs. concentration of bismuth (c_{Bi}) in the liquid Bi – Mg alloy at 975 K.

3.3 Transport properties

The viscosities of constituent elements, η_{i0} , and corresponding activation energies at fixed temperature are taken from Ref [24]. These values are optimised for the temperature of investigation by using Equation (21). Using the obtained values of heat of mixing at different composition, the computation of the viscosity of the liquid Bi- Mg alloy at 975 K is then done by Equation (20). The compositional dependence of the viscosity along with the ideal value is shown in Figure 9. The viscosities obtained are greater than the ideal values over the entire compositional range. The positive deviation from ideality increases up to $c_{Bi} = 0.4$ at which the deviation is maximum (= 0.001427). The plot of η at different temperature with respect to c_{Bi} (Figure 10) shows that there is decreasing tendency of η as temperature increases and the difference, $\eta_{1775K} - \eta_{975K}$ is maximum (0.001519) around stoichiometric composition.

The mixing tendency of the liquid alloy is also studied at the microscopic level by investigating the mutual and intrinsic-diffusion coefficients. The ratio D_M/D_{id} explores the mixing behaviour of the binary components in terms of the degree of chemical ordering. $D_M/D_{id} > 1$, represents the tendency of compound formation; $D_M/D_{id} < 1$ indicates the separation of phase and $D_M/D_{id} = 1$ represents the ideality of the solution. The values of D_M/D_{id} are obtained from Equation (25) and are found to be positive and greater than one in the composition range 0.2 to 0.7 (Figure 11). The maximum value (greater than 18.33) occurs at the compound forming composition. This value is so large that this further clarifies the theoretical analysis of the presence of the strong chemical order in the liquid state of Bi-Mg alloy at 975 K.

It is also observed that the increase in temperature causes decrease in D_M/D_{id} indicating the phase separation tendency with rise in temperature. The increasing value of $S_{cc}(0)$, thereby decreasing the gap between ideal values and theoretical values with increase in temperature indicates the tendency of like atom pairing, leading towards homo co-ordination. Further increase in temperature drives the solution towards ideality. The variation of α_1 with temperature supports the phase separating tendency with larger values of temperature as shown by variation of free energy of

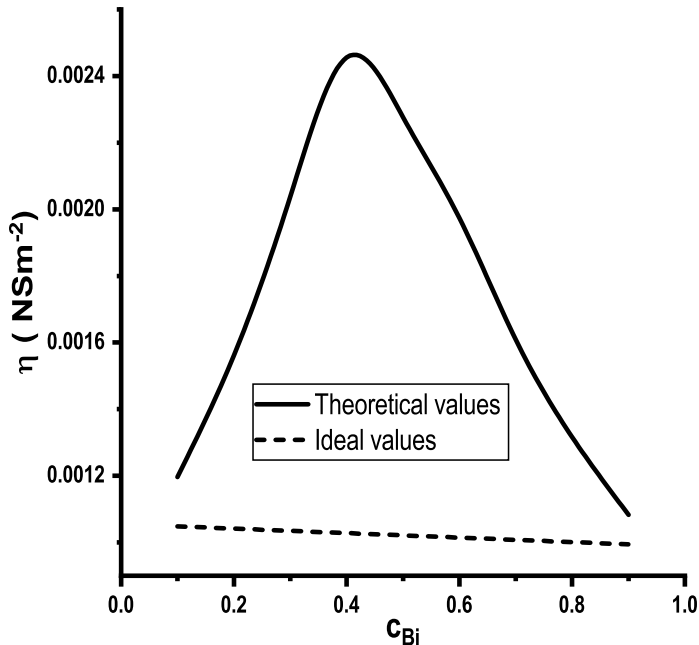


Figure 9. Viscosity (η) vs. concentration of bismuth (c_{Bi}) in the liquid Bi – Mg alloy at 975 K.

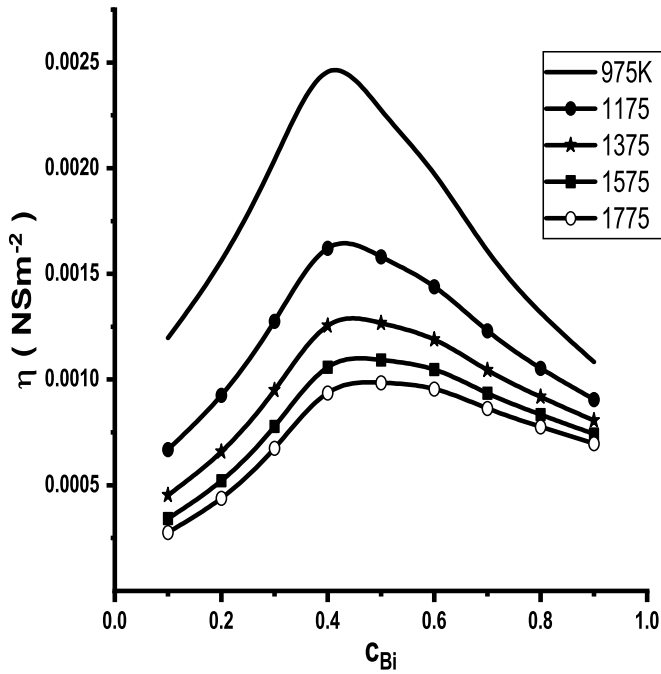


Figure 10. Compositional dependence of viscosity (η) of liquid Bi – Mg alloy at different temperatures.

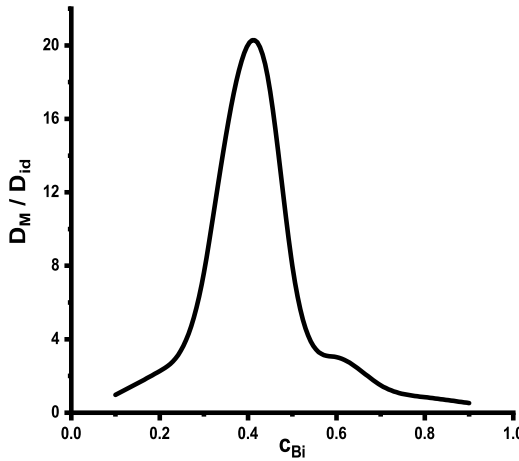


Figure 11. The ratio of mutual and intrinsic diffusion coefficients (D_M/D_{id}) vs. concentration of bismuth (c_{Bi}) of liquid Bi – Mg alloy at 975 K.

mixing with temperature. The very small change in the values of $S_{cc}(0)$, α_1 and D_M/D_{id} with increase of temperature cause the corresponding plots indistinguishable so we present here only the numerical analysis.

4. Conclusions

From the theoretical analysis following conclusion can be drawn:

- (1) The interaction parameters are found to be concentration independent and temperature dependent.
- (2) Asymmetry is observed in number of complexes, free energy of mixing, heat of mixing and entropy of mixing.
- (3) Surface concentration of Bi increases with increase in bulk concentration in all temperature of study, i.e. 975 K, 1175 K, 1375 K, 1575 K and 1775 K. And, with compare to temperature of study, it decreases as temperature of investigation increases.
- (4) At all temperature of investigation, the surface tension decreases with the increase in bulk concentration of Bi. The surface tension decreases with increase in temperature.
- (5) The concentration fluctuation in long wavelength limit is minimum and very small than ideal value at stoichiometric composition suggesting the strong tendency of compound formation at that composition.
- (6) The Warren – Cowley short-range order parameter has negative values at almost compositions. This also supports the strong interaction in the selected binary system.
- (7) The ratio of diffusion coefficients, $D_M/D_{id} > 1$ at almost compositions, which indicate that there is tendency of hetero co-ordination.
- (8) Positive deviation of viscosity isotherms from linear law is observed. The viscosity decreases with increase in temperature.
- (9) The temperature variation investigations of all the properties reveal that the compound forming tendency of Bi-Mg liquid alloy decreases as temperature increases.

Disclosure statement

No potential conflict of interest was reported by the authors.

ORCID

D. Adhikari  <http://orcid.org/0000-0002-6022-3615>

References

- [1] Koirala I, Jha IS, Singh BP, et al. Thermodynamic, transport and surface properties in In-Pb liquid alloys. *Phys B Condens Matter*. 2013;423:49–53.
- [2] Awe OE. Thermodynamic investigation of thermophysical properties of thallium-based liquid alloys. *Phys Chem Liq*. 2019;57:296–310.
- [3] Bhatia AB, Hargrove WH. Concentration fluctuations and thermodynamic properties of some compound forming binary molten systems. *Phys Rev B*. 1974;10:3186–3196.
- [4] Akinlade O, Singh RN, Sommer F. Thermodynamics of liquid Al-Fe alloys. *J Alloys Compd*. 2000;299:163–168.
- [5] Bhatia AB, Singh RN, Quasi-lattice A. Theory for compound forming molten alloys. *Phys Chem Liq*. 1984;13:177–190.
- [6] Novakovic R, Ricci E, Gnecco F. Surface and transport properties of Au – in liquid alloys. *Surf Sci*. 2006;600:5051–5061.
- [7] Jha IS, Koirala I, Singh BP, et al. Concentration dependence of thermodynamic, transport and surface properties in Ag–Cu liquid alloys. *Appl Phys A*. 2014. DOI:10.1007/s00339-014-8282-x
- [8] Adhikari D, Jha IS, Singh BP. Thermodynamic and microscopic structure of liquid Cu-Sn alloys. *Phys B Condens Matter*. 2010;405:1861–1865.
- [9] Koirala I, Singh BP, Jha IS. Theoretical assessment on segregating nature of liquid In–Tl alloys. *J Non Cryst Solids*. 2014;398:26–31.
- [10] Singh BP, Koirala I, Jha IS, et al. The segregating nature of Cd-Pb liquid binary alloys. *Phys Chem Liq*. 2014;52:457–470.
- [11] Prasad LC, Singh RN. Surface segregation and concentration fluctuation at the liquid-vapor interface of molten Cu-Ni alloys. *Phys Rev B*. 1991;44:768–771.
- [12] Hultgren R, Desai PD, Hawkins DT, et al. Selected values of the thermodynamic properties of binary alloys. Metal Park, Ohio: American Society for Metals; 1973.

- [13] Jung I-H, Kang D-H, Park W-J, et al. Thermodynamic modeling of the Mg-Si-Sn system. *Calphad*. 2007;31:192–200.
- [14] Paliwal M, Jung I-H. Thermodynamic modeling of the Mg-Bi and Mg-Sb binary systems and short-range-ordering behavior of the liquid solutions. *Calphad*. 2009;33:744–754.
- [15] Fang D, Sun Z, Li Y, et al. Preparation, microstructure and thermal properties of Mg-Bi alloys as phase change materials for thermal energy storage. *Appl Therm Eng*. 2016;92:187–193.
- [16] Chunju NIU, Changrong LI, Zhenmin DU, et al. Thermodynamic assessment of the Bi-Mg binary system. *Acta Metall Sin*. 2012;25(1):19–28.
- [17] Butler JAV. The thermodynamics of the surfaces of solutions. *R Soc A*. 1932:348–375. <https://doi.org/10.1098/rspa.1983.0054>
- [18] Moelwyn-Hughes EA. *Physical chemistry*. Second ed. Oxford: Pergamon; 1964.
- [19] Bhatia AB, Thornton DE. Structural aspects of the electrical resistivity of binary alloys. *Phys Rev B*. 1970;2:3004–3012.
- [20] Bhatia AB, Hargrove WH, Thornton DE. Concentration fluctuations and partial structure factors of compound-forming binary molten alloys. *Phys Rev B*. 1974;9:435–444.
- [21] Warren BE. *X-ray diffraction*. New York: Dover Publication; 1990.
- [22] Cowley JM. An approximate theory of order in alloys. *Phys Rev*. 1950;77:669–675.
- [23] Singh RN, Pandey DK, Sinha S, et al. Thermodynamic properties of molten salt solutions. *Phys B*. 1987;145:358–364.
- [24] Brandes EA, Brook GB. 1992. *Smithells metals reference book*. 7th ed. Jordan Hill, Oxford: Butterworth-Heinemann Linacre House. DOI:10.1016/B978-075067509-3/50014-2.
- [25] Darken LS, Gurry RW. *Physical chemistry of metals*. New York: McGraw Hill; 1953.



Phase Transitions

A Multinational Journal

ISSN: (Print) (Online) Journal homepage: <https://www.tandfonline.com/loi/gpht20>

Phase segregating and complex forming Pb-based (=X-Pb) liquid alloys

Indra Bahadur Bhandari, Narayan Panthi, Ishwar Koirala & Devendra Adhikari

To cite this article: Indra Bahadur Bhandari, Narayan Panthi, Ishwar Koirala & Devendra Adhikari (2021): Phase segregating and complex forming Pb-based (=X-Pb) liquid alloys, Phase Transitions, DOI: [10.1080/01411594.2021.1933485](https://doi.org/10.1080/01411594.2021.1933485)

To link to this article: <https://doi.org/10.1080/01411594.2021.1933485>



Published online: 31 May 2021.



Submit your article to this journal [↗](#)



View related articles [↗](#)



View Crossmark data [↗](#)



Phase segregating and complex forming Pb-based (=X-Pb) liquid alloys

Indra Bahadur Bhandari^{a,b}, Narayan Panthi^{a,c}, Ishwar Koirala^a and Devendra Adhikari ^d

^aCentral Department of Physics, Tribhuvan University, Kirtipur, Nepal; ^bDepartment of Applied Sciences, Purwanchal Campus, Tribhuvan University, Dharan, Nepal; ^cDepartment of Physics, Patan Multiple Campus, Tribhuvan University, Lalitpur, Nepal; ^dDepartment of Physics, M.M.A.M.C., Tribhuvan University, Biratnagar, Nepal

ABSTRACT

We have used a theoretical model based on the assumption of compound formation in binary alloys to study the thermodynamic, microscopic and surface properties of Bi-Pb and In-Pb liquid alloys. A review of the phase diagrams for these alloys shows that one of the stable complexes for Bi-Pb liquid alloy is BiPb₃; also that In-Pb is a stable phase in liquid In-Pb alloys. Using the same interaction parameters that are fitted for free energy of mixing, we have been able to compute the bulk and thermodynamic properties of the alloys. From our observations, we are able to show that the Bi-Pb liquid alloy exhibits compound formation over the whole concentration range and the In-Pb alloys undergo phase separation. With regard to surface properties Pb segregates more to the surface in In-Pb alloys than in Bi-Pb alloys. The viscosity isotherms have positive deviation from ideality for both Bi-Pb and In-Pb alloys.

ARTICLE HISTORY

Received 9 December 2020
Accepted 24 March 2021

KEYWORDS

Bi-Pb; In-Pb; asymmetry; interaction parameters; deviation

1. Introduction

Numerous available models [1–28] have been used by a number of researchers to study the thermodynamic, structural, transport and surface properties of binary liquid alloys; the deviation of the properties of alloys from the ideal mixing condition is discussed in such model formulations in terms of the energy interaction of the constituent species of the respective alloys. It follows from the above that the main parameter for selecting a thermodynamic alloy is how far the thermodynamic properties of liquid alloys deviate from the ideal properties. On the basis of its deviation from the ideal thermodynamic properties, an alloy can be considered either as a compound-forming liquid alloy (hetero-coordinated) or as a segregating (homo-coordinated) system. One of the basic advantages of using such a thermodynamic model is that it can be easily extended to investigate the compositional dependence of structural properties [14,29] such as long wavelength fluctuations, chemical short-range order parameters, transport properties [30,31] such as diffusion coefficient, viscosity and surface properties [16,32] such as surface tension and surface composition. Departures from ideality are visible as asymmetries in thermodynamic properties away from equiatomic composition and are usually attributed to one of the following factors: the size effect, the difference in electronegativity or the interactions between solute and solvent atoms or the combination of these factors [33]. The industrial applications of liquid alloys could also be a very important basis for a detailed study. Lead and lead alloys have frequently been the subject of numerous experimental and theoretical research studies [34–50].

Lead (Pb) is among the top 10 essential commodities consumed in the industrial world. Lead has some exceptional properties: low melting point, easy casting, high density, softness, malleability, low strength, easy production, acid resistance and electrochemical reactions with sulfuric acid. Due to its excellent resistance to air, water and soil corrosion, Lead is one of the most stable materials produced. Lead is ductile and malleable and can be produced by rolling, extruding, forging, spinning and hammering in different shapes. Low tensile strength and very low creep strength make it unfit for use without the addition of alloy elements. Lead can be easily alloyed to a lot of other metals. Lead alloys with low melting points can be cast into many shapes using a variety of molding materials and casting processes. Antimony, calcium, tin, copper, tellurium, arsenic and silver are the main alloy elements used to strengthen lead. Minor alloy elements include selenium, sulfur, bismuth, cadmium, indium, aluminum and strontium. The main uses of lead alloys are lead-acid ammunition batteries; cable sheathing; construction of sheets, pipes and solders; bearings; gaskets; special castings; anodes; fusible alloys; shielding; and weights. Because of the corrosion resistance of lead and lead alloys, their applications are also associated with the formation of the protective corrosion film. Despite many useful applications, lead and its compounds are combined toxins and should be treated with recommended precautions. Such chemicals should not be used in diet or other consumption substances [51].

In-Pb alloys are generally recommended for soldering gold as alternative solders, as they do not easily leach or dissolve gold. In addition, In-Pb alloys are used as contact alloys for metal-glass or metal-ceramic connections due to their relatively low melting temperatures [40]. Elemental Pb and In are not easy to volatilize; therefore; the data obtained at high temperatures are sufficiently realistic and it is interesting to study the properties of Pb–In melts. Lead-bismuth alloys are of value for their corrosion protection and wear resistance properties [52]. The lead-bismuth alloy is a prospective heat transfer medium for nuclear power units [53].

The layout of the paper is as follows. Section 2 provides the theoretical basis for our work. Section 3 presents and discusses the results of this work. Finally, the conclusions are outlined in Section 4.

2. Theory

The advantages of complex formation model (CFM) [12,17,25,54] are that, it seeks to account stability of compound through concentration-dependent free energy of mixing G_M , heat of mixing H_M and concentration fluctuation in long wavelength limit $S_{cc}(0)$. Formalism in weak interaction approximation [55] was applied to liquid Bi-Pb and In-Pb alloys to describe the behavior of their mixing properties. In the framework of CFM, A-B liquid alloy is a pseudo-ternary mixture consisting of A-atoms, B-atoms and chemical complexes $A_\alpha B_\beta$ with intermetallic stoichiometry present in a solid state, all in chemical equilibrium with each other [56,57]. If there are x_1 number of A atoms, x_2 number of B atoms and x_3 number of $A_\alpha B_\beta$ complexes in the ternary mixture, then we have from the conservation of atoms,

$$x_1 = c - \alpha x_3, \quad x_2 = (1 - c) - \beta x_3 \quad \text{and} \quad x = x_1 + x_2 + x_3 = 1 - (\alpha + \beta - 1)x_3 \quad (1)$$

where α and β are small integers determined from the stoichiometry of energetically favored compound and c is the atomic fraction of A atoms. The value of x_3 can be calculated at a given pressure and temperature from the equilibrium state of free mixing energy, G_M as

$$\left(\frac{\partial G_M}{\partial x_3} \right)_{T,P,c} = 0 \quad (2)$$

where G_M for binary alloys can be written as

$$G_M = -x_3 \chi + RT \sum_{i=1}^3 x_i \ln \left(\frac{x_i}{x} \right) + \sum_{i<j} \Psi_{ij} \left(\frac{x_i x_j}{x} \right) \quad (3)$$

Here the first term $-x_3\chi$ stands for lowering of free energy due to the formation of complex $A_\alpha B_\beta$, χ is the formation energy of the complex, Ψ_{ij} ($i = 1, 2, 3$) are the average interaction energies among the species i and j . From Equations (2) and (3), the equilibrium value of x_3 is given by the equation

$$(x_3 x^{\alpha+\beta-1} x_1^{-\alpha} x_2^{-\beta})^{-1} = \exp\left(\Phi - \frac{\chi}{RT}\right) \quad (4)$$

where

$$\begin{aligned} \Phi &= \Phi_1 + \Phi_2 + \Phi_3 \\ \Phi_1 &= \left[(\alpha + \beta - 1) \frac{x_1 x_2}{x^2} - \alpha \frac{x_2}{x} - \beta \frac{x_1}{x} \right] \frac{\Psi_{12}}{RT} \\ \Phi_2 &= \left[(\alpha + \beta - 1) \frac{x_2 x_3}{x^2} - \beta \frac{x_3}{x} + \frac{x_2}{x} \right] \frac{\Psi_{23}}{RT} \\ \Phi_3 &= \left[((\alpha + \beta - 1) \frac{x_1 x_3}{x^2} - \alpha \frac{x_3}{x} + \frac{x_1}{x}) \right] \frac{\Psi_{13}}{RT} \end{aligned} \quad (5)$$

The heat formation, H_M , can be obtained through Equation (3) and the relation

$$H_M = G_M - T(\partial G_M / \partial T)_{P,c,N} \quad (6)$$

Equations (3) and (6) yield

$$H_M = -x_3 \left[\chi - T \left(\frac{\partial \chi}{\partial T} \right) \right] + \sum_{i < j} \sum \left(\frac{x_i x_j}{x} \right) \left[\Psi_{ij} - T \left(\frac{\partial \Psi_{ij}}{\partial T} \right) \right] \quad (7)$$

The other thermodynamic function entropy of mixing (S_M) can be expressed as

$$S_M = (H_M - G_M) / T \quad (8)$$

Using Equations (3) and (7) in Equation (8) we obtain

$$S_M = x_3 \frac{\partial \chi}{\partial T} - R \sum_{i=1}^3 x_i \ln \frac{x_i}{x} - \sum_{i < j} \sum \left(\frac{x_i x_j}{x} \right) \frac{\partial \Psi_{ij}}{\partial T} \quad (9)$$

Knowledge of surface properties is important for understanding surface-related properties such as wet joint capability, epitaxial growth, corrosion and phase transformation kinetics [58]. Centered on the assumption of a monatomic surface layer, Butler's method [59] for assessing surface tension, σ of liquid solution can be expressed as follows:

$$\sigma = \sigma_A + \frac{G_A^s - G_A^b}{S_A} + \frac{RT}{S_A} \ln \left(\frac{c^s}{c} \right) \quad (10)$$

$$= \sigma_B + \frac{G_B^s - G_B^b}{S_B} + \frac{RT}{S_B} \ln \left(\frac{1 - c^s}{1 - c} \right) \quad (11)$$

Equations (10) and (11) give the expression for surface tension in terms of partial excess free energy of mixing in bulk (G_i^b), partial excess free energy of mixing at the surface (G_i^s), bulk concentration (c) and surface concentration (c^s). Where σ_A and σ_B are the surface tensions of pure components A and B, respectively.

The monatomic surface area for each component is

$$S_i = 1.091 N_A^{1/3} V_i^{2/3} \quad (12)$$

where V_i is the molar volume of the component i that can be determined from its molar mass and density and N_A stands for Avogadro number. It is difficult to evaluate the coefficient in Equation

(12) for liquid alloys. For simplicity, it is usually set to 1.091 for liquid metals assuming close-packed structures [60].

The concentration fluctuations, in the long wavelength limit, $S_{cc}(0)$ indicate the preference for homo-coordination or hetero-coordination that defines the essence of mixing in liquid alloys in terms of chemical order and segregation. Once the Gibbs energy of mixing of the liquid phase, G_M is known, $S_{cc}(0)$ can be expressed by G_M as [61].

$$S_{cc}(0) = \left(\frac{1}{RT} \frac{\partial^2 G_M}{\partial c^2} \right)^{-1} \quad (13)$$

Theoretically computed values of $S_{cc}(0)$ can be compared with the observed values evaluated from the activity of constituent element at different composition by the following expression

$$S_{cc}(0) = \frac{c_B a_A}{(\partial a_A / \partial c_A)_{T,P,N}} = \frac{c_A a_B}{(\partial a_B / \partial c_B)_{T,P,N}} \quad (14)$$

Solving Equations (4) and (12) one obtains

$$S_{cc}(0) = \frac{RT}{RT \sum_{i=1}^3 \left(\frac{(x'_i)^2}{x_i} - \frac{(x')^2}{x} \right) + 2x \sum_{i < j} \sum \Psi_{ij} \left(\frac{x_i}{x} \right)' \left(\frac{x_j}{x} \right)'} \quad (15)$$

where the prime on x denotes its first differentiation with respect to c .

For ideal mixture Equation (15) reduces to

$$S_{cc}^{id}(0) = c_A c_B \quad (16)$$

The degree of order in the liquid alloy can be viewed using the Warren–Cowley short-range order parameter (α_1) [62, 63]. Experimentally, these quantities are not easily quantifiable by diffraction experiments. From the knowledge of the nearest neighbor contacts of unlike atoms in the melt, the expression for α_1 can be simply obtained [27]. Knowledge of α_1 provides a direct insight into the nature of the mixture's local arrangement of atoms. $\alpha_1 < 0$ refers to unlike atoms pairing as nearest neighbors, $\alpha_1 > 0$ corresponds to like atoms pairing in the first coordination shell, while $\alpha_1 = 0$ corresponds to a random distribution. The limiting values of α_1 for equiatomic composition fall in the range $-1 \leq \alpha_1 \leq +1$. The minimum possible value of α_1 is $\alpha_{\min} = -1$ representing complete ordering. On the other hand, the maximum value $\alpha_{\max} = +1$ implies total segregation leads to phase separation. Singh et al. [64] suggested that α_1 can be estimated from $S_{cc}(0)$.

$$\alpha_1 = \frac{S - 1}{S(z - 1) + 1}, \quad S = \frac{S_{cc}(0)}{S_{cc}^{id}(0)} \quad (17)$$

Here z is the coordination number of the alloy. It is taken as 10 for the present calculations, and the α_1 values are evaluated [6].

Viscosity is one of the most essential thermophysical properties of liquid alloys, deciding certain manufacturing processes and natural phenomena. By means of viscosity, the mixing behavior of binary melt can also be understood at the microscopic level. The Budai-Benko-Kaptay (BBK) model for viscosity of liquid alloy [65] is

$$\eta = P T^{1/2} \frac{\left(\sum_i c_i M_i \right)^{1/2}}{\left(\sum_i c_i V_i \right)^{2/3}} \exp \left[\frac{B}{T} \left(\sum_i c_i T_{m,i} - \frac{H_M}{qR} \right) \right] \quad (18)$$

The detailed formalism of the above-mentioned model and the values of the different parameters present in Equation (18) are explored in detail [66]. Here we have presented the main equation involved in the

measurement of viscosity. Many metallurgical processes and heterogeneous chemical reactions require transport properties, such as the diffusivity of liquid metals. For example, the rate of heterogeneous reactions between two liquid alloys, such as slag and metal, is limited by the diffusion of the reactant species [58]. The mixing behavior of the binary liquid alloys can also be explored at the microscopic level in terms of diffusion coefficient. The mutual diffusion coefficient (D_M) of liquid alloys can be displayed in terms of activity (a_i) and self-diffusion coefficient (D_{id}) of individual component applying Darken's equation [67].

$$D_M = c_i D_{id} \frac{d \ln a_i}{dc_i} \quad (19)$$

Here

$$D_M = c D_B + (1 - c) D_A \quad (20)$$

where D_A and D_B are the self-diffusion coefficients of pure components A and B, respectively. The ratio of mutual diffusion coefficient (D_M) and self-diffusion coefficient (D_{id}) is also associated with concentration fluctuation in long wavelength limit ($S_{cc}(0)$) as

$$\frac{D_M}{D_{id}} = \frac{c_A c_B}{S_{cc}(0)} \quad (21)$$

3. Results and discussion

3.1. Thermodynamic properties

In this work, we aim to investigate some of the transport and surface properties of Bi-Pb and In-Pb alloys, such as surface tension, surface concentration, mutual diffusivity and viscosity, using energetics derived from their experimental thermodynamic data. To use the CFM to obtain the required energy parameters, we consider the existence of a form $A_\alpha B_\beta$ chemical complex in the liquid state of the alloy. By choosing the values α and β , we continue to determine the free energy of the alloy mixing values by varying the energy parameters χ and Ψ_{ij} . The set of energy parameters that propagates to a reasonable extent the computed values of the free energy of mixing of liquid alloys will be used in the calculation of their enthalpy of formation H_M , mixing entropy S_M , concentration-concentration fluctuation at the long wavelength limit $S_{cc}(0)$ and mutual diffusivities D_M/D_{id} . The values of α and β used for the computation are obtained from phase diagrams. For Bi-Pb, the phase diagram [68] shows the formation of intermetallic compounds of the type BiPb_3 in the solid phase. We, therefore, presume that the compound will stay stable and remain in the liquid phase and affect the thermodynamic properties of the liquid alloy to a reasonable amount. However in the case of the In-Pb liquid alloy, the selection of α and β corresponding to the In-Pb complex was capable of reproducing, to a reasonable degree, the reported free energy of the mixing values of the alloy. The plot of G_M/RT with respective concentration of Bi and In for Bi-Pb and In-Pb liquid alloys is shown in Figure 1.

The points are experimental data due to Ref. [68] and the lines are the calculated values, at 700 K for Bi-Pb and at 673 K for In-Pb. The energy parameters used for the calculation are presented in Table 1. It should be noted that within the framework of the models mentioned above certain parameters, i.e. the coordination number, z and the order energy parameters χ , Ψ_{ij} do not depend on concentration. The exponential dependence of the interaction energies with temperature was used to remove artifacts present in the thermodynamic properties of liquid alloys calculated using R-K polynomial [69, 70]. But in our case, using a CFM, no artifacts were observed in such a way that we have made use of linear dependency of interaction energies with temperature [71]. The value of z is selected from the structural data and the order energy parameters are fitted from the thermodynamic data.

Figure 1 demonstrates calculations made using $\alpha = 1$ and $\beta = 3$ for BiPb_3 complex and $\alpha = 1$ and $\beta = 1$ for In-Pb complex. To a reasonable extent, the measured free energy of the mixing of liquid alloys indicates that these complexes are likely to occur in the liquid phase of the alloy. Both complexes

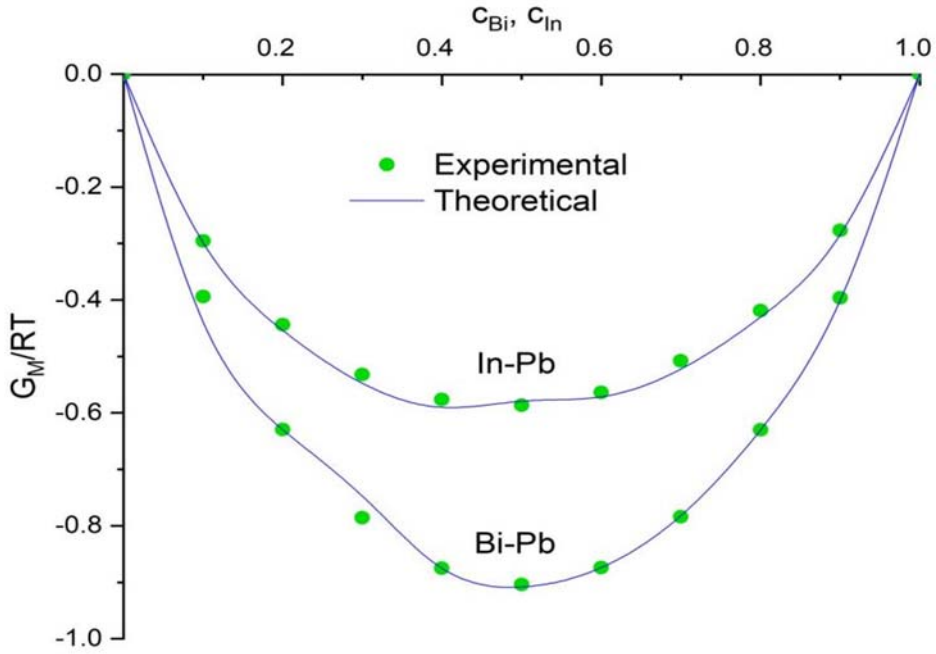


Figure 1. Free energy of mixing (G_M/RT) vs. bulk concentration for Bi-Pb and In-Pb alloys at 700 K and 673 K, respectively.

mentioned above show a good fit for the values of free energy at the given temperatures. We used experimental H_M values taken from Ref. [68] in conjunction with Equation (7) to fit the H_M versus concentration graph. Table 1 shows the values of the first derivatives of the interaction parameters with respect to temperature that give us the best fit for experimental H_M data. The values of H_M and S_M are in poor agreement with the experiment if energy parameters are taken as being temperature independent. We have, therefore, assumed the variation of these parameters with temperature to determine heat and entropy of formation with observed values [68]. Figure 2 illustrates that there is a good agreement between the experimental and calculated values of H_M/RT in both alloy systems. For the Bi-Pb system, the values of H_M/RT are negative throughout the whole concentration; this further confirms that Bi-Pb is a chemically favored system. However for In-Pb, the positive values of H_M/RT at all composition show that it is very weaker in complex formation than the previous system.

Table 1 shows that only Ψ_{12} of the first system has a negative temperature coefficient between the two systems; all energy parameters have positive temperature coefficients. The same interaction parameters fitted for experimental values of G_M and H_M are further used to calculate S_M/R through Equation (9). Figure 3 shows the reasonable agreement between the experimental values and calculated values of S_M for both systems.

3.2. Surface properties

The surface compositions and surface tension values for Bi-Pb and In-Pb liquid alloys were computed numerically from the expressions in Equations (10) and (11). The partial excess free energy of

Table 1. Interaction parameters and their temperature derivatives.

System	α	β	χ/RT	Ψ_{12}/RT	Ψ_{23}/RT	Ψ_{13}/RT	$\frac{1}{R} \frac{\partial \chi}{\partial T}$	$\frac{1}{R} \frac{\partial \Psi_{12}}{\partial T}$	$\frac{1}{R} \frac{\partial \Psi_{13}}{\partial T}$	$\frac{1}{R} \frac{\partial \Psi_{23}}{\partial T}$
Bi-Pb	1	3	1.880	-0.887	-0.714	0.519	1.580	-0.150	0.500	0.900
In-Pb	1	1	0.730	0.480	1.376	1.230	1.110	9.500	0.650	0.500

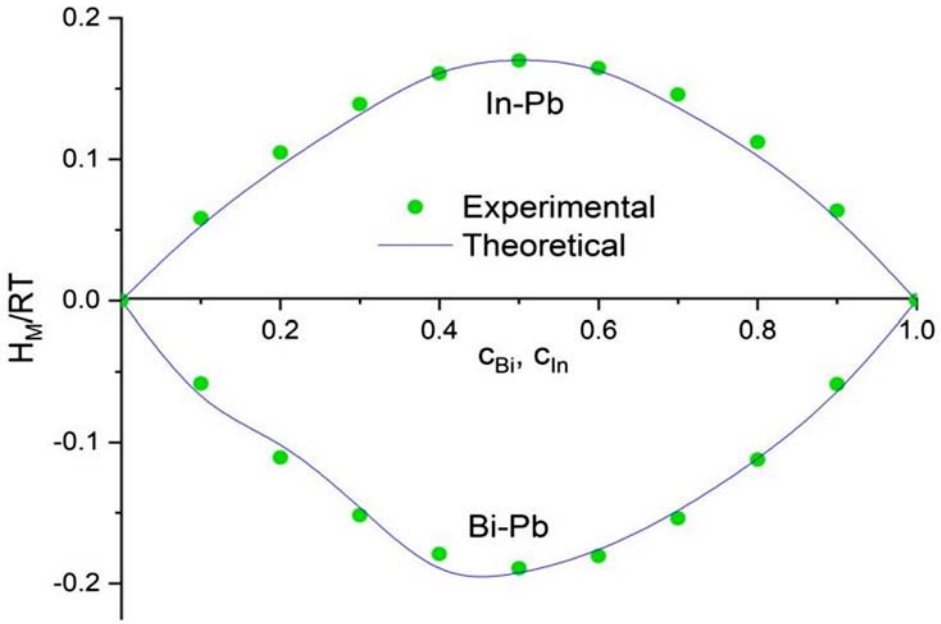


Figure 2. Heat of mixing (H_M/RT) vs. bulk concentration for Bi-Pb and In-Pb alloys at 700 K and 673 K, respectively.

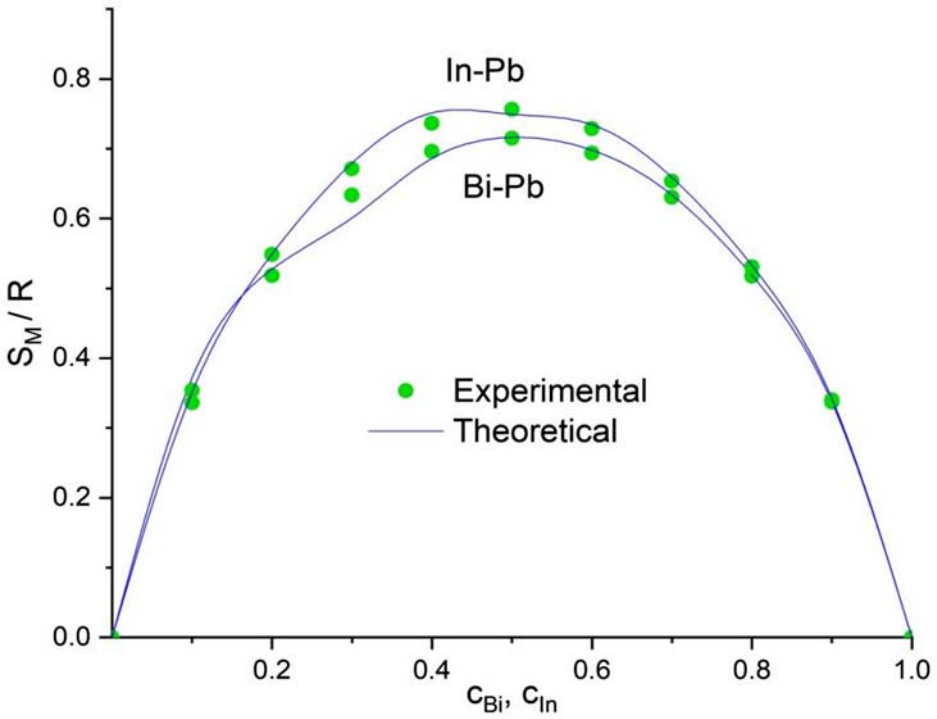


Figure 3. Entropy of mixing (S_M/R) vs. bulk concentration for Bi-Pb and In-Pb alloys at 700 K and 673 K, respectively.

Table 2. Input parameters for the calculation of surface tension and viscosity [72].

Element	$T_i^0(K)$	$\rho_i^0(kgm^{-3})$	$\Delta\rho_i(kgm^{-3}K^{-1})$	$\sigma_i^0(Nm^{-1})$	$\Delta\sigma_i(Nm^{-1}K^{-1})$	$\eta_i^0(Nsm^{-2})$	$E(J\ mol^{-1})$
Bi	544	10,068	-1.33	0.378	-7×10^{-5}	4.458×10^{-4}	6450
In	429.6	7023	-0.6798	0.556	-9×10^{-5}	3.02×10^{-4}	6650
Pb	600	10,678	-1.3174	0.468	-1.3×10^{-4}	4.636×10^{-4}	8610

mixing in bulk (G_i^b) and partial excess free energy of mixing at the surface (G_i^s) for Bi, Pb and In in both alloys were taken from Ref. [68]. The surface tension (σ_i^0), density (ρ_i^0) at fixed temperature (T_i^0) of the components of the alloy system were taken from Ref. [72] (where i denote In, Pb and Mg) are presented in Table 2. However, to obtain surface tension and density at working temperatures of 700 K and 673 K for Bi-Pb and In-Pb, respectively, the relationship between the temperature dependence of the surface tension and the density of the liquid metals used is shown below.

$$\rho_i(T) = \rho_i^0 + (T - T_i^0)\Delta\rho_i \quad (22)$$

$$\sigma_i(T) = \sigma_i^0 + (T - T_i^0)\Delta\sigma_i \quad (23)$$

Here $\Delta\rho_i$ and $\Delta\sigma_i$ are the temperature coefficients of density and surface tension, respectively, for the metal component of the alloys, and T is the working temperature in Kelvins.

Variation of the surface concentration of Bismuth and Indium by their bulk concentration for both Bi-Pb and In-Pb liquid alloys is shown in Figure 4. The surface concentration plot for Bi-Pb alloy showed that there is a surface segregation of Bismuth in this alloy. Lead, on the other hand, segregates to the surface for the In-Pb alloy.

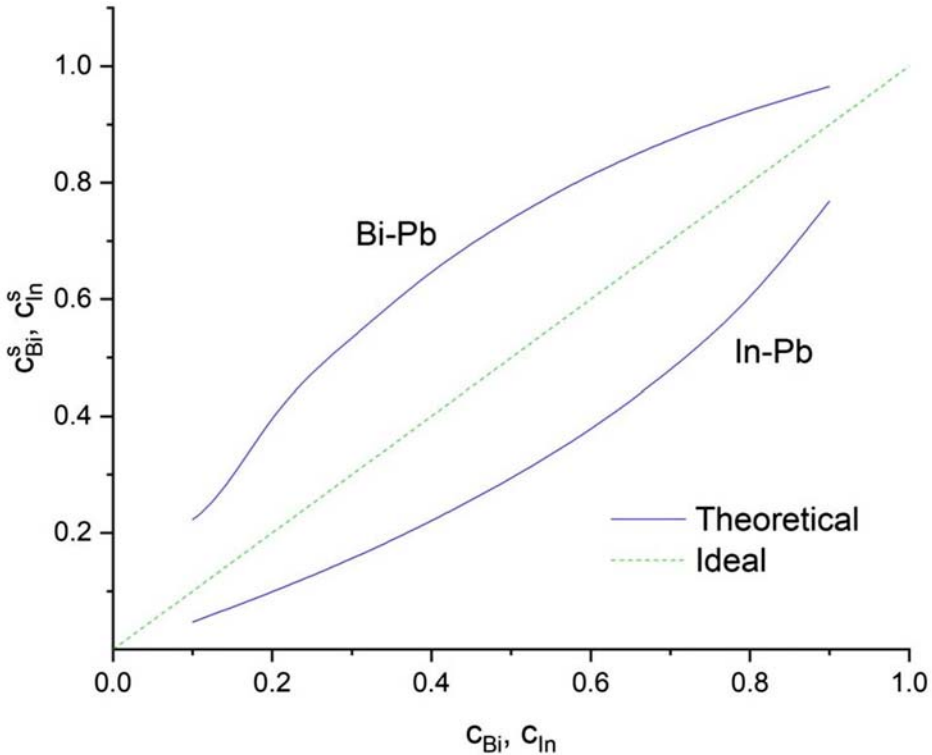


Figure 4. Surface concentrations (c_{Bi}^s, c_{In}^s) vs. bulk concentrations (c_{Bi}, c_{In}) for Bi-Pb and In-Pb alloys at 700 K and 673 K, respectively.

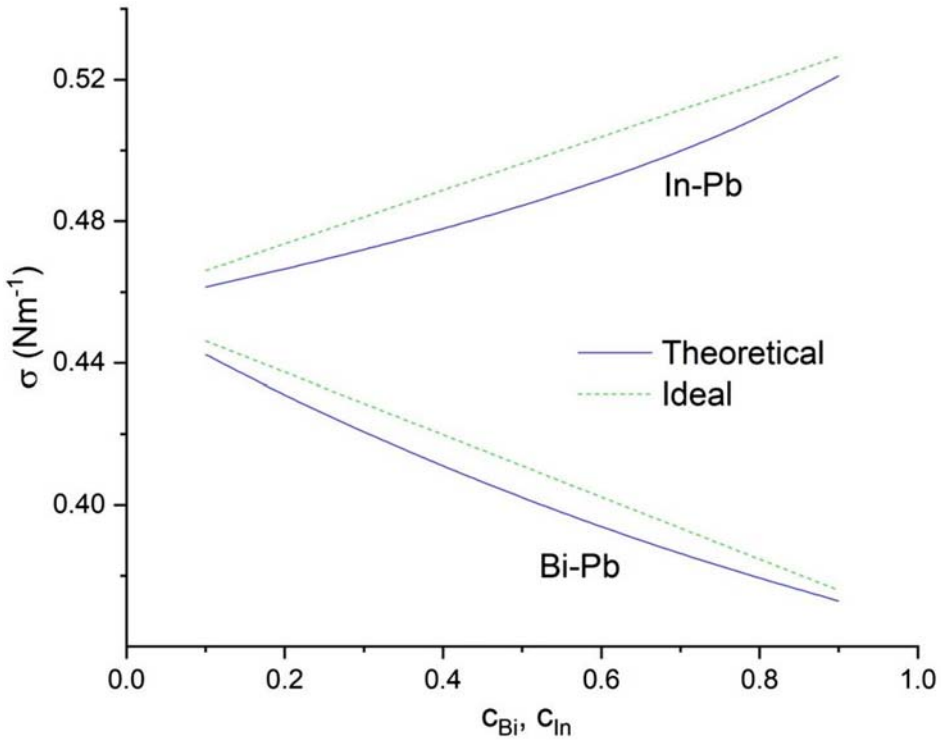


Figure 5. Surface tension (σ) vs. bulk concentration for Bi-Pb and In-Pb alloys at 700 K and 673 K, respectively.

Surface tension values for Bi-Pb and In-Pb liquid alloys over the entire bulk concentration range of the corresponding component are presented in [Figure 5](#).

The surface tension values of Bi-Pb decrease with little addition of Bismuth atoms. The surface tension of Bi is less than that of Pb. As most Bismuth atoms migrate to the surface and populate it, the surface tension of the alloy reduces the value of Lead and approaches the surface tension value of pure Bismuth. An increase in surface tension with an increase in the bulk concentration of Indium was observed for In-Pb. The surface tension values increase with the bulk concentration and reach a largest value of about 0.5211 at 0.9 atomic fraction of indium, which is close to the surface tension of the individual indium component.

3.3. Structural properties

Due to the difficulties in diffraction experiments, the theoretical estimation of concentration fluctuations in the long wavelength limit $S_{cc}(0)$ is of great significance when the nature of the atomic interactions in the melt has to be investigated. We calculated $S_{cc}(0)$ and the Warren–Cowley short-range order parameter (α_1) using the energy parameters estimated from our earlier calculations. In general, for a liquid binary alloy, when $S_{cc}(0) > S_{cc}^{id}(0)$, the liquid alloy is said to be phase-segregating or exhibits homo-coordination. $S_{cc}^{id}(0)$ is the ideal value of $S_{cc}(0)$ which is associated with ideal mixture. When $S_{cc}(0) < S_{cc}^{id}(0)$, the liquid alloys have a tendency of compound formation or manifest the hetero-coordination. In addition, the chemical short-range order parameter (α_1) provides a measure of the degree of compound formation in the liquid alloy. The maximum value of α_1 is 1 which shows complete separation of alloy components, while the minimum value of α_1 is -1 which means complete ordering in a liquid alloy. The plots of $S_{cc}(0)$ and the chemical short-range order parameter (α_1) for Bi-Pb and In-Pb complexes are shown in [Figures 6](#) and [7](#), respectively.

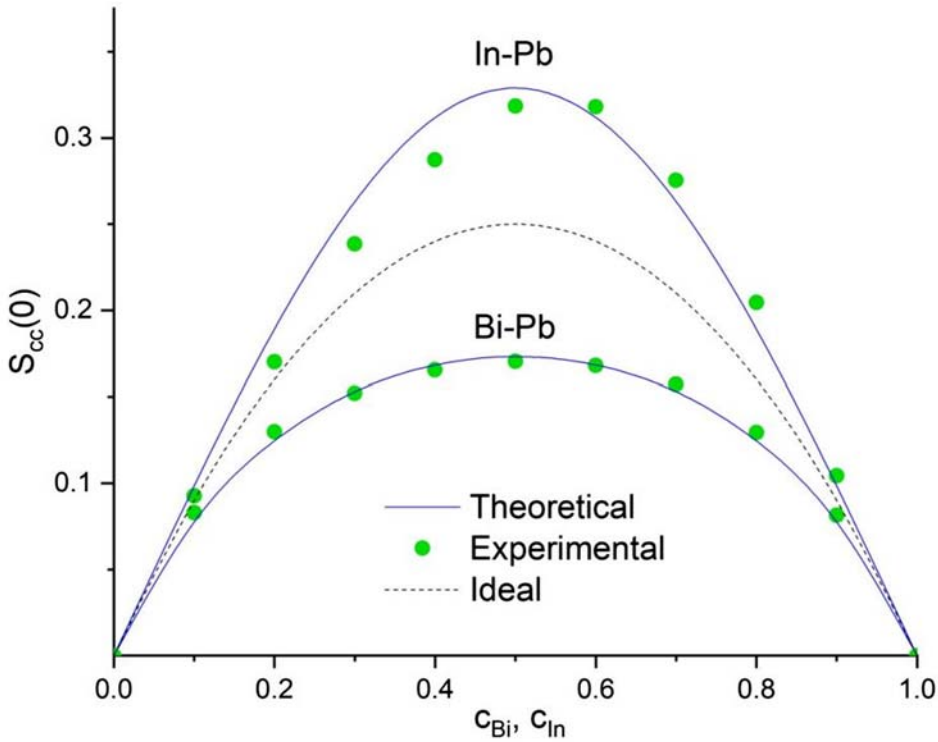


Figure 6. Concentration fluctuation at long wavelength limit ($S_{cc}(0)$) vs. bulk concentration for Bi-Pb and In-Pb alloys at 700 K and 673 K, respectively.

The lines are calculated values, while the points are experiment values calculated with Equation (14) using the activity data from Ref. [68] and the dashed line is for ideal values of $S_{cc}(0)$. Figure 6 shows that In-Pb is a phase-segregating almost the entire concentration range. This is supported by the chemical short-range order value, which has positive values throughout the entire region. For Bi-Pb liquid alloy, the computed $S_{cc}(0)$ values are smaller than the ideal values $S_{cc}^{id}(0)$ so the Bi-Pb liquid alloys have a good tendency for compound formation at all compositions. It can also be seen that α_1 values for Bi-Pb complex appear stronger with a minimum depth of $\alpha_1 = -0.0425$ at equiatomic composition. This strongly suggests that the first of the two Bi-Pb and In-Pb complexes have a higher tendency for complex formation.

3.4. Transport properties

Taking the necessary input data from Ref. [70, 72], the viscosity of the Bi-Pb liquid alloy at 700 K and the In-Pb alloy at 673 K is calculated out by Equation (18). The compositional dependency of the viscosity of both systems can be seen in Figure 8. The viscosity obtained for each alloy has opposite behavior. The viscosity value for Bi-Pb first increases with the bulk composition and achieves the highest value with the equiatomic composition. It decreases with a further rise in bismuth concentration. In the case of In-Pb, the viscosity isotherm almost displays the symmetric behavior with minima at $c_{In} = 0.5$. In comparison to the behavior seen in the previous one, the viscosity values for the In-Pb values decrease initially with the increase in corresponding composition. It is observed to decrease with more increase in concentration following equiatomic composition.

The computed values of $S_{cc}(0)$ for Bi-Pb and In-Pb were further used to evaluate the ratio of mutual diffusivities to intrinsic diffusivities (D_M/D_{id}) as a function of composition using Equation

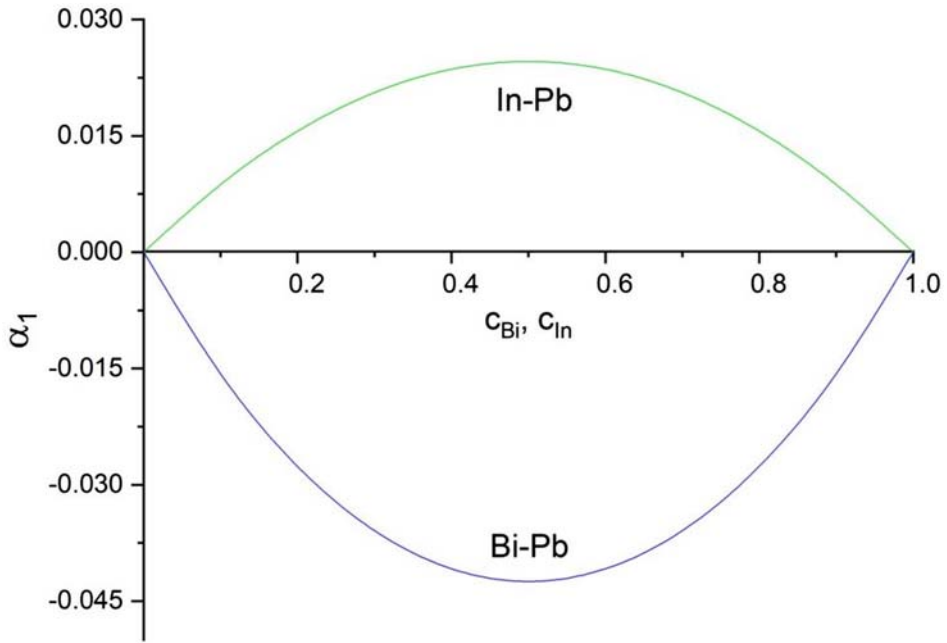


Figure 7. Chemical short-range order (α_1) vs. bulk concentration for Bi-Pb and In-Pb alloys at 700 K and 673 K, respectively.

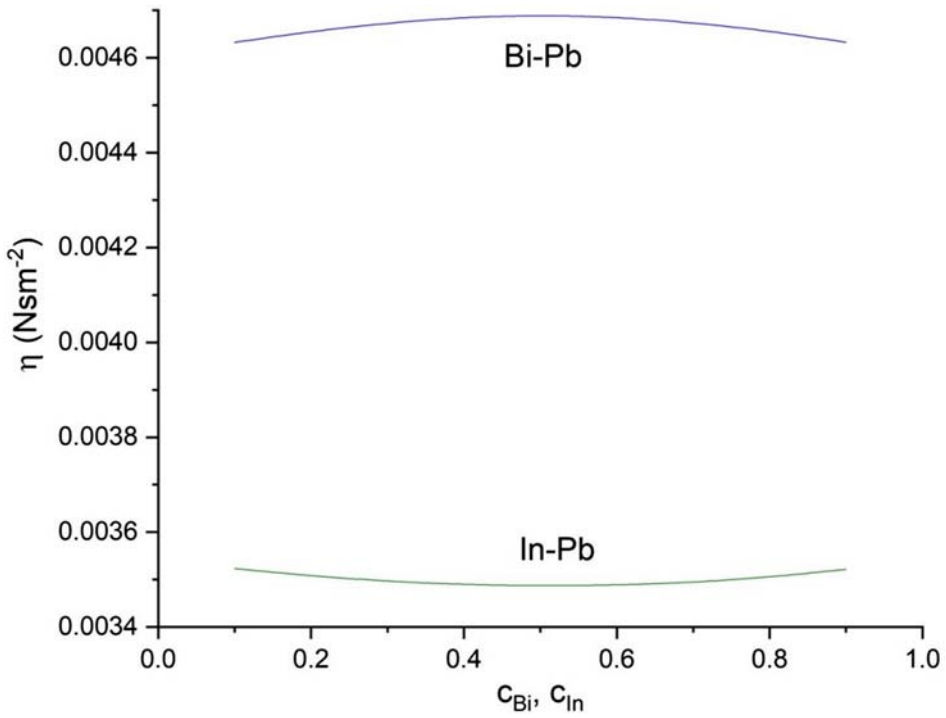


Figure 8. Viscosity (η) vs. bulk concentration for Bi-Pb and In-Pb alloys at 700 K and 673 K, respectively.

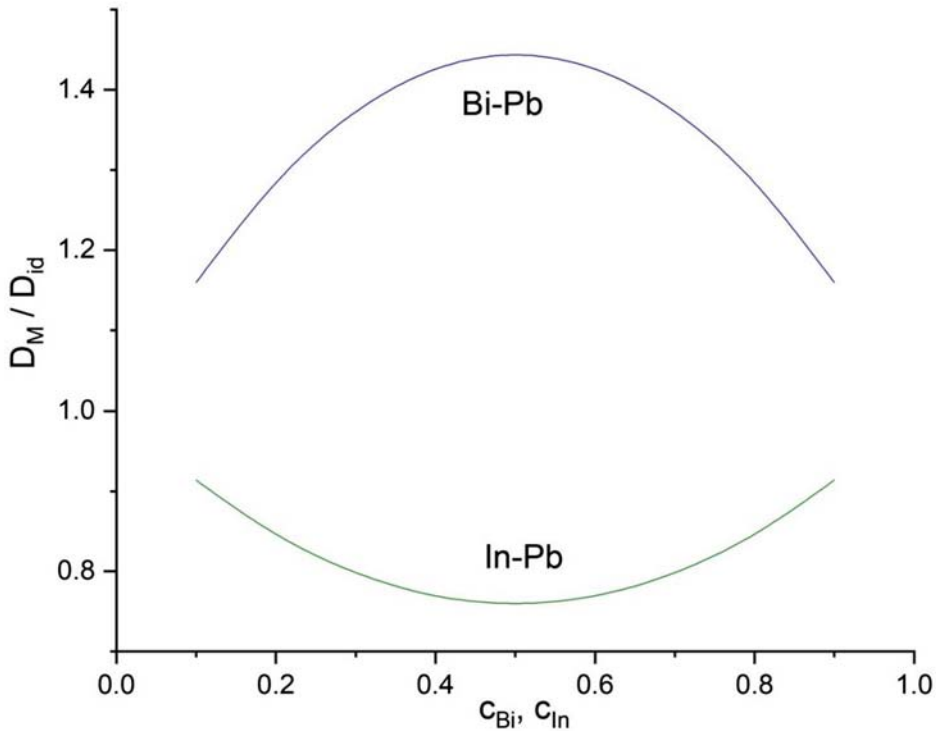


Figure 9. Ratio of mutual and intrinsic diffusion coefficients (D_M/D_{id}) vs. bulk concentration for Bi-Pb and In-Pb alloys at 700 K and 673 K, respectively.

(21). It is noted here that this ratio of diffusivities can also be used to indicate the level of order in a liquid binary alloy. If $D_M/D_{id} = 1$, the alloy has a regular mixture of components leading to the ideal solution. Hence $D_M/D_{id} > 1$ shows a tendency to hetero-coordination, while $D_M/D_{id} < 1$ shows a tendency to homo-coordination. The plots of D_M/D_{id} against concentration are presented in Figure 9.

The Bi-Pb alloy is stronger by better predicting the measured $S_{cc}(0)$. We, therefore, expect it to better emulate the other properties of the alloy. The values of D_M/D_{id} for Bi-Pb liquid alloy based on the energy parameters, due to the BiPb_3 complex, showed values that are greater than 1 throughout the concentration range. This undoubtedly showed that the Bi-Pb alloy is strongly compound-forming in the entire concentration range. For In-Pb, our calculated values of D_M/D_{id} suggest segregation throughout the whole composition range and, therefore, further support the very small tendency of compound formation in the alloy.

4. Conclusion

Thermodynamic and microscopic investigations of selected systems show that Bi-Pb alloys have a complex formation behavior, while the In-Pb system is undergoing phase separation. It has been observed that a component with a higher surface concentration, compared to its bulk concentration or a component with a lower surface tension segregates over the surface of the alloy. The evaluation of the coefficient of diffusion promotes the same tendency of the selected systems, as predicted in structural and thermodynamic properties. In the present study of viscosity, it is interesting to notice that both the alloys show symmetric behavior about equiatomic composition. However, in the case of variation with bulk composition, they exhibit opposite behavior.

Disclosure statement

No potential conflict of interest was reported by the author(s).

ORCID

Devendra Adhikari  <http://orcid.org/0000-0002-6022-3615>

References

- [1] Adhikari D, Jha IS, Singh BP. Structural asymmetry in liquid Fe-Si alloys. *Philos Mag.* 2010;90:2687–2694. DOI:10.1080/14786431003745302.
- [2] Adhikari D, Singh BP, Jha IS. Structural and energetic anomaly in liquid Na–Sn alloys. *J Mol Liq.* 2012;167:52–56. DOI:10.1016/j.molliq.2011.12.010.
- [3] Brillo J, Kolland G. Surface tension of liquid Al–Au binary alloys. *J Mater Sci.* 2016;51, DOI:10.1007/s10853-016-9794-x.
- [4] Chatterjee SK, Prasad LC, Bhattarai A. Interionic pair potential and entropy of mixing of Al–Mg compound forming binary molten alloys. *J Alloys Compd.* 2010;496:100–104. DOI:10.1016/j.jallcom.2010.02.013.
- [5] Egry I, Brillo J, Holland-Moritz D, et al. The surface tension of liquid aluminium-based alloys. *Mater Sci Eng A.* 2008;495:14–18. DOI:10.1016/j.msea.2007.07.104.
- [6] Godbole RP, Jha SA, Milanarun M, et al. Thermodynamics of liquid Cu–Mg alloys. *J Alloys Compd.* 2004;363:187–193. DOI:10.1016/S0925-8388(03)00326-8.
- [7] Jha IS, Koirala I, Singh BP, et al. Concentration dependence of thermodynamic, transport and surface properties in Ag–Cu liquid alloys. *Appl Phys A.* 2014;116:1517–1531.
- [8] Jha N, Rafique SM, Mishra AK, et al. Thermodynamic properties and electrical resistivity of liquid MgZn alloys. *Indian J Phys.* 2001;75(A):519–523.
- [9] Koirala I, Singh BP, Jha IS. Theoretical assessment on segregating nature of liquid In–Tl alloys. *J Non Cryst Solids.* 2014; 398–399. DOI:10.1016/j.jnoncrysol.2014.04.018.
- [10] Koirala RP, Koirala I, Adhikari D. Energetics of mixing and transport phenomena in Cd-X (X = Pb, Sn) melts. *Bibechana.* 2017;15:113–120. DOI:10.3126/bibechana.v15i0.18751.
- [11] Kumar A, Rafique SM, Jha N, et al. Structure, thermodynamic, electrical and surface properties of Cu–Mg binary alloy: complex formation model. *Phys B.* 2005;357:445–451. DOI:10.1016/j.physb.2004.12.031.
- [12] Novakovic R, Giuranno D, Ricci E, et al. Bulk and surface properties of liquid Sb–Sn alloys. *Surf Sci.* 2011;605:248–255. DOI:10.1016/j.susc.2010.10.026.
- [13] Akinlade O, Singh RN, Sommer F. Thermodynamics of liquid Al–Fe alloys. *J Alloys Compd.* 2000;299:163–168. DOI:10.1016/S0925-8388(99)00682-9.
- [14] Novakovic R. Thermodynamics, surface properties and microscopic functions of liquid Al – Nb and Nb – Ti alloys. *J Non Cryst Solids.* 2010;356:1593–1598. DOI:10.1016/j.jnoncrysol.2010.05.055.
- [15] Odusote Y.A., Hussain L.A., Awe O.E. Bulk and dynamic properties in Al–Zn and Bi–In liquid alloys using a theoretical model. *J Non Cryst Solids.* 2007;353:1167–1171. DOI:10.1016/j.jnoncrysol.2006.12.023.
- [16] Prasad LC, Singh RN. Surface segregation and concentration fluctuation at the liquid–vapor interface of molten Cu–Ni alloys. *Phys Rev B.* 1991;44:13768–13771.
- [17] Sharma N, Thakur A, Ahluwalia PK. Thermodynamic, surface and transport properties of liquid Hg–Pb and Hg–In amalgams. *J Mol Liq.* 2013;188:104–112. DOI:10.1016/j.molliq.2013.10.004.
- [18] Shrestha GK, Singh BK, Jha IS, et al. Optimization method for the study of the properties of Al–Sn binary liquid alloys. *Phys B Condens Matter.* 2017;514:1–7. DOI:10.1016/j.physb.2017.03.005.
- [19] Sommer F. Thermodynamics of liquid alloys. *Mater Sci Eng A.* 1997;226:757–762.
- [20] Yadav SK, Jha LN, Dhungana A, et al. Thermo-Physical properties of Al–Mg alloy in liquid state at different temperatures. *Mater Sci Appl.* 2018;09:812–828. DOI:10.4236/msa.2018.910058.
- [21] Yadav SK, Mehta U, Gohivar RK, et al. Reassessments of thermo-physical properties of Si–Ti melt at different temperatures. *Bibechana.* 2019;17:146–155. DOI:10.3126/bibechana.v17i0.26877.
- [22] Anusionwu BC, Adebayo GA, Madu CA. Thermodynamics and surface properties of liquid Al–Ga and Al–Ge alloys. *Appl Phys A.* 2009;97:533–541. DOI:10.1007/s00339-009-5428-3.
- [23] Attri KS, Ahluwalia PK, Sharma KC. Concentration fluctuations and thermodynamics of compound formation in mercury indium liquid alloy. *Phys Chem Liq.* 1994;26:225–235. DOI:10.1080/00319109408029495.
- [24] Awe OE, Odusote YA, Hussain LA, et al. Temperature dependence of thermodynamic properties of Si–Ti binary liquid alloys. *Thermochim Acta.* 2011;519:1–5. DOI:10.1016/j.tca.2011.02.028.
- [25] Bhatia AB, Hargrove WH. Concentration fluctuations and thermodynamic properties of some compound forming binary molten systems. *Phys Rev B.* 1974;10:3186–3196.

- [26] Bhatia AB, Singh RN. Thermodynamic properties of compound forming molten alloys in a weak interaction approximation. *Phys Chem Liq.* 1982;11:343–351. DOI:10.1080/00319108208080755.
- [27] Bhatia AB, Singh RN. A Quasi-lattice Theory for compound forming molten alloys. *Phys Chem Liq.* 1984;13:177–190. DOI:10.1080/00319108608078511.
- [28] Boyo AO. The study of thermodynamic properties of liquid NaCs alloys. *African J Sci Technol.* 2005;6:73–80.
- [29] Bhatia AB, Hargrove WH, Thornton DE. Concentration fluctuations and partial structure factors of compound-forming binary molten alloys. *Phys Rev B.* 1974;9:435–444. DOI:10.1103/PhysRevB.9.435.
- [30] Koirala I, Jha IS, Singh BP. Theoretical investigation on ordering nature of Cd-Bi alloys in the molten state. *Bibechana.* 2014;11:70–78.
- [31] Awe OE. Thermodynamic investigation of thermophysical properties of thallium-based liquid alloys. *Phys Chem Liq.* 2019;57:296–310. DOI:10.1080/00319104.2018.1443453.
- [32] Prasad LC, Singh RN, Singh VN, et al. Correlation between bulk and surface properties of AgSn liquid alloys. *J Phys Chem B.* 1998;102:921–926. DOI:10.1021/jp971042l.
- [33] Novakovic R, Giuranno D, Ricci E, et al. Surface and transport properties of In–Sn liquid alloys. *Surf Sci.* 2008;602:1957–1963. DOI:10.1016/j.susc.2008.03.033.
- [34] Anusionwu BC, Adebayo GA. Mixing properties in the In–Pb and In–Mg liquid alloys. *Phys B Condens Matter.* 2010;405:880–887. DOI:10.1016/j.physb.2009.10.007.
- [35] Kurata Y, Futakawa M, Kikuchi K, et al. Corrosion studies in liquid Pb–Bi alloy at JAERI: R & D program and first experimental results. *J Nucl Mater.* 2002;301:28–34. DOI:10.1016/S0022-3115(01)00720-6.
- [36] Yu J, Zhang Y, Zu FQ, et al. The abnormal changes of electrical resistivity in liquid Pb–In alloys. *Phys Chem Liq.* 2006;44:401–408. DOI:10.1080/00319100600574127.
- [37] Okajima K, Sakao H. On surface- and body-activities of components in the binary molten alloys. *Trans Japan Inst Met.* 1970;11:180–184. DOI:10.2320/matertrans1960.11.180.
- [38] Jesser WA, Shneck RZ, Gile WW. Solid-liquid equilibria in nanoparticles of Pb–Bi alloys. *Phys Rev B – Condens Matter Mater Phys.* 2004;69:1–13. DOI:10.1103/PhysRevB.69.144121.
- [39] Plevachuk Y, Sklyarchuk V, Gerbeth G, et al. Surface tension and density of liquid Bi–Pb, Bi–Sn and Bi–Pb–Sn eutectic alloys. *Surf Sci.* 2011;605:1034–1042. DOI:10.1016/j.susc.2011.02.026.
- [40] Minic D, Zivkovic D, Zivkovic Z. Calorimetric investigation of the Pb–In binary system. *Thermochim Acta.* 2001;372:85–91. DOI:10.1016/S0040-6031(01)00443-9.
- [41] Deloffre P, Balbaud-Célérier F, Terlain A. Corrosion behaviour of aluminumized martensitic and austenitic steels in liquid Pb–Bi. *J Nucl Mater.* 2004;335:180–184. DOI:10.1016/j.jnucmat.2004.07.014.
- [42] Bermúdez-Salguero C, Gracia-Fadrique J. Phase segregation at the liquid–air interface prior to liquid–liquid equilibrium. *J Phys Chem B.* 2015;119:10304–10315.
- [43] Popović MP, Olmsted DL, Bolind AM, et al. A study of the effects of minor additives to Pb–Bi eutectic: designing novel Pb–Bi–X liquid alloys for heat transfer applications. *Mater Des.* 2018;159:240–251. DOI:10.1016/j.matdes.2018.08.044.
- [44] Lukas HL. The Bi–Pb (Bismuth–Lead) system. *Bull Alloy Phase Diagrams.* 1980;1:67–70. DOI:10.1007/BF02881192.
- [45] Awe OE, Odusote YA, Akinlade O, et al. Energetics of mixing in Bi–Pb and Sb–Sn liquid alloys. *Phys B Condens Matter.* 2008;403:2732–2739. DOI:10.1016/j.physb.2008.02.005.
- [46] Ilinčev G. Research results on the corrosion effects of liquid heavy metals Pb, Bi and Pb–Bi on structural materials with and without corrosion inhibitors. *Nucl Eng Des.* 2002;217:167–177. DOI:10.1016/S0029-5493(02)00158-9.
- [47] Odusote YA, Fayose OO, Odigie PJ. Mixing properties of X–Pb, (X = Cd, In) liquid binary alloys. *J Non Cryst Solids.* 2007;353:4666–4671. DOI:10.1016/j.jnoncrysol.2007.07.006.
- [48] Fruehan RJ. Mass spectrometric determination of activities for alloys with complex vapor species: Bi–Pb and Bi–Ti. *Metall Trans.* 1971;2:1213–1218. DOI:10.1007/BF02664254.
- [49] Awe OE, Akinlade O, Hussain LA. Thermodynamic investigations of Bi–Cd, In–Pb, and Ni–Pd liquid alloys. *Zeitschrift Fuer Met Res Adv Tech.* 2005;96:89–93. DOI:10.3139/146.018076.
- [50] Klement W. Hexagonal close-packed structures in Bi–Pb alloys and the polymorphism of lead at high pressure. *J Chem Phys.* 1963;38:298–299. DOI:10.1063/1.1733654.
- [51] King M, Ramachandran V, Prengaman RD, et al. Updated by staff, lead and lead alloys. *Kirk–Othmer Encycl Chem Technol.* 2005;14, DOI:10.1002/0471238961.1205010411091407.a01.pub2.
- [52] Fratesi R, Roventi G, Maja M, et al. Electrodeposition of lead alloys from fluoborate baths. *J Appl Electrochem.* 1984;14:505–510. DOI:10.1007/BF00610816.
- [53] Barbin N, Terentiev D, Alexeev S, et al. Thermodynamic modeling of the Pb + Bi melt evaporation under various pressures and temperatures. *Comput Mater Sci.* 2013;66:28–33. DOI:10.1016/j.commatsci.2012.06.013.
- [54] Jha IS, Singh RN, Srivastava PL, et al. Stability of HgNa and HgK liquid alloys, *philos. Mag. B phys. condens. matter; stat. mech. electron. Opt Magn Prop.* 1990;61:15–24. DOI:10.1080/13642819008208649.
- [55] Novakovic R, Ricci E, Giuranno D, et al. Thermodynamics and surface properties of liquid Bi–In alloys. *CALPHAD.* 2009;33:69–75. DOI:10.1016/j.calphad.2008.09.002.

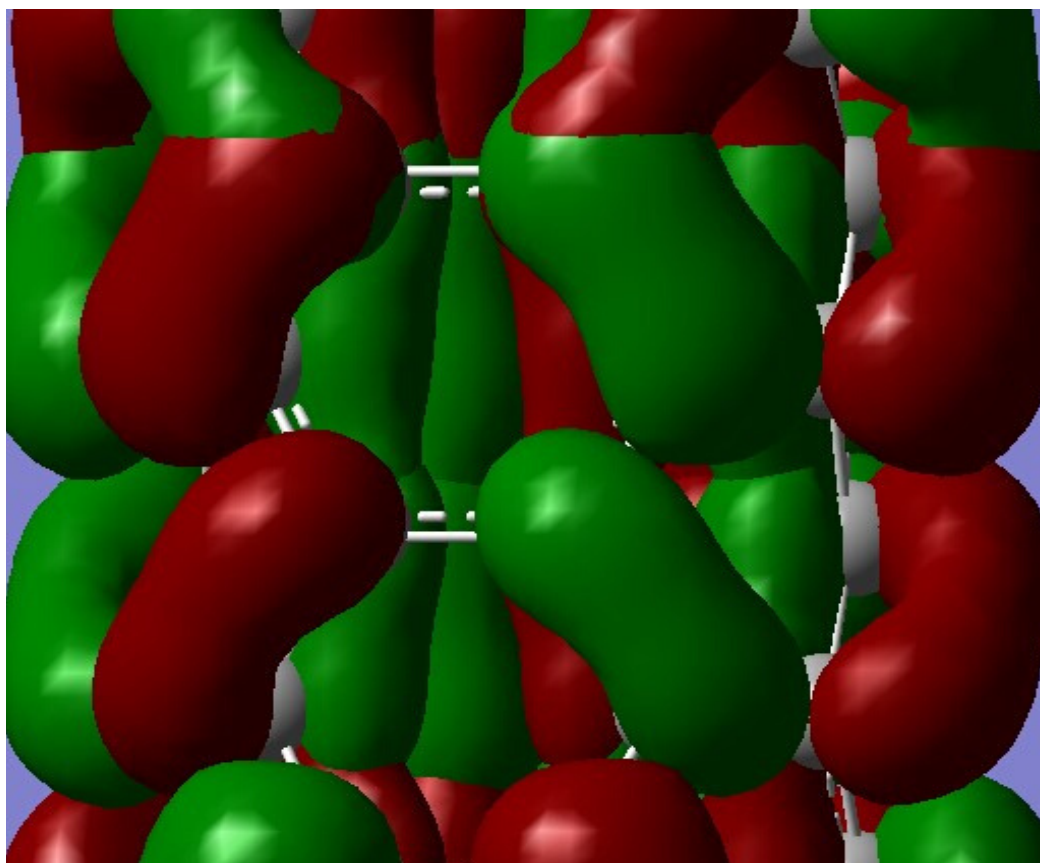
- [56] Novakovic R, Tanaka T, Muolo ML, et al. Bulk and surface properties of liquid Ag–X (X = Ti, Hf) compound forming alloys. *Surf Sci.* 2005;591:56–69. DOI:10.1016/j.susc.2005.06.022.
- [57] Singh RN. Free energy and heat of mixing of alloys. *J Phys F Met Phys.* 1981;11:389–396. DOI:10.1088/0305-4608/11/2/011.
- [58] Iida Takamichi IL, Rodericj G. The physical properties of liquid metals. Oxford University Press; 1988.
- [59] Butler JAV. The Thermodynamics of the surfaces of solutions. *R Soc A.* 1932: 348–375. DOI:10.1098/rspa.1983.0054.
- [60] Moser Z, Gasior W, Gasior J, et al. Surface tension of liquid Ag–Sn alloys: experiment versus modeling. *J Phase Equilib.* 2001;22(3):254–258.
- [61] Bhatia AB, Thornton DE. Structural aspects of the electrical resistivity of binary alloys. *Phys Rev B.* 1970;2:3004–3012. DOI:10.1103/PhysRevB.2.3004.
- [62] Warren BE. X-ray diffraction. New York: Dover Publication; 1990.
- [63] Cowley JM. An approximate theory of order in alloys. *Phys Rev.* 1950;77:669–675. DOI:10.1103/PhysRev.77.669.
- [64] Singh RN, Pandey DK, Sinha S, et al. Thermodynamic properties of molten salt solutions. *Phys B.* 1987;145:358–364. DOI:10.1007/978-94-009-3863-2_2.
- [65] Budai I, Benkő MZ, Kaptay G. Comparison of different theoretical models to experimental data on viscosity of binary liquid alloys. *Mater Sci Forum.* 2007;537-538:489–496.
- [66] Zhang F, Wen S, Liu Y, et al. Modelling the viscosity of liquid alloys with associates. *J Mol Liq.* 2019;291:111345.
- [67] Darken LS, Gurry RW. Physical chemistry of metals. New York: McGraw Hill; 1953.
- [68] Hultgren R, Desai PD, Hawkins DT, et al. Selected values of the thermodynamic properties of binary alloys. Metal Park, OH: American Society for Metals; 1973.
- [69] Kaptay G. A coherent set of model equations for various surface and interface energies in systems with liquid and solid metals and alloys. *Adv Colloid Interface Sci.* 2020;283:102212.
- [70] Kaptay G. The exponential excess Gibbs energy model revisited. *Calphad.* 2017;56:169–184.
- [71] Bhandari IB, Koirala I, Adhikari D. Temperature-dependent mixing behaviours of Bi–Mg liquid alloys. *Phys Chem Liq.* 2020:1–14. <https://doi.org/10.1080/00319104.2020.1863402>.
- [72] Brandes EA, Brook GB. *Smithells Metals reference book*, seventh, Butterworth-Heinemann Linacre House. Oxford: Jordan Hill; 1992; DOI:10.1016/B978-075067509-3/50014-2.

Volume 8, December 2019

ISSN 2542-2545

The
**HIMALAYAN
PHYSICS**

A peer-reviewed Journal of Physics



*Department of Physics, Prithvi Narayan Campus, Pokhara
Nepal Physical Society, Western Chapter, Pokhara*

Thermodynamics of liquid Gallium-Zinc alloy

Research Article

I. B. Bhandari^{1,2}, N. Panthi^{1,3}, I. Koirala^{1*}

1 Central Department of Physics, Tribhuvan University, Kathmandu, Nepal

2 Department of Applied Sciences, Institute of Engineering, Tribhuvan University, Kathmandu, Nepal

3 Department of Physics, Patan Multiple Campus, Tribhuvan University, Kathmandu, Nepal

Abstract: This research explores mixing behavior of Ga-Zn system through Complex Formation Model. The variables affecting to temperature are the interaction energy parameters in which the properties under investigation are projected. The study has inspected through different thermodynamic properties such as free energy of mixing, heat of mixing and entropy of mixing. Theoretical results are in a good acceptance with the corresponding literature data and support a homocoordinating tendency in Ga-Zn liquid alloys.

Keywords: Thermodynamic properties • Complex formation model • Segregation

1. Introduction

Gallium lies on group IIIB in the periodic table. It is proficiently applicable as a thermometric liquid and in doping semi-conductors and production of solid-state devices like transistors. Huge amounts of zinc are used to produce die castings. These applications of the components of liquid alloys studied make them good candidates for the current kind of study. In manufacturing semiconductor devices, Gallium alloys play the pivotal role. And it is promising materials for lead free solders, because they have the traits of low melting point, good wetting properties, adhesion and oxidation resistance [1–3]. Ga-Zn alloy possesses the constituents of different Gallium based multi component alloys i.e. applied in semiconducting industry. This research is significant for the study of the energetics of ternary systems such as Ga-Sn-Zn, Al-Ga-Zn, etc. It is specified that, this system is intensified low melting eutectic which is mentioned in literature [4–6].

The Ga-Zn system is analyzed through positive interaction energy, amplifying the formation of two phase structure, as presented by its simple eutectic phase diagram. The preliminary research of the empirical factors such as electronegativity difference ($= 0$) and size ratio $\Omega_{Ga}/\Omega_{Zn} \approx 1.19$ (Ω is atomic volume) [7, 8]. Ga-Zn system presents the values which are the characteristics for segregating alloys. However, the determining role is ascribed to the size ratio values. It purposes a limited solubility in the solid state and hence the presence of an eutectic reaction.

* Corresponding Author: ikphysicsstu@gmail.com

Thermodynamics of Ga-Zn system is examined through various experimental methods. There are numerous findings obtained applying EMF measurements. Besides this, there are some other results derived by thermodynamic calculation based on various theoretical models [9]. Numerous investigations have been performed for different system through various approaches [10–14]. This paper presents the results of thermodynamic analysis of Ga-Zn alloys according to Conformal Solution Model. The outcomes are analyzed and compared with literature data to explicate the accuracy of this method in thermodynamic description of the presented binary system.

2. Modelling

If c is the atomic concentration of A atoms then $(1-c)$ is atomic concentration for B atoms and such that $uA + vB = A_uB_v$ (u and v are small integer) then, number of A atoms, $N_A = c$. Number of B atoms, $N_B = (1-c)$, so that total number of atoms, $N = N_A + N_B$. When components A and B are blended together to form a binary A – B solution, thermodynamic properties are changed. The liquid alloy is assumed to be composed of three species; A atom, B atom and chemical complex A_uB_v , ternary mixture also called conformal solution. The number of free atoms will be reduced due to compound formation in the melt. Now for n_1 gm atoms of A, n_2 gm atoms of B and n_3 gm atoms of A_uB_v ,

$$n_1 = c - un_3 \text{ and } n_2 = (1 - c) - vn_3 \quad (1)$$

The total number of atoms after mixing,

$$n = n_1 + n_2 + n_3 \quad (2)$$

$$= 1 - (u + v - 1)n_3 \quad (3)$$

The free energy of mixing of the binary A-B mixture can be written as,

$$G_M = -n_3g + G' \quad (4)$$

Here, $-n_3g$ represents lowering of free energy due to compound formation, g is the formation energy of complex. G' is the free energy of mixing of the ternary mixture of A, B and A_uB_v . If the ternary mixture is an ideal solution,

$$G' = RT \sum n_i \ln \left(\frac{n_i}{n} \right) \quad (5)$$

If the effects of differences in sizes of the various constituents in the mixture cannot be ignored and the interaction ω_{ij} are small but not zero, the theory of regular solutions in the zeroth approximation [15] or the conformal solution approximation [16] is valid. For regular solution

$$G' = RT \sum n_i \ln \left(\frac{n_i}{n} \right) + \sum \omega_{ij} \left(\frac{n_i n_j}{n} \right) \quad (6)$$

This equation is also referred to as conformal solution approximation. where $\omega_{ij} = 0$ ($for\ i = j$) are termed as the interaction energies and by definition are independent of concentration, although they depend upon temperature and pressure. Now the expression for free energy of mixing G_M for the compound forming binary alloy is

$$G_M = -n_3g + RT \sum_{i=1}^3 n_i \ln \left(\frac{n_i}{n} \right) + \sum_{i<j} \sum \left(\frac{n_i n_j}{n} \right) \omega_{ij} \quad (7)$$

The expression for heat of mixing H_M is given by [17],

$$H_M = G_M - T \left(\frac{\partial G_M}{\partial T} \right)_P \quad (8)$$

$$H_M = -n_3g + RT \sum_{i=1}^3 n_i \ln \left(\frac{n_i}{n} \right) + \sum_{i<j} \sum \left(\frac{n_i n_j}{n} \right) \omega_{ij} - T \frac{\partial}{\partial T} \left[-n_3g + RT \sum_{i=1}^3 n_i \ln \left(\frac{n_i}{n} \right) + \sum_{i<j} \sum \left(\frac{n_i n_j}{n} \right) \omega_{ij} \right] \quad (9)$$

$$= -n_3 \left[g - T \left(\frac{\partial g}{\partial T} \right)_P \right] + \sum_{i<j} \sum \left(\frac{n_i n_j}{n} \right) \left[\omega_{ij} - T \left(\frac{\partial \omega_{ij}}{\partial T} \right)_P \right] \quad (10)$$

The expression for entropy of mixing S_M can be obtained as [17],

$$S_M = n_3 \frac{\partial g}{\partial T} - R \sum_{i=1}^3 n_i \ln \frac{n_i}{n} - \sum_{i<j} \sum \frac{n_i n_j}{n} \frac{\partial \omega_{ij}}{\partial T} \quad (11)$$

The equilibrium value of n_3 at a given pressure and temperature is given by

$$\left(\frac{\partial G_M}{\partial n_3} \right)_{T,P,N,C} = 0 \quad (12)$$

Substituting the value of G_M from Eq. 7 and after some algebraic calculation

$$\ln (n_3 n^{u+v-1} n_1^{-u} n_2^{-v}) + Y = \frac{g}{RT} \quad (13)$$

which is the equilibrium equation, where

$$Y = \left[\frac{n_1 n_2}{n^2} (u+v-1) - u \frac{n_2}{n} - v \frac{n_1}{n} \right] \frac{\omega_{12}}{RT} + \left[\frac{n_2 n_3}{n^2} (u+v-1) - v \frac{n_3}{n} + \frac{n_2}{n} \right] \frac{\omega_{23}}{RT} + \left[\frac{n_1 n_3}{n^2} (u+v-1) - u \frac{n_3}{n} + \frac{n_1}{n} \right] \frac{\omega_{13}}{RT}$$

3. Results and Discussion

Ga-Zn system has a eutectic point at 3.7 wt% Zn and at temperature of 25°C. The hexagonal (Zn) terminal solid solution has a maximum solubility of 2.36 wt% Ga at 260°C, while the orthorhombic (Ga) solid solution has a maximum solubility of 0.8 wt% Zn at 20°C [9]. Available experimental data [18] on the thermodynamic

properties as well as phase diagram information [18] have been used for the calculation of the order energy parameters for the Ga-Zn liquid phase by the CFM in a weak approximation. For the given temperatures the Gibbs free energy are negative and exhibit a flat minimum of -0.567 at the composition, $c = 0.45$]. Accordingly, the Ga-Zn compound was postulated as energetically less favored and the preferential arrangements of Ga and Zn constituent atoms does not so favor the formation of Ga-Zn complexes ($\mu = 1, v = 1$) in the liquid alloys. Keeping in mind the Ga-Zn phase diagram and the applications related to the different melting intervals of Ga-Zn alloys, all calculations have been done at $T = 750$ K. The optimized data set of the Gibbs energy of mixing of liquid Ga-Zn alloys together with the enthalpy of mixing and Ga and Zn activity data [18] have been used to calculate the interaction energy parameters at $T = 750$ K. The calculated interaction energy parameters for liquid Ga-Zn alloy, expressed in RT units at $T = 750$ K are; $g = 0.721$, $\omega_{12} = -6.091$, $\omega_{13} = 1.942$, $\omega_{23} = 1.808$

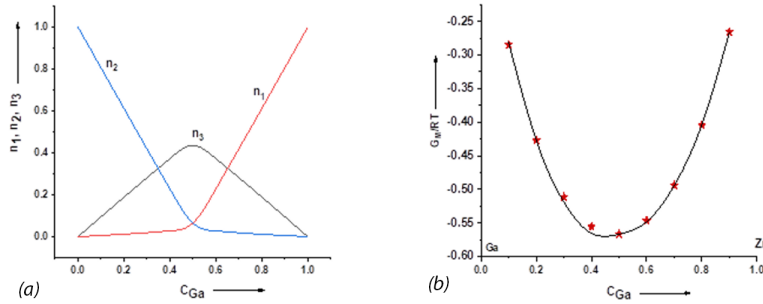


Figure 1. (a) Number of complexes (n_1, n_2, n_3) Vs concentration (c_{Ga}) of liquid Ga-Zn alloy at 750 K, (b) Free energy of mixing (G_M/RT) Vs concentration (c_{Ga}) of liquid Ga-Zn alloy at 750 K [Theoretical(-) and experimental(*) values [18]].

Equilibrium relation Eq. 13 along with Eqs. 1 and 3 are used to compute the number of complexes, n_3 , as a function of concentration. The values of interaction energy parameters are adjusted to give the concentration dependence of G_M which fits well with the corresponding thermodynamic data. The curves describing the Gibbs free energy of mixing of the Ga-Zn liquid phase are almost not symmetric with respect to the equiatomic composition. The concentration dependence of the equilibrium values of chemical complexes, n_3 , at $T = 750K$ exhibits the symmetry at the same composition, $c = 0.5$, with the maximum value of about 0.4365 (Fig. 1). With an increase in temperature, the inter-atomic forces become weaker, and the corresponding maximum value of n_3 decreases. Using the order energy parameters calculated at $T = 750K$, the enthalpy of mixing, H_M and the entropy of mixing S_M have been evaluated by Eqs. 10 and 11, respectively. The experimental data on the enthalpy of mixing measured at temperatures $T = 750K$ [18] have been used to calculate the variation in order energy parameters with temperature. The computed values of the derivatives are

$$\frac{1}{R} \frac{\partial g}{\partial t} = 1.224, \quad \frac{1}{R} \frac{\partial \omega_{12}}{\partial t} = 7.159, \quad \frac{1}{R} \frac{\partial \omega_{13}}{\partial t} = 0.444, \quad \frac{1}{R} \frac{\partial \omega_{23}}{\partial t} = 0.662 \quad (14)$$

A comparison between the calculated values of H_M and S_M by the CFM with the literature data [18] of liquid Ga-Zn alloy displays a good agreement between the two types of data (Fig. 2(a) and Fig. 2(b)).

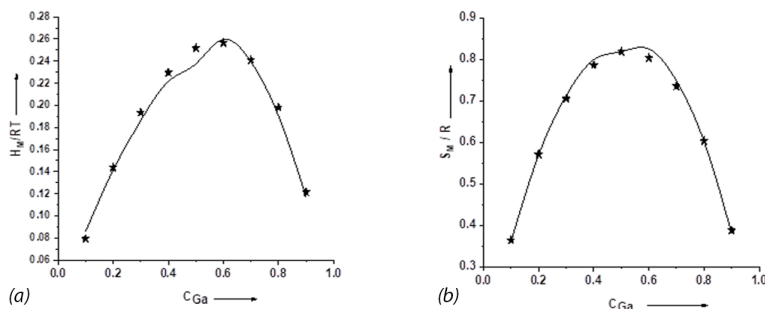


Figure 2. (a) Heat of mixing (H_M/RT), (b) Entropy of mixing (S_M/R) Vs concentration (c_{Ga}) of liquid Ga-Zn alloy at 750 K. [Theoretical(-) and experimental(*) values [18]]

4. Conclusions

Thermodynamic properties of Ga-Zn liquid alloy have been theoretically investigated by the CFM in a weak approximation. The thermodynamic data on mixing are used to obtain the interaction energy parameters, which are speculated to be invariant in all calculations. With the use same interaction parameters, the investigation of surface, transport and structural properties can be done further [14, 19–24]. The results obtained in the present work assure the applicability of this approach for a complete description of the thermodynamic of binary system which exhibit similar mixing properties. Moreover, it is found to be a useful tool in the interpretation of experimental results as well as in experimental planning.

References

- [1] Xu Q, Oudalov N, Guo Q, Jaeger HM, Brown E. Effect of oxidation on the mechanical properties of liquid gallium and eutectic gallium-indium. *Physics of fluids*. 2012;24(6):063101.
- [2] Wang H, Fang J, Xu Z, Zhang X. Improvement of Ga and Zn alloyed Sn–0.7 Cu solder alloys and joints. *Journal of Materials Science: Materials in Electronics*. 2015;26(6):3589–3595.
- [3] Liu NS, Lin KL. The effect of Ga content on the wetting reaction and interfacial morphology formed between Sn–8.55 Zn–0.5 Ag–0.1 Al– x Ga solders and Cu. *Scripta Materialia*. 2006;54(2):219–224.
- [4] Dutkiewicz J, Moser Z, Zabdyr L, Gohil DD, Chart TG, Ansara I, et al. The Ga-Zn (Gallium-Zinc) system. *Bulletin of Alloy Phase Diagrams*. 1990;11(1):77–82.
- [5] Genta V, Fiorani M, Valenti V. Thermodynamic Investigations of Metallic Systems, Note II: GaZn Liquid System. *Gazz Chim Ital*. 1955;85:103–110.
- [6] Predel B, Frebel M, Gust W. Untersuchung der thermodynamischen Eigenschaften flüssiger gallium-zinn- und gallium-wismut-Legierungen. *Journal of the Less Common Metals*. 1969;17(4):391–402.
- [7] Singh RN, Sommer F. Segregation and immiscibility in liquid binary alloys. *Reports on Progress in Physics*.

- 1997;60(1):57–150.
- [8] Iida T. Physical Properties of Liquid Metals. (II). Structure of Liquid Metals and Their (Number) Density. *Journal of the Japan Welding Society*. 1993;62(8):590–594.
- [9] Novakovic R, Zivkovic D. Thermodynamics and surface properties of liquid Ga-X (X = Sn, Zn) alloys. *Journal of Materials Science*. 2005 may;40(9-10):2251–2257.
- [10] Novakovic R, Ricci E, Gnecco F, Giuranno D, Borzone G. Surface and transport properties of Au–Sn liquid alloys. *Surface Science*. 2005;599(1-3):230–247.
- [11] Novakovic R, Ricci E, Giuranno D, Gnecco F. Surface properties of Bi–Pb liquid alloys. *Surface Science*. 2002;515(2-3):377–389.
- [12] Prasad LC, Singh RN, Singh VN, Chatterjee SK. Compound formation in Sn-based liquid alloys. *Physica B: Condensed Matter*. 1995;215(2-3):225–232.
- [13] Sharma N, Thakur A, Ahluwalia PK. Thermodynamic, surface and transport properties of liquid Hg–Pb and Hg–In amalgams. *Journal of Molecular Liquids*. 2013;188:104–112.
- [14] Awe OE, Akinlade O, Hussain LA. Thermodynamic properties of liquid Te–Ga and Te–Tl alloys. *Journal of Alloys and Compounds*. 2003;361(1-2):227–233.
- [15] Guggenheim EA. Statistical thermodynamics of mixtures with zero energies of mixing. *Proceedings of the Royal Society of London Series A Mathematical and Physical Sciences*. 1944;183(993):203–212.
- [16] Longuet-Higgins H. The statistical thermodynamics of multicomponent systems. *Proceedings of the Royal Society of London Series A Mathematical and Physical Sciences*. 1951;205(1081):247–269.
- [17] Lele S, Ramachandrarao P. Estimation of complex concentration in a regular associated solution. *Metallurgical Transactions B*. 1981;12(4):659–666.
- [18] Hultgren RK, Desai PD, Hawkins DT, Gleiser M, Kelley K. Selected values of the thermodynamic properties of binary alloys. 1st ed. American Society for Metals; 1993.
- [19] Bhatia AB, Hargrove WH. Concentration fluctuations and thermodynamic properties of some compound forming binary molten systems. *Physical Review B*. 1974;10(8):3186–3196.
- [20] Bhatia AB, Hargrove WH, Thornton DE. Concentration fluctuations and partial structure factors of compound-forming binary molten alloys. *Physical Review B*. 1974;9(2):435–444.
- [21] Koirala I, Singh BP, Jha IS. Theoretical assessment on segregating nature of liquid In–Tl alloys. *Journal of Non-Crystalline Solids*. 2014;398-399:26–31.
- [22] Jha IS, Singh RN, Srivastava PL, Mitra NR. Stability of HgNa and HgK liquid alloys. *Philosophical Magazine B*. 1990;61(1):15–24.
- [23] Jha IS, Koirala I, Singh BP, Adhikari D. Concentration dependence of thermodynamic, transport and surface properties in Ag–Cu liquid alloys. *Applied Physics A*. 2014;116(3):1517–1523.
- [24] Singh BP, Koirala I, Jha IS, Adhikari D. The segregating nature of Cd–Pb liquid binary alloys. *Physics and Chemistry of Liquids*. 2014;52(4):457–470.

BIBECHANA

ISSN 2091-0762 (Print), 2382-5340 (Online)

Journal homepage: <http://nepjol.info/index.php/BIBECHANA>

Publisher: Department of Physics, Mahendra Morang A.M. Campus, TU, Biratnagar, Nepal

Investigation on thermo-physical properties of liquid In-Tl alloy

I. B. Bhandari^{1,2}, N. Panthi^{1,3}, I. Koirala^{1*}

¹Central Department of Physics, Tribhuvan University, Kirtipur, Nepal

²Department of Applied Sciences, Purwanchal Campus, Tribhuvan University, Dharan, Nepal

³Department of Physics, Patan Multiple Campus, Tribhuvan University, Lalitpur, Nepal

*E-mail: ikphysicstu@gmail.com

Article Information:

Received: June 29, 2020

Accepted: August 8, 2020

Keywords:

Mixing properties

Ordering energy

Complex formation model

Segregation

ABSTRACT

This research explores mixing behaviour of liquid In – Tl system through thermodynamic and the structural properties on the basis of Complex Formation Model. The properties like surface tension and viscosity have been analyzed through simple statistical model and Moelwyn – Hughes equation. The interaction parameters are found to be positive, concentration independent and temperature dependent. Theoretical results are in a good agreement with the corresponding literature data which support homo-coordinating tendency in the liquid In-Tl alloy.

DOI: <https://doi.org/10.3126/bibechana.v18i1.29531>

This work is licensed under the Creative Commons CC BY-NC License. <https://creativecommons.org/licenses/by-nc/4.0/>

1. Introduction

Indium is a substance which is used in solder alloys which are applied in electronics for assembling semiconductor chips to a base and hybrid integrated circuits and to seal glass to metal in vacuum tubes. Fusible indium alloys are used to bend thin walled tubes without wrinkling the wall or changing the original cross-section. These alloys are not only used in fire control system, restraining links that hold alarm, water valve and door operating mechanism but also used as temperature indicators in situations where other methods of temperature measurements are impracticable and infeasible [1].

Indium is also used in nuclear reactor control rod alloys, low pressure sodium lamps and alkaline batteries. Additions of indium to lead–tin bearings are utilized in piston type aircraft engines, high performance automobile engines and in turbo–diesel truck engines. The addition of indium to gold dental alloys recuperates their mechanical properties and increases resistance to discoloring. Small amount of indium is used to improve the machinability of gold alloys for jewelry [1]. The indium–thallium alloy is a classic type of shape memory alloy with a low melting temperature. It has wide range of practical applications in the field of metallurgy which includes the use in

thermostats, hydraulic lines and electrical circuits [2]. Thallium alone is improper for direct use because of its properties of toxicity, unfavorable mechanical properties and significant tendency to oxidize. Thallium contains the most constant atomic vibration so far experimented. This property of Tl preceded it to be used in atomic clocks. Thallium immediately forms alloys with most other metals. There is incomplete mutual insolubility with iron and limited solubility in the liquid state with copper, aluminum, zinc, arsenic, manganese and nickel. Gold, silver, cadmium and tin formulate simple eutectic point with thallium. Thallium also forms binary alloys with antimony, barium, calcium, cerium, cobalt, germanium, lanthanum, lithium, magnesium, strontium, tellurium, bismuth and indium. The ternary alloys of thallium Tl–Pb–Bi, Tl–Al–Ag, In–Hg–Tl, Sn–Cd–Tl, Bi–Sn–Tl and Bi–Cd–Tl are used as semiconductors in ceramic compounds. Thallium has good wear resistance when it is used in bearing shafts. Thallium containing alloys are frequently recommended for bearings, electronics industry such as in solid state rectifiers, electrical fuses and soldering materials [1]. The study of In-Tl alloy is also useful to investigate the corresponding higher order alloy through different approaches [3]. There is difficulty in studying the properties of alloys in liquid state due to lack of long range atomic order. Therefore, theoreticians have exercised different models to understand the properties of various binary liquid alloys [4–22]. The different properties were studied at fixed temperature of 723 K through different models. In present work, we have explored the energetic of In – Tl alloy at a temperature of 723K using complex formation model [23]. The outcomes are analyzed and compared with literature data [24] to explicate the accuracy of this method in thermodynamic and structural description of the presented binary system.

2. Theory

Thermodynamic properties

If a binary alloy contains $N_A = x$ number of A atoms and $N_B = (1-x)$ number of B atoms, so that

total number of atoms is $N = N_A + N_B$. When components A and B are amalgamated together to form a binary A-B solution, thermodynamic properties are changed. The liquid alloy is considered to be ternary mixture of three species; A atom, B atom and chemical complex A_uB_v , is also called conformal solution. The number of free atoms will be reduced due to compound formation in the melt. Now for n_1g atoms of A, n_2g atoms of B and n_3g atoms of A_uB_v ,

$$n_1 = x - un_3 \text{ and } n_2 = (1 - x) - vn_3 \quad (1)$$

The total number of atoms after mixing can be given as

$$n = n_1 + n_2 + n_3 = 1 - (u + v - 1)n_3 \quad (2)$$

The free energy of mixing of the binary A-B mixture can be written as [23],

$$G_M = -n_3g + G' \quad (3)$$

Here, $-n_3g$ stands for lowering of free energy due to compound formation, g is the formation energy of complex. G' is the free energy of mixing of the ternary mixture of A, B and A_uB_v . If the ternary mixture is an ideal solution,

$$G' = RT \sum n_i \ln \left(\frac{n_i}{n} \right) \quad (4)$$

If the effects of differences in sizes of the various constituents in the mixture cannot be ignored and the interaction ω_{ij} are small but not zero, the theory of regular solutions in the zeroth approximation [25] or the conformal solution approximation [26] is valid. For regular solution

$$G' = RT \sum n_i \ln \left(\frac{n_i}{n} \right) + \sum \omega_{ij} \left(\frac{n_i n_j}{n} \right) \quad (5)$$

This equation is concerned to conformal solution approximation. Where $\omega_{ij} = 0$ (for $i = j$) are termed as the interaction energies and by definition are independent of concentration, although they are depended upon temperature and pressure.

Now the expression for free energy of mixing G_M for the compound forming binary alloy is

$$G_M = -n_3g + RT \sum_{i=1}^3 n_i \ln \left(\frac{n_i}{n} \right) + \sum \sum_{i<j} \left(\frac{n_i n_j}{n} \right) \omega_{ij} \quad (6)$$

The expression for heat of mixing H_M is given by [23]

$$H_M = G_M - T \left(\frac{\partial G_M}{\partial T} \right)_P \quad (7)$$

Substituting for G_M ,

$$H_M = -n_3 g + RT \sum_{i=1}^3 n_i \ln \left(\frac{n_i}{n} \right) + \sum_{i<j} \sum \left(\frac{n_i n_j}{n} \right) \omega_{ij} - T \frac{\partial}{\partial T} \left[-n_3 g + RT \sum_{i=1}^3 n_i \ln \left(\frac{n_i}{n} \right) + \sum_{i<j} \sum \left(\frac{n_i n_j}{n} \right) \omega_{ij} \right]$$

$$H_M = -n_3 \left[g - T \left(\frac{\partial g}{\partial T} \right)_P \right] + \frac{1}{n} \sum_{i<j} \sum (n_i n_j) \left[\omega_{ij} - T \left(\frac{\partial \omega_{ij}}{\partial T} \right)_P \right] \quad (8)$$

The expression for entropy of mixing S_M can be obtained as [23]

$$S_M = n_3 \frac{\partial g}{\partial T} - R \sum_{i=1}^3 n_i \ln \frac{n_i}{n} - \sum_{i<j} \sum \frac{n_i n_j}{n} \frac{\partial \omega_{ij}}{\partial T} \quad (9)$$

The equilibrium value of n_3 at a given pressure and temperature is given by [23]

$$\left(\frac{\partial G_M}{\partial n_3} \right)_{T,P,N,C} = 0 \quad (10)$$

Substituting the value of G_M from Equation (6) and after some algebraic calculation

$$\ln(n_3 n^{u+v-1} n_1^{-u} n_2^{-v}) + Y = \frac{g}{RT} \quad (11)$$

The Equation (11) is called equilibrium equation, where

$$Y = \left[\frac{n_1 n_2}{n^2} (u + v - 1) - u \frac{n_2}{n} - v \frac{n_1}{n} \right] \frac{\omega_{12}}{RT} + \left[\frac{n_2 n_3}{n^2} (u + v - 1) - v \frac{n_3}{n} + \frac{n_2}{n} \right] \frac{\omega_{23}}{RT} + \left[\frac{n_1 n_3}{n^2} (u + v - 1) - u \frac{n_3}{n} + \frac{n_1}{n} \right] \frac{\omega_{13}}{RT} \quad (12)$$

Structural Properties

The concentration fluctuation at long wavelength limit is of good interest because any deviation from ideal value $S_{cc}^{id}(0)$ is significant in describing the nature of ordering and phase segregation in molten alloys. This has been used to investigate the nature

of atomic order. The concentration fluctuation at long wavelength limit is related with free energy of mixing by the expression [27],

$$S_{cc}(0) = \frac{RT}{\frac{\partial^2 G_M}{\partial c^2}} \quad (13)$$

$$S_{cc}(0) = \frac{RT}{RT \sum_{i=1}^3 \left(\frac{(n_i')^2}{n_i} - \frac{(n')^2}{n} \right) + 2n \sum_{i<j} \sum \omega_{ij} \left(\frac{n_i}{n} \right)' \left(\frac{n_j}{n} \right)'} \quad (14)$$

Theoretically computed values of $S_{cc}(0)$ can be compared with the observed values computed from activity data by the expression,

$$S_{cc}(0) = (1-x) a_A \left(\frac{\partial a_A}{\partial c} \right)_{T,P,N}^{-1} = x a_B \left(\frac{\partial a_B}{\partial c} \right)_{T,P,N}^{-1} \quad (15)$$

The ideal value of $S_{cc}(0)$ can be expressed as,

$$S_{cc}^{id}(0) = x(1-x) \quad (16)$$

The Warren–Cowley short range order parameter quantify the degree of local order in the binary alloy [28,29]. The theoretical values of this parameter can be calculated as

$$\alpha_1 = \frac{(s-1)}{s(z-1)+1}, S = \frac{S_{cc}(0)}{S_{cc}^{id}(0)} \quad (17)$$

where z is coordination number, which is taken as 10 for our calculation.

Transport Properties

The mixing behaviour of the alloys forming molten alloy can also be studied at the microscopic level in terms of coefficient of diffusion. The mutual diffusion coefficient (D_M) of binary liquid alloys can be expressed in terms of activity (a_i) and self-diffusion coefficient (D_{id}) of pure component with the help of Darken's equation [30]

$$D_M = D_{id} x \frac{d \ln a_i}{dx} \quad (18)$$

with $D_M = c_A D_B + c_B D_A$

where D_A and D_B are the self – diffusion coefficients of pure components A and B respectively,

The expression for D_M in terms of $S_{cc}(0)$ can be given as

$$\frac{D_M}{D_{id}} = \frac{S_{cc}^{id}(0)}{S_{cc}(0)} \quad (19)$$

The mixing behaviour of liquid alloys at microscopic level can also be understood in terms of viscosity. The Moelwyn – Hughes equation for viscosity of liquid alloy [31] is

$$\eta = \eta_{id} \left[1 - x_A x_B \left(\frac{2g}{RT} \right) \right] \quad (20)$$

with

$$\eta_{id} = x\eta_A + (1 - x)\eta_B$$

where η_i is the viscosity of pure component i. At temperature T, it is given by [32]

$$\eta_i = \eta_{i0} \exp \left(\frac{E}{RT} \right) \quad (21)$$

Here η_{i0} a constant in the unit of viscosity and E is the activation energy.

Surface Properties

The surface properties of the liquid mixture give insight into the metallurgical phenomenon, such as crystal growth, welding, gas absorption and nucleation of gas bubbles [33]. The expressions for surface tension proposed by Prasad et al., [34,35], has been reduced in the simple form using zeroth approximation as

$$\tau = \tau_A + \frac{k_B T}{\xi} \ln \frac{x^s}{x} + \frac{g}{\xi} [p(1 - x^s)^2 + (q - 1)(1 - x)^2] \quad (22)$$

$$\tau = \tau_B + \frac{k_B T}{\xi} \ln \frac{(1-x^s)}{(1-x)} + \frac{g}{\xi} [p(x^s)^2 + (q - 1)(x)^2] \quad (23)$$

where τ_A and τ_B are the surface tensions of pure components A and B respectively, x and x^s are the bulk and surface concentration of the components of alloy, p and q are called coordination fractions, which are defined as the fraction of the total number of nearest neighbors made by atom within its own layer and that in the adjoining layer. The coordination fractions p and q are related to each other by the relation

$$p + 2q = 1, \text{ for closed packed structure, } p = 0.5 \text{ and } q = 0.25$$

The expression for the mean atomic surface area ξ is

$$\xi = \sum c_i \xi_i \quad (24)$$

The atomic surface are for each component is

$$\xi_i = 1.102 \left(\frac{\Omega_i}{N_A} \right)^{2/3} \quad (25)$$

where Ω_i is the molar volume of the component i and N_A represents Avogadro number. Equating equations (22) and (23), we can solve it for x^s as the function of x and hence compositional dependence of surface tension can be evaluated.

where τ_A and τ_B are the surface tensions of pure components A and B respectively, x and x^s are the bulk and surface concentration of the components of alloy, p and q are called coordination fractions, which are defined as the fraction of the total number of nearest neighbors made by atom within its own layer and that in the adjoining layer. The coordination fractions p and q are related to each other by the relation

$$p + 2q = 1, \text{ for closed packed structure, } p = 0.5 \text{ and } q = 0.25$$

The expression for the mean atomic surface area ξ is

$$\xi = \sum c_i \xi_i \quad (24)$$

The atomic surface are for each component is

$$\xi_i = 1.102 \left(\frac{\Omega_i}{N_A} \right)^{2/3} \quad (25)$$

where Ω_i is the molar volume of the component i and N_A represents Avogadro number. Equating equations (22) and (23), we can solve it for x^s as the function of x and hence compositional dependence of surface tension can be evaluated.

3. Results and Discussion

Thermodynamic properties

The experimental data on the thermodynamic properties as well as phase diagram information [24] have been used for the calculation of order energy parameters for liquid phase In–Tl system. The data set of the Gibbs energy of mixing (G_M) were taken as input data to calculate by the CFM the interaction energy parameters, i.e. g, ω_{12} , ω_{13} , ω_{23} . The starting values of g/RT and ω_{ij} /RT were obtained as suggested in ref. [23]. Equilibrium Equation (11) along with Equations (1) and (2) were applied to compute the number of complexes,

n_3 , as a function of concentration. The values of interaction energy parameters were adjusted to give the concentration dependence of free energy of mixing which fits well with the corresponding thermodynamic data. From the phase diagram [24] In-Tl alloy is expected to aggregate with stoichiometry In-Tl ($u = 1, v = 1$). The calculations were done at temperature of 723 K. The interaction energy parameters for In-Tl liquid alloys are found to be $g = 0.755 RT$, $\omega_{12} = 0.476 RT$, $\omega_{13} = 1.610 RT$ and $\omega_{23} = 1.481 RT$. The positive interaction energies imply the repulsion between the corresponding species.

The concentration dependence of the equilibrium values of chemical complexes, n_3 , (Fig. 1) displays the symmetry with the maximum value of 0.4178 at equiatomic composition. The curve describing the Gibbs free energy of mixing of the In-Tl liquid phase is symmetric with respect to the equiatomic composition (Fig. 2). Theoretical calculation of free energy of mixing for In-Tl liquid alloy shows that In - Tl alloy in liquid state is weakly interacting or homo-coordinating system. There is an excellent agreement between the experimental and calculated integral free energies. Very poor agreement of calculated values of H_M and S_M with experimental simply indicates the importance of the dependence of interaction energies on temperature. To account this, we have used Equations (8) and (9) to determine the variation in energy parameters with respect to temperature from experimental values of H_M and S_M [24]. The temperature dependent interaction energies at $T=723K$ are found to be

$$\frac{1}{R} \frac{\partial g}{\partial t} = 0.845, \quad \frac{1}{R} \frac{\partial \omega_{12}}{\partial t} = 0.383,$$

$$\frac{1}{R} \frac{\partial \omega_{13}}{\partial t} = 1.493,$$

$$\frac{1}{R} \frac{\partial \omega_{23}}{\partial t} = 1.430$$

It is found from the present analysis that the heat of mixing and entropy of mixing both are positive at all concentrations. Our theoretical calculation shows that the maximum value of the heat of mixing is 0.0512 RT at $x_{In} = 0.6$ (Fig.3) and the

maximum value of entropy of mixing is 0.6107 at $x_{In} = 0.5$ (Fig.4). There is excellent agreement between experimental and calculated values of H_M . The calculated values of S_M deviates from experimental values by maximum percentage of 8.31 at $x_{In} = 0.8$ and by minimum percentage of 5.56 at $x_{In} = 0.4$. This deviation is because of the propagation of error from previous calculation.

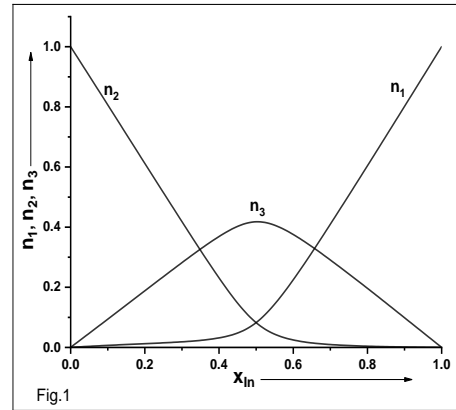


Fig.1: Number of complexes (n_1, n_2, n_3) vs. concentration x_{In} of liquid In - Tl alloy at 723K.

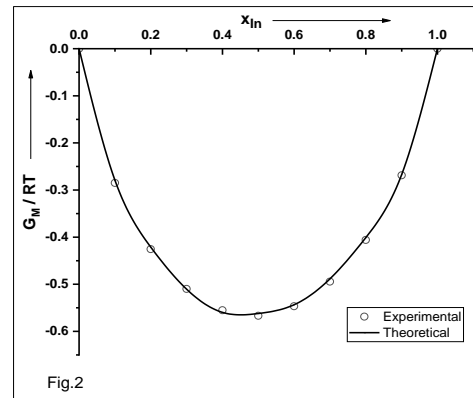


Fig. 2: Free energy of mixing (G_M/RT) vs. concentration (x_{In}) of liquid In - Tl alloy at 723K.

Structural Properties

It has been reported that when $S_{CC}(0) < S_{CC}^{id}(0)$, the existence of chemical ordering leading to complex

formation is expected while $S_{cc}(0) > S_{cc}^{id}(0)$, is an indication of segregation. The same interaction parameters used in the calculation of the thermodynamic properties were employed in the calculations of $S_{cc}(0)$ using Equation (14) while the experimental values of $S_{cc}(0)$ were obtained from Equation (15) using the experimental activity data. The results obtained from the above computations are plotted in Fig. (5). It is found that $S_{cc}(0) > S_{cc}^{id}(0)$ throughout the entire concentration range, this also confirms the presence of chemical segregation or a preference for like atoms to pair. The value of short range order parameter is positive through the whole concentration range which indicates that the alloy is segregating at all compositions. The value of short range order parameter has been found maximum (= 0.02438) at $x_{In} = 0.5$ at 723 K (Fig. (6)).

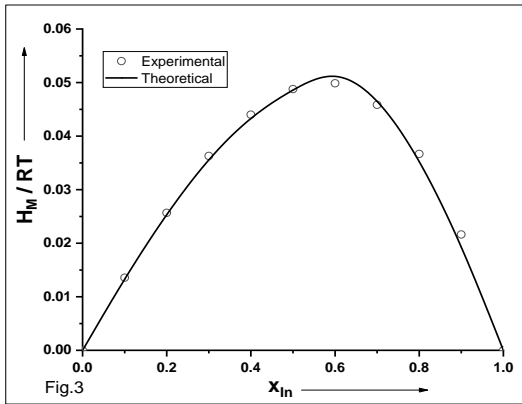


Fig. 3: Heat of mixing (H_M) vs. concentration of indium (x_{In}) in the liquid In - Tl alloy at 723K.

Transport Properties

The calculated values of $S_{cc}(0)$ by Equation (17) can be applied to evaluate the ratio of the mutual and intrinsic-diffusion coefficients (D_M/D_{id}) using Equation (19), against the concentration of indium. We note that the ratio of diffusivities can also be used to indicate levels of order in the liquid binary alloys. The presence of chemical order is indicated by $D_M/D_{id} > 1$. Similarly, $D_M/D_{id} < 1$ suggests the tendency for segregation. Fig. (7) shows the plots

D_M/D_{id} against concentration of indium. It can be observed that the ratio D_M/D_{id} is less than 1 throughout the whole concentration range. This indicates the homo – coordinating tendency in In–Tl alloys at the temperature of investigation. It is also noticed that D_M/D_{id} exhibits maximum peak at around the equi-atomic composition. The result predicted by D_M/D_{id} is in agreement with the results obtained from the free energy of mixing, concentration fluctuations and CSRO parameter.

The viscosity of the In–Tl liquid alloy has been calculated numerically using Equation (20). From the plot of η versus bulk concentration of indium (Fig. 8) small negative deviation from the linear law (Raoult's law) in viscosity isotherms $\eta(x)$ has been inspected.

Surface Properties

The surface concentrations and surface tension of In–Tl alloy have been computed numerically using Equations (22) and (23). The values of densities and surface tension at melting temperature (T^0) of pure atoms are taken from ref. [32]. These values have been optimized at required temperature (T) by using the expressions

$$\rho_i(T) = \rho_i^0 + (T - T_i^0) d\rho_i/dt \quad (26)$$

$$\tau_i(T) = \tau_i^0 + (T - T_i^0) d\tau_i/dt \quad (27)$$

where $d\rho_i/dt$ and $d\tau_i/dt$ represent temperature coefficients of density and surface tension respectively for the components of the metal alloys.

The computed values of surface concentration for molten In–Tl alloys at 723 K are depicted in Fig. (9). Surface concentration of indium in In–Tl alloys is found to increase with the increase of bulk concentration of In. The computed surface tension for In–Tl alloys at 723 K is less than ideal values at all concentrations of indium; i.e., there is negative departure of surface tension from ideality ($\tau = \tau_A x + \tau_B(1-x)$) throughout the bulk concentrations of indium in In–Tl alloys (Fig. 10). For the In–Tl melt, the surface tension of Tl is smaller than that of In atom. Therefore, Tl atoms having lower surface tension segregates on the surface phase but In

atoms remains in the bulk phase throughout the entire composition.

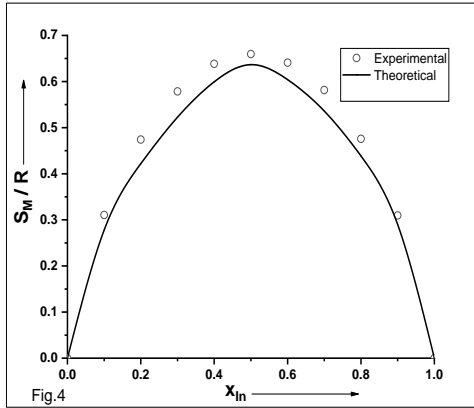


Fig. 4: Entropy of mixing (S_M) vs. concentration of indium (x_{In}) in the liquid In - Tl alloy at 723K.

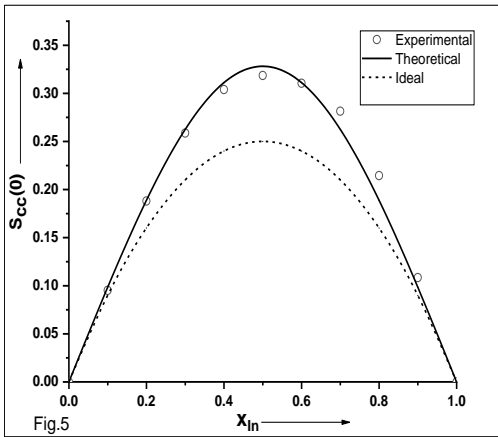


Fig. 5: Concentration fluctuation at long wavelength limit ($S_{cc}(0)$) vs. concentration of indium (x_{In}) in the liquid In - Tl alloy at 723K.

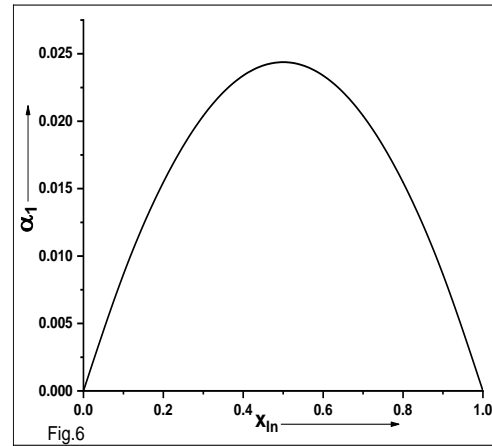


Fig. 6: Chemical short range order (α_1) vs. concentration of indium (x_{In}) in the liquid In - Tl alloy at 723K.

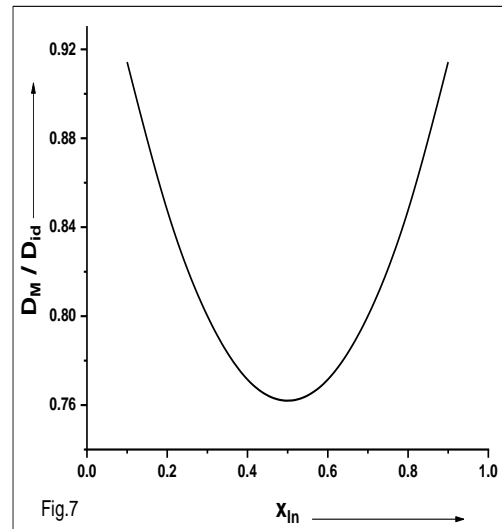


Fig. 7: Ratio of mutual and intrinsic diffusion coefficients (D_M/D_{id}) vs. concentration of indium (x_{In}) in the liquid In - Tl alloy at 723K.

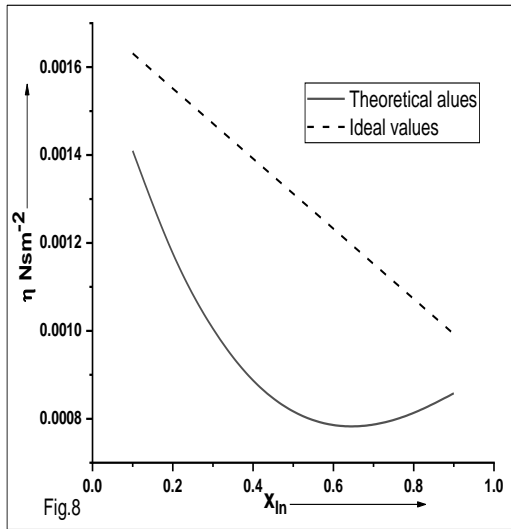


Fig. 8: Viscosity (η) vs. concentration of indium (x_{In}) in the liquid In - Tl alloy at 723K.

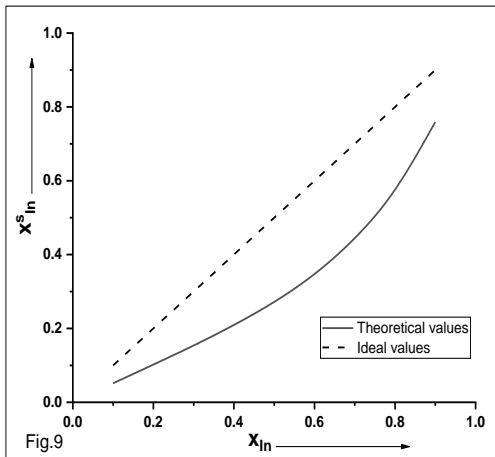


Fig. 9: Surface concentration of indium (x_{In}^s) vs. bulk concentration of indium (x_{In}) in the liquid In - Tl alloy at 723K.

4. Conclusions

The theoretical analysis of the thermodynamic properties reveals that there is a tendency of like atom pairing in the liquid In–Tl alloys at all concentrations. The ordering energy is found to be positive and temperature dependent. The study of

concentration fluctuation in long wavelength limit and CSRO show that there is tendency of phase separation in In–Tl liquid alloy. Negative deviation of viscosity isotherms from Raoult law is observed. Viscosity of the alloys decreases with increase in the concentrations of indium. The ratio of diffusion coefficients (D_M/D_{id}) is found to be greater than one at all compositions which also indicates segregating tendency of the system. At the temperature of investigation, the surface tension increases with the increase in the bulk concentration of In. The surface tension of the liquid In–Tl alloy is found to be smaller than ideal values.

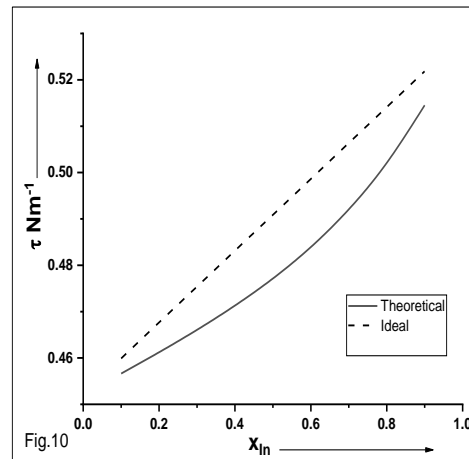


Fig. 10: Surface tension (τ) vs. bulk concentration of indium (x_{In}) in the liquid In - Tl alloy at 723K.

References

- [1] F. Habashi, ed., Alloys Preparation, Properties, Applications, First, Wiley-VCH (1998).
- [2] Z.P. Luo, An Overview on the Indium-Thallium (In-Tl) Shape Memory Alloy Nanowires, *Metallogr. Microstruct. Anal.* 1 (2012) 320. <https://doi.org/10.1007/s13632-012-0046-4>
- [3] U. Mehta, S.K. Yadav, I. Koirala, D. Adhikari, Thermo-physical properties of ternary Al–Cu–Fe alloy in liquid state, *Philos. Mag.* 0 (2020) 1. <https://doi.org/10.1080/14786435.2020.1775907>
- [4] D. Adhikari, A Theoretical study of thermodynamic properties of Cd-Bi liquid alloy, *BIBECHANA* 8 (2012) 90.

- <https://doi.org/10.3126/bibechana.v8i0.5693>
- [5] D. Adhikari, I.S. Jha, B.P. Singh, J. Kumar, Thermodynamic and structural investigations of liquid magnesium – thallium alloys, *J. Mol. Struct.* 985 (2011) 91. <https://doi.org/10.1016/j.molstruc.2010.10.026>
- [6] S. Lele, P. Ramachandrarao, Estimation of complex concentration in a regular associated solution, *Metall. Trans. B* 12 (1981) 659. <https://doi.org/10.1007/BF02654134>
- [7] R. Novakovic, Thermodynamics, surface properties and microscopic functions of liquid Al – Nb and Nb – Ti alloys, *J. Non. Cryst. Solids*. 356 (2010)1593. <https://doi.org/10.1016/j.jnoncrysol.2010.05.055>
- [8] R. Novakovic, D. Giuranno, E. Ricci, T. Lanata, Surface and transport properties of In – Sn liquid alloys, *Surf. Sci.* 602 (2008) 1957. <https://doi.org/10.1016/j.susc.2008.03.033>
- [9] Y.A. Odusote, Bulk and dynamic properties in Al – Zn and Bi – In liquid alloys using a theoretical model, *J. Non. Cryst. Solids*. 353 (2007) 1167. <https://doi.org/10.1016/j.jnoncrysol.2006.12.023>
- [10] L.C. Prasad, R.N. Singh, A quasi-lattice model for the thermodynamic properties of au-zn liquid alloys, *Phys. Chem. Liq.* 22 (1990) 1. <https://doi.org/10.1080/00319109008036406>
- [11] L.C. Prasad, R.N. Singh, V.N. Singh, S.K. Chatterjee, Compound formation in Sn-based liquid alloys, *Phys. B Phys. Condens. Matter*. 215 (1995) 225. [https://doi.org/10.1016/0921-4526\(95\)00393-N](https://doi.org/10.1016/0921-4526(95)00393-N)
- [12] R.N. Singh, A.B. Bhatia, Flory 's formula for the entropy of mixing of NaCs alloy, *J. Phys. F: Met. Phys.* 14 (1984) 2309. <https://doi.org/10.1088/0305-4608/14/10/009>
- [13] S.K. Yadav, S. Lamichhane, L.N. Jha, N.P. Adhikari, D. Adhikari, Mixing behaviour of Ni–Al melt at 1873 K, *Phys. Chem. Liq.* 54 (2016) 370. <https://doi.org/10.1080/00319104.2015.1095640>
- [14] S.K. Yadav, U. Mehta, R.K. Gohivar, A. Dhungana, R.P. Koirala, D. Adhikari, Reassessments of thermo-physical properties of Si-Ti melt at different temperatures, *BIBECHANA* 17 (2020) 146. <https://doi.org/10.3126/bibechana.v17i0.26877>
- [15] O. Akinlade, R.N. Singh, Bulk and surface properties of liquid In-Cu alloys, *J. Alloys Compd.* 333 (2002) 84. [https://doi.org/10.1016/S0925-8388\(01\)01733-9](https://doi.org/10.1016/S0925-8388(01)01733-9)
- [16] B.C. Anusionwu, G.A. Adebayo, Quasi-chemical studies of ordering in the Cu–Zr and Cu–Si melts, *J. Alloy. Compd.* 329 (2001) 162. [https://doi.org/10.1016/S0925-8388\(01\)01572-9](https://doi.org/10.1016/S0925-8388(01)01572-9)
- [17] O.E. Awe, Thermodynamic investigation of thermophysical properties of thallium-based liquid alloys, *Phys. Chem. Liq.* 57 (2019) 296. <https://doi.org/10.1080/00319104.2018.1443453>
- [18] O.E. Awe, O. Akinlade, L.A. Hussain, Thermodynamic properties of liquid Te–Ga and Te–Tl alloys, *J. Alloys Compd.* 361 (2003) 227. [https://doi.org/10.1016/S0925-8388\(03\)00451-1](https://doi.org/10.1016/S0925-8388(03)00451-1)
- [19] A.B. Bhatia, W.H. Hargrove, D.E. Thornton, Concentration fluctuations and partial structure factors of compound-forming binary molten alloys, *Phys. Rev. B* 9 (1974) 435. <https://doi.org/10.1103/PhysRevB.9.435>
- [20] A.B. Bhatia, R.N. Singh, A Quasi-lattice Theory for Compound Forming Molten Alloys, *Phys. Chem. Liq.* 13 (1984) 177. <https://doi.org/10.1080/00319108608078511>
- [21] I. Koirala, I.S. Jha, B.P. Singh, Theoretical investigation on ordering nature of Cd-Bi alloys in the molten dtatemolten state, *BIBECHANA*. 11 (2014) 70. <https://doi.org/10.3126/bibechana.v11i0.10382>
- [22] I. Koirala, B.P. Singh, I.S. Jha, Theoretical assessment on segregating nature of liquid In–Tl alloys, *J. Non. Cryst. Solids* 398 (2014) 26. <https://doi.org/10.1016/j.jnoncrysol.2014.04.018>
- [23] A.B. Bhatia, W.H. Hargrove, Concentration fluctuations and thermodynamic properties of some compound forming binary molten systems, *Phys. Rev. B* 10 (1974) 3186. <https://doi.org/10.1103/PhysRevB.10.3186>
- [24] R. Hultgren, P.D. Desai, D.T. Hawkins, M. Gleiser, K.K. Kelley, Selected Values of the Thermodynamic Properties of Binary Alloys., American Society for Metals, Metal Park, Ohio, (1973).
- [25] E.A. Guggenheim, *Mixtures*, Oxford University Press, London (1952).
- [26] H.C. Longuet-Higgins, The statistical thermodynamics of multicomponent systems, *Proc. R. Soc. London. Ser. A. Math. Phys. Sci.* 205 (1951) 247. <https://doi.org/10.1098/rspa.1951.0028>
- [27] A.B. Bhatia, D.E. Thornton, Structural aspects of the electrical resistivity of binary alloys, *Phys. Rev. B* 2 (1970) 3004.

- <https://doi.org/10.1103/PhysRevB.2.3004>
- [28] B.E. Warren, X-ray Diffraction, Dover Publication, New York, 1990.
- [29] J.M. Cowley, An approximate theory of order in alloys, Phys. Rev. 77 (1950) 669. <https://doi.org/10.1103/PhysRev.77.669>
- [30] L.S. Darken, R.W. Gurry, Physical Chemistry of Metals, McGraw Hill, New York (1953).
- [31] E.A. Moelwyn-Hughes, Physical Chemistry, Second, Pergamon, Oxford (1964).
- [32] E.A. Brandes, G.B. Brook, Smithells Metals Reference Book, Seventh, Butterworth-Heinemann Linacre House, Jordan Hill, Oxford, 1992. <https://doi.org/10.1016/B978-075067509-3/50014-2>
- [33] J.A.V. Butler, The Thermodynamics of the Surfaces of Solutions, R. Soc. A. (1932) 348. <https://doi.org/10.1098/rspa.1983.0054>
- [34] L.C. Prasad, R.N. Singh, V.N. Singh, G.P. Singh, Correlation between Bulk and Surface Properties of AgSn Liquid Alloys, J. Phys. Chem. B 102 (1998) 921. <https://doi.org/10.1021/jp971042l>
- [35] L.C. Prasad, R.N. Singh, Surface segregation and concentration fluctuation at the liquid-vapor interface of molten Cu-Ni alloys, Phys. Rev. B 44 (1991) 768. <https://doi.org/10.1103/PhysRevB.44.13768>

Temperature-dependent mixing behavior of Pb–Sb alloys in liquid state

Indra Bahadur Bhandari^{*,†,‡}, Narayan Panthi^{*}
and Ishwar Koirala^{*}

^{*}Central Department of Physics
Tribhuvan University, Kathmandu, Nepal

[†]Department of Applied Sciences
Purwanchal Campus, Tribhuvan University
Dharan, Nepal

[‡]bhandari.indra@gmail.com

Received 2 May 2021

Revised 26 June 2021

Accepted 26 June 2021

Published 4 August 2021

We have extended a computational model used to research the thermodynamic properties of binary liquid alloys to study chemical short-range order parameters and diffusion coefficients. Numerous simulations have also been employed for surface properties such as surface concentration and surface tension. The propensities for phase separation of the Pb–Sb alloy were also observed with a temperature rise. The structural and thermodynamic properties of the alloys were measured using the same interaction parameters that are suitable for the free energy of mixing and mixing enthalpy. The interaction parameters are discovered to be temperature-dependent but concentration-independent. Our results indicate that the liquid alloy Pb–Sb has a weakly interacting composition. According to the surface property review, the element Sb having a higher surface concentration than its bulk concentration segregates over the surface of the alloy.

Keywords: Segregation; deviation; ideality; symmetry; interaction parameters.

1. Introduction

The theoretical models used to analyze binary liquid alloy yield valuable knowledge as they deliver a substantial deviation from ideality in thermodynamic properties. On this basis, certain alloys are known to be symmetrical alloys [Adedipe *et al.*, 2019; Adhikari *et al.*, 2012a, 2012c; Akinlade and Boyo, 2004; Anusionwu, 2006; Attri *et al.*, 1996; Awe *et al.*, 2011; Jha *et al.*, 2014; Koirala *et al.*, 2014a, 2014b; Koirala, 2013; Novakovic *et al.*, 2014; Odusote, 2014; Rafique and Kumar, 2007; Singh *et al.*, 2014; Yadav *et al.*, 2015]. And alloys for which the deviation from

[‡]Corresponding author.

ideality of thermodynamic properties creates asymmetry apart from the equiatomic composition are recognized as asymmetric alloys [Adhikari *et al.*, 2012a, 2012c; Ajayi and Ogunmola, 2018; Akasofu *et al.*, 2020; Akinlade and Singh, 2002; Anusionwu *et al.*, 2009; Awe and Azeez, 2017; Bhandari *et al.*, 2020; Godbole *et al.*, 2004; Hoshino and Young, 1980; Ilo-Okeke *et al.*, 2005; Jha *et al.*, 2012, 2016; Koirala *et al.*, 2014a, 2014b; Kumar *et al.*, 2011; Mishra *et al.*, 2002; Novakovic *et al.*, 2014; Odusote and Popoola, 2017; Prasad *et al.*, 2007; Shrestha *et al.*, 2017; Singh *et al.*, 2012; Singh and Arafin, 2015; Yadav *et al.*, 2020]. The asymmetry in thermodynamic properties of binary melt is primarily related to the size effect [Singh, 1987] and disparity in electronegativity [Akinlade *et al.*, 2000]. In the case of Pb–Sb liquid alloy, the size ratio (≈ 1.074) and the electronegativity difference (≈ 0.28) are sufficiently small to induce appreciable thermodynamic properties asymmetry.

There are a variety of models available that can be used to estimate the thermodynamic properties of binary liquid alloys. The researchers have explored the energetics of liquid alloy through different theoretical models such as Quasi Chemical Approximation [Adhikari *et al.* 2012; Ajayi and Ogunmola, 2018; Anusionwu, 2006; Awe and Onifade, 2012; Jha *et al.*, 2016], Regular Associated Solution Model [Adhikari *et al.*, 2012; Jha *et al.*, 2012; Singh *et al.*, 2010; Yadav *et al.*, 2016], Four Atom Cluster Model [Akinlade *et al.*, 2003; Singh, 1993] and Flory Model [Adhikari, 2012; Odusote, 2014]. The Compound Formation Model [Akinlade and Boyo, 2004; Attri *et al.*, 1996; Awe and Oshakuade, 2016; Bhandari *et al.*, 2020; Godbole *et al.*, 2004; Kumar *et al.*, 2006; Mishra, 2007; Novakovic *et al.*, 2012; Rafique and Kumar, 2007], Regular Solution Model [Akasofu *et al.*, 2020], Simple Statistical Model [Anusionwu *et al.*, 1998; Anusionwu and Ilo-Okeke, 2005; Koirala *et al.*, 2014a, 2014b; Singh *et al.*, 2014, 2017], Singh and Sommer Model [Akinlade *et al.*, 1999; Anusionwu *et al.*, 2009; Anusionwu and Ilo-Okeke, 2005; Ilo-Okeke *et al.*, 2005] and Self-Association Model [Akinlade *et al.*, 2001; Awe and Azeez, 2017; Koirala *et al.*, 2015; Odusote *et al.*, 2016; Odusote and Popoola, 2017] are also widely used for the investigation of microscopic properties and thermodynamics of many binary liquid alloys. Recently, with the aid of RK Polynomial, Gohivar *et al.* clarified the miscibility gaps (artefacts) in the thermodynamics of certain binary melt [Gohivar *et al.*, 2020]. In addition, the complex-forming behavior of Cu–Sn alloy was studied by quasi-chemical approximation (QCA) and the temperature-dependent mixing behavior of Bi–Mg liquid alloy was evaluated by a compound formation model [Bhandari *et al.*, 2020; Panthi *et al.*, 2020]. The use of a model to conduct thermodynamic calculations can be a function of the class of the binary alloy (whether short-range ordered or phase separating). Interatomic interactions and associated energies of bonding between the A and B elements of binary alloys play an important role in the understanding of the mixing nature of the two metals. In the face of that, energetically, preferred hetero-coordination of A–B atoms as closest neighbors

over self-coordination of A–A and B–B atoms or vice versa leads to the grouping of all binary alloys into two distinct groups: short-range ordered or segregating.

Low melting point lead alloys can be cast into several forms using a number of molding materials and casting techniques. Antimony, calcium, tin, copper, tellurium, arsenic and silver are the primary alloy metals used to strengthen lead. The primary uses of lead alloys include lead-acid accumulator batteries; cable sheathing; sheet building, wire and welding; bearings; gaskets; special castings; anodes; fusible alloys; shielding and weights. Because of the corrosion resistance of lead and lead alloys, their use is often correlated with the development of protective corrosion film. Lead-antimony is the most commonly used lead alloy. These alloys are very important materials for use in industry as die casting alloys and in the production of acidic accumulators [Mostafa, 2004]. The addition of arsenic significantly increases the rate of ageing and final strength. The addition of tin increases fluidity and decreases the oxidation rate of molten lead-antimony alloys in conjunction with copper and arsenic. Large antimony alloys (>3.5% antimony) are reinforced mainly by the eutectic phase, whereas low antimony alloys are reinforced by precipitation. The primary application of lead-antimony alloys is as grids, posts and connectors for lead-acid batteries [Habashi, 1998]. The addition of Sb to Pb resulted in improved mechanical properties and improved castability, enabling the development of complicated shapes [Gancarz and Gasior, 2018]. According to the Pb–Sb phase diagram, with the eutectic point at 524.5 K for 16.75 at.% Sb, Pb–Sb alloys with 1–10 at.% Sb can be used in continuous casting and gravity casting applications, more often for lead electrodes for batteries [Okamoto, 2011]. Many studies have emphasized the Pb–Sb binary system in numerous ways in the past. In the past, several researchers have explored the Pb–Sb binary system in various ways. Thermodynamic properties of the Pb–Sb alloys were explored using emf measurements in the temperature range 720–890 K over a broad composition range [Arkhipov *et al.*, 2013]. The phase diagram of Pb–Sb system has been reproduced and the enthalpies and activities are re-assessed [Gierlotka *et al.*, 2013]. Electrical resistivity and viscosity of Pb–Sb alloys are measured and the temperature dependence of the resistivity varies constantly as the melts reach the undercooled liquid state [Guo *et al.*, 2012]. Lead-antimony alloy mixing enthalpies were calculated by direct liquid–liquid reaction calorimetry (DLLRC) and thermodynamic modeling at different temperatures [Hassam *et al.*, 2009]. Thermodynamic properties of the Pb–Sb alloys are analyzed by the emf measurement system at $T = 723\text{--}873\text{ K}$ for an expanded composition area [Zaikov *et al.*, 2007].

In this work, the free mixing energy, the mixing enthalpy and the mixing entropy as well as the concentration variations in the long-wavelength limit of liquid Pb–Sb alloys have been quantitatively discussed using the complex-forming model. The model is generalized to estimate short-range order parameters and diffusion coefficients and is further extended to observe the temperature-dependent nature of Pb–Sb liquid alloys. In particular, as regards the transport and surface properties

such as surface tension, diffusivity and viscosity of Pb–Sb liquid alloys, an absence of experimental observations at the investigation temperature was found. It is only possible to estimate the missing values by theoretical models.

In the next section, we will present the related formalism required for the present calculation; in Sec. 3, we will discuss our findings. At the end of the paper, we summarize our conclusions.

2. Theory

The benefit of the complex-formation model (CFM) [Bhatia and Hargrove, 1974; Jha *et al.*, 1990; Novakovic *et al.*, 2011; Sharma *et al.*, 2013] is that it attempts to take into account the stabilization of compound by the concentration-dependent free energy of mixing G_M , heat of mixing H_M and concentration fluctuation in the long-wavelength limit $S_{cc}(0)$. Within the context of the CFM, there are two approximations which make it possible to correctly approach the heteroatomic interactions of atoms in the liquid state: the approximation for strongly [Westbrook and Fleischer, 1995] and the approximation for weakly [Bhatia and Singh, 1984] interactive systems. The lack of clusters in the mixture reduces the formalism to a QCA for regular solutions [Guggenheim, 1952]. Formalism in weak interaction approximation is applied to liquid Pb–Sb alloys to describe the behavior of their mixing properties.

The mixing entropy is related to the free energy of mixing and enthalpy of mixing as follows:

$$S_M = (H_M - G_M)/T. \quad (1)$$

In the framework of CFM, A–B liquid alloy is considered to be a pseudo-ternary mixture consisting of A-atoms, B-atoms and chemical complexes $A_\alpha B_\beta$ with intermetallic stoichiometry present in a solid-state, all in chemical equilibrium with each other. If there are x_1 g moles of A atoms, x_2 g moles of B atoms and x_3 g moles of $A_\alpha B_\beta$ complexes in the mixture, then the free energy can be expressed as follows:

$$G_M = -x_3\chi + RT \sum_{i=1}^3 x_i \ln \left(\frac{x_i}{x} \right) + \sum_{i<j} \Psi_{ij} \left(\frac{x_i x_j}{x} \right). \quad (2)$$

Here, the first term $-x_3\chi$ stands for lowering of the free energy due to the formation of complex $A_\alpha B_\beta$, χ is the formation energy of the complex, Ψ_{ij} ($i = 1, 2, 3$) are the average interaction energies among the species i and j . The heat of formation is given as follows:

$$H_M = G_M - T(\partial G_M / \partial T)_{P,c,N}, \quad (3)$$

$$H_M = -x_3 \left[\chi - T \left(\frac{\partial \chi}{\partial T} \right) \right] + \sum_{i<j} \sum \left(\frac{x_i x_j}{x} \right) \left[\Psi_{ij} - T \left(\frac{\partial \Psi_{ij}}{\partial T} \right) \right]. \quad (4)$$

The values of the interaction energy parameters at the corresponding temperature can be used to observe the behavior of the liquid alloy at higher temperatures. The

value of the energy interaction parameters at the required temperature (T_R) can be determined from the following relation:

$$\Psi_{ij}(T_R) = \Psi_{ij}(T) + (T - T_R) \frac{\partial \Psi_{ij}}{\partial T}. \quad (5)$$

The value of x_3 can be calculated at a given pressure and temperature from the equilibrium state of the free mixing energy, G_M as follows:

$$\left(\frac{\partial G_M}{\partial x_3} \right)_{T,P,c} = 0. \quad (6)$$

From Eqs. (2) and (6), the equilibrium value of x_3 is given by the equation,

$$(x_3 x^{\alpha+\beta-1} x_1^{-\alpha} x_2^{-\beta})^{-1} = \exp \left(\Phi - \frac{\chi}{RT} \right), \quad (7)$$

where

$$\begin{aligned} \Phi &= \Phi_1 + \Phi_2 + \Phi_3 \\ \Phi_1 &= \left[(\alpha + \beta - 1) \frac{x_1 x_2}{x^2} - \alpha \frac{x_2}{x} - \beta \frac{x_1}{x} \right] \frac{\Psi_{12}}{RT} \\ \Phi_2 &= \left[(\alpha + \beta - 1) \frac{x_2 x_3}{x^2} - \beta \frac{x_3}{x} + \frac{x_2}{x} \right] \frac{\Psi_{23}}{RT} \\ \Phi_3 &= \left[(\alpha + \beta - 1) \frac{x_1 x_3}{x^2} - \alpha \frac{x_3}{x} + \frac{x_1}{x} \right] \frac{\Psi_{13}}{RT}. \end{aligned} \quad (8)$$

The number of complexes of A , B and $A_\alpha B_\beta$ are connected to each other as follows:

$$\begin{aligned} x_1 &= c - \alpha x_3, \quad x_2 = (1 - c) - \beta x_3 \quad \text{and} \\ x &= x_1 + x_2 + x_3 = 1 - (\alpha + \beta - 1)x_3, \end{aligned} \quad (9)$$

where α and β are small integers determined from the stoichiometry of energetically favored compounds and c is the atomic fraction of A atoms.

Using Eqs. (2) and (4) in Eq. (1) we get

$$S_M = x_3 \frac{\partial \chi}{\partial T} - R \sum_{i=1}^3 x_i \ln \frac{x_i}{x} - \sum_{i < j} \sum \left(\frac{x_i x_j}{x} \right) \frac{\partial \Psi_{ij}}{\partial T}. \quad (10)$$

Knowledge of diffusivity and viscosity provides a greater understanding of the mixing behavior of the binary liquid alloy at the atomic level. The Moelwyn-Hughes equation for the viscosity of liquid alloy [Budai *et al.*, 2005] is as follows:

$$\eta = (c_A \eta_A + c_B \eta_B) \times \left(1 - 2c_A c_B \frac{H_M}{RT} \right), \quad (11)$$

where η_i is the viscosity of pure component i . In terms of activation energy (E) and temperature (T), it can be expressed as follows [Brandes and Brook, 2013]:

$$\eta_i = \eta_i^0 \exp \left(\frac{E}{RT} \right). \quad (12)$$

Here, η_i^0 is a constant in the unit of viscosity.

For several metallurgical processes and heterogeneous chemical reactions, transport properties such as diffusivity of metals in the liquid state are required. For example, the rate of heterogeneous reactions between two liquid alloys, such as slag and metal, is restricted by the diffusion of the reactant species [Iida and Guthre, 1988]. The mutual diffusion coefficient (D_M) of liquid alloys can be displayed in terms of activity (a_i) and self-diffusion coefficient (D_{id}) of individual components [Darken and Gurry, 1953].

$$D_M = c_i D_{id} \frac{d \ln a_i}{dc_i}. \quad (13)$$

Here

$$D_M = cD_B + (1 - c)D_A, \quad (14)$$

where D_A and D_B are the self-diffusion coefficients of pure components A and B , respectively. One of the advantages of the presented model is that, the ratio of mutual diffusion coefficient (D_M) and self-diffusion coefficient (D_{id}) can be estimated in terms of concentration fluctuation in the long-wavelength limit ($S_{cc}(0)$).

$$\frac{D_M}{D_{id}} = \frac{c_A c_B}{S_{cc}(0)}. \quad (15)$$

Similarly, knowledge of surface properties is crucial for the understanding of surface-related properties such as wet joint capacity, epitaxial growth, corrosion and phase transition kinetics [Iida and Guthre, 1988; Thwaites, 1984]. Centered on the assumption of a monatomic surface layer, Butler's method [Butler, 1932] for assessing surface tension, σ of liquid solution can be expressed as follows:

$$\sigma = \frac{\mu_A^s - \mu_A^b}{S_A} = \frac{\mu_B^s - \mu_B^b}{S_B} = \dots = \frac{\mu_i^s - \mu_i^b}{S_i}, \quad (16)$$

where μ_i^s and μ_i^b are chemical potential of the hypothetical surface and the chemical potential of the bulk, respectively. S_i indicate the molar surface area of a pure element i . The expression for the surface tension of the binary liquid alloys in terms of partial excess free energy of mixing in the bulk (G_i^b), the partial excess free energy of mixing at the surface (G_i^s), the bulk concentration (c) and surface concentration (c^s) can be written as follows [Trybula *et al.*, 2016]:

$$\begin{aligned} \sigma &= \sigma_A + \frac{G_A^s - G_A^b}{S_A} + \frac{RT}{S_A} \ln \left(\frac{c^s}{c} \right) \\ &= \sigma_B + \frac{G_B^s - G_B^b}{S_B} + \frac{RT}{S_B} \ln \left(\frac{1 - c^s}{1 - c} \right), \end{aligned} \quad (17)$$

where σ_A and σ_B are the surface tensions of pure components A and B , respectively.

The monatomic surface area for each component is as follows:

$$S_i = 1.091 N_A^{1/3} V_i^{2/3}, \quad (18)$$

where V_i is the molar volume of the component i , can be determined from its molar mass and density and N_A stands for Avogadro number.

The surface tension value of the constituent element at a certain temperature (T_i^0) is available in the literature [Brandes and Brook, 2013]. These values can be optimized for working temperature (T) by using the expression,

$$\sigma_i(T) = \sigma_i^0 + (T - T_i^0)\Delta\sigma_i. \quad (19)$$

Here, $\Delta\sigma_i$ is the temperature coefficient of surface tension for the metal component of the alloys and T is the working temperature in Kelvins.

The concentration fluctuations in the long-wavelength limit $S_{cc}(0)$ indicate the preference for short-range ordering or phase-separation that defines the essence of mixing in liquid alloys in terms of chemical order and segregation. Once the Gibbs energy of mixing of the liquid phase G_M is known, $S_{cc}(0)$ can be expressed by G_M [Bhatia and Thornton, 1970].

$$S_{cc}(0) = \left(\frac{1}{RT} \frac{\partial^2 G_M}{\partial c^2} \right)^{-1}. \quad (20)$$

Theoretically computed values of $S_{cc}(0)$ can be compared with the observed values estimated from the activity of constituent elements at different compositions.

$$S_{cc}(0) = \frac{c_B a_A}{(\partial a_A / \partial c_A)_{T,P,N}} = \frac{c_A a_B}{(\partial a_B / \partial c_B)_{T,P,N}}. \quad (21)$$

Solving Eqs. (2) and (20) one obtains

$$S_{cc}(0) = \frac{RT}{RT \sum_{i=1}^3 \left(\frac{(x'_i)^2}{x_i} - \frac{(x')^2}{x} \right) + 2x \sum_{i < j} \Psi_{ij} \left(\frac{x_i}{x} \right)' \left(\frac{x_j}{x} \right)'}, \quad (22)$$

where the prime on x denotes its first differentiation with respect to c .

For ideal mixture, Eq. (22) reduces to

$$S_{cc}^{id}(0) = c_A c_B. \quad (23)$$

The degree of order in the liquid alloy can be viewed using the Warren–Cowley short-range order parameter (α_1) [Cowley, 1950; Warren, 1990]. Experimentally, this parameter is not readily quantifiable by diffraction experiments. From the knowledge of the nearest neighbor contacts of unlike atoms in the melt, the expression α_1 can simply be obtained. Singh *et al.* [1987] have suggested that α_1 can be estimated from $S_{cc}(0)$.

$$\alpha_1 = \frac{S - 1}{S(z - 1) + 1}, \quad S = \frac{S_{cc}(0)}{S_{cc}^{id}(0)}. \quad (24)$$

Here, z is the coordination number of the alloy. It is taken as 10 for the present calculations, and the α_1 values are evaluated.

3. Results and Discussion

3.1. Thermodynamic properties

Using energetics derived from experimental thermodynamic findings, we plan to investigate some of the transport and surface characteristics of Pb–Sb alloys such as viscosity, mutual diffusivity, surface concentration and surface tension. In order to use the CFM to obtain the required energy parameters, we consider the existence of a form $A_\alpha B_\beta$ chemical complex in the liquid state of the alloy. By choosing the values α and β from the phase diagram, we proceed to determine the mixing free energy values of the alloy by varying the energy parameters χ and Ψ_{ij} . The set of energy parameters that propagates to a reasonable extent the computed values of the free energy of mixing of liquid alloys will be further used in the calculation of their enthalpy of formation H_M , mixing entropy S_M and concentration–concentration fluctuation at the long-wavelength limit $S_{cc}(0)$. We extended the calculation to observe the short-range order parameter α_1 and mutual diffusivities D_M/D_{id} . The experimental data set of the Gibbs energy of mixing, G_M of liquid Pb–Sb alloys together with the enthalpy of mixing, H_M [Hultgren *et al.*, 1973] have been used to calculate the interaction energy parameters, i.e., χ , Ψ_{12} , Ψ_{13} and Ψ_{23} and their temperature derivatives at $T = 905$ K (Table 1). Simultaneously, Eq. (7) is solved for x_3 , whose values can further be used in Eqs. (2) and (4) for the calculation of G_M and H_M . At the compound forming composition, $c_c = 0.5$, the concentration dependence of the equilibrium values of chemical complexes, x_3 exhibits the maximum value of 0.4314; reflects the symmetric behavior of the alloy. It should be remembered that, within the context of the models described above, energy parameters χ and Ψ_{ij} do not depend on concentration but depend on temperature.

The values of the interaction energy parameters were adjusted to give the concentration dependences of G_M that fit well with the corresponding thermodynamic data. From Table 1, it is seen that only Ψ_{12} of the first system has a negative temperature coefficient in the presented system; all energy parameters have positive temperature coefficients. Figure 1 shows the excellent agreement of computed free energy of mixing by the presented model with the experimental data [Hultgren *et al.*, 1973]. The values of H_M and S_M are found to be in poor agreement with the experiment if energy parameters are taken as being temperature independent. Therefore, we have considered the variation of these parameters with temperature to ascertain the variation of heat and entropy of formation with observed values.

The enthalpies of mixing H_M and entropies of mixing S_M have been evaluated in Eqs. (4) and (10), respectively, and compared with available experimental data. The calculated enthalpies and entropies of mixing are in good agreement with

Table 1. Interaction parameters and their temperature derivatives.

χ/RT	Ψ_{12}/RT	Ψ_{23}/RT	Ψ_{13}/RT	$\frac{1}{R} \frac{\partial \chi}{\partial T}$	$\frac{1}{R} \frac{\partial \Psi_{12}}{\partial T}$	$\frac{1}{R} \frac{\partial \Psi_{13}}{\partial T}$	$\frac{1}{R} \frac{\partial \Psi_{23}}{\partial T}$
1.05	-0.23	1.10	1.10	1.044	1.990	0.980	0.994

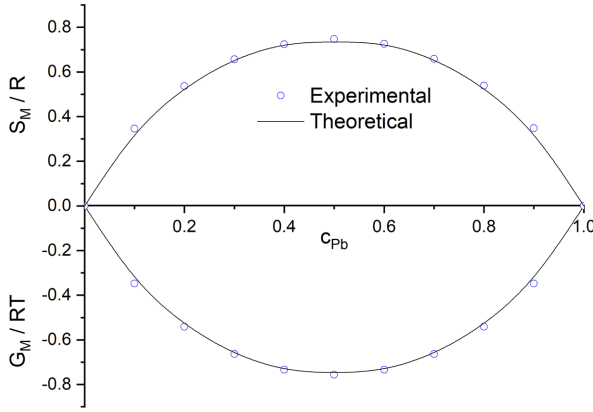


Fig. 1. The free energy of mixing (G_M/RT) and entropy of mixing (S_M/R) vs. concentration of lead (c_{Pb}) in the liquid Pb-Sb alloy at 905 K.

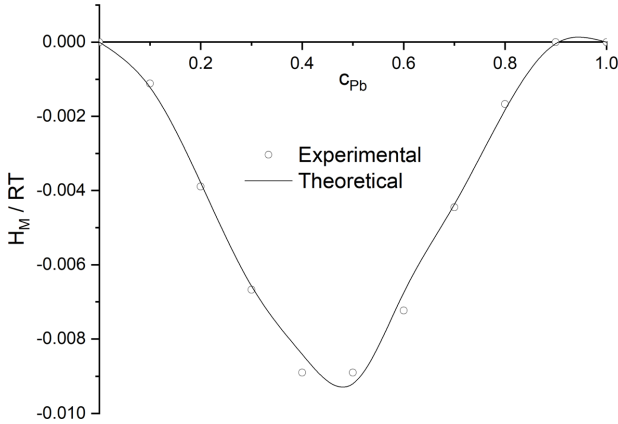


Fig. 2. Enthalpy of mixing (H_M/RT) vs. concentration of lead (c_{Pb}) in the liquid Pb-Sb alloy at 905 K.

experimental data as presented in Figs. 1 and 2. For all compositions, the mixing properties, i.e., the Gibbs free energy (Fig. 1) and enthalpy (Fig. 2) are small negative indicate weak interaction.

The variation of interaction energy parameters at higher temperatures is calculated by using Eq. (5) and presented in Fig. 3. The temperature dependence of interaction energy parameters excellently follows linear fit. However, the variation of ψ_{12} with temperature fits the second-order polynomial, $(\psi_{12}/RT) = p + qT + rT^2$, where p , q and r are constants having different values for different interaction parameters as presented in Table 2. These interaction parameters at different temperatures are used in Eq. (4) to obtain the variation of G_M/RT with temperature (Table 3). The negative values of G_M are observed to be decreasing showing phase separation tendency with an increase in temperature.

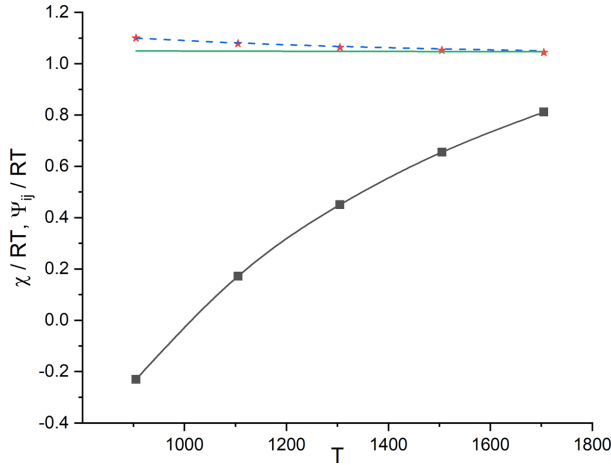


Fig. 3. Variation of the interaction parameters (χ and ψ_{ij}) with temperature (T). The solid line is for χ , a solid line with square symbols is for ψ_{12} , dashed line is for ψ_{23} and star symbols are for ψ_{13} .

Table 2. Values of coefficients for fit of various interaction parameters.

Coefficients	Ψ_{12}/RT	Ψ_{13}/RT	Ψ_{23}/RT	χ/RT
p	-2.93892	1.15799	1.15123	1.0529
$q(K^{-1})$	0.00391	-6.93655×10^{-5}	-6.12729×10^{-5}	-3.46828×10^{-6}
$r(K^{-2})$	-1.00803×10^{-6}			

Table 3. Variation of the free energy of mixing with temperature.

c_{Pb}	905 K	1105 K	1305 K	1505 K	1705 K
0.1	-0.3413	-0.3412	-0.3411	-0.3408	-0.3408
0.2	-0.5360	-0.5356	-0.5353	-0.5344	-0.5342
0.3	-0.6659	-0.6653	-0.6647	-0.6633	-0.6628
0.4	-0.7388	-0.7380	-0.7373	-0.7355	-0.7349
0.5	-0.7497	-0.7487	-0.7480	-0.7460	-0.7453
0.6	-0.7388	-0.7381	-0.7376	-0.7361	-0.7357
0.7	-0.6659	-0.6655	-0.6651	-0.6642	-0.6639
0.8	-0.5360	-0.5358	0.5356	-0.5352	-0.5351
0.9	-0.3413	-0.3413	-0.3413	-0.3413	-0.3413

3.2. Transport properties

The calculation of the viscosity of the Pb-Sb liquid alloy at 905 K is carried out by Eq. (11). The necessary fundamental data for the constituent elements at fixed temperature are taken from Ref. Brandes and Brook [2013]. These values are optimized for the investigation temperature by using Eq. (12). The compositional dependence of the viscosity with temperature is shown in Fig. 4. The viscosity obtained for the selected system alloy has been observed to decrease with the bulk concentration for

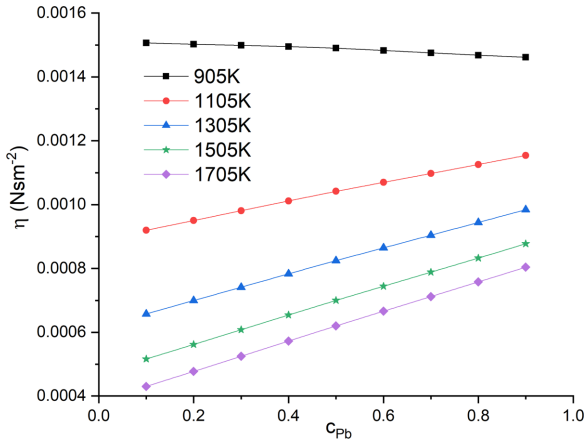


Fig. 4. Compositional dependence of viscosity (η) of liquid Pb-Sb alloy at different temperatures.

temperature 905 K. For higher temperature, it is found to be increasing with respect to the bulk concentration of Pb. As the temperature of the investigation increases, the viscosity is decreased.

The computed values of $S_{cc}(0)$ can be used to evaluate the ratio of mutual diffusivities to intrinsic diffusivities (D_M/D_{id}) as a function of composition using Eq. (15). The mixing behavior of binary liquid alloys can also be explained in terms of the ratio of diffusivities. The unity value of D_M/D_{id} tells that the alloy has a regular mixture of components leading to the ideal solution. The value of D_M/D_{id} greater than unity shows the tendency to short-range ordering in the alloy system while the smaller value of D_M/D_{id} leads the alloy towards phase separation. The plots of D_M/D_{id} against concentration at various temperatures are presented in Fig. 5. For the temperature of 905 K, it is clearly demonstrated in Fig. 5 that the ratio of mutual diffusivity is greater than unity throughout the entire compositional range. This undoubtedly showed that there is a presence of chemical order in the system at that temperature. For higher temperatures, it is getting even smaller leading the selected alloy towards homo-co-ordination.

3.3. Surface properties

The surface compositions and surface tension values for Pb-Sb liquid alloys have been computed numerically from Eq. (17). The surface tensions and density of the components of the alloy system at fixed temperature were taken from Ref. Brandes and Brook [2013] (Table 4). Equation (19) is used to achieve surface tension and density values at operating temperatures such as 905 K, 1105 K, 1305 K, 1505 K and 1705 K. The partial excess free energy of mixing in the bulk (G_i^b) and partial excess free energy of mixing at the surface (G_i^s) for Pb and Sb were taken from Ref. Hultgren *et al.* [1973].

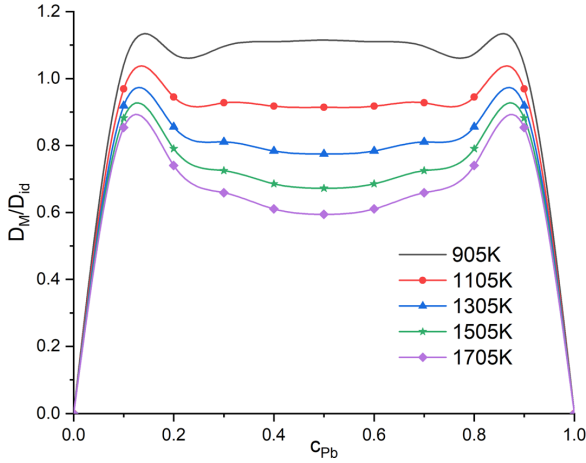


Fig. 5. Compositional dependence of the ratio of mutual and intrinsic diffusion coefficients (D_M/D_{id}) vs. concentration of lead (c_{Pb}) in the liquid Pb-Sb alloy at different temperatures.

Table 4. Input parameters for calculation of surface tension and viscosity.

Element	$T_i^0 (K)$	ρ_i^0 (Kgm^{-3})	$\Delta\rho_i$ ($Kgm^{-3}K^{-1}$)	σ_i^0 (Nm^{-1})	$\Delta\sigma_i$ ($Nm^{-1}K^{-1}$)	η_i^0 (Nsm^{-2})	E ($Jmol^{-1}$)
Pb	600	10678	-1.3174	0.468	-1.3×10^{-4}	4.636×10^{-4}	8610
Sb	903.5	6483	-0.565	0.367	-5×10^{-5}	8.12×10^{-5}	22000

The surface concentration of Pb is found to be increasing and that of Sb is observed to be decreasing with the bulk concentration (c_{Pb}). A negative deviation from ideality for the surface concentration of Pb and a positive deviation from ideality for the surface concentration of Sb has been observed. The surface concentration values of Sb are observed to be larger with their corresponding bulk concentration; confirms that the surface of the alloy is enormously rich with Sb atoms. With a rise in temperature, the surface concentration of Pb has been found to increase and that of Sb has been observed to decrease (Fig. 6). Surface tension values for Pb-Sb liquid alloys over the entire bulk concentration range of the corresponding component are presented in Fig. 7. The surface tension values of Pb-Sb increase with little addition of Lead atoms. In addition, as can be seen in Fig. 7, the surface tension isotherm with respect to the surface composition of Pb calculated by the above-mentioned model for the presented melt deviate negatively with respect to that calculated by the ideal solution model ($\tau_{ideal} = \tau_1c_1 + \tau_2c_2$), confirming that liquid alloys with negative excess Gibbs energy in the bulk exhibit negative surface tension deviations with respect to their ideal mixture [Westbrook and Fleischer, 1995]. The surface tensions of Pb-Sb alloy with respect to the bulk concentration of Pb at different temperatures are plotted in the same figure. It has been observed that the surface tension of the alloy decreases with an increase in the temperature.

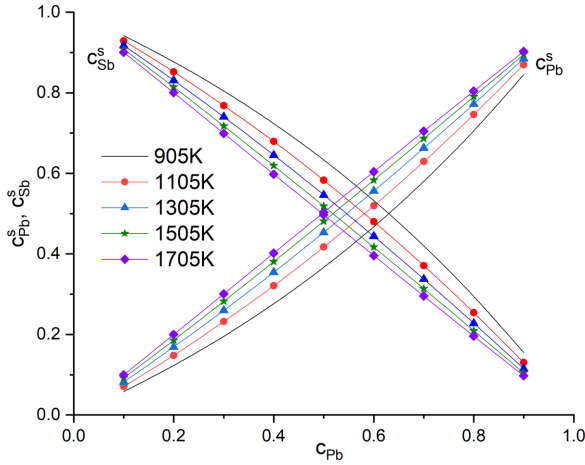


Fig. 6. Compositional dependence of the surface concentration of lead and antimony (c_{Pb}^s, c_{Sb}^s) vs. concentration of lead (c_{Pb}) in the liquid Pb-Sb alloy at different temperatures.

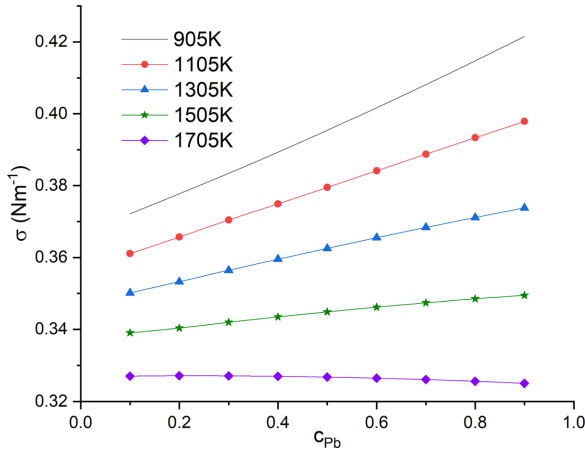


Fig. 7. Compositional dependence of viscosity (η) of liquid Pb-Sb alloy at different temperatures.

3.4. Structural properties

The theoretical calculation of concentration variations in the long-wavelength limit $S_{cc}(0)$ is of considerable importance because of difficulties in diffraction experiments when it is required to explore the essence of the atomic interactions in the melt. We determined $S_{cc}(0)$ and the Warren-Cowley short-range order parameter (α_1) using the energy parameters estimated in our earlier calculations. In general, in the case of a liquid binary alloy, when $S_{cc}(0) > S_{cc}^{id}(0)$ the system is assumed to be phase-segregating or to exhibit homo-coordination and when $S_{cc}(0) < S_{cc}^{id}(0)$ the system is said to be short-range ordering. $S_{cc}^{id}(0)$ is the ideal value of $S_{cc}(0)$ related with the ideal mixture. In addition, awareness of α_1 offers a clear glimpse into the

essence of the local arrangement of atoms of the mixture. $\alpha_1 < 0$ applies to atoms pairing as closest neighbors, $\alpha_1 > 0$ corresponds to like atoms pairing in the first co-ordination shell, while $\alpha_1 = 0$ corresponds to a random distribution. The limit values of α_1 for equiatomic composition fall within the range $-1 \leq \alpha_1 \leq +1$. The minimum possible value of α_1 is $\alpha_{\min} = -1$, which reflects complete ordering. On the other hand, the maximal value $\alpha_{\max} = +1$ is the absolute separation leading to the separation of phases. The plot of $S_{cc}(0)$ with respect to the bulk concentration of Pb at various temperatures for Pb–Sb complexes is shown in Fig. 8.

The lines are calculated values while the circles are experiment values calculated with Eq. (21) using the activity data from Ref. Hultgren *et al.* [1973] and the dashed line is for ideal values of $S_{cc}(0)$. Figure 8 shows that Pb–Sb is an ordering

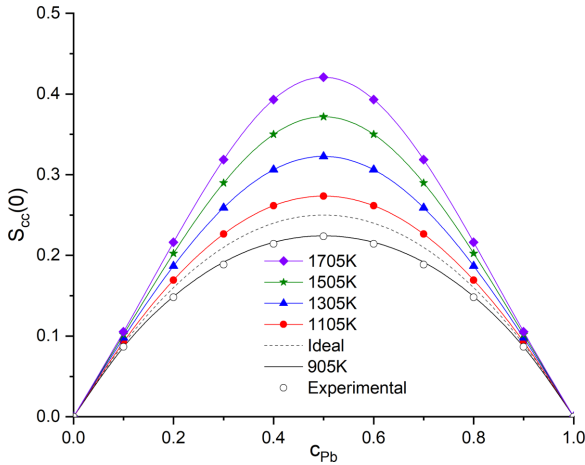


Fig. 8. Compositional dependence of $S_{cc}(0)$ in liquid Pb–Sb alloy at different temperatures.

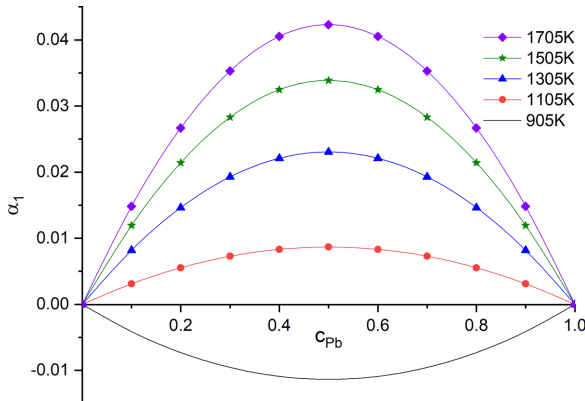


Fig. 9. Compositional dependence of chemical short-range order parameter (α_1) of liquid Pb–Sb alloy at different temperatures.

alloy almost through the entire concentration range. This is also supported by the chemical short-range order value, which has negative values throughout the entire region (Fig. 9).

The variation of both α_1 and $S_{cc}(0)$ with temperature supports the phase separating tendency with larger values of temperature as shown by variation of the free energy of mixing with temperature.

4. Conclusion

The thermodynamic, microscopic, transport and surface properties of Pb-Sb liquid alloys at different temperatures have been successfully explained through the different theoretical models. The theoretical analysis of thermodynamic properties reveals that Pb-Sb is a weakly interacting system. Except Ψ_{12} , all interaction parameters decrease with rise in temperature. Symmetry is observed in the free energy of mixing and entropy of mixing while asymmetric behavior is seen in enthalpy of mixing. Except for 905 K, the viscosity values are observed to be increasing with the bulk composition which is an interesting point for further investigation. The ratio of diffusion coefficients, $D_M/D_{id} > 1$ at all compositions which indicates that there is the tendency of compound formation over the whole composition range. The surface tension of the presented system is found to be smaller than ideal values. In the context of different temperatures, as the temperature of the study increases, it decreases. This study shows that component with larger surface concentration than its bulk composition tends to segregate on the surface of molten alloys. The study of concentration fluctuation in long-wavelength limit and CSRO show that there is the tendency of hetero co-ordination in liquid Pb-Sb alloy. The temperature variation investigations of all the properties reveal that the compound forming tendency of Pb-Sb liquid alloy decreases as temperature increases.

References

- Adedipe, A. M., Odusote, Y. A., Ndukwe, I. C. and Madu, C. A. [2019] "Energetics of compound formation in liquid Bi-Sb, Bi-Sn and Sb-Sn binary alloys," *Phys. J.* **3**, 37–48.
- Adhikari, D. [2012] "A theoretical study of thermodynamic properties of Cd-Bi liquid alloy," *BIBECHANA* **8**, 90–95. <https://doi.org/10.3126/bibechana.v8i0.5693>.
- Adhikari, D., Singh, B. P. and Jha, I. S. [2012] "Structural and energetic anomaly in liquid Na-Sn alloys," *J. Mol. Liq.* **167**, 52–56. <https://doi.org/10.1016/j.molliq.2011.12.010>.
- Adhikari, D., Singh, B. P. and Jha, I. S. [2012] "Energetics of Cd-based binary liquid alloys," *J. Non-Cryst. Solids* **358**(11), 1362–1367. <https://doi.org/10.1016/j.jnoncrystol.2012.03.008>.
- Adhikari, D., Singh, B. P. and Jha, I. S. [2012] "Phase separation in Na-K liquid alloy," *Ph. Trans.* **85**(8), 675–680. <https://doi.org/10.1080/01411594.2011.635903>.
- Ajayi, A. A. and Ogunmola, E. D. [2018] "Investigation on compound formation in Mg-Sb and Cu-Sb liquid alloys" *Int. J. Adv. Mater. Res.* **4**(2), 29–34.

- Akasofu, T., Kusakabe, M. and Tamaki, S. [2020] "An interpretation on the thermodynamic properties of liquid Pb–Te alloys," *High Temp. Mater. Processes*. **39**(1), 297–303. <https://doi.org/10.1515/htmp-2020-0068>.
- Akinlade, O., Ali, I. and Singh, R. N. [2001] "Correlation between bulk and surface phenomena in Ga-(Bi,In) and In-Bi liquid alloys," *Int. J. Mod. Phys B* **15**(22), 3039–3053. <https://doi.org/10.1142/S0217979201007178>.
- Akinlade, O. and Boyo, A. O. [2004] "Thermodynamics and surface properties of Fe–V and Fe–Ti liquid alloys," *Z. Metallkd.* **95**(5), 387–395. <https://doi.org/10.3139/146.017963>.
- Akinlade, O., Boyo, A. O. and Ijaduola, B. R. [1999] "Demixing tendencies in some Sn-based liquid alloys," *J. Alloys Compd.* **290**(1–2), 191–196. [https://doi.org/10.1016/S0925-8388\(99\)00232-7](https://doi.org/10.1016/S0925-8388(99)00232-7).
- Akinlade, O., Hussain, L. A. and Awe, O. E. [2003] "Thermodynamics of liquid Al–In, Ag–In and In–Sb alloys from a four-atom cluster model," *Z. Metallkd.* **94**(12), 1276–1279. <https://doi.org/10.3139/146.031276>.
- Akinlade, O. and Singh, R. N. [2002] "Bulk and surface properties of liquid In–Cu alloys," *J. Alloys Compd.* **333**(1–2), 84–90. [https://doi.org/10.1016/S0925-8388\(01\)01733-9](https://doi.org/10.1016/S0925-8388(01)01733-9).
- Akinlade, O., Singh, R. N. and Sommer, F. [2000] "Thermodynamics of liquid Al–Fe alloys," *J. Alloys Compd.* **299**(1–2), 163–168. [https://doi.org/10.1016/S0925-8388\(99\)00682-9](https://doi.org/10.1016/S0925-8388(99)00682-9).
- Anusionwu, B. C. [2006] "Thermodynamic and surface properties of Sb–Sn and In–Sn liquid alloys," *Pramana — J. Phys.* **67**(2), 319–330. <https://doi.org/10.1007/s12043-006-0076-z>.
- Anusionwu, B. C., Akinlade, O. and Hussain, L. A. [1998] "Assessment of size effect on the surface properties of some binary liquid alloys," *J. Alloys Compd.* **278**(1–2), 175–181. [https://doi.org/10.1016/S0925-8388\(98\)00530-1](https://doi.org/10.1016/S0925-8388(98)00530-1).
- Anusionwu, B. C. and Ilo-Okeke, E. O. [2005] "Segregation and surface properties of In–Zn liquid alloys," *Phys. Chem. Liq.* **43**(1), 25–36. <https://doi.org/10.1080/0031910042000303527>.
- Anusionwu, B. C. and Ilo-Okeke, E. O. [2005] "Temperature effect on demixing and surface properties of Sn–Zn liquid alloys," *J. Alloys Compd.* **397**(1–2), 79–84. <https://doi.org/10.1016/j.jallcom.2004.12.048>.
- Anusionwu, B. C., Madu, C. A. and Orji, C. E. [2009] "Theoretical studies of mutual diffusivities and surface properties in Cd–Ga liquid alloys," *Pramana — J. Phys.* **72**(6), 951–967. <https://doi.org/10.1007/s12043-009-0088-6>.
- Arkipov, P. A., Kumkov, S. I., Khalimullina, Yu. R. and Kholkina, A. S. [2013] "Estimation of the activity of lead in the binary Pb–Sb and Pb–Bi systems," *Russ. Metal. (Metally)*, **2013**(2), 115–122. <https://doi.org/10.1134/S0036029513020043>.
- Attri, K. S., Ahluwalia, P. K. and Sharma, K. C. [1996] "Two-compound formation in liquid binary alloys: Temperature dependence of thermodynamic functions in mercury indium alloy," *Phys. Chem. Liq.* **31**(4), 231–244. <https://doi.org/10.1080/00319109608031657>.
- Awe, O. E. and Azeez, A. A. [2017] "Temperature dependence of the bulk and surface properties of liquid Zn–Cd alloys," *Appl. Phys. A* **123**(5), 1–10. <https://doi.org/10.1007/s00339-017-0977-3>.
- Awe, O. E., Odusote, Y. A., Hussain, L. A. and Akinlade, O. [2011] "Temperature dependence of thermodynamic properties of Si–Ti binary liquid alloys," *Thermochim. Acta* **519**(1–2), 1–5. <https://doi.org/10.1016/j.tca.2011.02.028>.
- Awe, O. E. and Onifade, A. [2012] "Effects of surface coordination of atoms on the surface properties of some liquid binary alloys" *Phys. Chem. Liq.* **50**(5), 579–595. <https://doi.org/10.1080/00319104.2011.637627>.

- Awe, O. E. and Oshakuade, O. M. [2016] "Computation of infinite dilute activity coefficients of binary liquid alloys using complex formation model," *Physica B: Condens. Matter* **487**, 13–17. <https://doi.org/10.1016/j.physb.2016.01.023>.
- Bhandari, I. B., Koirala, I. and Adhikari, D. [2020] "Temperature-dependent mixing behaviours of Bi–Mg liquid alloys," *Phys. Chem. Liq.* 1–14. <https://doi.org/10.1080/00319104.2020.1863402>.
- Bhatia, A. B. and Hargrove, W. H. [1974] "Concentration fluctuations and thermodynamic properties of some compound forming binary molten systems," *Phys. Rev. B*, **10**(8), 3186–3196.
- Bhatia, A. B. and Singh, R. N. [1984] "A quasi-lattice theory for compound forming molten alloys," *Phys. Chem. Liq.* **13**(3), 177–190. <https://doi.org/10.1080/00319108408080778>.
- Bhatia, A. B. and Thornton, D. E. [1970] "Structural aspects of the electrical resistivity of binary alloys," *Phys. Rev. B*, **2**(8), 3004–3012. <https://doi.org/10.1103/PhysRevB.2.3004>.
- Brandes, E. A. and Brook, G. B. (Eds.). [2013] *Smithells Metals Reference Book* (Elsevier).
- Budai, I., Benkó, M. Z. and Kaptay, G. [2005] "Analysis of literature models on viscosity of binary liquid metallic alloys on the Example of the Cu–Ag System," *Mate. Sci. Forum* **473**, 309–314. <https://doi.org/10.4028/www.scientific.net/MSF.473-474.309>.
- Butler, J. A. V. [1932] "The thermodynamics of the surfaces of solutions," *Proc. R. Soc. London Series A Contain. Papers Math. Phys. Character* **135**(827), 348–375.
- Cowley, J. M. [1950] "An approximate theory of order in alloys," *Phys. Rev.* **77**(5), 669.
- Darken, L. S. and Gurry, R. W. [1953] *Physical Chemistry of Metals* (McGraw Hill).
- Gancarz, T. and Gasior, W. [2018] "Density, surface tension, and viscosity of liquid Pb–Sb alloys," *J. Chem. Eng. Data* **63**(5), 1471–1479. <https://doi.org/10.1021/acs.jced.7b01049>.
- Gierlotka, W., Lee, C., Chumpanaya, P., Rahman, Md. A. and Ko, T.-N. [2013] "Thermodynamic re-optimization of the binary Pb-Sb system," *J. Phase Equilibria Diffus.* **34**(5), 421–424. <https://doi.org/10.1007/s11669-013-0252-z>.
- Godbole, R. P., Jha, S. A., Milananun, M. and Mishra, A. K. [2004] "Thermodynamics of liquid Cu–Mg alloys," *J. Alloys Compd.* **363**(1–2), 187–193. [https://doi.org/10.1016/S0925-8388\(03\)00326-8](https://doi.org/10.1016/S0925-8388(03)00326-8).
- Gohivar, R. K., Koirala, R. P., Yadav, S. K. and Adhikari, D. [2020] "Temperature dependence of interaction parameters of Cu–Si liquid alloy," *AIP Adv.* **10**(8), 1–6. <https://doi.org/10.1063/5.0012834>.
- Gohivar, R. K., Yadav, S. K., Koirala, R. P. and Adhikari, D. [2020] "Artifacts in Al–Mn liquid alloy," *Physica B: Condens. Matter* **595**, 1–6. <https://doi.org/10.1016/j.physb.2020.412348>.
- Guggenheim, E. A. [1952] *Mixtures: The Theory of the Equilibrium Properties of Some Simple Classes of Mixture Solutions and Alloys* (Clarendon Press).
- Guo, F., Wang, W., Yang, H., Qin, J. and Tian, X. [2012] "Abnormal resistivity and viscosity behavior in Sb-rich Pb–Sb melts," *T. Nonferr. Metal Soc.* **22**(12), 3113–3119. [https://doi.org/10.1016/S1003-6326\(11\)61579-3](https://doi.org/10.1016/S1003-6326(11)61579-3).
- Habashi, F. (Ed.). [1998] *Alloys: Preparation, Properties, Application* (First) (Wiley-VCH Verlag GmbH).
- Hassam, S., Boa, D., Fouque, Y., Kotchi, K. P. and Rogez, J. [2009] "Thermodynamic investigation of the Pb – Sb system," *J. Alloys Compd.* **476**(1–2), 74–78. <https://doi.org/10.1016/j.jallcom.2008.09.002>.
- Hoshino, K. and Young, W. H. [1980] "Entropy of mixing of compound forming liquid binary alloys," *J. Phys. F Met. Phys.* **10**(7), 1365–1374. <https://doi.org/10.1088/0305-4608/10/7/006>.

- Hultgren, R., Desai, P. D., Hawkins, D. T., Gleiser, M. and Kelley, K. K. [1973] *Selected Values of the Thermodynamic Properties of the Elements* (National Standard Reference Data System).
- Iida, T. and Guthrie, R. I. L. [1988] *The Physical Properties of Liquid Metals* (Clarendon Press).
- Ilo-Okeke, E. O., Anusionwu, B. C. and Popoola, O. [2005] "Thermodynamic evaluation of viscosity in In–Zn and Sn–Zn liquid alloys," *Phys. Chem. Liq.* **43**(4), 333–342. <https://doi.org/10.1080/00319100500087964>.
- Jha, I. S., Adhikari, D. and Singh, B. P. [2012] "Mixing behaviour of sodium-based liquid alloys," *Phys. Chem. Liq.* **50**(2), 199–209. <https://doi.org/10.1080/00319104.2011.569887>.
- Jha, I. S., Khadka, R., Koirala, R. P., Singh, B. P. and Adhikari, D. [2016] "Theoretical assessment on mixing properties of liquid Tl–Na alloys," *Philos. Mag.* **96**(16), 1664–1683. <https://doi.org/10.1080/14786435.2016.1177668>.
- Jha, I. S., Koirala, I., Singh, B. P. and Adhikari, D. [2014] "Concentration dependence of thermodynamic, transport and surface properties in Ag–Cu liquid alloys," *Appl. Phys. A*, **116**(3), 1517–1523.
- Jha, I. S., Singh, R. N., Srivastava, P. L. and Mitra, N. R. [1990] "Stability of HgNa and HgK liquid alloys," *Philos. Mag. B* **61**(1), 15–24. <https://doi.org/10.1080/13642819008208649>.
- Koirala, I., Singh, B. P. and Jha, I. S. [2014] "Theoretical assessment on segregating nature of liquid In–Tl alloys," *J. Non-Cryst. Solids* **398**, 26–31.
- Koirala, R. P. [2013] "Thermodynamic and structural behaviour of liquid Al–Ga alloys," *Adv. Mater. Lett.* **4**(4), 283–287. <https://doi.org/10.5185/amlett.2012.8412>.
- Koirala, R. P., Kumar, J., Singh, B. P. and Adhikari, D. [2014] "Bulk and surface properties of Co–Fe and Fe–Pd liquid alloys," *J. Non-Cryst. Solids* **394**, 9–15. <https://doi.org/10.1016/j.jnoncrysol.2014.04.001>.
- Koirala, R., Singh, B., Jha, I. and Adhikari, D. [2015] "Energetics and local order in In-based liquid alloys," *BIBECHANA* **13**, 60–71. <https://doi.org/10.3126/bibechana.v13i0.13359>.
- Kumar, A., Jha, I. S. and Singh, B. P. [2011] "Quasi-lattice model for the thermodynamic properties and microscopic structure of molten Fe–Si alloy," *Physica B: Condens. Matter* **406**(23), 4338–4341. <https://doi.org/10.1016/j.physb.2011.08.060>.
- Kumar, A., Rafique, S. M. and Jha, N. [2006] "Study of glass forming tendency of Ca–Mg binary alloy and its physical properties: Pseudomolecule formation model," *Physica B: Condens. Matter* **373**(1), 169–176. <https://doi.org/10.1016/j.physb.2005.11.142>.
- Mishra, A. K. [2007] "Thermodynamic properties, surface properties and volume of mixing of liquid Cd–Na alloys — complex formation model incorporating volume interaction terms," *High Temp. Mater. Process.* **26**(3), 201–208. <https://doi.org/10.1515/HTMP.2007.26.3.201>.
- Mishra, P. P., Milanarun, M., Jha, N. and Mishra, A. K. [2002] "Thermodynamic properties of liquid glass-forming Ca–Mg alloys," *J. Alloys Compd.* **340**(1–2), 108–113. [https://doi.org/10.1016/S0925-8388\(01\)01988-0](https://doi.org/10.1016/S0925-8388(01)01988-0).
- Mostafa, M. M. [2004] "Steady state creep characteristics of the eutectic Pb–Sb alloy," *Physica B: Condens. Matter* **349**(1–4), 56–61. <https://doi.org/10.1016/j.physb.2004.01.159>.
- Novakovic, R., Giuranno, D., Delsante, S. and Borzone, G. [2014] "Bulk and surface properties of liquid Cr–Nb–Re alloys," *J. Phase Equilibria Diffus.* **35**(4), 445–457. <https://doi.org/10.1007/s11669-014-0316-8>.

- Novakovic, R., Giuranno, D., Ricci, E., Delsante, S., Li, D. and Borzone, G. [2011] "Bulk and surface properties of liquid Sb-Sn alloys," *Surf. Sci.* **605**, 248–255. <https://doi.org/10.1016/j.susc.2010.10.026>.
- Novakovic, R., Giuranno, D., Ricci, E., Tuissi, A., Wunderlich, R., Fecht, H.-J. and Egry, I. [2012] "Surface, dynamic and structural properties of liquid Al-Ti alloys," *Appl. Surf. Sci.* **258**(7), 3269–3275. <https://doi.org/10.1016/j.apsusc.2011.11.080>.
- Odusote, Y. A. [2014] "Thermodynamic and dynamical properties of liquid Al-X (X = Sn, Ge, Cu) systems," *J. Non-Cryst. Solids* **402**, 96–100. <https://doi.org/10.1016/j.jnoncrsol.2014.05.028>.
- Odusote, Y. A. and Popoola, A. I. [2017] "Thermodynamic and surface properties of Cr-X, (X = Mo, Fe) liquid alloys," *Am. J. Condens. Matter Phys.* **7**(3), 57–66.
- Odusote, Y. A., Popoola, A. I. and Oluyamo, S. S. [2016] "Bulk and surface properties of demixing liquid Al-Sn and Sn-Tl alloys," *Appl. Phys. A*, **122**(2), 80. <https://doi.org/10.1007/s00339-015-9591-4>.
- Okamoto, H. [2011] "Pb-Sb (Lead-Antimony)," *J. Phase Equilibria Diffus.* **32**(6), 567. <https://doi.org/10.1007/s11669-011-9952-4>.
- Panthi, N., Bhandari, I. B., Jha, I. S. and Koirala, I. [2020] "Complex formation behavior of Copper-Tin alloys at its molten state," *Adv. Mater. Lett.* **12**(1), 1–7.
- Prasad, L. C., Chatterjee, S. K. and Jha, R. K. [2007] "Atomic order and interionic pair potentials in Cu-Sn liquid alloys," *J. Alloys Compd.* **441**(1–2), 43–51. <https://doi.org/10.1016/j.jallcom.2006.09.079>.
- Rafique, S. M. and Kumar, A. [2007] "Thermodynamic properties and alloying behavior of liquid binary alloy: CdZn," *Indian J. Phys.* **81**(1), 35–39.
- Sharma, N., Thakur, A. and Ahluwalia, P. K. [2013] "Thermodynamic, surface and transport properties of liquid Hg-Pb and Hg-In amalgams," *J. Mol. Liq.* **188**, 104–112. <https://doi.org/10.1016/j.molliq.2013.10.004>.
- Shrestha, G. K., Singh, B. K., Jha, I. S., Singh, B. P. and Adhikari, D. [2017] "Optimization method for the study of the properties of Al-Sn binary liquid alloys," *Physica B: Condens. Matter*, **514**, 1–7. <https://doi.org/10.1016/j.physb.2017.03.005>.
- Singh, B. P., Adhikari, D. and Jha, I. S. [2010] "Concentration dependence of the structure and thermodynamic properties of silver-antimony alloys," *J. Non-Cryst. Solids* **356**(33–34), 1730–1734. <https://doi.org/10.1016/j.jnoncrsol.2010.06.004>.
- Singh, B. P., Adhikari, D. and Jha, I. S. [2012] "Short range order in molten Al-Si alloys," *Phys. Chem. Liq.* **50**(6), 697–704. <https://doi.org/10.1080/00319104.2012.682259>.
- Singh, B. P., Koirala, I., Jha, I. S. and Adhikari, D. [2014] "The segregating nature of Cd-Pb liquid binary alloys," *Phys. Chem. Liq.* **52**(4), 457–470. <https://doi.org/10.1080/00319104.2013.871668>.
- Singh, B. P., Singh, B. K., Jha, I. S., Shrestha, G. K. and Koirala, I. [2017] "Thermodynamic and transport properties of molten Bi-In alloys," *Himalayan Phys.* 5–9. <https://doi.org/10.3126/hj.v6i0.18349>.
- Singh, R. N. [1987] "Short-range order and concentration fluctuations in binary molten alloys," *Can. J. Phys.* **65**(3), 309–325. <https://doi.org/10.1139/p87-038>.
- Singh, R. N. [1993] "Higher order conditional probabilities and short range order in molten alloys," *Phys. Chem. Liq.* **25**(4), 251–267. <https://doi.org/10.1080/00319109308030365>.
- Singh, R. N. and Arafin, S. [2015] "Chemical short range order in MgPb alloys," *Phys. Chem. Liq.* **53**(1), 38–45. <https://doi.org/10.1080/00319104.2014.915712>.
- Singh, R. N., Pandey, D. K., Sinha, S., Mitra, N. R. and Srivastava, P. L. [1987] "Thermodynamic properties of molten salt solutions," *Physica B*, **145**, 358–364. <https://doi.org/10.1007/978-94-009-3863-2-2>.

- Thwaites, C. J. [1984] "Soldering technology — decade of developments," *Int. Met. Rev.* **29**(1), 45–74. <https://doi.org/10.1179/imtr.1984.29.1.45>.
- Trybula, M. E., Gancarz, T. and Gasior, W. [2016] "Density, surface tension and viscosity of liquid binary Al–Zn and ternary Al–Li–Zn alloys," *Fluid Ph. Equilibria*, **421**, 39–48. <https://doi.org/10.1016/j.fluid.2016.03.013>.
- Warren, B. E. [1990] *X-ray Diffraction* (Dover Publication).
- Westbrook, J. H. and Fleischer, R. L. (Eds.). [1995] *Intermetallic Compounds: Principles and Practice* (Wiley).
- Yadav, S., Jha, L. and Adhikari, D. [2015] "Thermodynamic, structural, transport and surface properties of Pb–Ti liquid alloy," *BIBECHANA*, **13**, 100–113. <https://doi.org/10.3126/bibechana.v13i0.13443>.
- Yadav, S. K., Lamichhane, S., Jha, L. N., Adhikari, N. P. and Adhikari, D. [2016] "Mixing behaviour of Ni–Al melt at 1873 K," *Phys. Chem. Liq.* **54**(3), 370–383. <https://doi.org/10.1080/00319104.2015.1095640>.
- Yadav, S. K., Mehta, U., Gohivar, R. K., Dhungana, A., Koirala, R. P. and Adhikari, D. [2020] "Reassessments of thermo-physical properties of Si–Ti melt at different temperatures," *BIBECHANA*, **17**, 146–155. <https://doi.org/10.3126/bibechana.v17i0.26877>.
- Zaikov, Yu. P., Arkhipov, P. A., Plekhanov, K. A., Ashikhin, V. V., Khalimulina, Yu. R., Chebykin, V. V. and Molchanova, N. G. [2007] "Thermodynamic characteristics of Pb–Sb alloys," *Russ. J. Non-Ferr. Met.* **48**(2), 92–98. <https://doi.org/10.3103/S1067821207020034>.



4th International Conference on Nanomaterials Science and Mechanical Engineering
University of Aveiro, Portugal, July 6-9, 2021

July 12, 2021

Organizing committee

Prof. Dr. Robertt Angelo Fontes Valente,
University of Aveiro, Portugal, E-mail:

robertt@ua.pt

Prof. Dr. Vítor António Ferreira da Costa,
University of Aveiro, Portugal, E-mail:

v.costa@ua.pt

Prof. Dr. António Manuel de Bastos Pereira,
University of Aveiro, Portugal, Email:

abastos@ua.pt

Dr. Paula Alexandrina de Aguiar Pereira
Marques University of Aveiro, Portugal, E-mail:

paula@ua.pt

Dr. Duncan Paul Fagg,

University of Aveiro, Portugal, Email:

duncan@ua.pt

Dr. Igor Bdikin,

University of Aveiro, Portugal, E-mail:

bdikin@ua.pt

Dr. Gonzalo Guillermo Otero Irurueta,

University of Aveiro, E-mail:

otero.gonzalo@ua.pt

Dr. Gil Gonçalves

University of Aveiro, E-mail:

ggoncalves@ua.pt

Editorial Board

Dr. Igor Bdikin (UA, Portugal)

Dr. Gil Gonçalves (UA, Portugal)

Raul Nunes Simões (UA, Portugal)

Technical Program Committee

Dr. Duncan Paul Fagg (UA, Portugal)

Dr. Paula Alexandrina de Aguiar Pereira

Marques (UA, Portugal)

Dr. Igor Bdikin (UA, Portugal)

Dr. Gonzalo Guillermo Otero Irurueta (UA,
Portugal)

Dr. Pukazh Selvan Dharmakkon (UA, Portugal)

Dr. Sergey Mikhalev (UA, Portugal)

Raul Nunes Simões (UA, Portugal)

Conference Contacts

TEMA-icnmsme2021.aveiro@ua.pt

Telephone: +351 234 370 830

Conference Web

<http://icnmsme2021.web.ua.pt>

Certificate of Attendance

We hereby confirm that

Mr. Indra Bahadur Bhandari

**Central Department of Physics, Tribhuvan University,
Kirtipur, Nepal**

**Department of Applied Sciences, Institute of
Engineering, Tribhuvan University, Nepal**

attended the

**4th International Conference on Nanomaterials Science
and Mechanical Engineering (ICNMSME2021) with**

Oral Presentation “Temperature-dependent mixing

behaviors of Bi -Mg liquid alloys”,

held in the

University of Aveiro, Portugal from 6 to 9 July 2021.

**For and on behalf of the ICNMSME2021 Organizing
Committee.**



Dr. Igor Bdikin
(ICNMSME-2021 Organizing Committee Co-Chair)

Department of Mechanical Engineering

University of Aveiro, Aveiro 3810-193, Portugal

Fax: (+351) 234 370 953

Tel: (+351) 234 370 830

Email: bdikin@ua.pt



Workshop on Low-dimensional materials: experiment, theory, application
University of Aveiro, Portugal, July 6, 2021

July 12, 2021

Organizing committee

Dr. Paula Alexandrina de Aguiar Pereira Marques University of Aveiro, Portugal, E-mail:
paula@ua.pt

Dr. Duncan Paul Fagg,
University of Aveiro, Portugal, Email:
duncan@ua.pt

Dr. Igor Bdikin,
University of Aveiro, Portugal, E-mail:
bdikin@ua.pt

Dr. Gonzalo Guillermo Otero Irurueta;
University of Aveiro, E-mail:
otero.gonzalo@ua.pt

Dr. Gil Gonçalves
University of Aveiro, E-mail:
ggoncalves@ua.pt

Editorial Board

Dr. Igor Bdikin (UA, Portugal)
Dr. Gil Gonçalves (UA, Portugal)
Raul Nunes Simões (UA, Portugal)

Technical Program Committee

Dr. Duncan Paul Fagg (UA, Portugal)
Dr. Paula Alexandrina de Aguiar Pereira Marques (UA, Portugal)
Dr. Igor Bdikin (UA, Portugal)
Dr. Gonzalo Guillermo Otero Irurueta (UA, Portugal)
Dr. Pukazh Selvan Dharmakkon (UA, Portugal)
Raul Nunes Simões (UA, Portugal)

Conference Contacts

TEMA-icnmsme2021.aveiro@ua.pt

Telephone: +351 234 370 830

Conference Web

<http://icnmsme2021.web.ua.pt/>

Certificate of Attendance

We hereby confirm that

Mr. Indra Bahadur Bhandari

**Central Department of Physics, Tribhuvan University,
Kirtipur, Nepal**

attended the

Workshop on Low-dimensional materials: experiment,

theory, application (WLDM-2021), held in the

University of Aveiro, Portugal,

6 July 2021.

**For and on behalf of the WLDM-2021 Organizing
Committees.**



Dr. Igor Bdikin
(WLDM-2021 Organizing Committee Co-Chair)
Department of Mechanical Engineering
University of Aveiro, Aveiro 3810-193, Portugal
Fax: (+351) 234 370 953
Tel: (+351) 234 370 830
Email: bdikin@ua.pt




International Conference on
Nanosciences and High Energy Physics
(ICNHEP-2019)
February 4-6, 2019
Central Department of Physics
Tribhuvan University, Kirtipur, Nepal





Certificate

This is to Certify that Dr./Mr./Ms *Indra* *Bd* *Bhandari* has participated in "ICNHEP-2019" and presented a invited talk/ research paper.

The title of the talk / paper is


Prof. Dr. Ram Pd. Khatiwada
Dean, IoST, TU, Kirtipur


Dr. Gopi Chandra Kaphle
Convener, ICNHEP-2019


Prof. Dr. Binil Aryal
Head CDP, TU, Kirtipur

2021 Second International Conference on

Advances in Physical Sciences and Materials (ICAPSM 2021)

12 - 13, August 2021 | Coimbatore, India | www.icapsm.com

CERTIFICATE

Publication Partner

IOPscience

PSM 3020

Peer Reviewed

This certificate is presented to



Indra Bahadur Bhandari

Central Department of Physics,
Tribhuvan University, Kirtipur, Nepal.
Department of Applied Sciences, Purwanchal Campus,
Tribhuvan University, Dharan, Nepal.

for presenting the research paper entitled “**Effect of Temperature on Mixing Behavior and Stability of Liquid Al-Fe Alloys**” in the Second International Conference on Advances in Physical Sciences and Materials (ICAPSM 2021) held at Coimbatore, Tamil Nadu, India during 12 -13, August 2021. Proceedings of the ICAPSM 2021 will be published by the Institute of Physics, United Kingdom in the IOP: Journal of Physics Conference Series (JPCS), a conference proceedings journal.

Dr. Thangaprakash Sengodan
Chair - TPC

Academic Partner



Department of Mechatronics
SNS COLLEGE OF TECHNOLOGY
Coimbatore, Tamil Nadu, INDIA

CMS Partner


DILIGENTEC SOLUTIONS

ICAPSM 2021



Tribhuvan University
Institute of Science and Technology
Dean's Office

SEMESTER EXAMINATION 2075

Name of Student: Indra Bahadur Bhandari

Exam Roll No.: 100010

Level: Ph.D.

Ph.D. Enrolment No.: 100/074

Department: Central Dept. of Physics

T.U. Regd. No.: 5.2-33-643-2003

Semester: I

Grade Sheet

Code No.	Course Title	Cr. Hrs.	Grade Point	Grade
PHS 911	Philosophy of Science	3	3.7	A-
RM 912	Research Methodology	3	3.3	B+
Sem 913	Seminar	3	4	A

SGPA: 3.7

Verified By: *Dndu*

Date: *oct. 9, 2018*



Shrestha
Asst. Dean



Tribhuvan University
Institute of Science and Technology
Dean's Office

SEMESTER EXAMINATION-2075

Name of Student: Indra Bahadur Bhandari Exam Roll No.: 200010

Level: Ph.D.

Ph.D. Enrolment No.: 100/074

Department: Central Dept. of Physics

T.U. Regd. No.: 5-2-33-643-2003

Semester: 2


Grade Sheet

Code No.	Course Title	Cr. Hrs.	Grade Point	Grade
PHY 951	Advanced Research Methodology	3	4	A
PHY 960	Materials Thermodynamics B	3	4	A
PHY 952	Seminar	3	4	A

SGPA: 4.00

Verified By: 

Date: - Sept. 16, 2019


Asst. Dean